COMPARATIVE STUDY ON PERFORMANCE OF PTFE AND PVDF MEMBRANES FOR WATER DESALINATION USING VACUUM MEMBRANE DISTILLATION

Submitted in fulfillment of the requirements of the degree of

DOCTOR OF PHILOSOPHY IN CHEMICAL ENGINEERING

By

JITENDRA KUMAR SINGH

(2011RCH7107)

SUPERVISOR

Dr. S. P. Chaurasia

Professor

Department of Chemical Engineering

MALAVIYA NATIONAL INSTITUTE OF TECHNOLOGY JAIPUR

Jan 2017

MALAVIYA NATIONAL INSTITUTE OF TECHNOLOGY JAIPUR

DEPARTMENT OF CHEMICAL ENGINEERING

JLN MARG, JAIPUR-302017 (RAJASTHAN) INDIA

CERTIFICATE

We are hereby pleased to certify that the thesis submitted by Mr. Jitendra Kumar Singh (Student ID: 2011RCH7107) entitled **"Comparative Study on Performance of PTFE and PVDF Membrane for Water Desalination Using Vacuum Membrane Distillation",** is approved for the award of the degree of Doctor of Philosophy (Ph.D.) in Chemical Engineering.

Prof. S.P. Chaurasia
(Supervisor)
Date:

Prof. K.K. Pant
(External Examiner)
Date:

ACKNOWLEDGEMENT

It is my pleasant duty to express my deep sense of gratitude to my supervisor, **Prof. S. P. Chaurasia**, Chemical Engineering Department, Malaviya National Institute of Technology Jaipur for his immeasurable inspiring guidance at each and every step during the course of this study as well as overall professional development. It was his constant encouragement and motivation which enabled me to bring this study to completion. I am extremely fortunate to have **Prof. S. P. Chaurasia** as my guide. I have no words to express my feeling towards my guide's extremely kind and tolerant attitude all the time.

I am also grateful to **Dr. Sushant Upadhyaya,** Assistant Professor, Chemical Engineering Department, MNIT Jaipur for his generous help in mathematical model validation and thesis writing. I would like to pay respect and thanks to the past **Director, Prof. I.K. Bhat, and the current Director, Prof. A.B. Gupta**, for providing all supports and funds from the institute for the installation of experimental setup. I would also like to acknowledge my friend **Dr. Manisha Sharma**, Assistant Professor, Chemical Engineering Department, Manipal University Jaipur for her continuous mutual motivation in all aspects. I express gratitude for the help and support by all other faculty members; especially my DRC committee members.

I would like to thank **Mr. Ramesh Sharma**, senior technician, Chemical Engineering Department, Malaviya National Institute of Technology Jaipur for his efforts in the modification and fabrication of the experimental set-up. I am thankful to **Mr. Rakesh Baghel, Miss Priya Pal** Research Scholar, and **Miss Khushboo Jagetita, Mr. Vaibhav Dhyani**, M.Tech Scholar, Chemical Engineering Department, also thankful to **Dr. Vipin Pal** and **Mr. Ashish Tyagi**MNIT Jaipur, for their support in thesis writing.

Last but not the least I am greatly thankful to my entire family, especially my father **Shri Rajpal Singh**, my mother **Smt. Rajrani Singh,** truly supportive and understanding my elder brothers, **Shri Pooran Singh, Shri Preetam Singh and Shri Dharmendra Singh**. I would also like to say special thanks to **Mrs. Vibha Upadhyaya and Miss Shweta Sumrai** for her moral support.

(Jitendra Kumar Singh)

(2011RCH7107)

ABSTRACT

The design of experiment (DOE) and ANOVA for determining the suitable parameters, membrane suitability and percentage contribution of operating parameters over response like permeate flux, salt rejection and specific energy consumption for two different type of membranes (PTFE & PVDF) of same pore size and different pore sizes have been done. The effect of various operating parameters like feed temperature, feed flow rate, feed concentration & membrane based parameters like pore diameter, membrane materials on permeate flux, salt rejection & energy consumption for VMD has been studied at constant permeate pressure of 9.0kPa. The effect of operating time was also observed and the membrane scaling /fouling has been studied using scanning electron microscope (SEM) technique. The heat transfer correlation has been developed for vacuum membrane distillation. Also, the ANN model has been developed using MATLAB. The vacuum membrane distillation has been compared with RO in terms of specific energy consumption and percent recovery. The mathematical model for recovery has been validated with the experimental recovery. From Taguchi optimization it is observed for the 0.22 µm PTFE & PVDF membranes, suitable feed temperature 65°C, feed flow rate 10 lpm, feed salt concentration 5000 ppm and for 0.45 µm PTFE and PVDF membranes, suitable feed temperature 65°C, feed flow rate 6 lpm and 4 lpm respectively, feed concentration of 5000 ppm was obtained from Taguchi analysis results for getting higher permeate flux & salt rejection with minimum specific energy consumption. The permeate flux increased linearly from 77 kg/m^2.hr to 98 kg/m^2.hr for 0.22 µm PTFE and from 78 kg/m^2.hr to 99 kg/m^2.hr for 0.22 µm PVDF membranes. Similarly for 0.45 µm PTFE & PVDF membranes, the flux increased from 134 kg/m^2.hr to 178 kg/m^2.hr and 318 kg/m^2.hr to 430 kg/m^2.hr, upon increasing of feed flow rate from 1 to 10 lpm at feed bulk inlet temperature of 65 °C, feed salt concentration of 5 g/l and permeate pressure of 9 kPa.

The gradual increment was found in permeate flux from 18.2 kg/m^2.hr to 98 kg/m^2.hr for 0.22µm PTFE and from 19 kg/m^2.hr to 99 kg/m^2.hr for 0.22 µm PVDF membranes. Similarly for 0.45µm PTFE & PVDF membranes, the flux increased from 44 kg/m^2.hr to 178 kg/m^2.hr and 205 kg/m^2.hr to 430 kg/m^2.hr, on increasing the feed bulk temperature from 45°C to 65°C, at feed flow rate of 10 lpm, feed salt concentration of 5000 ppm under 9.0 kPa of permeate pressure. The linear decrease in permeate flux was observed from 98.04 kg/m^2.hr to 84.24 kg/m^2.hr for 0.22 µm PTFE and from 98.93 kg/m^2.hr to 63.57 kg/m^2.hr for 0.22 µm PVDF membranes. Similarly for 0.45 µm PTFE & PVDF membranes, the flux decreased from 78.30

kg/m^2.hr to 155.62 kg/m^2.hr and 430.20 kg/m^2.hr to 389.66 kg/m^2.hr, on increasing the feed inlet salt concentration from 5000 ppm to 50,000 ppm at feed flow rate of 10 lpm, feed bulk inlet temperature of 65 °C under 9.0 kPa of permeate pressure.The salt rejection decreased from 99.9% to 99.5% for 0.22 µm PTFE and from 99.1% to 98.0% for 0.22 µm PVDF membranes. Similarly, for 0.45 µm PTFE & PVDF membranes, the salt rejection decreased from 99.5% to 78.13% and 99.1% to 16.15%, on increasing the feed flow rate, feed inlet temperature, and feed salt concentration from 1 to 10 lpm, 45 to 65 ºC, 5000 to 50000 ppm respectively. The linear decrement in specific energy consumption was found from 10.2 to 6.5 kWh/kg for 0.22 µm PTFE and from 8.4 to 4.4 kWh/kg for0.22 µm PVDF membranes, on increasing the feed flow rate from 1 to 10 lpm.

The specific energy consumption decreased linearly from 20.7 to 8.95 kWh/kg for 0.22 µm PTFE and from 18.65 to 4.4 kWh/kg for 0.22 µm PVDF membranes, on increasing the feed bulk temperature from 45°C to 65°C. The linear increase in specific energy consumption was observed from 6.5 kWh/kg to 12.2 kWh/kg for 0.22 µm PTFE and from 4.4 kWh/kg to 10.1 kWh/kg for 0.45 µm PVDF membranes, on increasing the feed salt concentration from 5,000 to 50,000 ppm.The decline in permeate flux was observed as 1.7% & 4.0 % for 0.22 µm PTFE membrane and 4.0 % & 9.0 % for 0.22 µm PVDF membrane in 200 hrs and 340 hrs continuous run respectively. Similarly the decline in permeate flux was observed for 0.45 µm PTFE & PVDF membranes, 2.6 % & 7.2% and 6.3% & 12.5% respectively in 200hrs and 340 hrs continuous run. This minor scale deposition is also evident from pore size distribution (PSD) which indicated that average pore size in PSD curve shifted from 0.22 µm to 0.18 µm and this little problem was very easily overcome by water washing.The experimental recovery was found to be 81% at 52 hr. Heat transfer correlation was obtained as $Nu= 0.158\ Re^{0.854}\ Pr^{0.33}$ under 9kPa permeate pressure at varied feed flow rate and temperature. The developed ANN model was found in good agreement with experimental results as compared to Upadhyaya et al. (2015) mathematical model. The percentage increment in specific energy consumption for VMD was found to be less as compared to RO and percentage recovery was observed higher in VMD than RO.

Contents

LIST OF FIGURES

LIST OF TABLES

LIST OF NOTATIONS

C_F	Sodium Chloride (NaCl) salt Concentration in Feed Tank
C_P	Sodium Chloride (NaCl) salt Concentration in Permeate
C_R	Sodium Chloride (NaCl) salt Concentration in Retentate
d	Membrane Pore Diameter(m)
D_{AB}	Diffusivity of A in B (m^2/s), where A is water vapour, and B is air
ΔC	Concentration Difference Across the Membrane
ΔH	Latent Heat ofVaporization of Water, J/kmol
ΔP	Pressure Difference across the Membrane
h_m	Membrane Heat Transfer Coefficient ($W/m^2 \cdot K$)
h_p	Permeate Side Heat Transfer Coefficient ($W/m^2 \cdot K$)
h_f	Feed Side Heat Transfer Coefficient ($W/m^2 \cdot K$)
K_f	Mass Transfer Coefficient (m/s)
$k_f^{'}$	Mass Transfer Coefficient (s/m)
K_n	Knudsen Number
M	Molecular Weight of Water (kg/kmol)
N	Total Trans – Membrane Flux ($kmol/m^2 \cdot h$)
$N_{A,M\text{-}K\text{-}P}$	Total Trans – Membrane Flux ($kmol/m^2 \cdot s$)
$N_{A,P}$	Flux Due to Poiseuille Flow ($kmol/m^2 \cdot s$)
$N_{A,K}$	Knudsen Diffusion ($kmol/m^2 \cdot s$)
$N_{A,M}$	Molecular Diffusion ($kmol/m^2 \cdot s$)
P_{pm}	Permeate Side Membrane Pressure (kPa)
P_{fm}	Feed Side Membrane Pressure (kPa)
R	Universal Gas Constant ($J/kmol \cdot K$)
r	Membrane Pore Radius (m)
T_f	Feed Bulk Temperature (K)
T_{fm}	Feed Side Membrane SurfaceTemperature (K)
T_{pm}	Permeate Side Membrane Surface Temperature (K)
V	Feed Volume in Feed Tank
V_m	Feed Section Volume of Membrane Module
y_A	Mole Fraction of Water Vapour

Greek Letters

δ	Membrane Thickness (m)
ε	Membrane Porosity
λ_{PTFE}	Thermal Conductivity of PTFE Membrane (W/m·K)
λ_{air}	Thermal Conductivity of Water Vapour (W/m·K)
η	Viscosity of Water Vapour (kg/m·s)
τ	Membrane Tortuosity

LIST OF PUBLICATIONS

List of Research Papers Published in Refereed Journals

1. ***Jitendra Kumar Singh***, Sushant Upadhyaya, and S.P. Chaurasia, "Application of vacuum membrane distillation for removal of fluoride", International journal of chemistry and chemical engineering ISSN 2248-9924, volume 3, number 3, pp 209-214 (2013).
2. ***Jitendra Kumar Singh***, Sushant Upadhyaya, S.P. Chaurasia, and Rakesh Baghel, "Process Optimization and Energy Consumption Study on Vacuum Membrane Distillation for Desalination"Journal of desalination published by Elsevier (Communicated).

List of Papers Presented/Published in International Conferences Proceedings

1. ***Jitendra Kumar Singh***, Sushant Upadhyaya, and S.P. Chaurasia, "Energy Consumption study for PTFE and PVDF membrane in Vacuum Membrane Distillation for Desalination" International Conference on Desalination for the Environment: Clean Water and Energy, Organised by Elsevier at Marriott Park Hotel, Rome, Italy, 22–26 May 2016.
2. ***Jitendra Kumar Singh***, Sushant Upadhyaya, S.P. Chaurasia, and Rakesh Baghel, "Energy Consumption Study on Vacuum Membrane Distillation for Desalination", in International conference on Clean India Technology- Role of Desalination and Water Purification (InDA-APDA Conference 2016) Organised by Indian Desalination Association, Chennai India, February 11, 12, 13-2016.
3. ***Jitendra Kumar Singh***, Sushant Upadhyaya, and S.P. Chaurasia, "Effects of operating parameters on energy consumption and permeate flux in vacuum membrane distillation for desalination", in "CHEMCON-2015", the 68th Annual Session of Indian Institute of Chemical Engineers, IIT Guwahati , 27-30 December.
4. ***Jitendra Kumar Singh***, Sushant Upadhyaya and S.P. Chaurasia, "Experimental study on water desalination by vacuum membrane distillation", International conference,"CHEMCON-2014", the 67th Annual Session of the Indian Institute of Chemical Engineers, organized by Chandigarh Regional Center Indian Institute of Chemical Engineers and Dr. S. S. Bhatnagar University Institute of Chemical Engineering & Technology, Panjab University Chandigarh.
5. ***Jitendra Kumar Singh***, Sushant Upadhyaya, and S.P. Chaurasia, "Application of vacuum membrane distillation for removal of fluoride", International conference on Chemical, Environmental and Bioprocess Engineering, JNU Delhi, Organized by Krishi Sanskrit Dec. 21 - 22, 2013.

6. ***Jitendra Singh,*** Sushant Upadhyaya and S.P. Chaurasia, "Studies on separation of NaCl from water by vacuum membrane distillation", International conference on water desalination treatment and management Organised by MNIT Jaipur and Indian Desalination Annual Congress (InDACON-13) Jaipur Feb. 21-22, 2013.

7. ***Jitendra Singh***, Sushant Upadhyaya and S. P. Chaurasia, "Separation of ethanol-water azeotropic mixture by vacuum membrane distillation", International conference on sustainable technologies for energy and environment in process industries and Indo-US joint international conference on energy and environment organized by IIChE Doaba Regional Centre and Department of Chemical Engineering, NIT Jalandhar, Punjab.

List of Papers Presented/Published in National Conferences Proceedings

1. ***Jitendra Kumar Singh***, Sushant Upadhyaya,S.P. Chaurasia, "Energy Consumption Study for PVDF membrane in vacuum membrane distillation for desalination"4th Rajasthan Science Congress at JK Lakshmipat University Jaipur, Rajasthan,October 15-17,2016.

2. ***Jitendra Singh***, S.P. Chaurasia, Sushant Upadhyaya and Rajeev Kumar Dohare, "Studies on Separation of Multi-Ions by Membrane Distillation" presented in National Conference on Water Quality Management Organised by MNIT Jaipur and CCDU & PHED Rajasthan at Jaipur, Rajasthan (India) Dec. 20-22, 2012.

List of Allied Papers

International Journal Publication (04)

1. Alka Dubey, Jyoti Jain, ***Jitendra Singh***, Potential of membrane bioreactors in ethanol and biogas production a review, International journal of chemistry and chemical engineering ISSN 2248-9924, volume 3, number 3, pp 131-138 (2013).

2. Jain Jyoti, Dubey Alka, ***Singh Jitendra Kumar***, Application of membrane bio reactor in waste water treatment a review, International journal of chemistry and chemical engineering ISSN 2248-9924, volume 3, number 2, pp 115-122 (2013).

3. Vijay Shankar Gautam, ***Jitendra Singh***, S.P. Chaurasia, Nitrate removal by vacuum membrane distillation from water, International journal of environmental research and development ISSN No.2249-3131, volume 3, number 7, pp 5-8, (2013).

4. Upadhyaya Sushant, Chaurasia S.P., Singh Kailash, ***Singh Jitendra***, Desalination of water by vacuum membrane distillation for sustainable development, International journal of environmental engineering and management ISSN 2231-1319, volume 3(3), pp 349-352, (2012).

National Journal Publication (01)

1. Jyoti Jain, ***Jitendra Kumar Singh***, S. P. Chaurasia, "Experimental analysis of process parameters on energy consumption for nitrate removal from water using VMD", Journal of energy research and environmental technology, ISSN: 2394-1561, volume 1, number 1, pp 38-42 (2014).

International Conference Publication (12)

1. Sushant Upadhyaya, Kailash Singh, ***Jitendra Singh***, Rakesh Baghel, & S.P. Chaurasia, "Artificial Neural Network Modeling of Vacuum Membrane Distillation for Desalination" International Conference on Desalination for the Environment: Clean Water and Energy, Organised by Elsevier at Marriott Park Hotel, Rome, Italy, 22–26 May 2016 (accepted).
2. Vaibhav Dhyani, ***Jitendra K. Singh***, Priya Pal and S. P. Chaurasia, "Desalination by vacuum membrane distillation: Application of Taguchi method", Proceedings of 5th International Symposium on Fusion of Science and Technology, Organized by National Agriculture Science Center, Pusa, New Delhi, India, January 18-22,2016 (Paper ID: 2016-ISFT-299).
3. Sushant Upadhayaya, Kailash Singh, S. P. Chaurasia, and ***Jitendra Kumar Singh***, "Robust design optimization of vacuum membrane distillation for desalination", 2nd International conference on desalination using membrane technology, organized by Elsevier at Nanyang Technological University, Singapore Expo Convention and Exhibition Centre, 26 - 29 July 2015.
4. Swati Dubey, Sushant Upadhyaya, ***Jitendra Kumar Singh*** and S. P. Chaurasia, "Treatment of textile wastewater containing methylene blue dye by vacuum membrane distillation", International conference, "CHEMCON 2014", the 67th Annual session of the Indian Institute of Chemical Engineers, organized by Chandigarh Regional Center Indian Institute of chemical Engineers and Dr. S. S. Bhatnagar University Institute of Chemical Engineering & Technology, Panjab University Chandigarh.
5. Jyoti Jain, ***Jitendra Singh***, Sushant Upadhyaya, and S. P. Chaurasia, "Experimental Analysis of process parameters on energy consumption for nitrate removal from water using VMD", International conference, "CHEMCON 2014", the 67th Annual session of the Indian Institute of Chemical Engineers, organized by Chandigarh Regional Center Indian Institute of chemical Engineers and Dr. S. S. Bhatnagar University Institute of Chemical Engineering & Technology, Panjab University Chandigarh.
6. Jyoti Jain, ***Jitendra Kumar Singh***, Sushant Upadhyaya, S. P. Chaurasia, "Application of vacuum membrane distillation for Nitrate removal", International conference on innovative

technology and management for water security organized by NIOT Chennai and InDACON-2014.

7. Jain Jyoti, Dubey Alka, ***Singh Jitendra Kumar***, "Application of membrane bio reactor in waste water treatment a review", International conference on Chemical, Environmental and Bioprocess Engineering, JNU Delhi, Organized by Krishi Sanskrit Dec. 21 -22, 2013.

8. Alka Dubey, Jyoti Jain, ***Jitendra Singh***, "Potential of membrane bioreactors in ethanol and biogas production a review", International conference on Chemical, Environmental and Bioprocess Engineering, JNU Delhi, Organized by Krishi Sanskrit Dec. 21 -22, 2013.

9. Sushant Upadhyaya, S.P. Chaurasia, K. Singh and ***Jitendra Singh***, "Heat transfer correlation using computational fluid dynamics for desalination by vacuum membrane distillation" International conference on sustainable technologies for energy and environment in process industries and Indo-US Joint International conference on energy and environment organized by IIChE Doaba Regional Centre and Department of Chemical Engineering, NIT Jalandhar, Punjab.

10. Akhilesh Kushwaha, V. Gautam, ***Jitendra Singh***, Sushant Upadhyaya and S.P. Chaurasia, "Studies on Boron removal for desalination applications by reverse osmosis membrane" International conference on water desalination treatment and management Organised by MNIT Jaipur and Indian Desalination Annual Congress (InDACON-13) at Jaipur, Feb. 21-22, 2013.

11. Vijay Shankar Gautam, Akhilesh Kushwaha, ***Jitendra Singh, Sushant*** Upadhyaya and S. P. Chaurasia, "Nitrate removal by polyamide RO membrane and effect of di-hydrogen phosphate ions on its removal", International conference on water desalination treatment and management Organised by MNIT Jaipur and Indian Desalination Annual Congress (InDACON-13) at Jaipur, Feb. 21-22, 2013.

12. Vijay Shankar Gautam, ***Jitendra Singh***, S. P. Chaurasia, "Nitrate removal by vacuum membrane distillation from water", International conference on Sustainable Innovative Techniques in Civil and Environmental Engineering by Krishi Sanskriti at J.N.U. New Delhi, 5th & 6th June 2013.

National Conference Publication (03)

1. Alka Dubey, Jyoti Jain, ***Jitendra Kumar Singh***, S. P. Chaurasia, "An experimental study on effect of operating parameters on flux for ethanol water separation using vacuum membrane distillation (VMD)" presented in the National conference on Innovation and Development in Chemical Technology (IDCT-2014) Feb 28 - March 1, 2014 organized by University School of Chemical Technology, Guru Gobind Singh Indraprastha University, Dwarka, New Delhi.

2. Jyoti Jain, ***Jitendra Kumar Singh***, Sushant Upadhyaya, S. P. Chaurasia, "Study of Process Parameters for Nitrate Removal by Vacuum Membrane Distillation" presented in the National conference on Innovation and Development in Chemical Technology (IDCT-2014) Feb 28 - March 1, 2014 organized by University School of Chemical Technology, Guru Gobind Singh Indraprastha University, Dwarka, New Delhi.
3. Upadhyaya Sushant, Chaurasia S.P., Singh Kailash, ***Singh Jitendra***, Desalination of water by vacuum membrane distillation for sustainable development, National conference on emerging trends in engineering, technology & science for sustainable development-2012, organized by Krishi Sanskriti at J.N.U. New Delhi.

CHAPTER 1. INTRODUCTION

While the demand for pure water is enhancing in the economic and social sectors, there is a tremendous decline in its availability. Meeting the safe water requirements in the urban and rural area is a major challenge in our country. Multi-ions are observed beyond the permissible limit in 90% of the available groundwater which is alarming for the treatment method for producing safe drinking water. Total water reservoir comprises in the world in the form of salty water and fresh water. Moreover, the percentage of saline water is found to be 97% and that of fresh water is 3%. Latter fresh water is available in the form of glaciers. North poles, south poles, and icecaps. However, the proper usage of this water is cumbersome, only 0.5% of the fresh water available in the form of ground water can be used by the human being for their drinking purpose. However, deterioration in groundwater was observed due to the increases in population and demand. Therefore, the planet will be suffering more in terms of ground water and surface water availability in near future.

However, water pollution continuously increases the atmosphere, so it's needed to rework against water supply problem with the help of some new technologies adopted by the industry. While desalination is also an effective approach. Many processes adapted for resolving these problem out of which membrane distillation (MD) is a novel process as it provides effective result in somewhat content. Membrane distillation is getting help to desalination to get pure drinking water with minimum energy requirement with the future content by 2030. 60% of world population faces serious water shortage and expected for future that 90% of water are causes of diseases. So required pure water and it's very important to sustain life in better way.

The Salinity of sea represent the saltiness, salinity is represented in terms of per mile. It's defined as gram salt dissolved ina kilogram of solution. The term saline represents the quantity of dissolved solid. The total dissolved solids present in the fresh water, brackish, saline, and brine water are less than one gram per liter, one to twenty gram per liter, twenty to fifty gram per liter and more than fifty gram per liter respectively. Salinity is expressed in milligram per liter or parts per million for chemical analysis of the solution. In past era around 1978 salinity word refer for chlorine amount dissolved in water. In other way salinity also defined as the ratio of the conductivity of sea water sample to the standard solution potassium chloride solution. The practical salinity scale is dimensionless and abbreviated as PSU.

Desalination technologies have been accepted as the elemental approach of producing ample water provisions and the usage as well as the ability of desalination technologies development estimate of around four percentage yearly (U.S. Bureau of Reclamation 2003). As a result of this sense, industries have engaged the desalination approach to producing potable and safe water from saline water. Assorted technologies such as membrane, thermal and recycling, reuse technologies are applicable for desalination and purification of briny water. The concept of all technologies is saline water convert into potable water. Any desalination and purification technologies having two output streams viz; the first one is permeate (product) and second is stream and retentate (brine or concentrated) stream.

Several technologies have been considered for the desalination of water and segregation of salts. In the research field, the most frequently using technology is reverse osmosis as compared to other techniques such as thermal technologies and evaporation(Kurbiela and Rybicki 1996). The major demerits of the reverse osmosis processes is extremely high pressure requirement at high solute concentration specifically in the case of highly briny industrial water (Mariah 2006). In the reverse osmosis processes the high pressure is required to break the osmotic pressure barrier in concentrate processing. While in the thermal evaporation, the high temperature must be required to achieve evaporation and recovery of salts.

Membrane distillation is relatively a new competitor of the membrane depending separation processes. Membrane distillation is first of the forthcoming non-isothermal membrane separation processes to appreciate for coming about 50 years. The advantage of the membrane distillation is to approximately an entire water recovery. Membrane Distillation is a thermal driven transport process of vapor through hydrophobic membranes, the essential driving force involved in Membrane distillation is the trans-membrane pressure difference. In the other membrane separation processes, the essential active force is the difference in chemical potential across the membrane (Khayet et al. 2011). The different configurations of membrane distillation are direct contact membrane distillation, sweeping gas membrane distillation, air gap membrane distillation and vacuum membrane distillation. These have been enormously used for numerous application like desalination, water reuse, food processing industry, medical, etc. the essential driving force is trans-membrane pressure difference generate a flux of water vapor through the membrane, and the aqueous brine solutions may be crystallized and concentrated. This operation may be used for high solute concentration at feed side, modest temperature, at small concentration gradients and atmospheric pressure (Mariah et al. 2006).

These are the following advantages of vacuum membrane distillation as compared to other famous technologies are hundred percent elimination of ions, colloids, macromolecules, and other non-volatile component at minimal performing pressure as compared to other pressure driven membrane separation processes, less performing temperature as compared to the distillation processes, lower vapour pressure in contrast to traditional distillation processes.Vacuum membrane distillation conflict with another membrane technologies in that the propulsive force for desalination is the difference in vapor pressure of water across the membrane, rather than total pressure. Vacuum membrane distillation process is trusted to be active in the field of desalination, concentration of an aqueous solution. Vacuum membrane distillation process is an arriving technology for desalination. It is not only the cost-effective process but also utilization of low-grade waste energy and renewable energy sources such as geothermal and solar energy. Countless theoreticians and researchers worldwide have been studied about the vacuum membrane distillation process. Today, vacuum membrane distillation process is considered as a promising substitute to many other conventional separation techniques. A membrane may be prepared from chemical antagonistic polymers such as poly-tetra-fluoro-ethylene (PTFE), Poly-vinylidene-fluoride (PVDF) and Polypropylene(Lawson and Lloyd 1997). A micro porous membrane for membrane distillation is basically identify by the following parameters such as: thickness of the membrane δ (m), porosity of the membrane ε (it is define as the porous volume fraction relative to the total volume of the membrane), tortuosity of the membrane τ (it is define as the ratio of pore length to membrane thickness), pore diameter of the membrane pore d (m). The membrane synthesis methods play a vital role in finding the surface porosity. In the present scenario, the porosity of the membrane as high as 90% and also commercially available (Cath et al. 2004). In the vacuum membrane distillation process, the membranes must be good thermal stability at higher temperature as 100 ºC; membrane matrix also must have very low thermal conductivity; the pore size distribution must be narrow in the membrane; membrane permeability must be high, and also high chemically resistance to several types of mixture/solutions, and its liquid entry pressure must be high to sustain water from entering the membrane pore. The membrane pore size varies from 100 nm to 1 µm; on increasing the pore diameter of the membrane the vacuum membrane distillation flux increases rapidly. For the calculation the trans-membrane flux the tortuosity factor may be taken as two (Bandini et al. 1997; Lawson and Lloyd 1997). As an evidence, the trans-membrane flux must be directly proportional to the opposite of the tortuosity and thickness of the membrane (Pangarkar et al. 2010b). From the vacuum, membrane distillation experiments measured the heat transfer

coefficient at the boundary layer for developing the empirical constants in the Dittus-Boelter equation. By using the gas dusty model for finding the vacuum membrane distillation flux.The dusty gas model does not explain the molecular diffusion. and also the flow over the non-porous passage of the membrane was not expected in this model in spite of great communication between the membrane material and components present in the mixture to be separated (Khayet et al. 2004).

The production of potable /distilled water from briny or brackish water and for the brine concentration (Li et al. 2003; Li and Sirkar 2005; Safavi and Mohammadi 2009). In between the topmost stated vacuum membrane distillation flux was near 70 kg/m2hr while treatment of one weight percent NaCl aqueous feed solution at a feed bulk temperature of 80 °C, at a constant downstream pressure of 8kPa using the modified polly propylene MXFR3 membrane.

In the present work, stress has been given on effects of operating conditions on permeate flux salt rejection as well as energy consumption. The Taguchi optimization was carried to identify the suitable operating and membrane parameters for getting the higher permeate flux, high rejection of salt and minimum energy requirement. The main task of this research work is find out the suitable operating conditions for better performance of VMD and also with best available model and compare the VMD performance with RO in terms of energy consumption and recovery.

1.1 Salient points of study in present work:

a) To find out the effect of the process operating parameters such as inlet temperature, salt concentration and flow rate on the permeate flux, rejection of salt and specific energy consumption for Polly-tetra-fluoro-ethylene (PTFE) and Polly-vinylidene-fluoride (PVDF) membranes.
b) To find out the response of the membrane parameters such as membrane pore diameter and membrane material on the rejection of salt, flux, and specific energy consumption.
c) To development the heat transfer correlation for the vacuum membrane distillation.
d) The study about the optimization of the operating parameters by Taguchi and analysis of variance for finding the suitable parameters for getting higher permeate flux & rejection with minimal energy requirements.
e) The study of the prediction of flux by ANN and validation of the experimental flux with Upadhyaya (2015) model.

f) Comparison of Reverse Osmosis and Vacuum Membrane distillation processon the basis of energy consumption and recovery.

1.2 **Organization of the present works**

The present research works explains into fivesections as follows:

Chapter number 1: Contains the introduction to membrane distillation process, research work and the scope of this work is merged together for desalination.

Chapter number 2: Summary of the appropriate literature review and sketch of essential concept compulsory for desalination by vacuum membrane distillation process and aim of the present research work.

Chapter number 3: Represents the details of the raw materials for experiments and operating procedure for vacuum membrane distillation experimental setup.

Chapter number 4: Represents all the results and their subsequent analysis about the dissimilar learnings carried out in the present research work.

Chapter number 5: contains the summary of the all findings in the present research work as conclusions and recommendations for future work.

The references and appendices have been provided at the end of the thesis.

CHAPTER 2. LITERATURE REVIEW

The production of the fresh water from salt water by using the desalination technology as a commercial level in the industries, rural and urban areas(Mariah 2006). Desalination comes in the categories of the membrane distillation processes and thermal desalination. The feed water is heated up to its boiling point for formation of water vapors in the thermal technique, while in the membrane distillation the fresh water production is done by transport of either water or salt through a permeable membrane because of the concentration difference in between the two sides

In the 1960s artificial membrane were used in separation processes, but they playing an increasingly vital role in the water desalination by 1980s(Shatat et al. 2012). The municipal water treatment basically membrane technologies were narrow such as micro filtration and desalination, while after the development of new membrane modules, its utilization has expanded not only to the water industry but also more return processes such as enzyme concentration, chemical segregation, and beverage distillation. The desalination technology uses a permeable membrane to move either water or salt to activate two zones of different concentrations to making potable water. The sizes of the body, molecules, ions and suspended particles which are blocked or granted to pass through membranes, is distinction between the several processes in membrane technology.The pre-treatment phase of desalination to eliminate large particles, ions, bacteria, and water softening is done by ordinary separation processes like ultrafiltration, microfiltration, and nanofiltration.The details of the diversified membrane desalination processes are presented as below(Shatat et al. 2012).

2.1 Reverse Osmosis (RO)

Theapproaches of “reverse osmosis” and “osmosis” have been accepted for long time. In evidence, studies on osmosis were borne as early as 1748 by the scientist Nollet, and countless researchers explored this development over the next two centuries(Reid 1966; Jianhui et al. 1991).The reverse osmosis is used as attainable separation process as compared to others, this is relatively young technology.In actually that only in the later stage of 1950's did the task of Reid show the cellulose acetate reverse osmosis membranes were efficient of severing salt from water, although the water fluxes attained were too cramped to practical (Reid and Breton 1959; Ferguson 1980; Lonsdale 1982).Loeb and Sourirajan in the 1960's

grown an approach for preparation asymmetric cellulose acetate membranes with comparatively more water fluxes and separations, thus building reverse osmosis separations both achievable and practical(S Loeb 1962; Loeb 1981).

Since then, the development of new-generation membranes such as the thin-film, composite membrane that can tolerate wide pH ranges, higher temperatures, and harsh chemical environments and that have highly improved water flux and solute separation characteristics has resulted in many RO applications. In addition to the traditional seawater and brackish water desalination processes, RO membranes have found uses in wastewater treatment, production of ultrapure water, water softening, and food processing as well as many others(Bhattacharyya and Williams 1992).

The driving force for the development and use of RO membranes is the advantages that these have over traditional separation processes such as distillation, extraction, ion exchange, and adsorption. Reverse osmosis is a pressure-driven process so no energy-intensive phase changes or potentially expensive solvents or adsorbents are needed for RO separations. Reverse osmosis is a process that is inherently simple to design and operate compared to many traditional separation processes. Also, simultaneous separation and concentration of both inorganic and organic compounds is possible with the RO process. In addition, with nanofiltration membranes selective solute separations based on charge and molecular weight/size differences are possible. Finally, reverse osmosis technology can also be combined with ultrafiltration, pervaporation, distillation, and other separation techniques to produce hybrid processes that result in highly efficient and selective separations (Bhattacharyya and Williams 1992).

The RO process is comparatively new in correlation to other technologies, and was introduced as a successfully commercialized technology in desalination industry in the early 1970s(Shatat et al. 2012). Reverse osmosis is a method for desalting water by passing feed solution to membranes that are permeable to water but non-permeable to salt without the needing any heating or phase change. The pressurized saline water passes by pumping to the feed side of the membrane and water with negligible salt comes out at low pressure as permeate to the downstream side. The membrane property of rejecting tiny solutes from water was known to mankind since a very long time. The osmotic phenomenon for ceramic membrane was investigated in starting of the 1850s by Traube and Pfeffer. The process of desalting of water was patented in 1931, and this method was termed as RO(Horvath et al.

1931). The same process was studied for better outcome by Reid and Breton (1959), using cellulose acetate films with thickness ranges from 5-20 µm. Low fluxes were obtained by this membrane but by pressurizing the feed solution up to 1000 psi, the salt rejection in the permeate was more than 98% (Khedr 2003).An astonishing development in the field of RO, converting the process into the practical zone was made by Loeb–Sourirajan employing cellulose acetate membranes of anisotropic morphology. This anisotropic membrane produced flux ten times greater than that obtained by Reid and Breton giving the same level of rejection(S Loeb 1962). This development strengthened the practical process to a great extent and after few years later a demonstration set up was installed. First, plate and frame and then tubular type membrane modules were developed for application in RO and in due time the development of spiral wound membrane modules came in the account by meticulous designing practice(Bray 1968; Westmoreland Julius C 1968).

In 1975, the composite membranes were used for desalination, and it was observed that by using these membranes, high level salt rejections as well as better transmembrane fluxes were obtained. For the production of ultra-pure water, plants were installed in Japan, Europe, and the United States, as well as huge desalination plants for conversion of brackish ground water and sea water into municipal drinking water, were installed in the desert regions and the Middle East.

2.1.1. Reverse Osmosis working principle

In this process, an external pressure greater than the osmotic pressure is applied, so that the flow of water takes place from the salt solution to the fresh water. The process called as reverse osmosis because this type of flow is reverse flow.

For 5000 to 50000 ppm salt concentration, operating pressure in the range of 14-68 bar have been reported. Operating pressure in the range of 6-14 bar has been reported, for low salt concentration (150-5000 ppm). Because of low temperature (generally an ambient temperature), less corrosion in RO process has been reported. High selectivity, the large variety of polymeric membranes availability, fewer corrosion problems compared to MED and MSF. The disadvantages include low water recovery, scaling and biological fouling of membranes and the high-pressure need at high salt concentrations.

2.1.2. Problems Associated in Desalination by RO

The noticeable problem associated with desalination of water by RO is membrane scaling that highly increases during the presence of high salt concentration content in feed solution, such as sea water. The precipitation of minerals from the feed stream on the membrane surface is termed as scaling (Vrouwenvelder et al. 1998). The hard salts ($CaSO_4$) and its derivatives, and also soft salt ($CaCO_3$), are responsible components for membrane scaling (van de Lisdonk et al. 2000).The solubility of hard salts is inversely proportional to the temperature, at high temperatures. Because of this reason the deposition of non-alkaline hard salts increases with temperature.

The concentration of dissolved salts in retentate stream increases with the course of time,in RO process for the production of fresh water. There is deposition of salts layer as precipitates on the membrane surface, as a result. These depositions are responsible for huge scaling on the surface of the membrane and cause a scaling phenomenon that hinders the overall operation of RO setup and reduces its potential by half(Ohya et al. 2001).Membrane fouling on the surface of RO membrane is another major problem encountered. Fouling takes place because of high concentration of the electrolytes in feed solution and presence of certain impurities, micro-organisms, and macro particles.

High pressure is needed for removing the high TDS levels from the source water. This high-pressure requirement may cause economic unbalance. High osmotic pressure is created by high concentration of salts in feed solution. The external pressure should be higher than the osmotic pressure, to perform the RO process (Mariah 2006) to maintain the effective driving force or the pressure difference for better transport.

2.1.3. Remedies for Scaling and Fouling Problems in RO Process

Following methods can be used to overcome the membrane scaling problems:
Acid can be added to the feed for partial conversion of bicarbonates into sulfate and conversion to carbon dioxide, for reducing the scaling of calcium carbonate.Anti-scaling agents can be used to retard the growth of scale and thus reduce the scale formation. To prevent scaling, the anti-scaling agents like sodium-hexa-meta phosphate may be useful. Reduction of operating pressure may also help in reducing the scaling phenomena since it reduces the overall recovery and hence minimizes the salt deposition.Feed stream can be pre-treated before sending it to the RO system. Pre-treatment can be done using soda ash or lime.

Adding them may help in the precipitation of carbonates as calcium carbonate. Membrane scaling reduces to some extent, as a result.For minimizing the fouling on the membrane surface, it is better to pre-treat the feed water before it enters the membrane module. The proper pre-treatment of the source water will help in preventing the salt precipitation and stop the growth of microbes on the membrane surface.

2.2 Nano Filtration Processes

The nanofiltration (NF) membrane is a kind of pressure-driven membrane which has its properties in between reverse osmosis (RO) and ultrafiltration (UF) membranes. NF offers many benefits such as less operation pressure, higher flux, and higher retention of multivalent-ion salts and of organic molecular above 300, comparatively low investment, and low cost of operation and maintenance. Because of these benefits, the application of NF worldwide have increased (Lu et al. 2002). The history of NF dates back to the 1970s when RO membranes with a reasonable water flux operating at relatively low pressures were developed. Therefore, the high pressures usually used in RO resulted in a considerable energy cost. Thus, membranes with lower rejections of dissolved components, but yielding high water permeability, would be a great improvement for separation technology. Such low-pressure RO membranes were later called, NF membranes (Bruggen and Vandecasteele 2003). By the second half of the 1980s, NF had become an established technology, and the first applications were reported (William J Conlon 1989; Schaep et al. 1998).

2.2.1. NF membranes in water treatments

In addition to having the capability to reducethe ionic strength of the solution, NF membranescan remove hardness, organics and particulatecontaminants. Many researchers have used NF toachieve those objectives and the followingsections highlight their major findings.

Ground water

The softening of ground water using NF hasbeen studied by many investigators (Watson and Hornburg 1989; Bergman 1995; Bergma 1996; Sombekke et al. 1997; Schaep et al. 1998). Schaep et al. (1998) used several different types of NF membranes for hardness removal. Retentions higher than 90% were found for multivalent ions, whereas monovalent ions were retained for about60–70%. Sombekke et al. (1997) compared NFmembranes with pellet softening and granularactivated carbon for softening water. Both methods gave good results;

however, NF membraneshave several advantages from the point of view ofhealth aspects and lower investment costs.Removal of natural organic matter (NOM) anddisinfection by-product (DBP) precursors werealso studied(P. Fu et al. 1994; Fu et al. 1995; Jacangelo et al. 1997; Alborzfar et al. 1998; Escobar et al. 2000; Everest and Malloy 2000; Khalik and Praptowidodo 2000; Gorenflo et al. 2002). Jacangelo et al. (1997) reportedthat both RO and NF are used in the US forremoval of NOM. To date, NF has been employed primarily for groundwater containingrelatively low total dissolved solids but with hightotal hardness, color, and DBP precursors. Escobar et al. (2000) found that the rejection of assailable organic carbon was greater than 90% atpH 7.5 and greater than 75% at pH 5.5 by usingTFC-S NF membranes.

The removal of pesticides and some micro pollutants from ground water has been studied bymany researchers (Montovay et al. 1996; Berg et al. 1997; Bruggen et al. 1998; Wittmann et al. 1998; Ducom and Cabassud 1999; Kiso et al. 2000; Bruggen et al. 2001; Kiso et al. 2002). Bruggen et al. (1998) showed that the NF70 membrane can rejectpesticides such as atrazine, simazine, diuron andisoproturon over 90%. Similarly, removal oftrichloroethylene and tetra-chloro-ethylene can beachieved using several different types of NFmembranes (Ducom and Cabassud 1999).

Surface waters often have a changing chemistry or composition due to seasonal changes orafter dilution with rain. NF is a reliable option for surface water treatment, although the focus ishere rather on removal of organics than on softening (Bruggen and Vandecasteele 2003). Hardness removal from a lake in Taiwan has been studied by Yeh et al. (2000) using different methods such as a conventional processfollowed by ozone, GAC and pellet softening,and an integrated membrane process (UF/NF) andthe conventional process. Softening was achievedby all processes, but water produced by the membrane process had the best quality as measured byturbidity (0.03 NTU), total hardness rejection(90%), and dissolved organics rejection (75%).Removal of DBP precursors and NOM fromsurface water sources has been studied by manyinvestigators(Agbekodo et al. 1996; Ericsson et al. 1996; Visvanathan et al. 1998; Cho et al. 1999; Levine et al. 1999). Visvanathan et al. (1998)studied the effect of the presence of ions, operating pressure, feed, pH, and suspended solids onrejection properties, and concluded that higherpressure and suspended solids content increaserejection, while rejections are somewhat lower athigher ionic strength. Also, they conclude thatboth high and low pH of the feed water producelow rejection, while better

rejection has beenfound at a pH range of 7–9, which indicates thatpH adjustment of the feed may not be required.

2.2.2. NF as pre-treatment for desalination

Feed pretreatment is one of the major factors determining the success or failure of a desalination process. Different methods of pretreatment for desalination process were suggested by many researchers. Traditional pretreatment is based on mechanical treatment (media filters, cartridge filters) supported by extensive chemical treatment(Bruggen and Vandecasteele 2002). In the past, conventional pretreatment (i.e., coagulation, flocculation, acid treatment, pHadjustment, addition of anti-scalant and media filtration) was usually used(Sikora et al. 1989). The main problem in using conventional pretreatment is corrosion and corrosion products. For example, in the acid dosing system, corrosion of metallic surfaces and corrosion products will roughen the surface of the equipment, which provides active sites for precipitation of more scale deposits (Sikora et al. 1989; Al-Ahmad and Aleem 1993). In addition, this pretreatment is known to be complex, labor intensive and space consuming (Hoop et al. 2001).

2.3 Membrane Distillation

2.3.1 Introduction

Membrane distillation (MD) is a thermally driven desalination process that involves phase conversion from liquid to vapor on one side of the membrane and condensation of vapor to liquid on the other side(Lawson and Lloyd 1997). The exploitation of waste heat energy sources such as solar energy enables MD more promising separation technique for industrial scale. Growing economics and water scarcity are driving desalination as a solution for water supply problems. Membrane distillation in the application of water desalination makes this technology a prospective one in the research areas. The membrane facilitates the transport of water vapor through its pores but does not participate in the actual separation process. Membrane distillation can be employed in four different configurations namely DCMD, AGMD, VMD and Sweeping gas membrane distillation. Those of which DCMD and AGMD are best suited for the desalination applications where water is the major permeate component. These two configurations are applied to produce fresh water from a salt solution(Alklaibi and Lior 2004)

For the operations under the heading of Membrane Distillation (MD), a variety of terms such as membrane distillation, capillary distillation, trans-membrane distillation, etc. are used. The desired requirements for an MD process are:

i) The membrane must be porous.
ii) At least one side of the membrane must be kept in touch with the process liquid.
iii) Capillary condensation of vapor should not take place inside the membrane pores.
iv) For each component, the driving force in this operation is the partial pressure gradient of the vapor phase inside the pores.
v) The liquid should not wet the membrane.
vi) The membrane does not change the vapor-liquid equilibrium (VLE) of different component of the process liquid.

Both MD and conventional distillation process depend on the Vapor-Liquid equilibrium and both processes require that latent heat of vaporization in order to produce the vapor phase. However, the essential difference between these two processes is that in conventional distillation the liquid solution is needed to be heated up to boiling point, whereas this requirement is not present the case of MD. The MD can be well operated with the feed temperature less than its boiling point. Moreover, the components to be separated may have close boiling points or may from an azeotropic mixture. Hence, MD is a special case of distillation process (Zhang et al. 2015).

Membrane distillation is categorized under the heading of thermal separation process where vapor enters the hydrophobic micro-porous membranes. The liquid feed should be in direct contact to feed side of the membrane section even though the liquid is not transferred through the pores of the membranes. The hydrophobicity of the membrane creates a resistance for the liquid feed solutions, and does notallow it to pass through the pores of the membrane because ofsurface tension. Due to this, at interface vapor-liquid equilibrium is attained on the feed side of the porous membrane. The main driving force for MD is the trans-membrane vapor pressure difference (El-Bourawi et al. 2006).

MD is a novel method for desalination, and it is different from rest of the membrane technologies because of the driving force for desalination in MD is the difference of vapor pressure across the membrane, and not total pressure. Hydrophobic-micro-porous membranes are used for MD, which permit water vapor to pass through the membrane and not the liquid

water. The feed water is heated to increase its vapor pressure and thus establish a vapor pressure gradient. Many methods have been examined to build up the vapor pressure difference across the micro-porous hydrophobic membranes and in all cases, the hot saline feed water must be kept in direct contact with the membrane(Walton et al. 2000).

MD is betted as an alternative to many conventional separation techniques and it is considered asaneffective technique in the area of desalination and concentration of the aqueous solution.

2.3.2 Historical prospective

The first patent on membrane distillation (Lawson and Lloyd 1997) was filed byBodell in (1968), and the very first paper on MD was published in International Journal of Industrial and Engineering Chemistry Process Design Development, authored by Findley (M.E.Findley 1967) after mere four years of Bodell's patent. In this paper, Findley highlighted the ideal properties of membrane needed for MD process in order to improve the economic reception, through experimental calculation at enhanced temperature. He used many membranes types, such as cellophane, wood, paper plate, nylon, aluminum foil, paper hot cup, diatomaceous earth material and gum wood in direct contact membrane distillation configuration. Hydrophobicity is an essential property of membrane and it was made by using PTFE and silicone as a coating material. His idea was focused on improving the life span of the membrane under high operating temperature and to make membranes available at cheaper rates.

The second patent on direct contact membrane distillation (Lawson and Lloyd 1997; Hilal et al. 2004) was filed by Weyl in (1967) with the description of a process to produce demineralized water by adopting modified procedure and equipment from saline water. Here, a PTFE hydrophobic membrane of thickness 31.75 cm, porosity 42% and pore size of 90 µm was used. The idea of using other hydrophobic polymeric membrane materials like polypropylene, polyethylene, and polyvinyl chloride was indicated in this patent. The idea of using non-hydrophobic membrane wrapped by porous hydrophobic material in MD was introduced by Weyl (1967) in his patent as an alternative. The spiral wound membrane module was fabricated by coiling the membrane over a cylinder. Multistage operation procedure was a fresh method suggested in this patent. Another patent was granted toBodell (1968)for the production of drinking water from importable solution using membrane

distillation. He used the parallel arrangement of tubular membranes made of silicone having an inner and outer diameter 300 μms and 640 μms respectively. In this method, the air passes through the space between the permeate side and the membrane side continuously, and the vapors are condensed in an external condenser. This method was termed as sweeping gas membrane distillation (SGMD). Desalination of sea water was done economically in Bodell (1968) patent of MD. In his patent, the set up described had the provision of treating sewage, wastewater, brine, urine, and other impure water sources effectively for the production of drinking water. In this configuration, it was recommended that the vapor pressure of water in the air gap should be at least 0.04 atmospheres less than the feed solution. The usage of vacuum on the permeate side was also described in this patent. This method of generating vapor at low temperature by applying vacuum through an external vacuum pump was termed as Vacuum Membrane Distillation (Tang et al. 2009; Sushant Upadhyaya, S.P.Chaurasia 2012; Abu-Zeid et al. 2015)

Findley published his second paper, explaining the heat and mass transfer phenomena involved associated with the transfer of vapors from the feed side to the permeate side. An empirical correlation based on temperature difference as the driving force was also made to represents all the experimental data (M.E.Findley 1967). The diffusion of vapor through stagnant gas present in the membrane pores was suggested as the main parameter influencing the mass transfer flux in this experimental study.

After this, the research-excitement in the MD process saw a decline because of the less flux compared to the RO process and also because of the unavailability of desirable membrane modules at that time. In 1972, a patent by Rodgers was filed describing desalination operation using multi-stage assembly or a stack of micro porous flat sheet membrane in the DCMD configuration (Rodgers 1968; Rodgers 1969; Zhang et al. 2012). A thermal gradient was maintained in membrane assembly in order to produce distillate from the feed. The latent heat that is transferred from feed side of membrane via membrane to the permeate side was recovered by transferring heat to a feed stream. In this patent, it was clearly mentioned the membranes used in MD should be hydrophobic and highly porous (>80%) with uniform pore size distribution. The suitable polymeric membranes that could be used for MD were identified as polycarbonate, polypropylene, polyethylene, polyvinylidene fluoride (PVDF), etc. The application of silicone coating as a water repellant on the porous membrane was also

discussed in this patent for providing better hydrophobic characteristics to the membrane (Kuo et al. 2008; García-Payo et al. 2009).

After the successive improvement in required membrane properties for MD, the MD process again got its reputation in desalination field under academic research in the beginning of 1980's. During this time, quality membranes were developed.

An expanded PTFE membrane (Gore-Tex membrane) was used first(Esato et al. 1979) as an inert membrane of thickness 50 µms and pore size of 0.5 µms. Subsequently, this Gore-Tex membrane made of PTFE with porosity 80%, pore size range 0.2-0.45 µm and membrane thickness 25 µms was proposed by the Gore-Tex for membrane distillation in a spiral wound membrane module.

Cheng and Wiersma (1983)were granted many patents regarding MD membranes types, module arrangements, procedures, and setup(Upadhyaya 2013). The various patents granted to them in MD are as follows: The first patent was filed with a design aiming to improve the MD process and providing a continuous production of fresh water for a long run. A composite layer membrane was used in this process, the composite layer being made by fastening thin hydrophobic and hydrophilic membrane of a micro-porous grade. Towards the feed section, the hydrophilic side of the membrane was kept; and towards the permeate section (distillate side), hydrophobic side layer was placed. The membrane layers were well supported with the help of support layers to prevent the membrane puncture. The hydrophobic part made from PTFE and PVDF polymers whereas the hydrophilic part made of cellulose nitrate, polysulfone, cellulose acetate of the composite membrane was also suggested in this patent. The hydrophilic layer of the membrane minimizes the disturbances made by feed stream in the pores of the hydrophobic layer. The phenomenon of evaporation and condensation took place in the hydrophobic membrane pores. For salt water desalination, higher flux was observed with this composite membrane when the smaller pore size for hydrophilic membrane layer was used instead of the hydrophobic membrane layer. The hydrophobic layer having a pore size less than 0.5 µms gave the best results in this case.

In other patents, several other composite membranes were used and structured by sandwiching thin micro porous layers of hydrophobic material on both side by coating a thin layer of hydrophilic material (Cheng and Wiersma 1983a; Cheng and Wiersma 1983b).Hydrophobic layers different from each other were also tested. The materials used for

this testing were cellulose acetate, polysulfone, cellulosic esters, etc. The pure water flux of 3.13 kg/m2.hr was obtained when feed bulk temperature was 62.8°C and permeate side temperature was 56.7°C. But when the composite membrane of same structure was used witha non-hydrophilic layer coating on permeate side over the hydrophobic layer, the process conditions remaining the same; it was discovered that the flux was decreased to 2.14 kg/m2.hr. So in this patent, it was focused that the use of a hydrophilic material layer on the permeate side of hydrophobic membrane yielded higher fluxes.

Various MD papers regarding desalination and reuse of water were presented in 2nd world congress (Upadhyaya 2013).These works on MD revoked the interest in upgrading the hydrophobic porous membrane characteristics (Drioli et al. 1987; Kimura et al. 1987; Gostoli and Sarti 1989) for different MD configuration. Later, it was also discovered that the academic research increased much in comparison to the industrial research and most of work gained reputation through publication in various reputed national as well as international journals such as the Journal of Desalination. The number of MD papers published in journals per year since 1983 is shown in Figure 2.1.

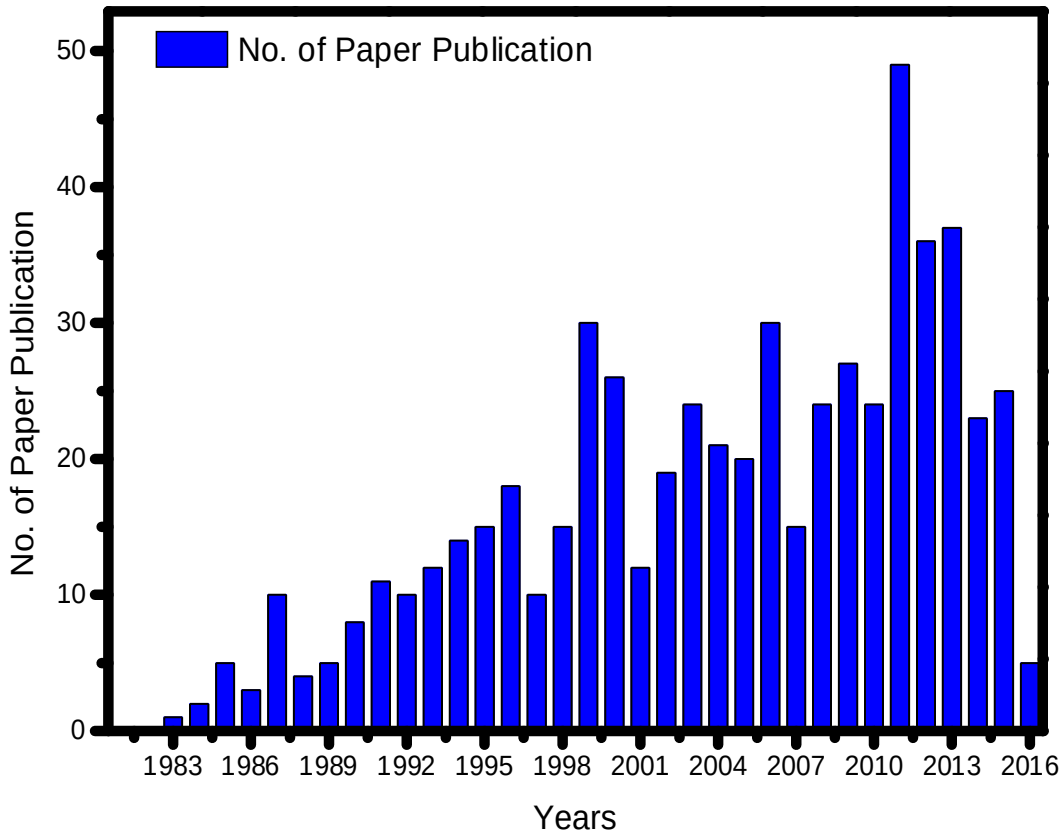

Figure 2.1: Research publication on MD Process Till 2016

2.3.3 Configurations of Membrane Distillation

Four configurations have been developed to perform MD process. These are direct contact membrane distillation (DCMD),air gap membrane distillation (AGMD), sweeping gas membrane distillation (SGMD), and vacuum membrane distillation (VMD). The method in which the vapor molecule is condensed, is the difference among these configurations.

2.3.3.1 Vacuum Membrane Distillation

In vacuum membrane distillation, the feed stream contacts directly with the membrane surface, and is maintained at a pressure lower than the minimum liquid entry pressure (LEP).At the rear side of the membrane, the permeate pressure is usuallykeptdown to the equilibrium saturation pressure by vacuum. In this configuration, the vapor permeate does not condense in cooling chamber, but is taken out by vacuum and condenses externallyin a condenser. VMD configuration is displayed in Figure 2.2. The pressure difference between the two sides of the membrane develops a convective mass flow along the pores that results to the total mass transfer of VMD. However, in DCMD and AGMD, there is only the diffusive flux of volatile constituents within the membranes pores. Therefore, mass flux of VMD is generally higher than that of other MD configurations. This advantage makes VMD very thermally efficient. However, application of VMD is similar to that of SGMD, more successful examples are yet to be developed.

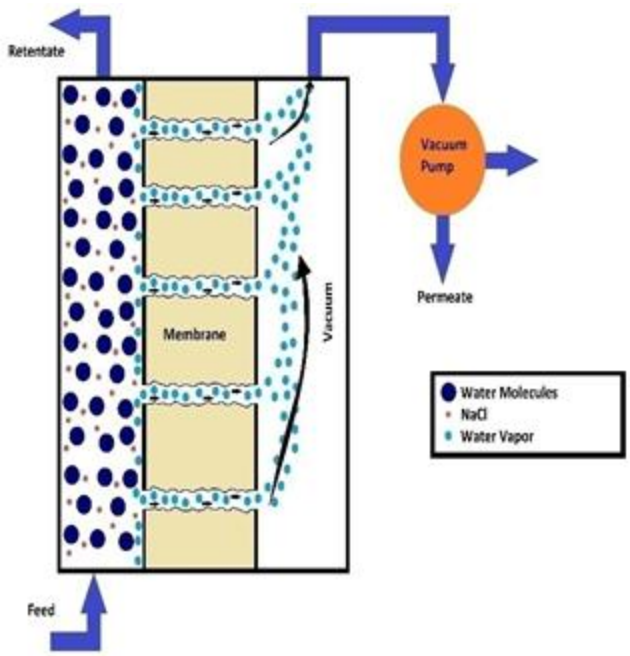

Figure 2.2: VMD Configuration

2.3.3.2 Direct contact membrane distillation

DCMD configuration is shown in Figure 2.3, where a micro-porous membrane separates the two compartments. The feed and permeate stream flows through the two chambers respectively. The high volatile constituents gets vaporized at interface of liquidand vapor andtravel across the membrane to the permeate side where it condensates. The direct contact reveal that both the process and permeate liquid are in direct contact with the membrane in the compartments.

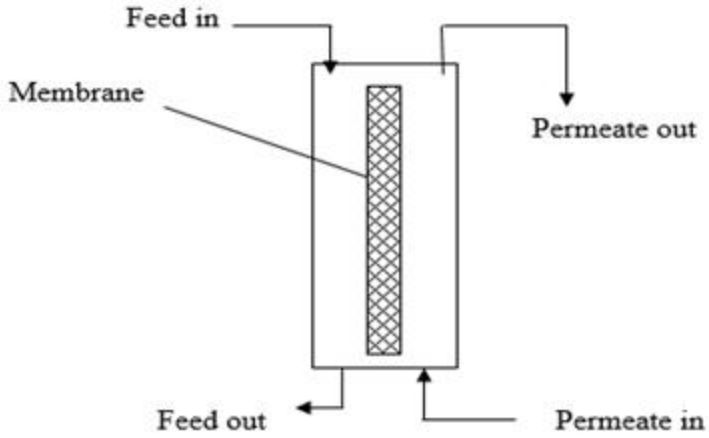

Figure 2.3: DCMD Configuration

Out of the four configurations, usually DCMD is used because of the simple fabrication. Some limitations are associated with DCMD application. Despite of the poor conductivity of polymeric material, the temperature difference between feed and permeate side provides a driving force for mass transfer and it also introduces heat conduction across membrane. Therefore, only part of the heat energy given to the feed is used for evaporation. In DCMD, because of the permeate flow in the cooling chamber is directly contacted with the membrane, the heat losses by the heat conduction is much larger than the other configurations. Thermal efficiency is small comparatively. The operator must prepare enough permeate fluid in prior for its direct contact with membrane while it flows through the cooling compartment. Moreover, as the condensate is mixed with the fluid in cooling chamber, spotting the leakage of the membrane is not so easy. Due to the unique advantage, DCMD is relevant for desalination (Lawson and Lloyd, 1996b).

2.3.3.3 Sweeping Gas Membrane Distillation

The advantages of AGMD over DCMD is high thermal efficiency because of the presence of air gap on the permeate side. As the stagnant air gap causes resistance to mass transfer, masstransfer across the air gap is the controlling step. This problem can be reduced by enhancing the mass transfer in this region. In SGMD, this is done by flowing air in the condensing chamber and creating the air flow on the membrane surface, rather than using a static air layer comparting the membrane and the condensing surface. SGMD configuration is displayedin Figure.

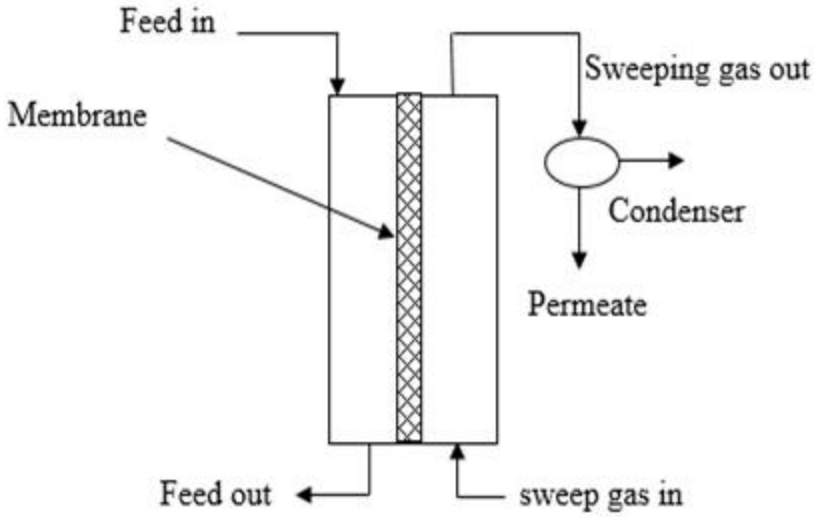

Figure 2.4: SGMD Configuration

The vapors of volatile constituents are taken from the chamber by the air flow and then it gets condensed in the condenser. Hence, SGMD can be taken as the combination of high mass transfer coefficient of DCMD and the less heat loss of AGMD. Very few works has been done in the field of SGMD. This may be because of the fact that the permeate should be collected externally. The layer sweeping gas flow is needed forgetting significant permeate yield, and extra cost related with transporting gas will be spent (K.Mohamed et al., 2000). SGMD is good for removing the volatile organic component or dissolved gas.

2.3.3.4 Air Gap Membrane Distillation

Air gap membrane distillation (AGMD) configuration is displayedin Figure, where an air gap is maintained with the help of a plate to minimize the cooling chamber from the membrane.

In this configuration, the migrated vapors molecule out of the membrane pores pass across the air gap and then condense on the plate, the condensate generated getsdrained out of the air gap by gravity. Coolant is used for removing the latent heat released during the condensation of vapor to liquid, in the cooling chamber. The static air in the air gap presents a new resistance to mass transfer, which in turn results in a low mass flux through the membrane. The air gap is broader than that of membrane, transport process across air gap is usually the controlling step in the AGMD (Garcia-Payo et al., 2000). However because of the low heat conductivity, air gap decreases the heat loss by conduction considerably. Therefore, in AGMD the thermal efficiency is greater than that of the DCMD. Since the product (i.e. the condensate) can be achieved directly, it is easy to decide whether there is wetting or membrane leakagehappeningby investigating the product composition. Whereas compared with other MD configuration, AGMD output can be weighted precisely. These advantages make AGMD particular in experimental studies.

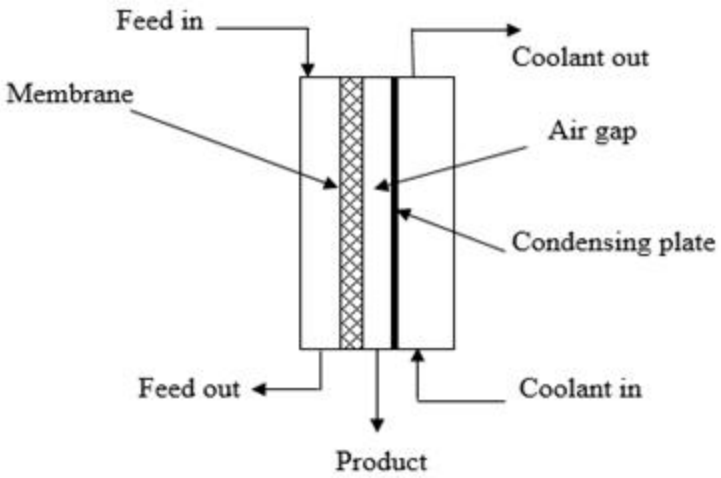

Figure 2.5: AGMD Configuration

2.3.4 Characterization of MD Membranes

The membrane characterization for MD, which is based on the physical methods, can be categorized as follows:

a) Conventional physical methods to determine parameters like pore size and pore size distribution, which are permeation based.

b) Microscopic methods which providea better apprehension of membrane morphology and structural properties (Khayet and Matsuura, 2011) such as photographical images from

scanning electron microscopy (SEM), Transmission Electron Microscopy (TEM),field emission scanning electron microscopy (FESEM) and atomic force microscopy (AFM).

c) Spectroscopic techniquessuch as Infrared (IR) spectroscopy, Fourier Transform Infrared (FTIR) Spectroscopy, Raman Spectroscopy (RS), Nuclear Magnetic Resonance (NMR) which provide the savvy of structural properties of the membrane at a molecular level(Singh et al., 1998).
d) Methods of determining the bulk properties of membranes such as thermal properties from Differential Scanning Calorimetry (DSC) and mechanical properties including tensile strength from UTM.
e) Other methods including contact angel and zeta potential measurement

2.3.4.1. Physical Methods

There are many acknowledged physical techniques for estimating membrane pore size for flat sheet, hollow fiber and capillary membranes. Some of the techniques are given below:

1) Gas Permeation Test
2) Wet/Dry Flow Method
3) Mercury Porosimetry
4) Bubble gas transport method

2.3.4.2. Transport Mechanism in MD Process

The simultaneous heat and mass transfer takes place acrossa micro-porous hydrophobic membrane in MD operation. Through membrane pores as well as membrane material, the heat transfer takes place, but mass transport takes place only via the membrane pores. The heat transfer within the membrane pore is because of the vapor flux (N, kmol/m^2 ·sec) and latent heat (ΔH, kJ/kmol) of the volatile component and heat energy transferred across the gas–filled membrane pores is in the form of latent heat and membrane material itself because of conduction (Khayet and Matsuura, 2011). Due to the hydrophobic property of the membrane, only the volatile componentis able to cross the membrane pores, from the feed side to the permeate side. In each MD configuration, a boundary layer of fluid is present on both sides of the membrane which builds a resistance to both mass and heat transfer, and this phenomenon is labeled as concentration and temperature polarization respectively. When feed contains more than two volatile component then concentration gradient come into account and effects of both concentration polarization and temperature polarization are encountered in MD process whereas, if only single volatile component are in feed solution to

be treated than there would be no concentration gradient (El-Bourawi et al., 2006) in scene and therefore only temperature polarization effect comes into existence. Each MD configurations has different picture of the polarization effects due to its different geometry and conditions.

Based on the transport of vapors through a membrane in different MD configurations, their performance is analyzed. Various mathematical models have been developed based on the kinetic theory of gases and tested on these MD configurations. The membrane used in MD is a porous media and the transport of mass through it can be monitored by three fundamental mechanisms. These mechanisms are based on Knudsen diffusion flow model, viscous or Poiseuille flow model and molecular diffusion model.

The mass transfer across the membrane is affected by two important parameters viz mean free path (λ) and membrane mean pore diameter (d). The mean free path (λ) can be defined as the average distance traveled by any molecule before collision (Lawson and Lloyd, 1997). The mean free path can be calculated with the help of expression given in equation 2.11. The dimensionless number (λ/d) used to define the transport occurring in MD is known as Knudsen number (Kn) and is defined as the ratio of the mean free path to mean pore diameter of membrane.

$$\lambda = \frac{k_B T}{\sqrt{2\pi p \sigma^2}} \qquad 2.1$$

Where σ is the collision diameter of a molecule (2.641A ° for water vapour), k_B is the Boltzmann constant, $\overline{p}$ the mean pressure within the membrane pores and T the absolute temperature.

In reality, all of the three mechanisms (Knudsen diffusion, molecular diffusion, and viscous flow models) take place simultaneously. The dusty gas modelincludes all the three mechanisms(Guijt et al., 2005, Izquierdo-Gil et al., 1999) and is also acknowledges the effects of membrane parameter in it equations. Is the most versatile model for flux prediction through a porous medium (Mason and Malinauskas, 1983).

Theonly problem with the application of the DGM theory on MD is that it is a non-isothermal process. DGM that was initially derived for isothermal flux but has been successfully applied to non-isothermal systems via the inclusion of terms for thermal diffusion and thermal

transpiration. However, it can be easily shown (Jackson, 1977) that these terms are negligible, and T_{avg} in the membrane can be used in place of T in the DGM equations.
It is worth citing that of the total heat flux across the membrane (typically 50 to 80%) is consumed in latent heat for permeate production, while the remaining is lost in thermal conduction. As a matter of fact, the heat loss via conduction through the membrane matrix become less significant when the MD system works under high operating temperatures, which are lower than the boiling point of the feed aqueous solution. This may be considered one method to minimize heat loss through the membrane, which is one of the inconveniences of MD process.

In VMD, resistance offered by the boundary layer in the permeate side and the contribution of conduction to the heat transported through the membrane are often neglected (Lawson and Lloyd, 1997, El-Bourawi et al., 2006, Bandini et al., 1997). Because of this VMD of pure wateris useful for estimating the feed side temperature of the membrane surface (T_{fm}) as it cannot be determined directly and therefore the coefficient of heat transfer at the boundary layer of the membrane module can be determined (Mengual et al., 2004). This method has been put on use for selecting the adequate empirical heat transfer correlation for any given MD system, which is a complex task whiledeveloping theoretical models for determining the temperature polarization coefficients. In fact, the usage of empirical heat transfer correlations in MD has been questioned and even criticized as these correlations were originally developed for heat exchangers.

2.3.5 Membrane selection criteria for membrane distillation

Following requirements should be satisfied by the membranes for being used for MD:

2.3.5.1 Pore size distribution

The pore size range may vary from several nanometers to few micrometers. The distribution of pore size must be as narrow as possible and the feed liquid must not enter into the pores. The LEP must be as high as possible. It can be defined as the minimum transmembrane pressure that is needed for distilled water or other feed solutions to enter into the pores of the membrane by overcoming the hydrophobic forces. Otherwise, pore wetting will take place and it will lead to the requirement of a large surface area for a given production rate and decline in the salt rejection. The LEP is characteristic of any membrane. A high LEP can be

achieved by using materials of low surface energy or high hydrophobicity (i.e. large contact angle for water or feed solutions) and small maximum pore size. On the other hand, a small maximum pore size leads to a small mean pore size and, thus, low membrane permeability. Therefore, a compromise between the high LEP and the high productivity must be made by choosing an appropriate pore size and pore size distribution. The membrane may be composed of a single layer or multi-layers. But, at least one of these layers should be hydrophobic and be porous.

2.3.5.2 Membrane Porosity

The porosity (void volume fraction open to MD vapour flux) of the single-layer membrane or that of the hydrophobic layer in the case of the multi-layered membrane should be as high as possible. This is proportional to the MD membrane permeability. In fact, membranes with higher porosity can provide large spaces for evaporation. Therefore, it is generally agreed upon that the higher membrane porosity results in the higher permeate flux regardless of the MD configuration.

2.3.5.3 Membrane thickness

The thickness of the single-layer membrane must be suitable as the thickness is inversely proportional to the rate of mass and heat transport by conduction through the membrane. In the case of a multi-layered membrane, the hydrophobic layer thickness must be as thin as possible. While a high mass transport is favored for the MD process, a high heat transport is considered to be a heat loss. Therefore, compromise should be made, again, between the mass and the heat transfer, by properly adjusting the membrane thickness. One advantage of the multi-layered membrane is that a high mass transport is allowed by making the hydrophobic layer as thin as possible, while a low heat transfer is enabled by making the overall membrane thickness (hydrophobic layer þ hydrophilic layer) as thick as possible.The tortuosity factor (i.e. the measure of the digression of the pore structure from straight cylindrical pores normal to the surface) should be small. This is inversely proportional to membrane permeability. In MD studies, in order to predict the transmembrane fluxes, a value of 2 is frequently assumed for membrane tortuosity factor.

2.3.5.4 Thermal conductivity of membrane material

The thermal conductivity of the membrane material must be as low as possible. It must be mentioned here that most of the hydrophobic polymers have similar thermal conductivity within the same order of magnitude. The thermal conductivity of commercial membranes ranges from 0.04 W/m.K to 0.06 W/m.K. It is possible to diminish the membrane heat transfer by conduction using membranes of high porosities, since the conductive heat transfer coefficients of the gases trapped in the pores are of magnitude of order smaller than most of the used membrane materials. This possibility is also aligned to the requirement in order to achieve high MD permeability. The membrane surface which is in touch with the feed solution mustfabricated with a material of high fouling resistance, even though fouling effect in MD is not as strong as that in pressure-driven membrane separation processes. The membrane surface modification is needed, when hydrophobic layer is in contact with the feed solution. Depending on the feed solution to be treated,this can be achieved by coating the surface with a thin layer of a fouling resistant material.

2.3.5.5 Thermal stability of membrane

The membrane must have good thermal stability. Long-term stability is expected from MD membranes at temperatures as high as 100ºC.The membrane material must have good chemical resistance against various feed solutions. Resistance to acid and base is necessary if the membrane has to be cleaned. The membrane in MD acts only as a support for the vapor/liquid interfaces and does not alter the VLE of the aqueous solutions which are in contact with it.

2.3.5.6 Membrane life and cost

The membrane should be having a long and stable life (permeability and selectivity) when used on commercial scale. Anotheressential requirement is that the membrane should be of low cost.

2.3.6 Modelling in Membrane Distillation

In MD processes, heatand mass transport are coupled. In the VMD process used in present study, feed solution is brought into contact with one side of a micro porousmembrane and vacuum is applied on the opposite side. In this condition, a transmembrane water vapor pressure difference is created. The driving force for mass transfer in MD systems is the

inequalityof the partial pressure of water vapor across micro porous hydrophobic membrane. Therecognized transport mechanisms for mass transfer across the membrane are usuallyKnudsen and molecular diffusion and, sometimes, viscous flow. Molecular diffusion has a partial pressure difference as its driving force. And non-identical molecules that are in the way forms the resistance to mass transfer. The driving force for Knudsen diffusion is also a partial pressure difference, but in this situation molecules bounce into the membrane matrix, which generates the resistanceto mass transfer. Knudsen diffusion is thus important for small (micro) pores and / or low pressure. Lastly, viscous flow has a total pressure difference as driving force, and the membrane matrix forms the resistance against it(Lawson and Lloyd, 1996a, Xu et al., 2006, Mengual et al., 2004, Pangarkar et al., 2010). In a VMD configuration, the molecular diffusion is not sufficient due to the verylow value of the partial pressure of the air inside the pores. Therefore, the Knudsen and viscous flow diffusion should be a chosen as more appropriated(Lawson and Lloyd, 1997, Mengual and Peña, 1997). In MD, heat and mass transfer happens simultaneously and both temperature and concentration polarization effects should be taken into consideration. Part of the heattransfer takes place by the void space of the membrane where gases are entrappedand the other part through conduction in the membrane matrix. Hence, the membrane parameters play important role in the heat and mass transfer phenomena. Therefore, all these factors result in complicated modeling steps. However, despite the numerous mathematical models that have been found by MD investigators and regardless of their accuracy in predicting the MD permeate flux, there are many issues which are still need to be fully understood.

Various many mathematical models for various membrane distillation configurations have been developed. The guessing of permeate flux with respect to operating, membrane based parameters is the main work of the developed model (Xiuli et al., 2003, Khayet et al., 2000, Banat and Simandl, 1994, Bandini et al., 1992, Mengual et al., 2004, Phattaranawik et al., 2003b, Lawson and Lloyd, 1996a, F.A.Bannat and J.Simandl, 1998, Bandini et al., 1997, Bandini and Sarti, 1999, Martinez-Diez and Vazquez-Gonzalez, 1998, Martinez-Diez and Vazquez-Gonzalez, 1999, Schofield et al., 1990a, Schofield et al., 1990b, Khayet et al., 2004b, Ugrozov and Elkina, 2002, Martinez-Diez et al., 2002, Khayet and Matsuura, 2004, Foster et al., 2001, Chernyshov et al., 2003, Gryta et al., 1997, Gryta and Tomaszewska, 1998, Ding et al., 2003, Alklaibi and Lior, 2005b,Criscuoli, Carnevale, & Drioli, 2013; Lee & Kim, 2013; Lovineh, Asghari, & Rajaei, 2013; Shi, Zhao, & Zhu, 2014; Soukane, Chelouche, & Naceur, 2014; Tavakolmoghadam & Safavi, 2012; Upadhyaya, Singh, Chaurasia, Dohare, & Agarwal, 2015; Zhang et al., 2013; Zuo, Guan, & Wang, 2014). Moreover, the membrane

selectivity was also given when using VMD configuration byKhayet and Matsuura, 2004. It is worth noting here that complete relationships in MD modeling have been reviewed in literature Lawson and Lloyd, 1997,Khayet et al. 2004, Mengual et al. 2004studied other equations peculiarly those involving the pore size distribution, which are not considered inLawson & Lloyd, 1997.

The model recommend a linear relationship between the water flux, N, and the water vapor pressure difference between condensing and evaporating surface.

$$N = K_M \Delta P_V = K_M(PV - P_0) \qquad 2.2$$

Where $K_M$is known as MD coefficient, $P_0$is the pressure in the vacuum side and P_v is the water vapor pressure in the membrane surface at the temperature T_w. Coefficient $K_M$depends on temperature and some geometric characteristics of the membrane. Based on the Kinetic Theoryof Gases or the Dusty Gas Model, there is a Knudsen type diffusion of water molecules acrossthe membrane pores and the permeation flux, N, was written(Lawson and Lloyd, 1997).

$$N = 1.0663 \frac{r\varepsilon}{\tau}\left(\frac{M}{RT}\right)^{\frac{1}{2}} \frac{\Delta P_V}{\delta} \qquad 2.3$$

Where r is the pore size, ε is known as fractional void volume of the membrane, δ is the membrane thickness, τ is the pore tortuosity, M is the water molecular mass and R is the gas constant. As it is well known, the water vapor pressure at liquid –vapor interface (in Pa) may vary with the temperature (in K), according to Antoine's equation

$$P_V = \exp\left(23.1964 - \frac{3816.44}{T - 46.13}\right) \qquad 2.4$$

VMD is a thermally driven process, heat and mass transfer are occurring simultaneously and boundary layers are formed near the membrane surface. Consequently, there is a reduction in the driving force due to polarization effects of temperature and concentrations. When a molecular mixture is brought to the membrane surface by the driving force action, some molecules will permeate across the membrane while other molecules will be retained. This results to an accumulation of the retained components and a depletion of the more permeating components in the boundary layer adjacent to the membrane surface. This phenomenon is called as concentration polarization.

In VMD process, heat transfer occurs by two major mechanisms: (i) the latent heat transfer along with the transmembrane vapor flux, and (ii) heat transferred by conduction across the membrane matrix(Lawson and Lloyd, 1997).Therefore, there is rather complex relationship between both mass and heattransfer. The temperature at the membrane surface is lower than the analogous value at the bulk phase. This forms temperature gradients in the liquid film adjoining the membrane. This phenomenon is known as temperature polarization(Lawson and Lloyd, 1997, Mengual and Peña, 1997,Alsaadi et al. 2014).

Heat transfer through the boundary layer in a MD module is usually the rate limiting step for mass transfer, because such alarge quantity of heat must be needed to the vapor liquid interface to vaporize the liquid. The heat transfer coefficient , h_f, of the VMD feed side boundary layer, is defined by Lawson and Lloyd (1996a)

$$Q = h_f \Delta T_f \qquad 2.5$$

Where Q is the rate of heat transfer through the boundary layer and $\Delta T_f$is the temperature difference across the boundary layer. In VMD, the conductive heat transfer across the membrane is minute because of the low pressure on the permeate side of the membrane(Lawson and Lloyd, 1996a, Lawson and Lloyd, 1997) consequently, the heat transfer through the liquid boundary layer and the energy transported through the membrane for VMD(Lawson and Lloyd, 1996a, Mengual et al., 2004) is:

$$h_f \Delta T_f = N \Delta H_v \qquad 2.6$$

Where ΔH_v is the latent heat of vaporization of water. The empirical correlation like a Dittus-Boelter equation gives the value of $h_f$for turbulent liquid flow written in the simplified form (Lawson and Lloyd, 1996a):

$$h d / k^T = Nu = a\,\mathrm{Re}^a\,\mathrm{Pr}^b \qquad 2.7$$

Where d is knows as effective tube diameter, k^T is called the thermal conductivity of the water, Nu, Re and Pr are the Nusselt, Reynolds and Prandtl numbers respectively, and a, b and c are known as the characteristic constants of the module design and liquid flow regimes. The viscosity correction factor usually associated with the Dittus-Boelter equation $(\mu / \mu_{wall})^{0.14}$, is very small for MD application(Lawson and Lloyd, 1996a).

When both heat and mass transfer are happening simultaneously, the mass and heat transfer coefficients may be related by the Reynolds analogy(Pangarkar et al., 2010):

$$\frac{h_f}{k_f} = \rho C_P \left(\frac{Sc}{\mathrm{Pr}} \right)^{2/3} \qquad 2.8$$

Where k_f is called the mass transfer coefficient of boundary layer, ρ is the density of water, Cp is the specific heat capacity, and Sc is the Schmitt number

2.4 Membrane Parameters Affecting Membrane Distillation Process

The membranes used in MD process are made for micro-filtration purposes and most of them are prepared using PP, PTFE, andPVDF. These membranes are available in flat-sheet or capillary forms (Ding et al., 2003). The required membrane parameters for MD process were given by many researchers(Lawson and Lloyd, 1997, Khayet and Matsuura, 2001, Schneider et al., 1988). Very few authors have considered the possibility of membrane designing (Khayet and Matsuura, 2001, Lawson and Lloyd, 1996b). The effects of membrane based parameters on MD performance are discussed below:

2.4.1 Membrane Pore Size

The pore diameter for MD process range between 100 nanometer to 1µm and it is agreed on increasing the pore diameter of membrane, the flux for MD increases. This may be due to the Knudsen-viscous transition (Cath et al., 2004, Schneider et al., 1988Hailin Zhu, Hongjie Wang, FengWang, Yuhai Guo 2013; Lovineh et al. 2013; Sun et al. 2014). For maintaining the hydrophobicity of the membrane, the pore size should be made small creating a conflict for MD permeability. The Knudsen number defines the role of transfer mechanism and helpful for optimizing the pore size of the membrane in order to get suitable flux.

2.4.2 Membrane Thickness

The MD flux is directly proportional to the reciprocal of membrane thickness. Membrane thickness creates a resistance to mass transfer through MD. For getting more flux, the membrane should be kept thinner. On the other side, for excellent heat efficiency the membrane should be thicker since heat dissipation through conduction take place by membrane material (Lawson and Lloyd, 1997, Schofield et al., 1990b, Schofield et al., 1990a, Lagan et al., 2000,Drioli et al. 2013; Lee and Kim 2013; Lovineh et al. 2013; Zhang et al. 2013; Zhou et al. 2014; Zuo et al. 2014). Using simulation and accounting the effect of thermal conductivity, the optimum thickness of membrane was calculated in the range of 30–60 µm(Lagan et al., 2000).

2.4.3 Pore Tortuosity

Membrane tortuosity is the mean length of the pores compared to the thickness of the membranes. Generally, tortuosityvalue of 2 is considered for estimation of flux (Lawson and Lloyd, 1997, Bandini et al., 1997, Khayet et al., 2004a, Lovineh et al. 2013). Moreover, a tortuosity of nearly 4 was observed by others (Fernandez-Pineda et al., 2002). In real sense, the membrane pores are not linear across the membrane so, the vapor molecules travelthrough tortuous way, which declines MD flux. To our survey, no systematic study has been done on the effect of tortuosity for the permeate flux in MD. The correction factor was generally considered during the estimation of permeate flux since it is cumbersome to calculate the tortuosity value clearly. Hence, actual effect of tortuosity on flux needs to be investigated further. The gas permeation test along with porosity measurement testis used to determine this value (Khayet et al., 2004a, Khayet et al., 2004b).

2.4.4 Membrane Porosity

Membrane porosity was defined as void volume. It is effective parameter for MD performance and selectivity. The MD membrane porosity ranges between 30 and 85%. It is known that greater porosity, creates higher permeate fluxes in all types of MD configuration. It should be remembered that heat loss due to conduction was less in the membrane of higher porosity. This is due to the very low heat transfer coefficient of the gas as compared to the membrane material (Lawson and Lloyd, 1997, Schofield et al., 1990b).

2.4.5 Pore Size Distribution

The membranes employed in MD exhibit a pore size distribution rather than a uniform pore size. Therefore, more than one mechanism can take place simultaneously to different extent depending on the pore size and on the MD operating conditions. The effect of pore size distribution on the MD flux has been rarely studied in VMD (Khayet et al., 2004a, Khayet and Matsuura, 2004, Lovineh et al. 2013). It was observed when using commercial membranes that the predicted DCMD flux assuming uniform pore size is quite similar to that calculated using pore size distribution. In contrast, when using laboratory made membranes, which exhibit pore size distribution with geometric standard deviations far from unity, the difference between the calculated permeate fluxes is higher(Khayet et al., 2004b). Further studies are needed to clarify this effect using other membranes and MD configurations.

2.5 Operating variables affecting Membrane Distillation process

The operating variables play a very significant role in the estimation of MD flux. The effects to these process based parameters on VMD performance are discussed separately in the subsection as:

2.5.1 Feed Temperature

The effect of the feed temperature on MD flux has been studied for various types of geometries. The feed temperature was kept below the boiling point of the feed solution and the range for feed temperature range for desalination was taken in the range 25 to 85 °C at constant feed flow rate and other operating parameters. It is accepted that the permeate flux increases exponentially on increasing the feed bulk inlet temperature. It was also observed by many workers that temperature polarization effect increases with the feed bulk temperature (Phattaranawik et al., 2003b, Lawson and Lloyd, 1996a, Lagan et al., 2000). The permeate flux increases exponentially but selectivity ceases in MD, when the volatile component has to be removed from the feed solution. Such effect has been reported by several MD investigators (Bandini et al., 1992, Lawson and Lloyd, 1996a, Rivier et al., 2002, Bandini et al., 1997, Desalination and Distillation 2009; Fan and Peng 2012; Hasanoğlu et al. 2012; Chen et al. 2013; Ji et al. 2013; Lovineh et al. 2013; Sivakumar et al. 2013; Zhang et al. 2013; Criscuoli et al. 2013b; Zhao et al. 2013b; Abdallah et al. 2014; Mohammadi et al. 2014; Naidu et al. 2014; Shi et al. 2014; Shim et al. 2014; Sun et al. 2014; Tang et al. 2014; Zhou et al. 2014; Zuo et al. 2014; Upadhyaya et al. 2015). This may be considered to increased effect of both temperature and concentration polarization with the increase of feed temperature. However for cross flow pattern in membrane modules, simultaneous temperature and pressure drop has been seen. In all of MD process, the inlet temperature is not same to outlet temperature and is a function of feed flow rate. For this particular reason it was advised to consider a general temperature polarization coefficient, and an overall was valid for the complete process. The overall is calculated from the experimental data (Khayet et al., 2000). Usage of mixing cells (i.e. known as Lewis cells) made the inlet and outlet temperature nearly identical

2.5.2 Feed Circulation Velocity

The feed flow rate and feed mixing rate increase the feed side heat transfer coefficient and minimizes the temperature and concentration polarization effect. This as a result improves the MD flux Asymptotic increment in permeate flux with higher feed flow rate was seen by

some workers for DCMD, AGMD and VMD configurations (Banat and Simandl, 1994, Alklaibi and Lior, 2005a, Desalination and Distillation 2009; Fan and Peng 2012; Hasanoğlu et al. 2012; Chen et al. 2013; Criscuoli et al. 2013a; Ji et al. 2013; Lee and Kim 2013; Lovineh et al. 2013; Sivakumar et al. 2013; Zhang et al. 2013; Zhao et al. 2013a; Criscuoli et al. 2013b; Zhao et al. 2013b; Abdallah et al. 2014; Figoli et al. 2014; Mohammadi et al. 2014; Naidu et al. 2014; Selvi and Baskaran 2014; Shim et al. 2014; Sun et al. 2014; Zuo et al. 2014; Upadhyaya et al. 2015) whereas the increment in flux for SGMD was negligible during separation of non-volatile solute in the feed solution (Khayet et al., 2000). It must be remembered that when volatile components are in the feed solutions, the process separation factor (selectivity) is most likely to be directly affected by the feed flow rate. The linear increment was also observed in MD flux with the feed flow rate by other workers (Mengual et al., 2004, Phattaranawik et al., 2003b). Turbulent condition was preferred for getting higher production from MD(Lawson and Lloyd, 1996a, Martinez-Diez and Vazquez-Gonzalez, 1998, Schofield et al., 1990a, Lawson and Lloyd, 1996b), which is obtained by creating extensive and rigorous mixing along at the cost of high Reynolds number experimentally. So, at higher feed flow rate the bulk temperature is near to feed side membrane temperature and as a result the MD flux is higher. But, this response is different for different MD configuration and experimental situation. Higher separation factors were obtained by different MD investigators in all MD (Bandini et al., 1992, Bandini et al., 1997, Bandini and Sarti, 1999). The increment of in the separation factor is because of excellent mixing at higher feed flow rates, which minimize the effect of the concentration polarization at boundary. Reynolds number (Re_N) is related linearly to the feed velocity (v), whereas the pressure drop (ΔP) is directly proportional to the length of the membrane test cell (L) and square of feed velocity as:

$$\mathrm{Re}_N = \frac{v d_h \rho}{\mu} \qquad 2.9$$

$$\Delta p = f \frac{L}{d_h} \rho \frac{v^2}{2} \qquad 2.10$$

Whered_h,f, ρ and μ are the hydraulic diameter of the flow channel, friction factor, fluid density and dynamic viscosity, respectively. Hence, the feed flow rate must be changed with great caution to avoid the problem of pore wetting at the membrane surface. This could be gained by maintaining the hydrostatic pressure less than the liquid entry pressure (LEP) of

feed solution into the membrane pores under turbulent condition. No study was observed regarding use of stirring cells in AGMD, SGMD and VMD.

2.5.3 Feed Inlet Concentration

The effect of feed concentration on trans-membrane flux depends strongly on the separation process itself. As it is well known MD can be used for the treatment of highly concentrated solutions (i.e. non-volatile solute) without suffering the large drop in permeability observed in other membrane processes such as the pressure-driven membrane processes (Lawson and Lloyd, 1997, Banat and Simandl, 1994, Cath et al., 2004). When non-volatile solutes are considered, the most likely effect of the feed concentration is to result in a decrease in the permeate flux in all MD configurations(Fan and Peng 2012; Lovineh et al. 2013; Sivakumar et al. 2013; Criscuoli et al. 2013b; Abdallah et al. 2014; Mohammadi et al. 2014; Naidu et al. 2014; Selvi and Baskaran 2014; Sun et al. 2014). This is attributed to the fact that the addition of non-volatile solute to water reduces the partial vapour pressure and consequently reduces the driving force of MD process. There is also the contribution due to the effect of the concentration polarization (i.e. formation of a boundary layer on the feed membrane surface). Nevertheless, this contribution is very small compared to that of the temperature polarization (Martinez-Diez and Vazquez-Gonzalez, 1998, Schofield et al., 1990a, Martinez-Diez and Vazquez-Gonzalez, 1999, Schofield et al., 1990b). On the other hand, when aqueous solutions containing volatile components (such as alcohols) are considered, the effect of increasing solute concentration is completely different and depends upon the thermodynamic properties of the involved volatile compound and its interaction with water. Generally, in such situations, increasing solute (volatile compound) concentration results in a higher permeate flux(Hasanoğlu et al. 2012). This is attributed to the increase of the trans-membrane partial pressure of the volatile component due to the increase of its concentration in the feed side. In this case, care must be taken to avoid membrane pore wetting. Another issue to be considered here is that the presence of a non- volatile component such as salts in diluted aqueous solutions containing organic compounds may alter the vapour pressure of the solution. For instance in case of a binary mixture of water/alcohol, the addition of salt may change the vapour pressure ratio and increases the MD selectivity (Banat and Simandl, 1999).

2.5.4 Vapour Pressure Difference

As discussed initially, the vapour pressure difference across the membrane is the driving force for MD process. This can be obtained by varying the temperature difference or by applying vacuum at the downstream side of the membrane. It is frequently agreed linear increment in the MD flux with the vapour pressure difference in every types of MD. Due to the fact that the temperature and the concentration polarization affect the permeate flux, it was also observed an implicit relation between the permeate flux and the bulk pressure difference (El-Bourawi et al., 2006, Hasanoğlu et al. 2012; Criscuoli et al. 2013a; Ji et al. 2013; Lovineh et al. 2013; Sivakumar et al. 2013; Zhao et al. 2013b; Abdallah et al. 2014; Shi et al. 2014; Sun et al. 2014; Wang et al. 2014; Zhou et al. 2014; Zuo et al. 2014; Upadhyaya et al. 2015). In VMD, the permeate flux and the transmembrane hydrostatic pressure increase with the decrease of the permeate pressure in the downstream side of the membrane and therefore the trouble of membrane wetting is more. Nevertheless, when a volatile organic compound (VOC) is present in the feed solution, the effect of decreasing the downstream pressure in VMD result total permeate flux (water and VOC) increment but on the other side it may also tend to comparatively bad selectivity of the process. To obtain more VOC in permeate, it is advised to work at higher permeate (Bandini et al., 1997, El-Bourawi et al., 2006). On the other hand, the effect of the trans-membrane hydrostatic pressure in MD is very evident and required to be studied.

2.6 Advantages of Membrane Distillation Process

Membrane distillation is a new process worldwide as a low cost, energy saving alternative to conventional separation process such as distillation and reverse osmosis.

The benefit of MD compared to other more popular separation processes stem from

The theoretically 100% rejection of ions, colloids, macro molecules & other non-volatiles. Lower operating pressure than conventional pressure driven membrane separation processes. Lower operating temperature, than conventional distillation. Reduced chemical interaction between membrane & process solutions. Less demanding membrane mechanical property requirements. Reduced vapor pressure spaces compared to conventional distillation processes.

The large vapor space required by a conventional distillation column is replaced in MD by the pore volume of a micro-porous membrane, which is generally of the order of 100μm thick. Where conventional distillation relies on high vapor velocities to provide intimate

vapor-liquid contact, MD employs a hydrophobic micro-porous membrane to support a vapor-liquid interface, Due to this reason, MD processes equipment can be much smaller, which translates to a savings in terms of real estate & the required operating temperature are much lower because it is not necessary to heat the feed liquids above the boiling point. Further, lower process temperature combined with reduced equipment surface area results in less heat lost to the environment through equipment surfaces. Feed temperature in MD typically ranges from 60 to 90^0C, although temperature as low as 30^0C have been used. Therefore, low grade, waste & for alternative energy sources such as geothermal & solar energy can be coupled with MD system for a cost efficient, energy efficient liquid separation system (Lawson and Lloyd, 1997).

Lower operating system temperatures have also made MD attractive in the food industry where concentrated fruit juices can be prepared with better flavor and color (Calabro et al., 1994). Since MD is a thermal driven process, operating pressure are generally on the order of zero to a few hundred kPa, relatively low compared to pressure driven processes such as RO. Lower operating pressure translates to lower equipment costs & increased process safety. Another benefit of MD is its efficiency in terms of solute rejection. Since MD operates on the principles of vapor-liquid equilibrium, 100%(theoretical) of ions, macromolecules, colloids & other non-volatile constituents are rejected, pressure driven processes such as RO, UF,& MF have not been shown to achieve such high levels of rejection.

Another advantage MD has over RO, UF, & MF arises from the minimal role that the membrane plays in actual separation. In MD the membrane acts mainly as a support for a vapor-liquid interface and does not distinguish between solution components as a chemical basis, nor does not it act as a sieve. Therefore MD membranes can be fabricated from chemical resistant polymers such as PTFE(Poly-tetra-fluro-ethylene), PP(Polypropylene), PVDF(Poly-vinyl-dene-fluoride), further membrane fouling is less of a problems in MD than in other membranes separation because the pores are relatively large compared to the 'pores' or diffusional pathways in RO or UF & are not easily clogged.

2.7 Model for Estimation of Feed Side Membrane Temperature

A computational fluid dynamics (CFD) simulation that coupled an established heat and mass transfer model was carried out for the vacuum membrane distillation (VMD) of NaCl solution to predict mass and heat behaviors of the process. The effects of feed bulk temperature, feed flow rate and vacuum pressure was studied simultaneously on permeate flux and compared with experimental data The temperature profile on membrane surface was

then generated under varied flow rate, feed bulk temperature and vacuum pressure in the fluent software.

2.7.1 Geometry and Computational Mesh Generation

PTFE membrane was used in the simulation. The membrane was purchased from Millipore, and the pore size of the membrane is 0.22 μm, with a porosity of 85 %, a membrane area of 0.00212 m^2. The liquid feed was NaCl aqueous solution with a certain concentration of 0.5 mol/l. NaCl aqueous solutions with temperature upto 65 °C flew into the membrane from the inlet. The inner section was defined as wall except the entry of the membrane silk, so that NaCl aqueous solution can only flow upto the silk, where the water molecules of NaCl aqueous solution evaporated, permeating through the membrane pores into the permeate section. The driving force of the whole process was vapor pressure difference. The produced volatile molecules were removed by applying vacuum at the downstream of the membrane and were condensed into condenser. The main dimensions of the membrane with test cell module were listed in Table 2.1.

Table 2.1: Test Cell Module Dimensions

Effective membrane diameter	52 mm
Feed section diameter	70 mm
Feed section length	123 mm
Permeate section length	73 mm

Figure 2.6schematically shows the geometry of computational domain setup in representing a channel section of the test cell of the membrane module with 200 mm height and diameter of 70 mm. Mesh was generated by the commercial grid-generation tool GAMBIT consisting of 57,871 nodes and the structured quadrilateral grid was used. A non-uniform mesh was adopted with the mesh density being higher near to the membrane surface. In all cases, the mesh independence of the solution was checked and made sure that there were sufficient cells in the temperature boundary layer. The automatic mesh partition of membrane silk was body fitted anisotropic mesh: the distance from the first mesh point to the boundary was 0.05, called first row; the growth factor was 1.01; the creating form was 1:1. The more detailed meshes were generated for the import and export of the membrane and the membrane silk vacuum ports. The whole mesh of the model in the membrane module section is shown

inFigure 2.7. Fluent was used as CFD simulation in this work to evaluate the flow conditions in this membrane module test cell.Figure 2.8 shows the flow chart of solution step to calculate the feed side membrane surface temperature (T_{fm}).

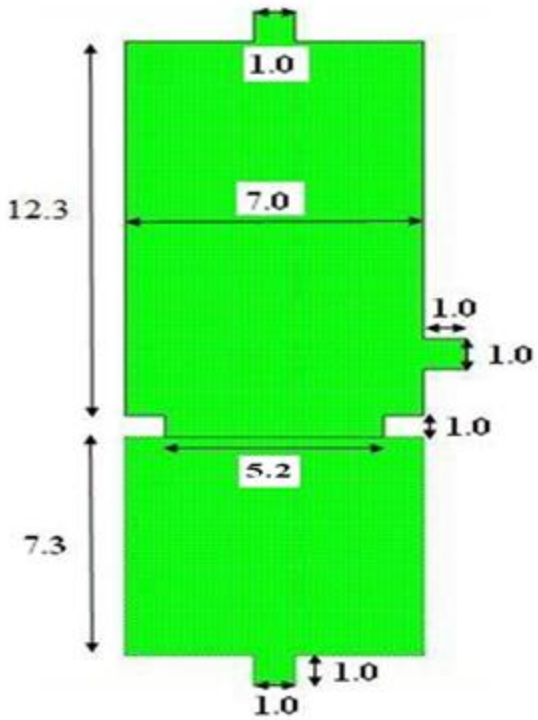

Figure 2.6: Membrane Module Test Cell

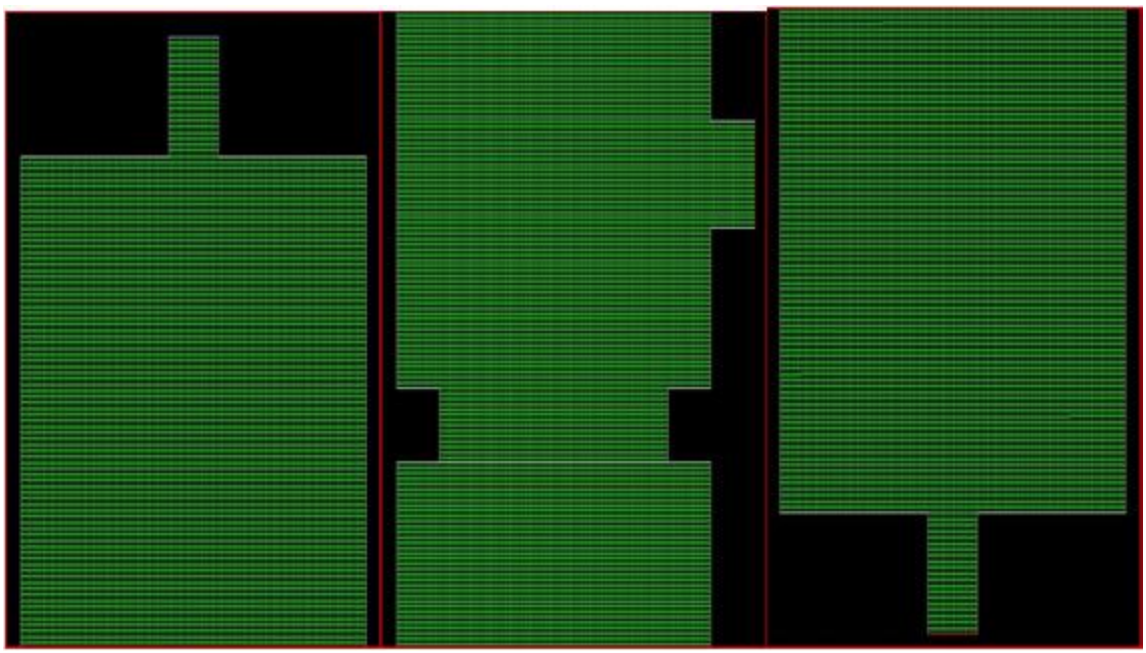

(a) **(b)** **(c)**

Figure 2.7: Membrane Module Section

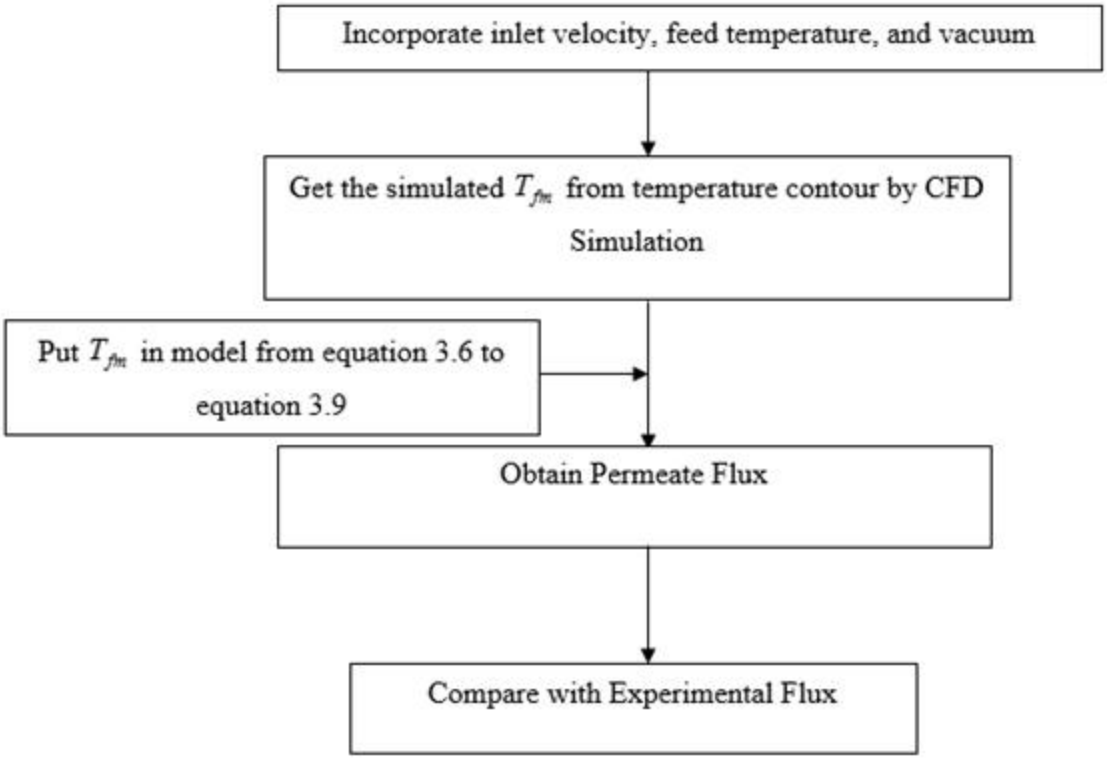

Figure 2.8: Flow Chart of Solution Step to calculate the T_{fm}

2.7.2 Boundary and initial conditions

Feed inlet

The inlet region of membrane model was simplified into a rectangular region, which was set to velocity-inlet. The inlet pressure was 1 atmospheric pressure, the feed flow rate varied from 1 10 lpm, and the gravitational acceleration was 9.81 m/s^2.

Pressure Outlet

The outlet was set to pressure-outlet. For outflow boundary condition, the velocity gradient of fluid was assumed to be zero, and the outlet temperature was 5°C lower than the inlet temperature.

Vacuum exports

Vacuum export was set to pressure-outlet, the pressure was in the range of 11 to 7 kPa, and the backflow of vapor was 0.

Porosity of the membrane silk

The flow through the porous field was calculated using the superficial velocity under the assumptions: membrane silk surface was considered as a wall (ignore the membrane flexibility), and the membrane surface was set to porous-jump.

2.8 Artificial Neural Network (ANN)

During the past years, neural networks have become widely used in chemical engineering for the simulation of complicated systems where the available information is experimental.Artificial neural network is an attempt to simulate within specialized hardware or sophisticated software, the multiple layers of simple processing elements called neurons. Each neuron is linked to certain of its neighbours with varying coefficients of connectivity that represent the strengths of these connections. Learning is accomplished by adjusting these strengths to cause the overall network to output appropriate results. A collection of nodes connected to each other forms the artificial neural network. A group of nodes called the input layer receives a signal from some external source. Another group of nodes, called the output layer, return signal to the environment. The remaining nodes in the network are called hidden nodes because they do not receive signal from or send a signal to an external source or location. The hidden nodes may be grouped into one or more hidden layers each of the arcs between two nodes (the lines between the circles) has a weight associated with it (Konar, 1999).

An artificial neural network is composed of many artificial neurons that are linked together according to specific network architecture. The objective of the neural network is to transform the inputs into meaningful outputs.

2.8.1 Definition

Hecht-Nielsen defined a neural network as: a computing system made up of a number of which processes information by its simple highly interconnected processing elements, dynamic state response to external inputs (Hecht-Nielsen, 1987).

An Artificial Neural Network (ANN) is a computer program that can recognize patterns in a given collection of data and produce a model for that data. It resembles the brain in two respects:

1. Knowledge is acquired by the network through a learning process (trial and error).
2. Interneuron connection strengths known as synaptic weights are used to store the knowledge.

2.8.1.1. The Analogy to Brain

The ANN modeling technique is a kind of artificial intelligence (AI) application that simulates the human brain's problem solving processes. Just as humans apply knowledge gained from past experience to new problems or situations, a neural network takes previously

solved examples, looks for patterns in these examples, learns these patterns and develops the ability to correctly classify new patterns. In addition, the neural network has the ability to resemble human characteristics in problem-solving that is difficult to simulate using the logical, analytical techniques of expert system and standard software technologies (Konar, 1999).

2.8.1.2. The Biological Neuron

The most basic element of the human is a specific type of cell, which provides us with the abilities to remember, think, and apply previous experiences to our every action. These cells are known as neurons, each of these neurons are connected with up to 200000 other neurons. The power of the brain comes from the numbers of these basic components and the multiple connections between them. A general biological neuron shown in Figure 2.9, with axons from two other neurons and dendrites for two other neurons.Several properties of the processing elements of artificial neural networks are suggested by the properties of biological neurons. A biological neuron has three types of components as dendrites, soma, and axon.

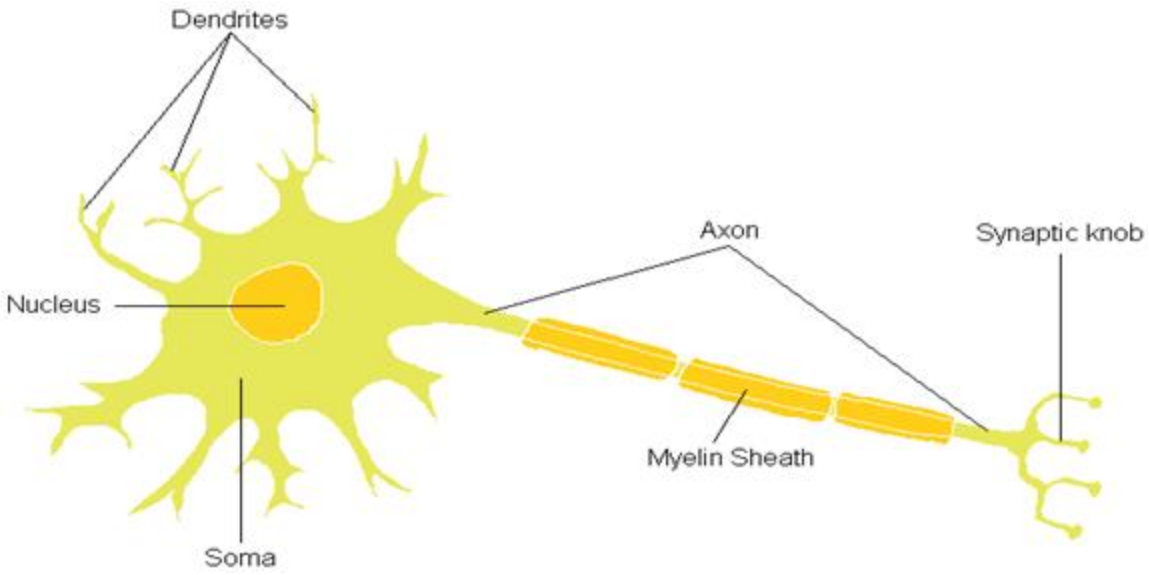

Figure 2.9: Biological Neuron

The neuron has four main regions to its structure as the cell body, offshoots, dendrites and axon. The cell body is the heart of the cell, containing the nucleus and maintaining protein synthesis. A neuron may have many dendrites, which branch out in a tree like structure, and receive signals from other neurons. A neuron usually only has one axon which grows out from a part of the cell body called the axon hillock which conducts electric signals. These electric signals are called action potentials that neurons use to convey information to the brain. Therefore, the brain determines what type of information is being received based on

the path that the signal took. Myelin is the fatty tissue that surrounds and insulates the axon. Often short axons do not need this insulation. There are un-insulated parts of the axon. These areas are called Nodes. At these nodes, the signal traveling down the axon is regenerated. This ensures that the signal traveling down the axon travels fast and remains constant (i.e. very short propagation delay and no weakening of the signal). The neurons do not actuallyphysically touch. They are separated by the synaptic cleft, and electric signals are sent through chemical interaction. Neurons can be classified by their number of processes (or appendages), or by their function. If they are classified by the number of processes, they fall into three categories. Unipolar neurons have a single process and are most common in invertebrates. In bipolar neurons, the dendrite and axon are the neuron's two separate processes. Finally, multipolar neurons are most common in mammals. Examples of these neurons are spinal motor neurons, pyramidal cells and Purkinje cells (in the cerebellum). If classified by function, neurons again fall into three separate categories. The first group is sensory, or afferent, neurons, which provide information for perception and motor coordination. The second group provides information (or instructions) to muscles and glands and is therefore called motor neurons. The last group, inter neuronal, contains all other neurons and has two subclasses(Shetty and Chellam, 2003).

The artificial neuron as depicted in Figure 2.10incorporates most features of a biological neuron. Neurons work by processing information. They receive and provide information in form of spikes. Spikes are interpreted as spike rates.

For example, like a neuron, the processing element (PE) has many inputs but has a single output, which can fan out to many other PEs in the network. The input connections are modeled as arrows from other processing elements. The input, i^{th} receives from the j^{th} PE indicated as x_j. Each connection to the i^{th} PE has associated with it a quantity called weight or connection strength. The weight on the connection from the j^{th} node to the i^{th} node is denoted by w_{ij}. The output of the PE corresponds to the firing frequency of the neuron and the weight corresponds to the strength of the synaptic connection between neurons.The inputs to the PE are segregated to various types. This segregation acknowledges that a particular input connection may have one of several effects. An input connection may be excitatory or inhibitory. For example, in our models excitatory connections have positive weights and inhibitory connections have negative weights. Each PE determines a net input value based on all its input connection. We typically calculate the net input by summing the input values, gated (multiplied) by their corresponding weights.

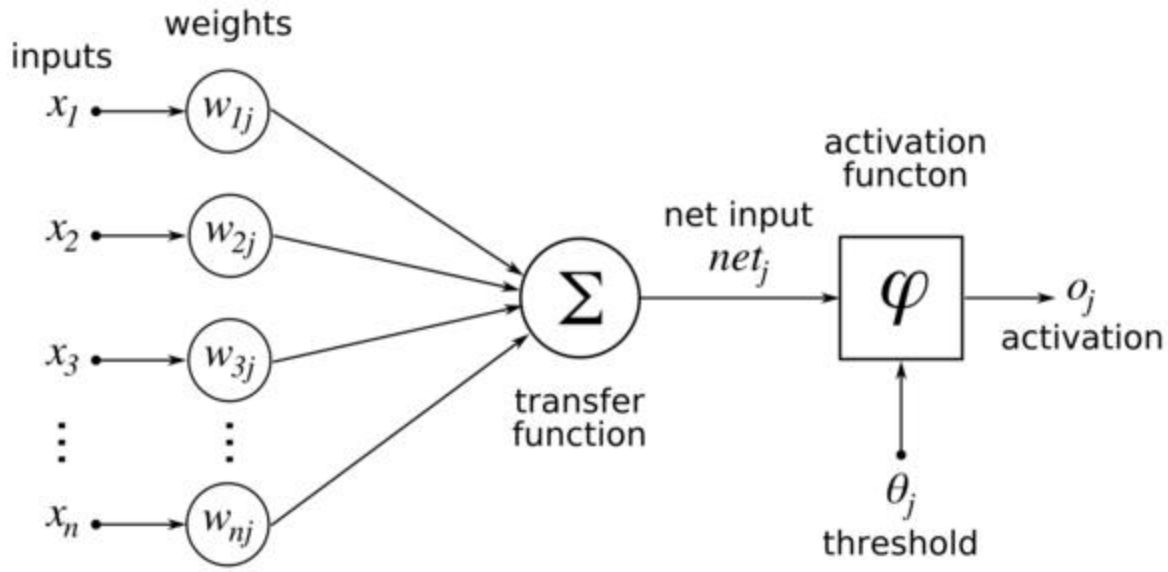

Figure 2.10: The Artificial Neuron

2.8.2 Models

Neural network models in artificial intelligence are usually referred to as artificial neural networks (ANNs); these are essentially simple mathematical models defining a function.

Each type of ANN model corresponds to a *class* of such functions.

Y = f(X) where

– X is a set of numeric inputs

– Y is a set of numeric outputs

– **f()** is an unknown functional relationship between the input and the output

The ANN must approximate f () in order to find the appropriate output for each set of inputs.

Activation Function

Activation function acts as a squashing function, such that the output of a neuron in a neural network is between certain values (usually 0 and 1, or -1 and 1). In general, there are three types of activation functions, denoted by Φ(.). First, there is the Threshold Function which takes on a value of 0 if the summed input is less than a certain threshold value (v), and the value 1 if the summed input is greater than or equal to the threshold value.

$$f(x) = \begin{cases} 1\,, & v \geq 0 \\ 0\,, & v < 0 \end{cases} \qquad 2.11$$

Secondly, there is the Piecewise-Linear function. This function again can take on the values of 0 or 1, but can also take on values between that depending on the amplification factor in a certain region of linear operation.

Thirdly, there is the sigmoid function. This function can range between 0 and 1, but it is also sometimes useful to use the -1 to 1 range. An example of the sigmoid function is the hyperbolic tangent function.

$$\phi(v) = \tanh\frac{v}{2} = \frac{1-e^{-v}}{1+e^{v}} \qquad 2.12$$

An artificial neural network comprises of a collection parallel processing units connected with each other by decision weights. Even though all artificial neural networks are constructed from this basic building block the fundamentals may vary. The process of designing a neural network is an iterative process. The developer must go through a period of trial and error in the design decisions before coming up with a satisfactory design. The design issues in neural networks are complex and are the major concerns of system developers.

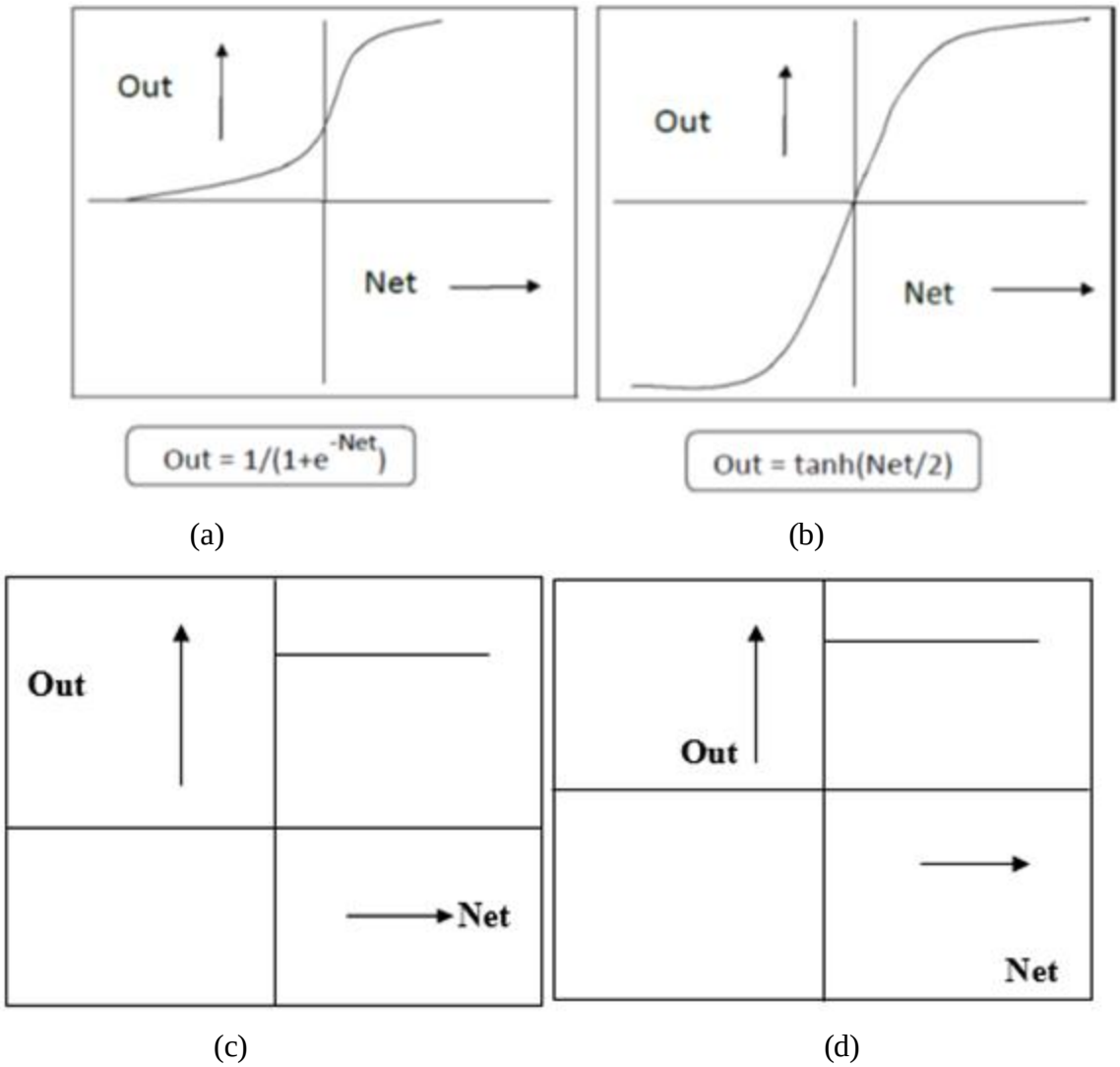

Figure 2.11: Common Non-linear Transfer Functions used for Synaptic Inhibition. Soft non- linearity: (a) Sigmoid and (b) Tanh; Hard non-linearity: (c) Signum and (d) Step.

Designing a neural network consists of the following steps:

• Arranging neurons in various layers.

• Deciding the type of connections among neurons fo r different layers, as well as among the neurons within a layer.

• Deciding the way a neuron receives input and prod uces output.

• Determining the strength of connection within the network by allowing the network learns the appropriate values of connection weights by using a training data set.

Biologically, neural networks are constructed in a three dimensional way from microscopic components. These neurons seem capable of nearly unrestricted interconnections. This is not true in any man-made network. Artificial neural networks are the simple clustering of the primitive artificial neurons. This clustering occurs by creating layers, which are then connected to one another as shown in Figure 2.11. How these layers connect may also vary. Basically, all artificial neural networks have a similar structure of topology. Some of the neurons interface the real world to receive its inputs and other neurons provide the real world with the network's outputs. All the rest of the neurons are hidden from view.

Figure 2.12 **(**with one hidden layer) shows that the neurons are grouped into layers. The input layer consist of neurons receive from the external environment. The output layer consists of neurons that communicate the output of the system to the user or external environment. There are usually a number of hidden layers between these two layers. When the input layer receives the input its neurons produce output, which becomes input to the other layers of the system. The process continues until a certain condition is satisfied or until the output layer is invoked and fires their output to the external environment.

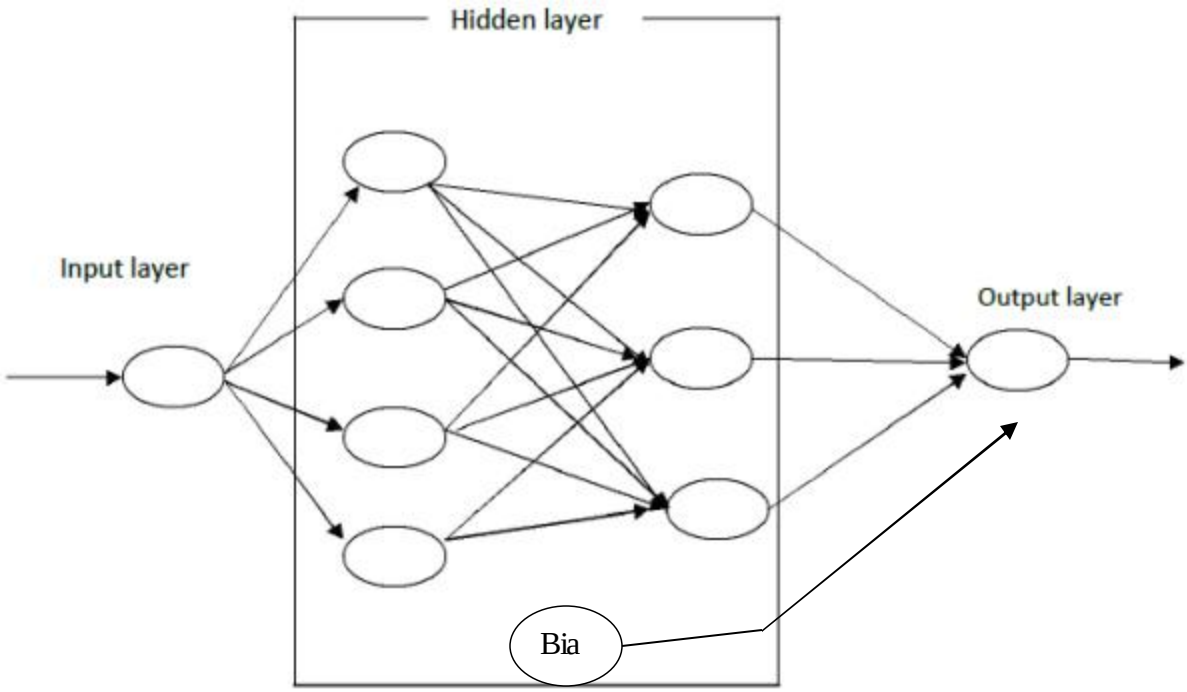

Figure 2.12: Basic Neural Network Structure

To determine the number of hidden neurons the network should have to perform its best, one are often left out to the method trial and error. If the hidden numbers of neurons are increased too much there will be an over fit, that is the net will have problem to generalize. The training set data will be memorized making the network useless on new data sets (Shetty and Chellam, 2003).

2.8.3 Applications of Neural Network

Emulation of biological system computational structures may yield superior computational paradigms for certain classes of problems. Among these are the classes NP-hard problems, which include labeling problems, scheduling problems, search problems and other constraint satisfaction problems, etc. A comprehensive application for ANNS may be provide as below:

a) Image processing and computer vision, processing, segmentation and analysis, stereo vision, processing and understanding of time varying images.
b) Signal processing, including seismic signal analysis and morphology.
c) Pattern recognition, radar signal classification and analysis, speech recognition, fingerprint identification character recognition and handwriting analysis.
d) Medicine, including electrocardiographic signal analysis and understanding, diagnosis of various diseases and medical image processing.

e) Military systems, including undersea mine detection, radar clutter classification, tactical speaker identification.
f) Financial systems, including stock market analysis, real estate appraisal, credit card authorization and security trading.
g) Artificial intelligence, including adductive systems and implementations of expert systems.
h) Power systems, including system state estimation, transient detection and classification, fault detection and recovery, load forecasting and security assessment.
i) Oil and Gas Exploration, including the excavation oil and natural gas wells in the ground.
j) Machine Diagnostics; include the detection of fault in the machine.
k) Artificial intelligence can be used in speech recognition as the speech input signals are mapped to the phoneme regions, the output units can be connected to the appropriate typewriter key to construct the phonetic type writer.

From the literature survey, following grey areas have emerged:

1. Various authors have studied the effect of various operating parameters like feed temperature, permeate pressure, feed flow rate and feed salt concentration on permeate flux and salt rejection, However, in literature no comparative study was observed under same operating condition to investigate the suitability of different membrane, made of different materials and different pore sizes, which is essential to determine the efficiency of membrane under large usage.

2. Few authors have studied the effect of feed flow rate and permeate pressure on specific energy consumption on vacuum membrane distillation for desalination. However, the effect of feed bulk temperature and feed salt concentration and membrane based parameter like pore size and membrane material was not seen in literature. The feed bulk temperature and feed salt concentration also plays a vital role in specific energy consumption beside feed flow rate and permeate pressure. Moreover, membrane materials also affect the specific energy consumption which needs to be investigated.

3. Simultaneous comparison of RO & VMD for desalination was not observed in literature in terms of energy consumption and recovery.

In view of the above gaps/hypothesis, objectives of the research work in the current study are as follows:

1. To perform design of experiment (DOE) and ANOVA for determining the optimum parameters, membrane suitability and percentage contribution of operating parameters over response like permeate flux, salt rejection and specific energy consumption for both membrane (PTFE & PVDF) of same pore size and different pore size.
2. To study the effects of various operating parameters like feed temperature, feed flow rate, feed concentration & membrane based parameters like pore diameter, membrane materials on permeate flux, salt rejection &energy consumption for VMD.
3. To study the effect of usage time on membrane scaling /fouling using scanning electron microscope (SEM) technique.
4. To develop the heat transfer correlation for VMD using Newton's method.
5. To develop the ANN model using MATLAB and Mathematical model (Upadhyaya, et al.2015) and to determine the degree of closeness of both models with the experimental data.
6. To compare the VMD process with RO in terms of specific energy consumption and recovery.

CHAPTER 3. EXPERIMENTAL MATERIALS AND METHODS

A detailed description of different materials and methods used in the present study is presented in this chapter.

3.1 Materials Used:

3.1.1 Distilled Water

Since the ancient time distilled water has been produced using distillation-the process of boiling the water in a pot or still, and then the collection of condensate. When the water evaporates and its vapours are condensed, distilled water is obtained which is free from impurities. Harmful microbes as well as harmless and beneficial minerals are removed. Distillation purifies the water to such extent which only filtration cannot do. Distilled water has various applications such as in industries and laboratories etc. Some important properties of water are given in Table 3.1. The distilled water for this experiment was collected from the distillation assembly available in biotechnology and bioprocessing engineering lab which consists of mainly three componentsRound Bottom Distilling flask, Condenser and Collector. Figure 3.1illustrated a typical laboratory distillation setup.

Table 3.1: Physical properties of water

Molecular formula	H_2O
Molar mass	18.02 g/mol
Appearance	White solid or almost colorless, transparent, with a slight hint of blue, crystalline solid or liquid
Odour	Odorless
Density	1000 kg/m^3= 1 g/cm^3, liquid (4 °C)
Melting point	0 °C, 32 °F, 273.15 K
Boiling point	99.98 °C, 211.97 °F, 373.13 K
Viscosity	0.001 Pa s at 20 °C
Thermal Conductivity	0.58 W/m K

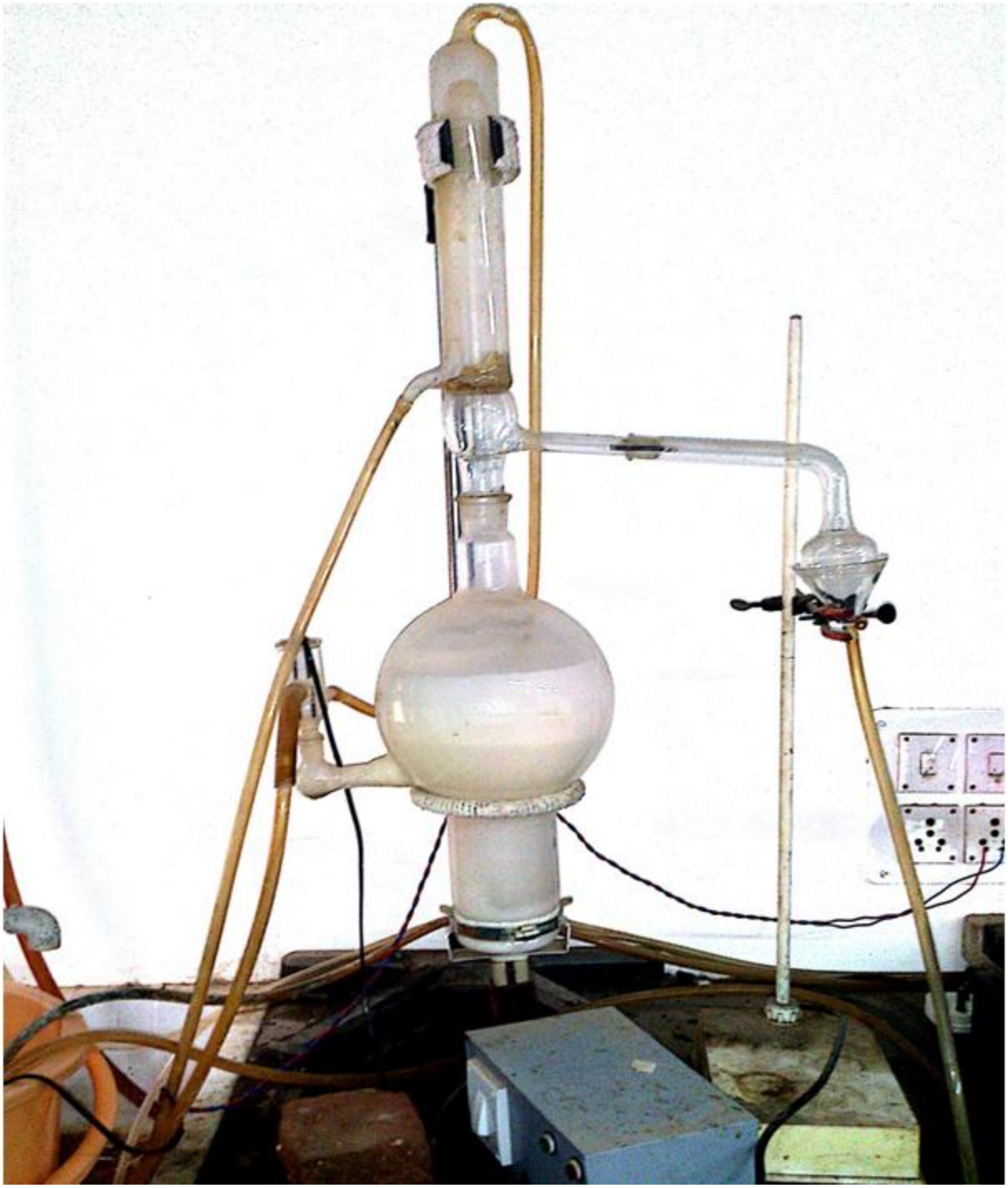

Figure 3.1: Laboratory distill water setup

3.1.2 Sodium Chloride (NaCl)

Sodium chloride, also known as salt, common salt, table salt or halite, is an ionic compound with the formula NaCl, representing equal proportions of sodium and chloride. Sodium chloride is the salt most responsible for the salinity of the ocean and the extracellular fluid of many multicellular organisms. As the major ingredient in edible salt, it is commonly used as a condiment and food preservative. The structure of sodium chloride is shown inFigure 3.2.

Figure 3.2: Structure of Sodium Chloride

Pure NaCl make of Merck was purchased from local market Jaipur. The properties of pure sodium chloride are given inTable 3.2.

Table 3.2: Physical Properties of Pure Sodium Chloride

Molecular formula	NaCl
Molecular weight – NaCl	58.44 g/mol
Appearance	Colorless Crystals
Odor	Odorless
Atomic weight - Na	22.99 (39.34%)
Atomic weight - Cl	35.45 (60.66%)
Density	2.17 g/cm^3
Specific gravity	2.1 - 2.6
pH of aqueous solution	Neutral
Solubility in water	359 $g\ l^{-1}$

3.1.3 Sodium Fluoride:

Sodium fluoride is a colorless solid; it is a source of the fluoride ion in diverse applications. Sodium fluoride is less expensive and less hygroscopic than potassium fluoride. The pure sodium fluoride was purchased from the local market, and its properties are given inTable 3.3. The permissible limit of F^- in water is 1ppm.

Table 3.3Physical Properties of Sodium Fluoride

Molecular formula	NaF
Molar mass	41.99 g/mol
Appearance	White solid
Odor	Odorless
Density	2.56 g/cm^3

3.2 Experimental Setup

In this study, a lab scale vacuum membrane distillation setup was fabricated. The schematic diagram of the experimental setup is shown in Figure 3.3. Flat sheet hydrophobic micro-porous PTFE and PVDF membranes with 90 mm were used for the experiments. The feed water was heated to required temperature 45-65ºC using a heating apparatus at the base of the feed tank. The feed temperature was monitored using a capillary type heating thermostat element. The feed solution was then pumped from feed tank using a feed pump to the membrane unit. The flow rate was regulated using a gate valve and the excess flow was bypassed using a UPVC solid valve to keep the feed flow rate constant. The feed was circulated through the membrane module. The membrane module comprised of a flat of different flat sheet membranes used in the module are mentioned in Table 3.4. The feed flow rate was measured using a Rota meter installed before the membrane unit. The temperature of fluids at inlet and outlet were monitored using digital thermometers. A vacuum pump was installed at the base to create the required vacuum at the permeate side by virtue of which the partial pressure difference across the membrane was maintained. The electrical energy consumed by the heating and pumping systems were measured by the electric meters.

A condensation unit (Helical coil Borosil glass condenser) was used at the permeate side to condense the vapor coming from the membrane unit. A cold water reservoir was housed in the setup to supply cold water for the condensation process. A permeate receiver (Borosil, 1000 ml capacity) was used to collect the pure water exiting the condensation unit. A pressure gauge (Gluck India Mfg. Co.) was used to measure the vacuum created and a vacuum release valve was used to vary the vacuum level.

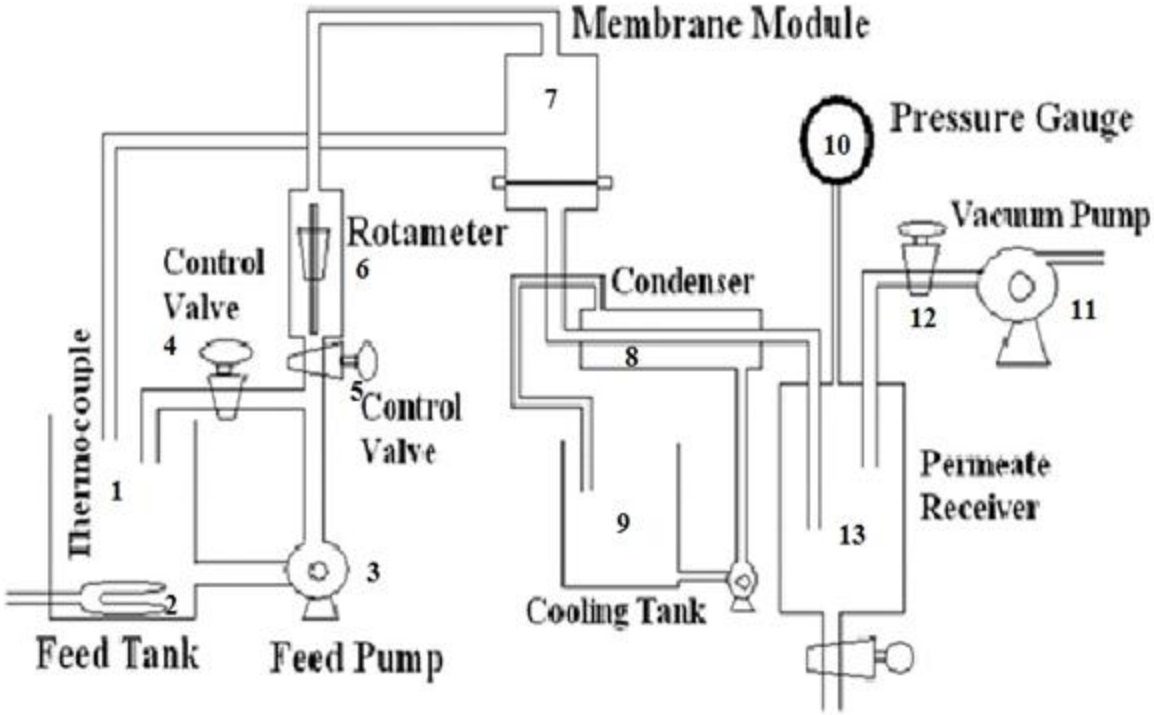

Figure 3.3: Schematic Diagram of VMD Set Up

The schematic diagram of VMD consists the following components

1. Feed Tank
2. Thermocouple
3. Feed pump
4. Bypass control valve
5. Feed Flow control valve
6. Rota meter
7. Membrane module
8. Condenser
9. Cooling water tank
10. Vacuum gauge
11. Vacuum pump
12. Vacuum control valve
13. Permeate receiver

(a) Experimental Setup of VMD

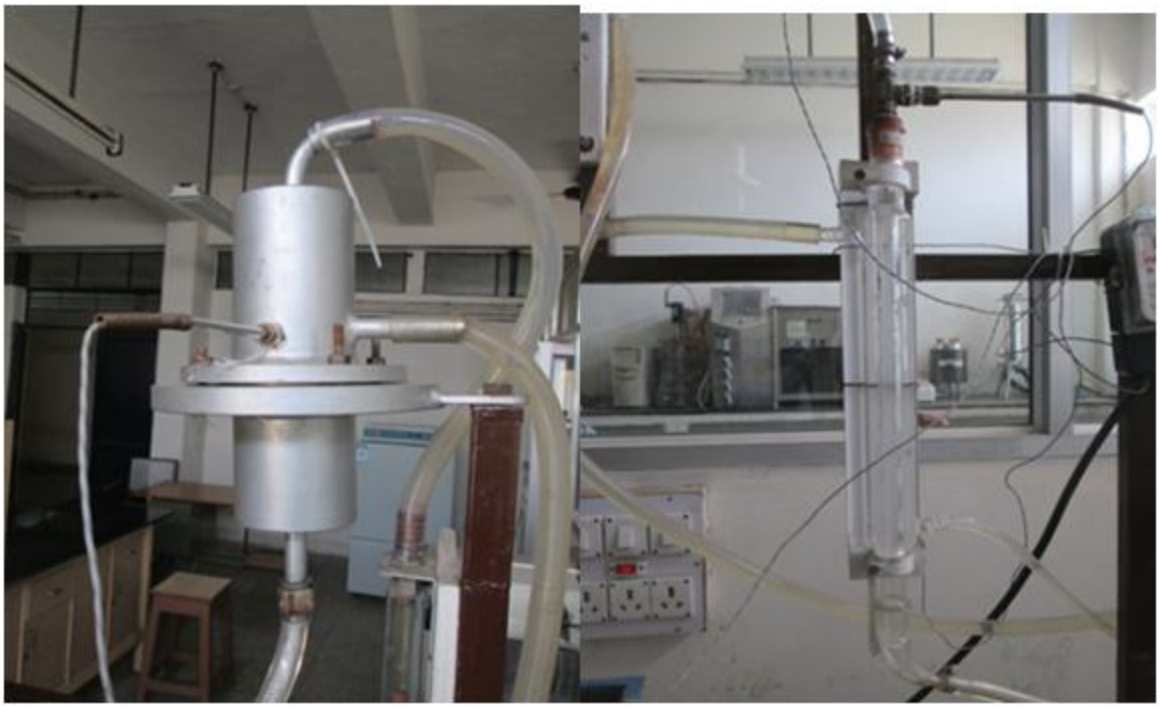

(b): Membrane Module of VMD Setup(c) Permeate Condenser

(d) Feed Tank **(e) Permeate Receiver**

(f) Energy meters (g) Control Board

Figure 3.4: Pictorial Diagram of VMD Setup

3.3 Experimental procedure

The procedures adopted for conducting experiment for desalination by VMD setup areas follows:

1. The experiments of VMD were carried out using a hydrophobic PTFE and PVDF micro-porous flat sheet membranes.
2. The aqueous feed solution of salts/(Na^+Cl^-) was prepared and continuously fed through a feed tank to the membrane module by feed pump.
3. On the permeate side of the membrane module, the vacuum pump was connected.
4. The permeate water vapor was condensed continuously in a condenser.
5. The membrane flux was measured by collecting permeate in a graduated receiver.
6. The temperature controller equipped with heater was connected to maintain the temperature of the feed solution in the feed tank.
7. Electrical conductivity of the distillate permeate was measured using a conductivity meter.

The maximum limit of feed side volumetric feed flow rate is to be decided as the liquid entry pressure (LEP) of membrane material of different pore size. The setup was run at various feed flow rate from 1 to 10 lpm & it was found that the feed side liquid pressure is varying 0.17 bar to 1.22 bar. The membrane properties are described in Table 3.4

Table 3.4: Properties of membranes

Properties	Specifications			
Membrane material	PTFE	PTFE	PVDF	PVDF
Surface property	Hydrophobic			
Diameter, mm	90			
Effective membrane diameter, mm	52			
Pore size, µm	0.22	0.45	0.22	0.45
Thickness, µm	175	175	125	125
Porosity %	70	85	70	85
Liquid Entry Pressure, bar	2.80	1.24	2.04	1.05
Effective membrane area, m^2	0.00212			
Maximum operating temperature, °C	130	130	90	90
Supplier	Millipore			

3.4 Calibration of conductivity meter for Analysis of NaCl Solution

Conductivity is a measure of how well a solution conducts electricity. Water with absolutely no impurities (which does not exist) conducts electricity very poorly. The impurities in water increase its conductivity. Thus, by measuring the conductivity of water, degree of impurity can be estimated. The current is carried almost entirely by dissolved ions. The ability of an ion to carry current dependent onits charge and its mass/size. Ions with more charge conduct more current; larger ions conduct less.

The conductivity is measured using conductivity meter. The actual amount of electricity that a given water solution conducts change with distance between the electrodes and water temperature. Conductivity is expressed in units of mhos. The meter has a probe with two electrodes, usually 1 centimeter apart. Most of the modern ones sense the temperature as well as electronically correct for its effects. Since the meter gives a reading that is corrected for temperature and electrode separating distance, the number is called "specific conductance," expressed in mhos per centimeter at 25° C. The SI unit of conductivity is siemen (S) named after the French physicist, and equivalent to the mho. Thus 1 microsiemen per meter (mS/m) is equivalent to 100 mmho/cm. Very often, a meter will read out in mS/cm or mS/cm (or just mS or mS which are assumed to be per centimeter). Pure water has a specific conductance of about one millionth of a mho/cm. Wells and lakes in Connecticut usually have a specific

conductance of about 50 to 500 times that. To make these numbers easy to write, usually a unit of micromhos per centimeter (mmhos/cm) is used. Thus, laboratory pure water is around 1 mmho/cm; tapwater is usually around 50 to 500 mmhos/cm.The conductivity was measured by electrical conductivity meter of Toshniwal (TCM15^{+}) make shown in Figure 3.5. The calibration curve is plotted inFigure 3.6.

a) Standard solutions of 1, 5, 10, 50, 100, 500, 1000,5000,10000,15000,20000,25000,30000,35000,40000,45000, 50000, 55000 ppm NaCl solution were prepared.

b) The electrodes in each of the standards were immersed in turn, starting with the least concentrated, and system was calibrated.

c) The conductivity of the standard was written down, and the calibration curve was plotted.

d) Permeate samples were same as the standard solutions. The electrodes were immersed and reading of the unknown conductivity was displayed on the meter.

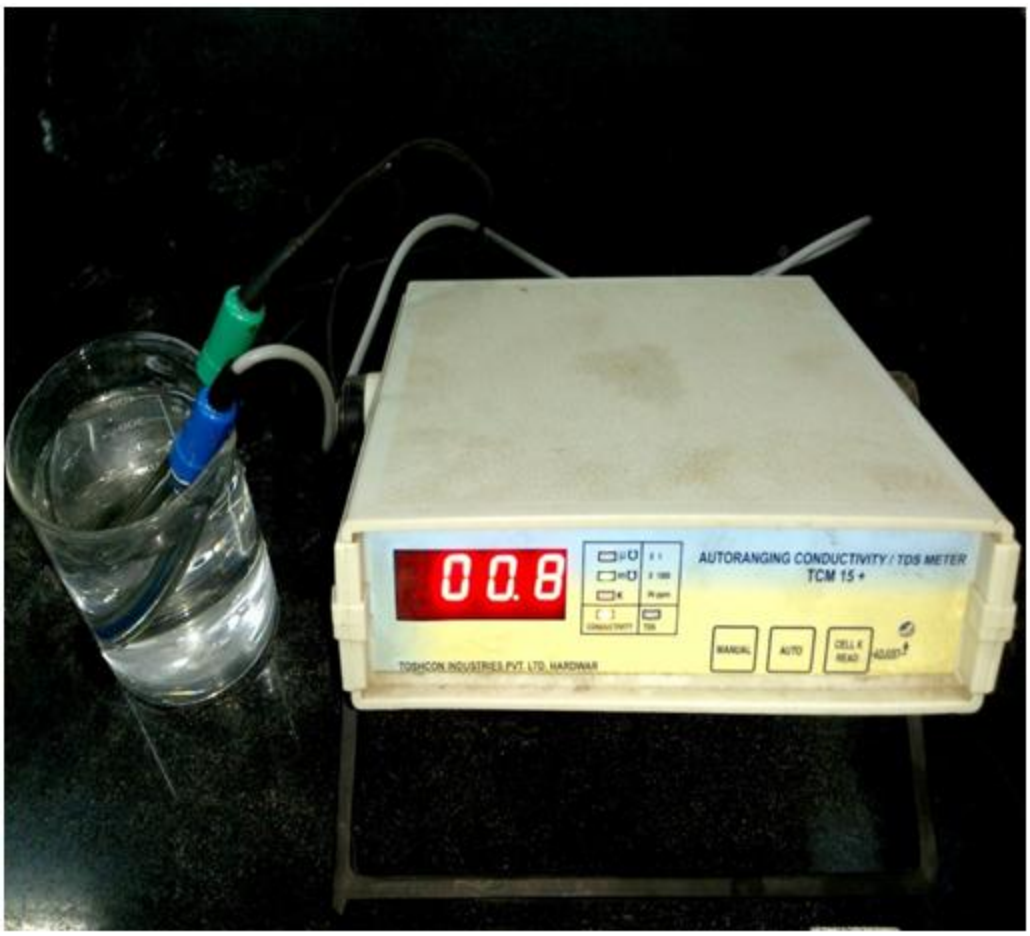

Figure 3.5: Conductivity Meter

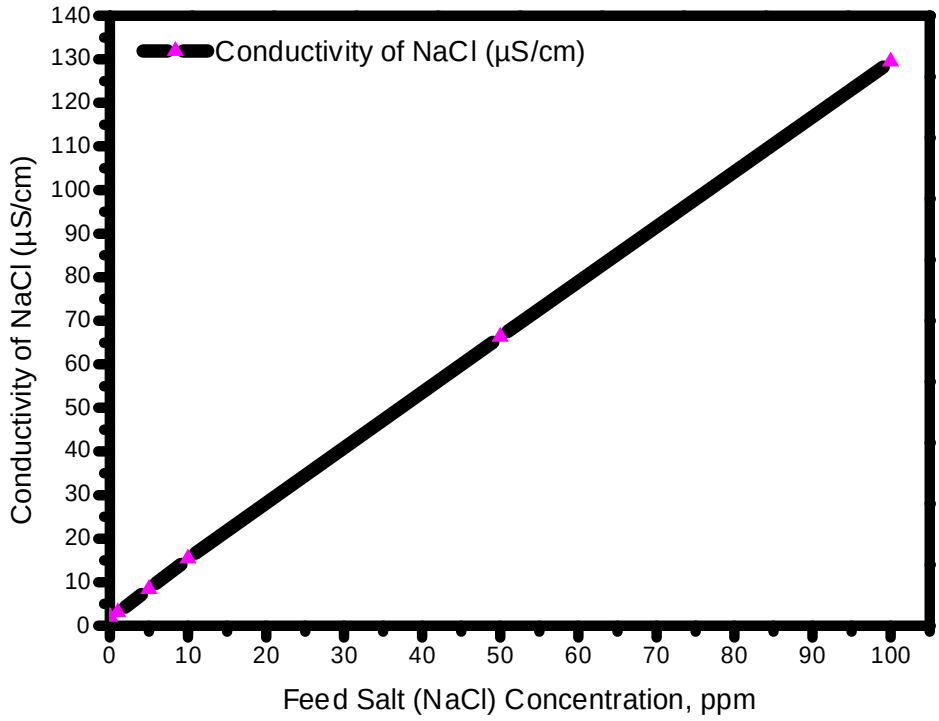

(a)

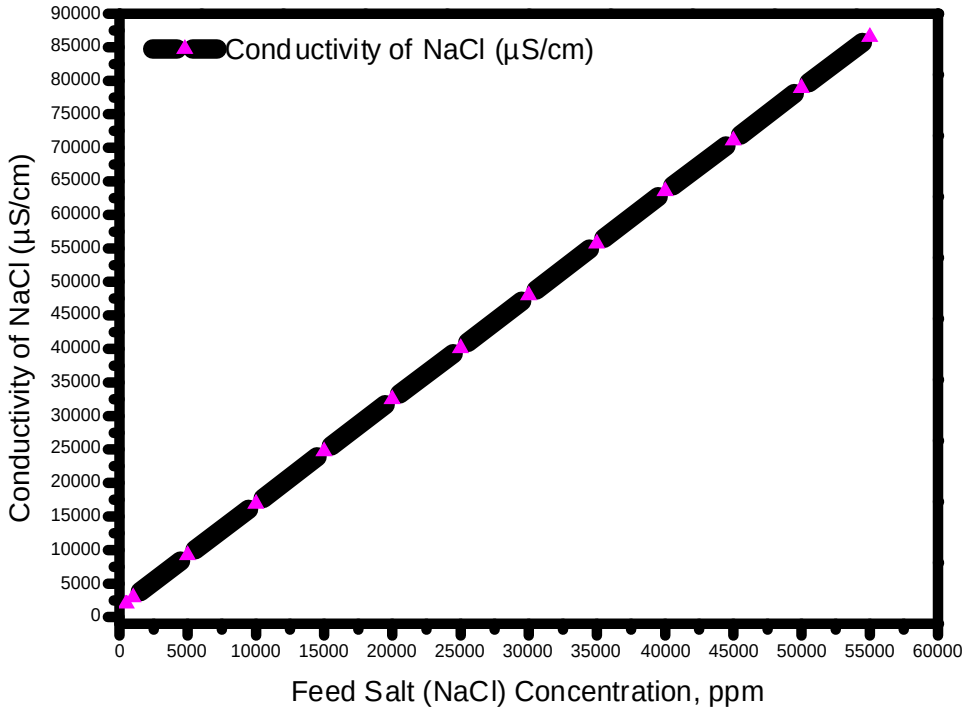

(b)

Figure 3.6: Calibration Curve (a) enlarged view in the range 0-100 ppm (b) for concentration range 0-60000 ppm

3.5 Characterization of Membrane by Microscopic Method

A scanning electron microscope (SEM) are used to characterize membrane shown in Figure 3.8. It is a type of electron microscope that produces images of a sample by scanning with a focused beam of electrons. The electrons interact with atoms in the sample, producing signals that can be detected, which contains information about the sample's surface topography and composition. The beam's position is combined with the signal to produce an image. SEM can have resolution finer than 1 nanometer. Specimens can be observed in high vacuum, in low vacuum, and in wet conditions. The most common mode of detection is by secondary electrons emitted by atoms excited by the electron beam. The number of secondary electrons depends on the angle between the surface and the beam. The types of signals produced by SEM include secondary electrons, characteristic X-rays, back-scattered electrons (BSE), light (cathodoluminescence) (CL). Due to very narrow electron beam, SEM micrographs produce a large depth of field yielding a characteristic 3D appearance, which is useful for understanding the surface structure of a sample. BSE images can provide information about the distribution of different elements in the sample.

3.5.1 Scanning process and image formation

Electronic amplifiers are used to amplify the signals, which are displayed as variations in brightness on a computer monitor. Each pixel is synchronized with the position of the beam on the specimen in the SEM, and the resulting image is therefore a distribution map of the signal emitted from the scanned area of the specimen. The hydrophobic PTFE and PVDF membranes morphology was characterized by SEM using the following two steps:

i. Gold coating of membrane sample was done by spitter coater
ii. The gold coated sample was mounted in the SEM holder
iii. SEM analysis was performed at different level of intensity for examine the morphology of the membrane.
iv. The sample was placed to the SEM chamber shown in Figure 3.8

Figure 3.7: Scanning Electron Microscope

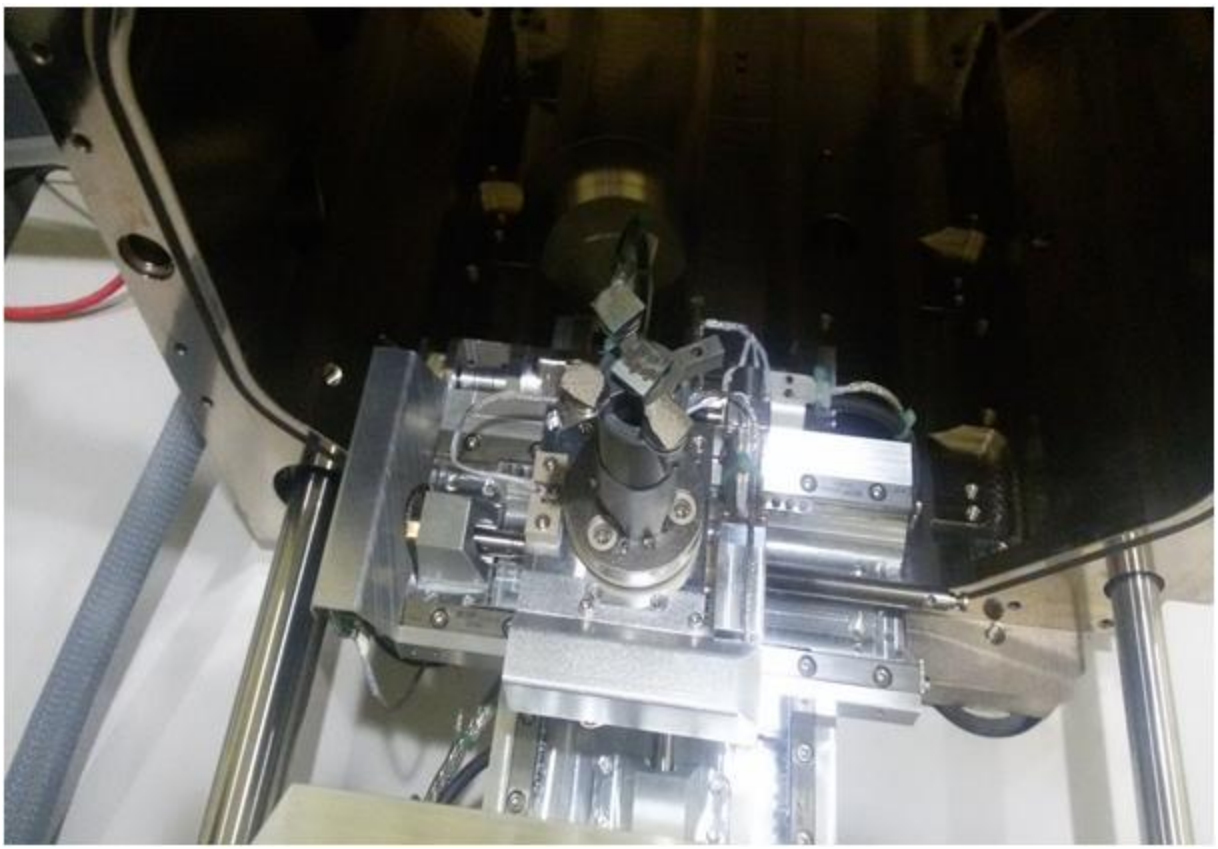

Figure 3.8: SEM Opened Sample Chamber

3.6 Calculation of Permeate Flux, Salt Rejection and Specific energy consumptions.

The MD flux (N, kg/m^2 h) is calculated by equation (3.1):

$$N_{\exp} = \frac{V \times \rho}{A \times t} \qquad 3.1$$

Where V is volume of permeate water (l); ρ is density of permeate water (kg/l); A is effective membrane area (m^2) and t is the running time of VMD.

The concentration of ionic species in the feed water (C_1, ppm) and in permeate water (C_2, ppm) were calculated by the conductivity meter. The percentage removal (% R) of the species was calculated from equation (3.2):

$$R = \left(\frac{C_1 - C_2}{C_1} \right) \times 100 \qquad 3.2$$

The Energy Consumption (EC, kWh/m^3) is calculated by the equation (3.3):

Energy Consumption (EC) =Total Energy Consumption/ Total Permeate Volume3.3

CHAPTER 4. RESULTS AND DISCUSSION

A detailed description of results obtained out of experimental investigations and its validation with existing mathematical models and subsequent discussion/ interpretation along with membrane characterization, Taguchi's Optimization, and recovery calculation have been given. Moreover, effects of various parameters on specific energy consumption were also discussed in this section.

VMD experiments were performed using NaCl solution as feed. Various parameters *viz* temperature, flow rate, concentration, membrane materials (PTFE & PVDF) and pore sizes were selected to investigate the process outcome in terms of permeate flux and specific energy consumption. In this work, temperature was varied from 45-65°C, flow rate from 1 to 10 lpm, concentration of feed salt from 5000-50000 ppm under constant permeate side pressure of 9.0 kPa. Moreover, to examine the process in terms of membrane based parameters, different membranes made of PTFE and PVDF were used and compared. The membrane were taken of two different pore size (0.22 and 0.45μm) in this experimental work. The percentage rejection were calculated by measuring the salt concentration of feed and permeate using an electrical conductivity meter of Toshniwal (TCM15$^{+)}$ make.

4.1 Taguchi Optimization for Experimental Permeate Flux

Taguchi design philosophy continually strives to reduce variation around the target value. This design methodology involves two steps; the first step towards improving quality is to achieve the population distribution as close to the target value as possible. To achieve this, Taguchi designed experiments using especially constructed tables known as "Orthogonal arrays (OA)" (Mohammadi and Safavi, 2009). The use of these tables make the design of experiments very easy and consistent, the second objective was to develop standard techniques for analysis of results. Through the use of "outer arrays" Tahuchi devised an effective way to study the influence of noise factors (uncontrollable sources) such as weather conditions; machinery wears etc. with the least number of repetitions. The end result is the robust design affected minimally by noise factors. Taguchi experimental design usually involves attempting to optimize a process which can involve several parameters (e.g., time, temperature, chemical composition etc.) at several levels. Taguchi L_{25} (5^3) OA_{25} involves three process parameters in five levels. The 25 in the designation OA_{25}represents the number of rows, which is also the number of treatment conditions. Each row, represents a trial

condition with factor levels indicated by numbers in the rows. The levels of the factors are feed bulk temperature (45, 50,55,60, 65 °C), feed flow rate (2, 4, 6, 8, 10 lpm) and salt concentration (5000, 15000, 25000, 35000, 50000ppm) respectively shown in Table 4.1 to Table 4.4as orthogonal array consisting parameters and its level with the corresponding permeate flux. Each run was conducted twice to study the effects of noise sources on the performance of the VMD setup.

Table 4.1: Taguchi Orthogonal Array for PTFE Membrane (0.22 µm pore size)

Temperature (°C)	Flow Rate (lpm)	Feed Concentration (ppm)	Permeate Flux ($Kg/m^2 \cdot hr$)		Mean	SN Ratio
			Trail 1	Trail 2		
45	2	5000	9.3	9.7	9.5	19.56
45	4	15000	10.1	10.3	10.2	20.19
45	6	25000	10.7	10.9	10.8	20.70
45	8	35000	11.1	11.3	11.2	20.99
45	10	50000	10.2	10.2	10.2	20.17
50	2	15000	15.6	15.4	15.5	23.80
50	4	25000	14.8	14.6	14.7	23.32
50	6	35000	14.3	13.9	14.1	22.99
50	8	50000	12.9	12.7	12.8	22.13
50	10	5000	26.7	27.1	26.9	28.61
55	2	25000	23.3	23.1	23.2	27.29
55	4	35000	21.2	20.8	21.0	26.44
55	6	50000	16.5	16.9	16.7	24.46
55	8	5000	39.3	39.1	39.2	31.86
55	10	15000	37.5	37.9	37.7	31.52
60	2	35000	33.7	33.3	33.5	30.49
60	4	50000	29.3	29.1	29.2	29.30
60	6	5000	57.9	58.3	58.1	35.29
60	8	15000	55.8	56.4	56.1	34.98
60	10	25000	53.98	54.02	54.0	34.65
65	2	50000	44.9	44.7	44.8	33.03
65	4	5000	85.5	85.7	85.6	38.65
65	6	15000	80.7	80.5	80.6	38.13
65	8	25000	77.7	77.9	77.8	37.82
65	10	35000	88.8	89	88.9	38.98

The signal- to- noise (S/N) ratio contribution were chosen as a proactive equivalent to the reactive loss function and to analyze the outcomes. For robust (optimal) design, the S/N ratio

represented by equation 4.1 should be maximized for system optimization so that response (permeate flux) will get maximized.

$$S/N = \frac{Amount\ of\ energy\ for\ \text{int}ended\ function}{Amount\ of\ energy\ wasted} = \frac{signal}{noise} = -10\log\left(\frac{1}{n}\sum_{i=1}^{n}\frac{1}{y_i^2}\right) \quad (4.1)$$

Where, n is the number of experiments and $y_i$is the response (permeate flux) of each set of experiment. In this work, the desalination experiment was performed through VMD set up and the idea was focused for desalination by VMD to increase the trans-membrane permeate flux, salt rejection and minimize the energy consumption using robust design process parameter optimization methodology

Table 4.2: Taguchi Orthogonal Array for PVDF Membrane (0.22 µm pore size)

Temperature (°C)	Flow Rate (lpm)	Feed Concentration (ppm)	Permeate Flux (Kg/m^2·hr)		Mean	SN Ratio
			Trail 1	Trail 2		
45	2	5000	10.3	10.10	10.2	20.16
45	4	15000	10.5	10.90	10.7	20.59
45	6	25000	11.1	11.30	11.2	20.96
45	8	35000	11.7	11.50	11.6	21.28
45	10	50000	10.8	10.60	10.7	20.56
50	2	15000	16.2	16.40	16.3	24.24
50	4	25000	15.3	15.50	15.4	23.73
50	6	35000	14.9	14.70	14.8	23.38
50	8	50000	13.5	13.30	13.4	22.51
50	10	5000	27.7	28.10	27.9	28.92
55	2	25000	23.7	24.10	23.9	27.57
55	4	35000	21.8	21.40	21.6	26.68
55	6	50000	17.5	17.10	17.3	24.77
55	8	5000	39.6	39.40	39.5	31.94
55	10	15000	37.1	37.30	37.2	31.41
60	2	35000	34.4	34.20	34.3	30.69
60	4	50000	29.7	30.10	29.9	29.51
60	6	5000	58.6	58.80	58.7	35.37
60	8	15000	56.9	56.70	56.8	35.08
60	10	25000	54.6	54.80	54.7	34.76
65	2	50000	59.8	60.00	59.9	35.55
65	4	5000	84.6	84.40	84.5	38.54
65	6	15000	85.2	85.00	85.1	38.60
65	8	25000	85.8	85.60	85.7	38.66
65	10	35000	86.7	86.50	86.6	38.75

Table 4.3: Taguchi Orthogonal Array for PTFE Membrane (0.45 µm pore size)

Temperature (°C)	Flow Rate (lpm)	Feed Concentration (ppm)	Permeate Flux ($Kg/m^2 \cdot hr$)		Mean	SN Ratio
			Trail 1	Trail 2		
45	2	5000	27.4	27.2	27.3	28.72
45	4	15000	31.3	31.1	31.2	29.88
45	6	25000	32.3	32.5	32.4	30.21
45	8	35000	33.3	32.9	33.1	30.40
45	10	50000	32.7	33.1	32.9	30.35
50	2	15000	52.4	52.6	52.5	34.40
50	4	25000	52.7	53.1	52.9	34.48
50	6	35000	54.3	54.1	54.2	34.67
50	8	50000	53.4	53.6	53.5	34.57
50	10	5000	71.3	70.9	71.1	37.04
55	2	25000	65.7	66.1	65.9	36.38
55	4	35000	68.7	69.1	68.9	36.76
55	6	50000	66.2	66.4	66.3	36.43
55	8	5000	90.6	90.8	90.7	39.15
55	10	15000	98.7	99.1	98.9	39.91
60	2	35000	99.3	99.5	99.4	39.95
60	4	50000	101.2	101.4	101.3	40.11
60	6	5000	125.5	125.3	125.4	41.96
60	8	15000	130.6	130.8	130.7	42.33
60	10	25000	135.6	135.4	135.5	42.64
65	2	50000	117.3	117.1	117.2	41.38
65	4	5000	147.8	147.6	147.7	43.39
65	6	15000	154.2	153.8	154.0	43.75
65	8	25000	157.7	158.1	157.9	43.97
65	10	35000	163.3	162.9	163.1	44.25

Table 4.4: Taguchi Orthogonal Array for PVDF Membrane (0.45 µm pore size)

Temperature (°C)	Flow Rate (lpm)	Feed Concentration (ppm)	Permeate Flux ($Kg/m^2 \cdot hr$)		Mean	SN Ratio
			Trail 1	Trail 2		
45	2	5000	64.90	64.87	64.93	36.24
45	4	15000	64.60	64.63	64.57	36.21
45	6	25000	62.20	62.29	62.11	35.88
45	8	35000	115.50	115.36	115.64	41.25
45	10	50000	160.70	160.79	160.61	44.12
50	2	15000	87.10	87.15	87.05	38.80
50	4	25000	88.00	88.05	87.95	38.89
50	6	35000	91.80	91.83	91.77	39.26
50	8	50000	150.70	150.65	150.75	43.56
50	10	5000	248.20	248.26	248.14	47.89
55	2	25000	115.60	115.57	115.63	41.26
55	4	35000	112.10	112.15	112.05	40.99
55	6	50000	98.20	98.24	98.16	39.84
55	8	5000	242.10	242.05	242.15	47.68
55	10	15000	287.30	287.25	287.35	49.17
60	2	35000	177.90	177.89	177.91	45.01
60	4	50000	174.70	174.73	174.67	44.85
60	6	5000	232.30	232.34	232.26	47.32
60	8	15000	281.90	281.93	281.87	49.00
60	10	25000	339.80	339.78	339.82	50.63
65	2	50000	295.80	295.82	295.78	49.42
65	4	5000	330.20	330.18	330.22	50.38
65	6	15000	332.50	332.53	332.47	50.44
65	8	25000	371.00	371.02	370.98	51.39
65	10	35000	400.00	399.89	400.11	52.04

4.1.1 Taguchi Approach for Permeate Flux forPTFE membrane (0.22 µm pore size)

The effect of feed bulk temperature on permeate flux and SN ratio is shown inFigure 4.1 and Figure 4.2. From this figure, it is obvious that on increasing feed bulk temperature, the mean permeate flux increases from 10.39 to 75.5 kg/m^2 h and SN ratio increases from 20.32 to 37.32. Therefore, for maximum permeate flux and SN ratio, the suitable value of feed inlet temperature is 65 °C.On increasing the feed flow rate from 2 to 10 lpm, it can be seen from theFigure 4.1 that mean permeate flux increases from 25.29 to 43.54 kg/m^2 h and from Figure 4.2 SN ratio increases from 26.84 to 30.79. Therefore, the suitable value of feed flow rate is found to be 10 lpm. The mean permeate flux decreases from 43.87 to 22.74 kg/m^2 h on increasing the salt concentration from 5000 to 50000 ppm. However, not much variation in SN ratio is observed on increasing the salt concentration. Since, the mean flux & SN ration is greater at lower concentration therefore, lower concentration favours the permeate flux. Hence, at 65°C of feed inlet temperature, 10 lpm of feed flow rate and 5000 ppm of feed NaCl concentration, the suitable permeate flux was found to be 98.0 kg/m^2 h and rejection was found to be nearly 99.9%.

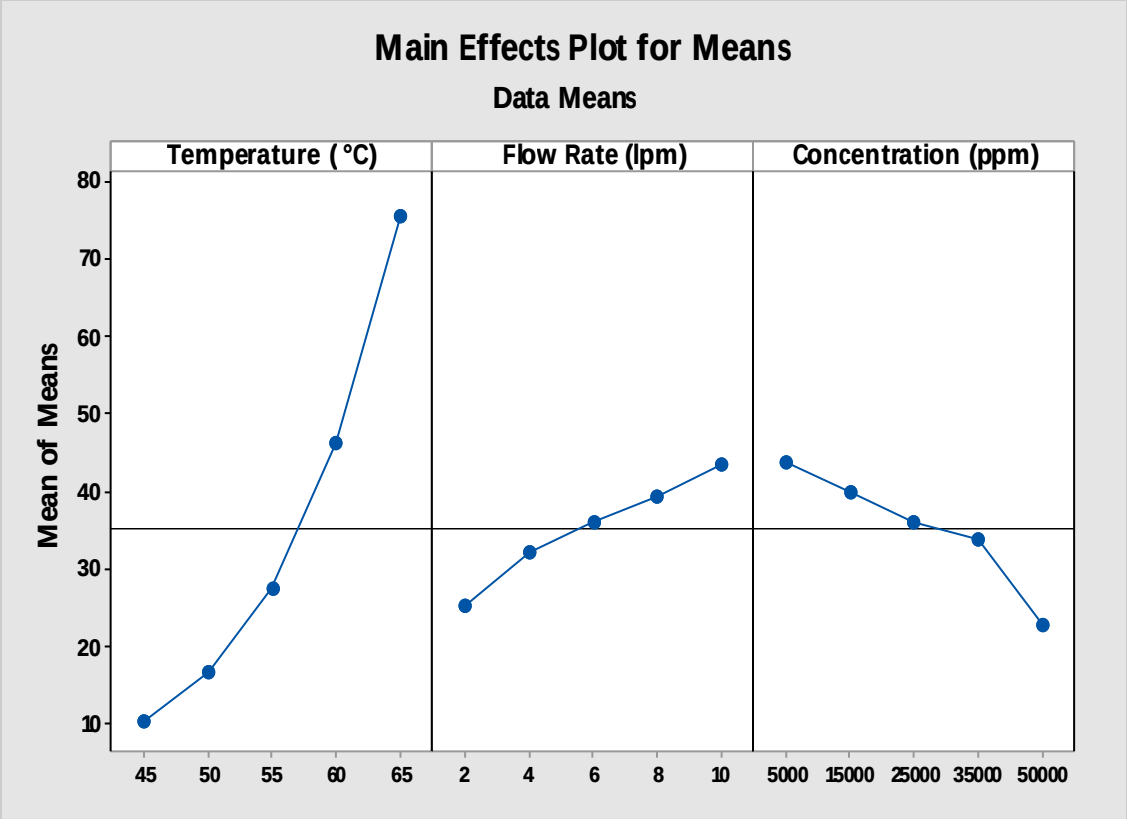

Figure 4.1: Effect of the operating parameters on mean of permeate flux for PTFE membrane (0.22 µm pore size)

Analysis of variance (ANOVA) is also performed on orthogonal experimental data to evaluate the significance of process parameters on permeate flux. Percent contribution of variance can be calculated as dependent on the following equations (Roy 1990; Oktem 2007):

Total degree of freedom, $f_T = nr - 1$ (4.2)

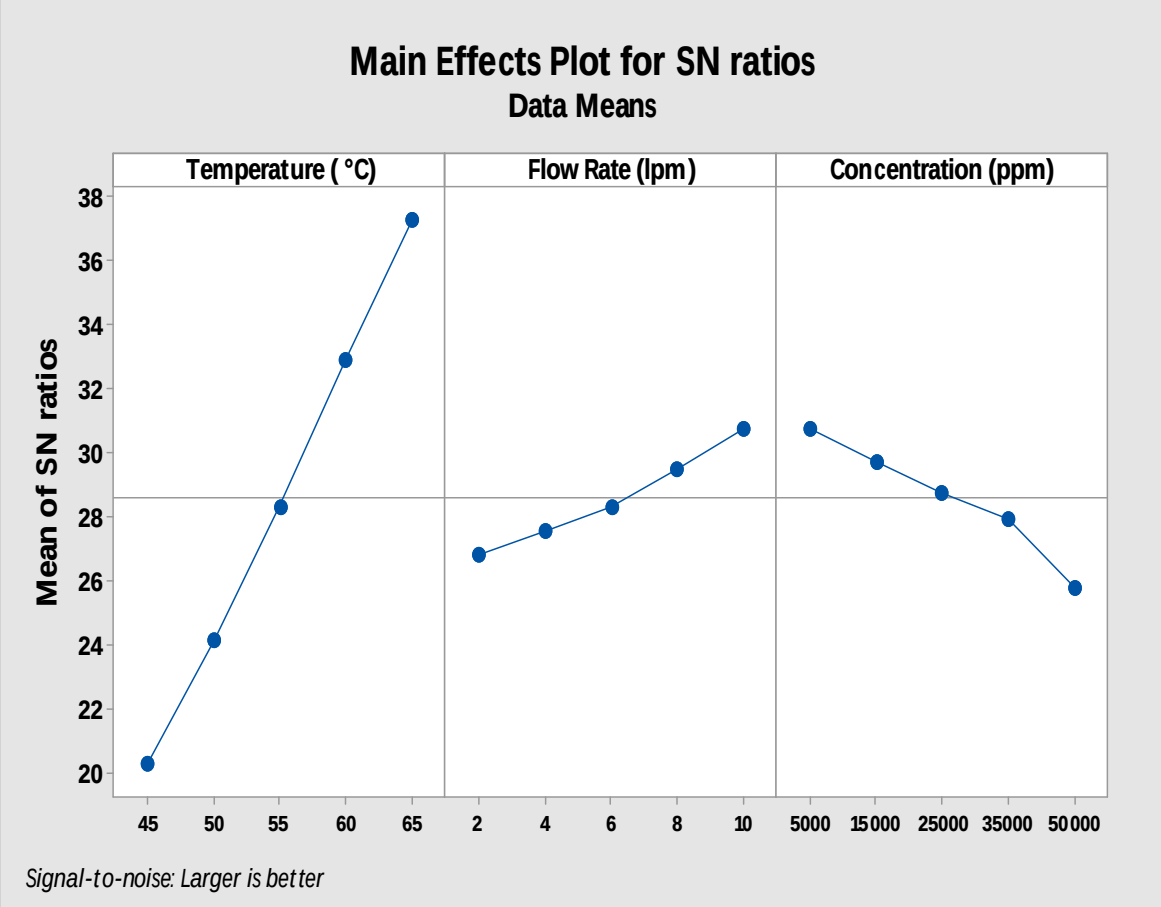

Figure 4.2: Effect of the operating parameters on mean of SN ratio for PTFE membrane (0.22 µm pore size)

Degree of freedom of input variable, $f_j = No.of\ levels - 1$ (4.3)

Degree of freedom of error, $f_e = f_T - \sum_{j=1}^{m} f_j$ (4.4)

Equation Correction factor, $CF = \frac{\left(\sum_{i=1}^{n} y_i\right)^2}{n}$ (4.5)

Total Sum of squares, $SS_T = \sum_{i=1}^{n} y_i^2 - CF$ (4.6)

Where $y_i$is the mean of trials, n is the number of experimental runs, r is the number of repetitions, and m is the total number of input variables.

Sum of aquares of input variables A (Temperature), B (Feed flow rate), C (Feed salt concentration) are:

$$SS_A = A_1^2 / N_{A1} + A_2^2 / N_{A2} + A_3^2 / N_{A3} + A_4^2 / N_{A4} + A_5^2 / N_{A5} - CF \quad (4.7)$$

$$SS_B = B_1^2 / N_{B1} + B_2^2 / N_{B2} + B_3^2 / N_{B3} + B_4^2 / N_{B4} + B_5^2 / N_{B5} - CF \quad (4.8)$$

$$SS_C = C_1^2 / N_{C1} + C_2^2 / N_{C2} + C_3^2 / N_{C3} + C_4^2 / N_{C4} + C_5^2 / N_{C5} - CF \quad (4.9)$$

Where A_1, A_2, A_3, A_4, A_5 are sum of mean values of flux corresponding to temperature of 45, 50, 55, 60, and 65 °C, respectively. Similarly, B_1, B_2, B_3, B_4, B_5, C_1, C_2, C_3, C_4, C_5 can be computed.

Means of squares is given by MS=SS /DOF, where DOF is degree of freedom. F-value is computed by,

$F = MS / MS\ of\ error$ (4.10)

Percentage contribution, $P = SS / Total\ SS$ (4.11)

The results of ANOVA as calculated from the above equations are shown in Table 4.5. It can be observed from this table that feed temperature, feed flow rate and feed salt concentration influence permeate flux by 84.37 %, 5.98% and 7.84% respectively.

Table 4.5: Analysis of variance for percent contribution for experimental permeate fluxfor PTFE membrane (0.22 µm pore size)

Parameter	DF	Adj SS	Adj MS	F-Value	% Contribution
Temperature (°C)	4	13804.5	3451.12	140.11	84.37
Flow rate (lpm)	4	978.7	244.67	9.93	5.98
Concentration (ppm)	4	1282.7	320.67	13.02	7.84
Error	12	295.6	7.13		
Total	24	16361.4			

4.1.2 Taguchi Approach forPermeate Flux for PVDFMembrane (0.22µmpore size)

Similarly, the Taguchi optimization was performed as per Table 4.2for PVDF membrane of pore size 0.22 µm. From the Figure 4.3 and Figure 4.4, it can be observed that mean permeate flux increases exponentially from 10.86 to 80.37 kg/m^2 h and SN ratio value increases linearly from 20.71to 38.02 on increasing the feed bulk temperature from 45 to 65 °C. This may be due to the reason that vapor pressure on membrane feed side increases exponentially as per Antoine relation on increasing the feed bulk temperature which as a result increases the driving force for mass transfer. Therefore, the suitable value of feed inlet temperature is 65 °C at which the mean permeate flux and SN value is found to be highest. In the same way, the most suitable value of feed flow rate and feed salt concentration were found to be 10 lpm and 5000 ppm from the Figure 4.3&Figure 4.4. Hence, the experimental suitable permeate flux is found to be 98.9 kg/m^2 hunder the optimised values *viz* 65°C of feed inlet temperature, 10 lpm of feed flow rate and 5000 ppm of feed NaCl concentration.The rejection in the retentate was found to be 98.0%. ANOVA was performed using *MINITAB 17* over the orthogonal array as given in Table 4.2. The ANOVA results is shown in Table 4.6. It can be observed from the Table 4.6 that feed temperature, feed flow rate and feed salt concentration contributes to permeate flux by 89.64 %, 4.21% and 5.65% respectively.

Table 4.6: Analysis of variance for percent contribution of operating parameters for PVDF membrane (0.22 µm).

Parameter	DF	Adj SS	Adj MS	F-Value	% Contribution
Temperature (°C)	4	15612.3	3903.08	547.23	89.64
Flow rate (lpm)	4	733.3	183.32	25.7	4.21
Concentration (ppm)	4	984.8	246.2	34.52	5.65
Error	12	85.6	7.13		
Total	24	17416			

It can be observed that the percentage contribution of feed temperature on permeate flux is more for PVDF membrane (89.64 %) as compared to PTFE membrane (84.37%) of 0.22 µm pore size. This may be due the fact heat loss through PVDF membrane under the same operating parameters is less compared to PTFE membrane since the thermal conductivity of PVDF membrane is less as compared to PTFE membrane.

However, the percentage contribution of feed flow rate is found to be less for PVDF membrane as compared to PTFE membrane which may be because the effect of

concentration polarization (function of flow rate) on PTFE membrane is less than the PVDF membrane under the same operating condition as the Coefficient of friction of PTFE is less than PVDF membrane. Moreover, the percentage contribution of feed concentration is less for PVDF membrane in contrast to PTFE membrane since activity coefficient for PVDF membrane will become less as the salt deposition on membrane surface will be more for PVDF since the coefficient of friction for PVDF is more than PTFE membrane.

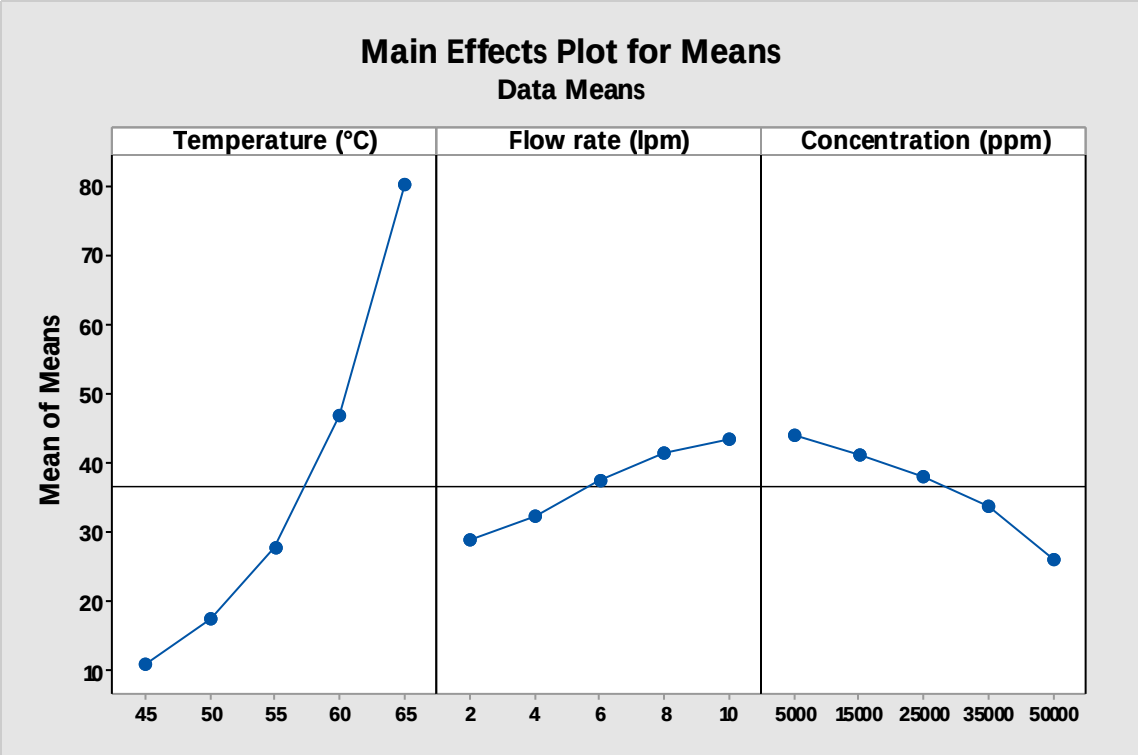

Figure 4.3: Effect of the operating parameters on mean of permeate for PVDF membrane (0.22 µm pore size)

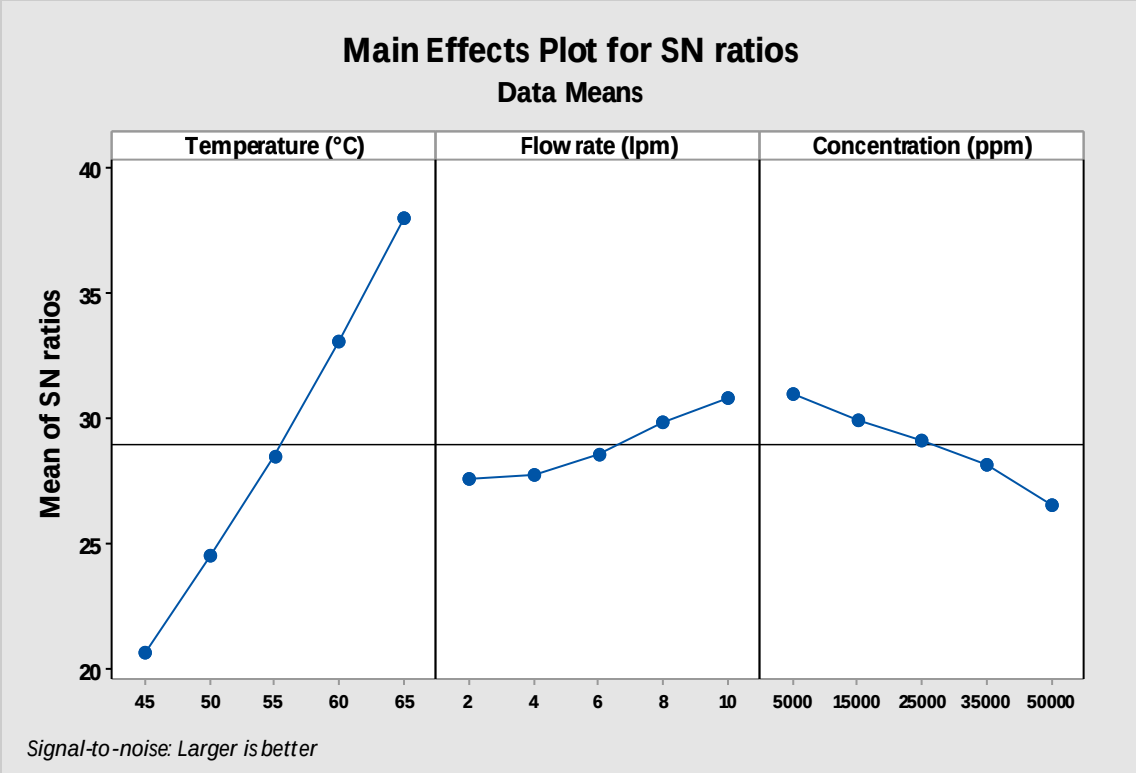

Figure 4.4: Effect of the operating parameters on mean of SN ratio for PVDF membrane (0.22 µm pore size)

4.1.3 Taguchi Approach for Permeate Flux for PTFE Membrane (0.45µm pore size)

The Tahuchi optimization was performed for PTFE membrane of 0.45 µm pore diameter. the suitable operating value on the basis of high mean permeate flux and mean SN ratio was found to be feed temperature of 65 °C, feed flow rate of 10 lpm, feed salt concentration of 5000 ppm as shown in Figure 4.5and Figure 4.6. Under these operating condition, the experimental flux was found to be 178 kg/m^2 h. and rejection was found to be 78.3%.The percentage contribution of feed flow rate, feed bulk temperature and feed salt concentration were found to be 4.93 %, 92.23% and 2.59 %, respectively using *ANOVA* as shown in Table 4.7.

Table 4.7: Analysis of variance for percent contribution of operating parameters for PTFEMembrane (0.45µm pore size).

Parameter	DF	Adj SS	Adj MS	F-Value	% Contribution
Temperature (°C)	4	43922.9	10980.7	1147.93	92.23
Flow rate (lpm)	4	2350.2	587.5	61.42	4.93
Concentration (ppm)	4	1234	308.5	32.25	2.59
Error	12	114.8	9.6		
Total	24	47621.9			

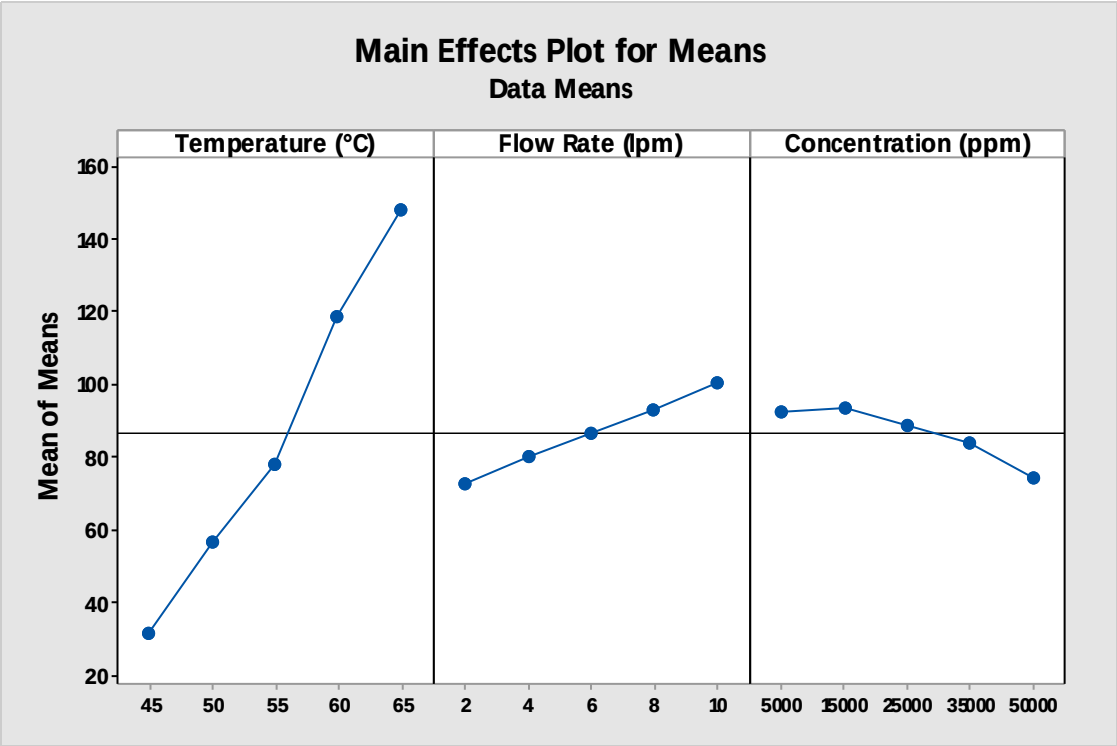

Figure 4.5: Effect of the operating parameters on mean of permeate for PTFE membrane (0.45 µm pore size)

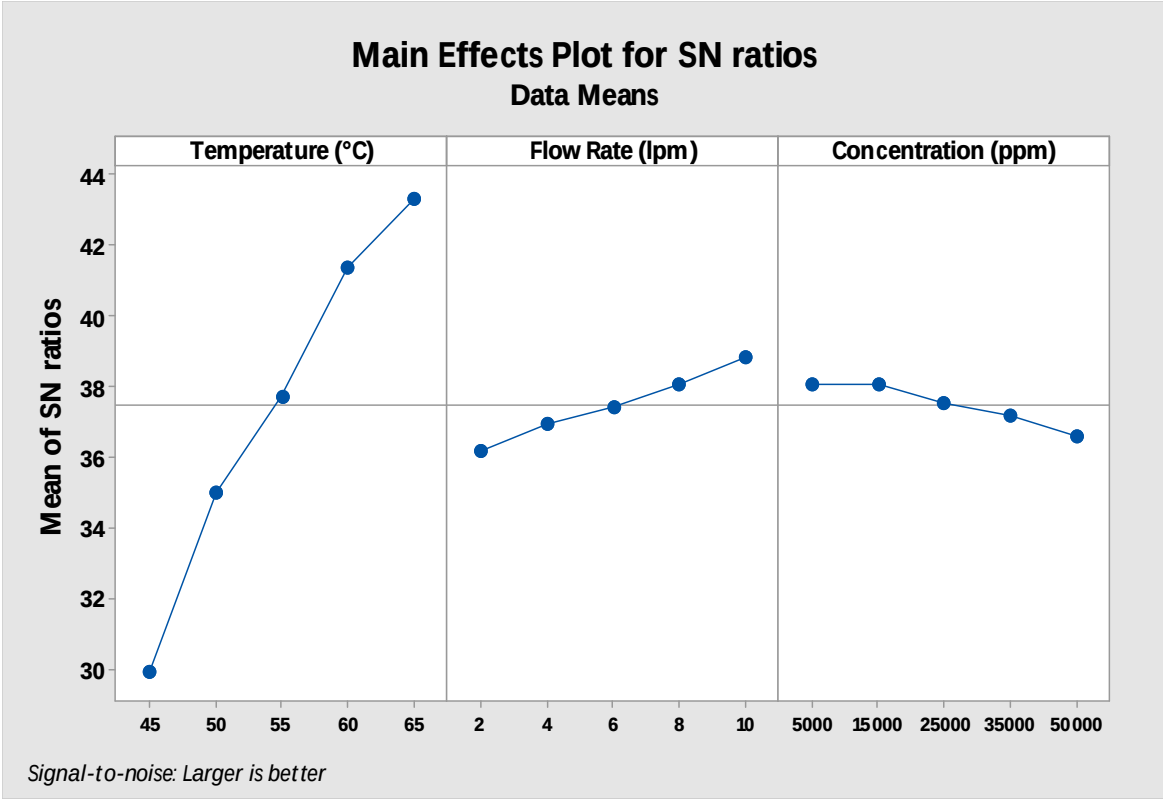

Figure 4.6: Effect of the operating parameters on mean of SN ratio for PTFE membrane (0.45 µm pore size)

4.1.4 Taguchi Approach for Permeate Flux for PVDF membrane of 0.45 µmpore size

The experimental suitable permeate flux was found to be 430 kg/m^2.h at most suitable operating parameters of 65 ºC feed bulk temperature, feed flow rate of 10 lpm and feed salt concentration of 5,000 ppm. These operating parameters can be depicted as suitable operating conditions from Figure 4.7and Figure 4.8 which was obtained using Taguchi approach. The rejection was found to be nearly 16.69%. The results of ANOVA as calculated using the equations 4.7 to 4.11 are shown inTable 4.8. It can be observed from ANOVA Table 4.8, that feed temperature, feed flow rate and feed salt concentration influence permeate flux by 70.24%, 26.15 % and 2.91% respectively.

It was found that the percentage contribution of feed flow rate is more for PVDF membrane (26%) as compared to PTFE membrane (5%) of same pore size of 0.45 µm. This may be due to the reason that membrane might have got punctured as the PVDF membrane has less mechanical strength compared to PTFE membrane, since the LEP of PVDF membrane is less as compared to PTFE membrane which makes PVDF membrane less hydrophobic compared to PTFE membrane.The salt rejection in case of PVDF membrane was found to be much lower (15%) than PTFE membrane (78%) which shows that PVDF membrane might have got ruptured at high flow rate. The contribution of feed bulk temperature for PVDF membrane was found to be less as compared to PTFE membrane this may be due to more contribution of feed flow rate. However, the contribution of feed salt concentration for both membrane was found to be almost same for pore size of 0.45 µm.

Table 4.8: Analysis of variance for percent contribution of individual parameters for experimental runs with 0.45µm PVDF membrane.

Parameter	DF	Adj SS	Adj MS	F-Value	% Contribution
Temperature (°C)	4	197929	49482.1	305.47	70.24
Flow rate (lpm)	4	73678	18419.6	113.71	26.15
Concentration (ppm)	4	8212	2053.1	12.67	2.91
Error	12	1944	162		
Total	24	281763			

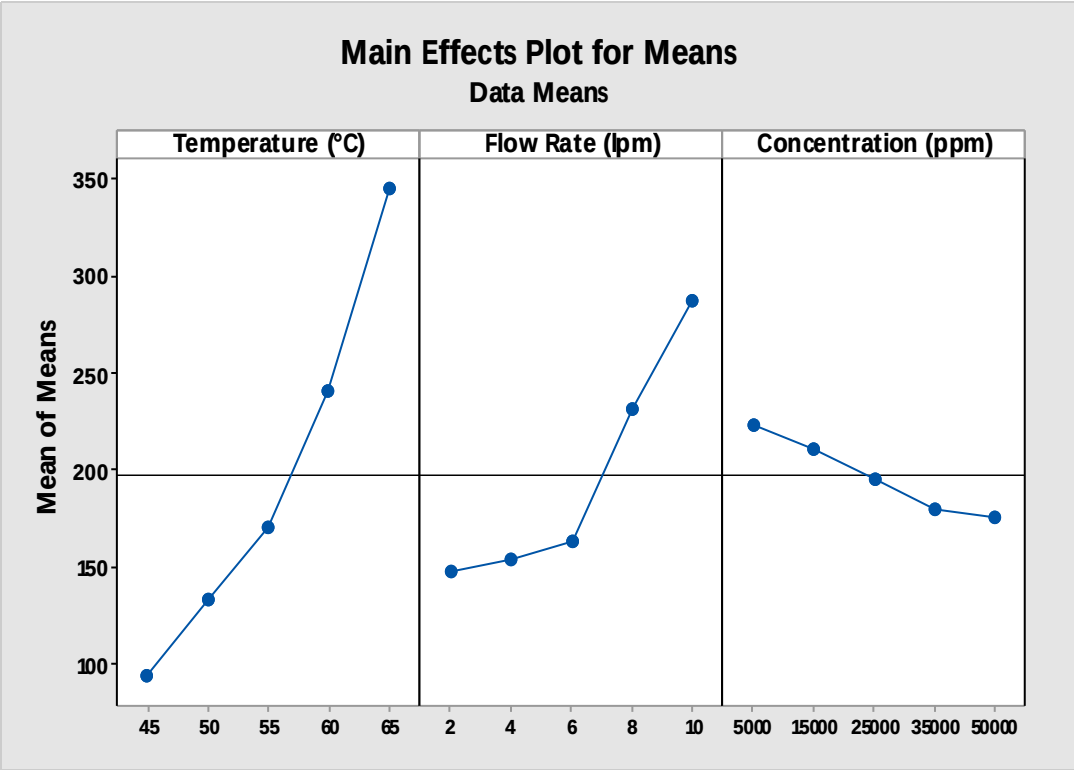

Figure 4.7: Effect of the operating parameters on mean of permeate for PVDF membrane (0.45 µm pore size)

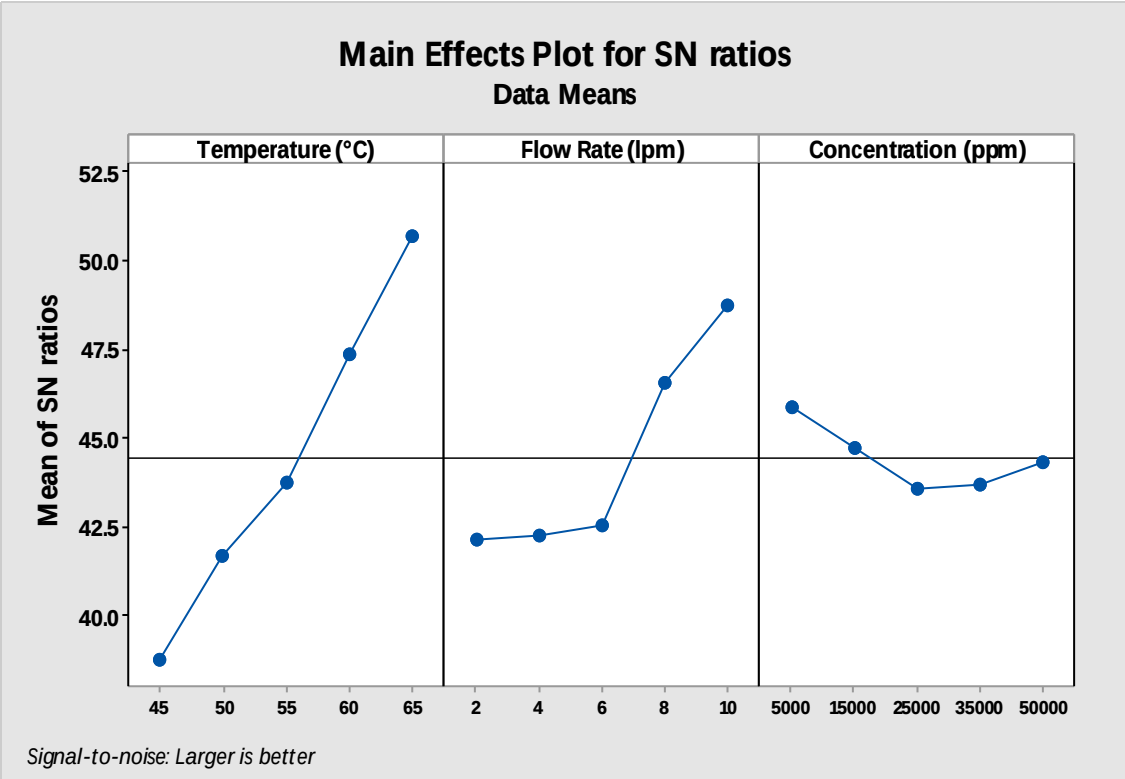

Figure 4.8: Effect of the operating parameters on mean of SN ratio for PVDF membrane (0.45 µm pore size)

Table 4.9: Taguchi analysis for permeate flux

Membrane	Suitable Parameters			Permeate Flux ($kg/m^2.h$)	Salt Rejection (%)
	Temperature (°C)	Feed flow rate (lpm)	Feed concentration (ppm)		
PTFE (0.22µm)	65	10	5,000	98.0	99.9
PTFE (0.45 µm)	65	10	5,000	178	78.6
PVDF (0.22 µm)	65	10	5,000	98.9	98.6
PVDF (0.45 µm)	65	10	5,000	430	15.2

4.2 Taguchi optimization for Experimental Salt Rejection

To determine the suitable parameters for higher salt rejection, the Taguchi approach was performed for different membranes (PTFE & PVDF) of two different pore size (0.22 & 0.45 µm). The Taguchi orthogonal array were made as shown in Table 4.10 to Table 4.13 representing five level of three factors as feed bulk temperature (45, 50,55, 60, 65 °C), feed flow rate (2, 4, 6, 8, 10 lpm) and salt concentration and five level (5000, 15000, 25000, 35000, 50000ppm) respectively with the corresponding salt rejection.

Table 4.10: Taguchi Orthogonal Array for 0.22 µm PTFE Membrane

Temperature (°C)	Flow Rate (lpm)	Concentration (ppm)	Salt Rejection (%)		Mean	S/N Ratio
			Trail 1	Trail 2		
45	2	5000	99.97	99.99	99.98	40.00
45	4	15000	99.96	99.94	99.95	40.00
45	6	25000	99.97	99.95	99.96	40.00
45	8	35000	99.99	99.97	99.98	39.99
45	10	50000	99.98	99.96	99.97	39.99
50	2	15000	99.99	99.99	99.99	40.00
50	4	25000	99.95	99.97	99.96	39.99
50	6	35000	99.97	99.99	99.98	39.99
50	8	50000	99.98	99.96	99.97	39.99
50	10	5000	99.98	99.96	99.97	40.00
55	2	25000	99.96	99.98	99.97	39.99
55	4	35000	99.97	99.97	99.97	39.99
55	6	50000	99.96	99.98	99.97	39.99
55	8	5000	99.99	99.97	99.98	40.00
55	10	15000	99.97	99.97	99.97	40.00
60	2	35000	99.99	99.97	99.98	39.99
60	4	50000	99.97	99.99	99.98	39.99
60	6	5000	99.98	99.96	99.97	40.00
60	8	15000	99.99	99.97	99.98	39.99
60	10	25000	99.97	99.99	99.98	39.99
65	2	50000	99.99	99.97	99.98	39.99
65	4	5000	99.97	99.99	99.98	40.00
65	6	15000	99.97	99.99	99.98	39.99
65	8	25000	99.99	99.97	99.98	39.99
65	10	35000	99.97	99.99	99.98	39.99

Table 4.11: Taguchi Orthogonal Array for 0.22 µm PVDF Membrane

Temperature (°C)	Flow Rate (lpm)	Concentration (ppm)	Salt Rejection (%)		Mean	S/N Ratio
			Trail 1	Trail 2		
45	2	5000	99.99	99.99	99.99	40.00
45	4	15000	99.98	100	99.99	40.00
45	6	25000	99.99	99.97	99.98	39.99
45	8	35000	99.98	99.94	99.96	39.86
45	10	50000	99.96	99.98	99.97	39.82
50	2	15000	99.97	99.99	99.98	40.00
50	4	25000	99.97	99.95	99.96	39.99
50	6	35000	99.98	99.96	99.97	39.99
50	8	50000	99.97	99.99	99.98	39.83
50	10	5000	99.99	99.99	99.99	39.82
55	2	25000	99.96	99.92	99.94	39.99
55	4	35000	99.95	99.97	99.96	39.99
55	6	50000	99.97	99.93	99.95	39.99
55	8	5000	99.987	99.993	99.99	39.89
55	10	15000	99.987	99.993	99.99	39.82
60	2	35000	99.97	99.99	99.98	39.99
60	4	50000	99.96	99.94	99.95	39.99
60	6	5000	99.97	99.99	99.98	40.00
60	8	15000	99.96	99.98	99.97	39.87
60	10	25000	99.98	99.96	99.97	39.82
65	2	50000	99.97	99.99	99.98	39.99
65	4	5000	99.989	99.991	99.99	39.99
65	6	15000	99.97	99.95	99.96	39.99
65	8	25000	99.94	99.96	99.95	39.85
65	10	35000	99.95	99.93	99.94	39.82

Table 4.12: Taguchi Orthogonal Array for 0.45 µm PTFE Membrane

Temperature (°C)	Flow Rate (lpm)	Concentration (ppm)	Salt Rejection (%)		Mean	S/N Ratio
			Trail 1	Trail 2		
45	2	5000	99.96	99.94	99.95	39.99
45	4	15000	99.64	99.66	99.65	39.97
45	6	25000	99.58	99.56	99.57	39.95
45	8	35000	84.29	84.27	84.28	38.50
45	10	50000	76.86	76.84	76.85	37.70
50	2	15000	99.69	99.67	99.68	39.97
50	4	25000	99.47	99.49	99.48	39.95
50	6	35000	99.36	99.34	99.35	39.94
50	8	50000	83.76	83.74	83.75	38.45
50	10	5000	79.36	79.34	79.35	37.98
55	2	25000	99.34	99.36	99.35	39.94
55	4	35000	99.24	99.26	99.25	39.93
55	6	50000	99.16	99.14	99.15	39.92
55	8	5000	84.77	84.79	84.78	38.56
55	10	15000	78.35	78.37	78.36	37.88
60	2	35000	99.17	99.15	99.16	39.92
60	4	50000	98.96	98.94	98.95	39.91
60	6	5000	99.57	99.59	99.58	39.96
60	8	15000	84.34	84.36	84.35	38.52
60	10	25000	77.45	77.43	77.44	37.77
65	2	50000	98.75	98.77	98.76	39.89
65	4	5000	99.55	99.57	99.56	39.96
65	6	15000	99.44	99.46	99.45	39.95
65	8	25000	83.96	83.94	83.95	38.48
65	10	35000	76.59	76.57	76.58	37.67

Table 4.13: Taguchi Orthogonal Array for 0.45 µm PVDF Membrane

Temperature (°C)	Flow Rate (lpm)	Concentration (ppm)	Salt Rejection (%)		Mean	S/N Ratio
			Trail 1	**Trail 2**		
45	2	5000	98.84	98.82	98.83	39.90
45	4	15000	98.80	98.74	98.77	39.89
45	6	25000	91.65	91.69	91.67	39.24
45	8	35000	35.97	35.99	35.98	31.12
45	10	50000	13.15	13.21	13.18	22.40
50	2	15000	98.90	98.70	98.80	39.90
50	4	25000	98.60	98.88	98.74	39.89
50	6	35000	89.35	89.37	89.36	39.02
50	8	50000	33.63	33.61	33.62	30.53
50	10	5000	18.85	18.87	18.86	25.51
55	2	25000	98.76	98.78	98.77	39.89
55	4	35000	98.72	98.70	98.71	39.89
55	6	50000	86.28	86.28	86.28	38.72
55	8	5000	38.33	38.35	38.34	31.67
55	10	15000	16.74	16.72	16.73	24.47
60	2	35000	98.75	98.73	98.74	39.89
60	4	50000	98.66	98.68	98.67	39.88
60	6	5000	92.45	92.43	92.44	39.32
60	8	15000	36.56	36.58	36.57	31.26
60	10	25000	14.61	14.59	14.60	23.29
65	2	50000	98.69	98.71	98.70	39.89
65	4	5000	98.76	98.74	98.75	39.89
65	6	15000	90.14	90.12	90.13	39.10
65	8	25000	34.81	34.79	34.80	30.83
65	10	35000	12.48	12.46	12.47	21.92

4.2.1 Salt Rejection by Taguchi Approach for PTFE membrane (0.22 µm pore size)

The effect of feed bulk temperature on mean of salt rejection is shown inFigure 4.9 and the mean of SN ratio in Figure 4.10. From these figure, it was found that on increasing feed bulk temperature, the mean salt rejection varies from 99.95 to 99.91 % and constant mean of SN ratio is to be found 39.99. Therefore, for maximum mean salt rejection and mean of SN ratio, the suitable value of feed inlet temperature is 65°C. On increasing the feed flow rate from 2 to 10 lpm, it can be seen from the Figure 4.9that mean salt rejection is constant 99.93% and from Figure 4.10 the mean of SN ratio was found to be constant 39.99. Therefore, the suitable value of feed flow rate is found to be 10 lpm. The mean of salt rejection is constant 99.9 % on increasing the salt concentration from 5000 to 50000 ppm. Since SN ratio remained almost constant for feed salt concentration in the range of 5000 ppm to 50000 ppm, considering the higher permeate flux at lower feed salt concentration, 5000 ppm of feed concentration advisable. At 65°C of feed inlet temperature, 10 lpm of feed flow rate and 5000 ppm of feed NaCl concentration, the experimental salt rejection was found to be 99.9 % and permeate flux was found to be 98.0 kg/m^2 h. The percentage contribution of various parameters is calculated by *ANOVA* using *MINITAB* 17 software are shown in Table. It was observed that feed salt concentration contribute to salt rejection in permeate side is very less 0.4% which may be due to the reason as the salt rejection is unaffected by varying the feed salt concentration. However, feed bulk temperature and feed flow rate contributes 9.69 % and 88.69% respectively to salt rejection.

Table 4.14: Analysis of variance for percent contribution for experimental salt rejection for 0.22 µm PTFE membrane

Source	DF	Adj SS	Adj MS	F-Value	% Contribution
Temperature (°C)	4	0.002504	0.000626	24.08	9.69
Flow rate (lpm)	4	0.022904	0.005726	220.23	88.69
Concentration (ppm)	4	0.000104	0.000026	1.00	0.40
Error	12	0.000312	0.000026		
Total	24	0.025824			

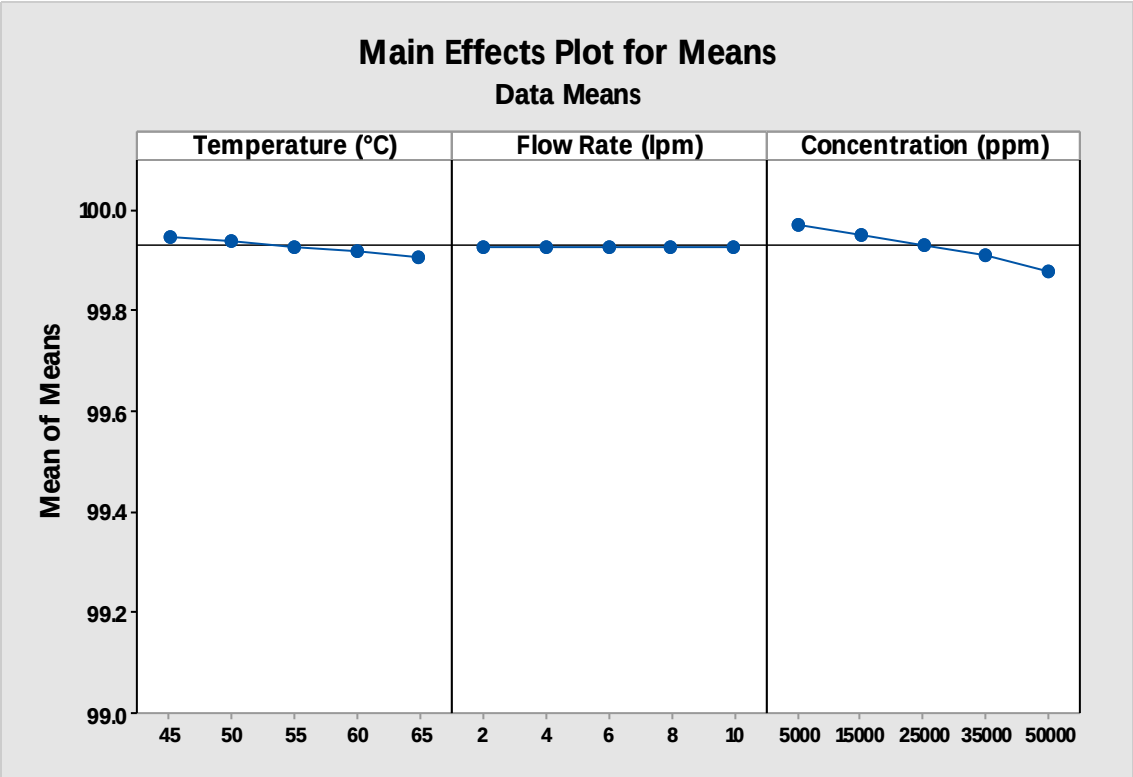

Figure 4.9: Effect of operating parameters on mean of salt rejection for PTFE Membrane (0.22µm pore size)

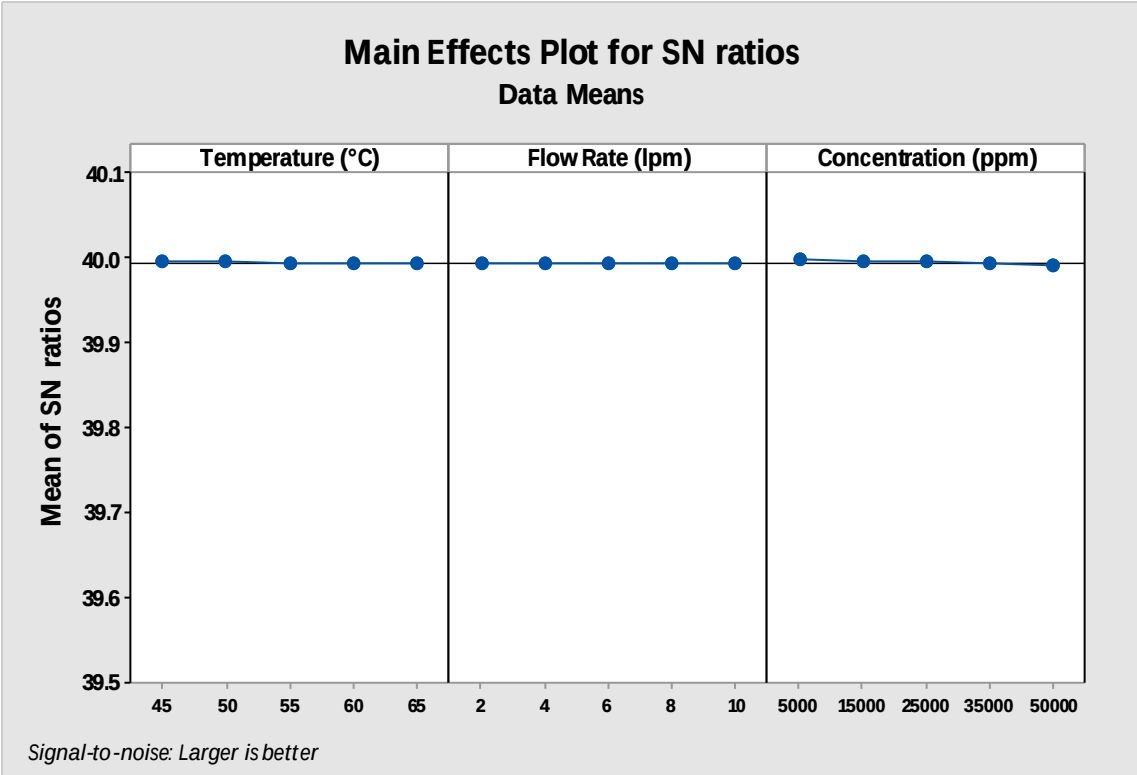

Figure 4.10: Effect of operating parameters on mean of SN ratio on salt rejection for PTFE Membrane (0.22 µm pore size)

4.2.2 Taguchi Approach for salt rejection for PVDF membrane (0.22 µm pore size)

The effect of feed bulk temperature on mean of salt rejection and mean of SN ratio is shown inFigure 4.11 and Figure 4.12 respectively. From these figure, it is obvious that on increasing feed bulk temperature, the mean of salt rejection varies from 99.25 to 99.18 % and constant SN ratio of 39.93. Therefore, for maximum permeate flux and SN ratio, the suitable value of feed inlet temperature is 65 °C. On increasing the feed flow rate from 2 to 10 lpm, it can be seen from the Figure 4.11that mean of salt rejection varies from99.92 to 97.98% and from the Figure 4.12 the mean of SN ratio also constant 39.9. Therefore, the suitable value of feed flow rate is found to be 10 lpm. The mean of salt rejection is constant of 99.31 on increasing the salt concentration from 5000 to 50000 ppm. However, not much variation in SN ratio is observed on increasing the salt concentration. Since, the mean flux & SN ratio is greater at lower feed concentration therefore, lower feed concentration favours the permeate flux. Hence, at 65°C of feed inlet temperature, 10 lpm of feed flow rate and 5000 ppm of feed NaCl concentration, the suitablesalt rejection was found to be 98.0 % and permeate flux was found to be 98.9kg/m^2 h. The percentage contribution of feed flow rate on salt rejection for PVDF membrane of 0.22 µm pore size was found to be 98.62 % using ANOVA as shown in Table 4.15 to Table 4.15 which is higher than membrane of PTFE of same pore size. This may be due to the reason as salt rejection decreases to 99.92 % to 97.98% on increasing the feed flow rate from 1 to 10 lpm in PVDF membrane while this rejection is almost constant for PTFE membrane on increasing the feed flow rate. Moreover, there might be probability that liquid entry pressure is lower which ultimately reduces the hydrophobic behaviour of PVDF membrane. It was also found that contribution of feed bulk temperature and feed salt concentration affects less on salt rejection for PVDF membrane of 0.22 µm pore size.

Table 4.15: Analysis of variance for percent contribution for experimental salt rejection for 0.22 µm PVDF membrane

Source	DF	Adj SS	Adj MS	F-Value	% Contribution
Temperature (°C)	4	0.04	0.010	1.01	0.22
Flow rate (lpm)	4	18.40	4.60	459.98	98.63
Concentration (ppm)	4	0.09	0.03	2.38	0.51
Error	12	0.12	0.01		
Total	24	18.66			

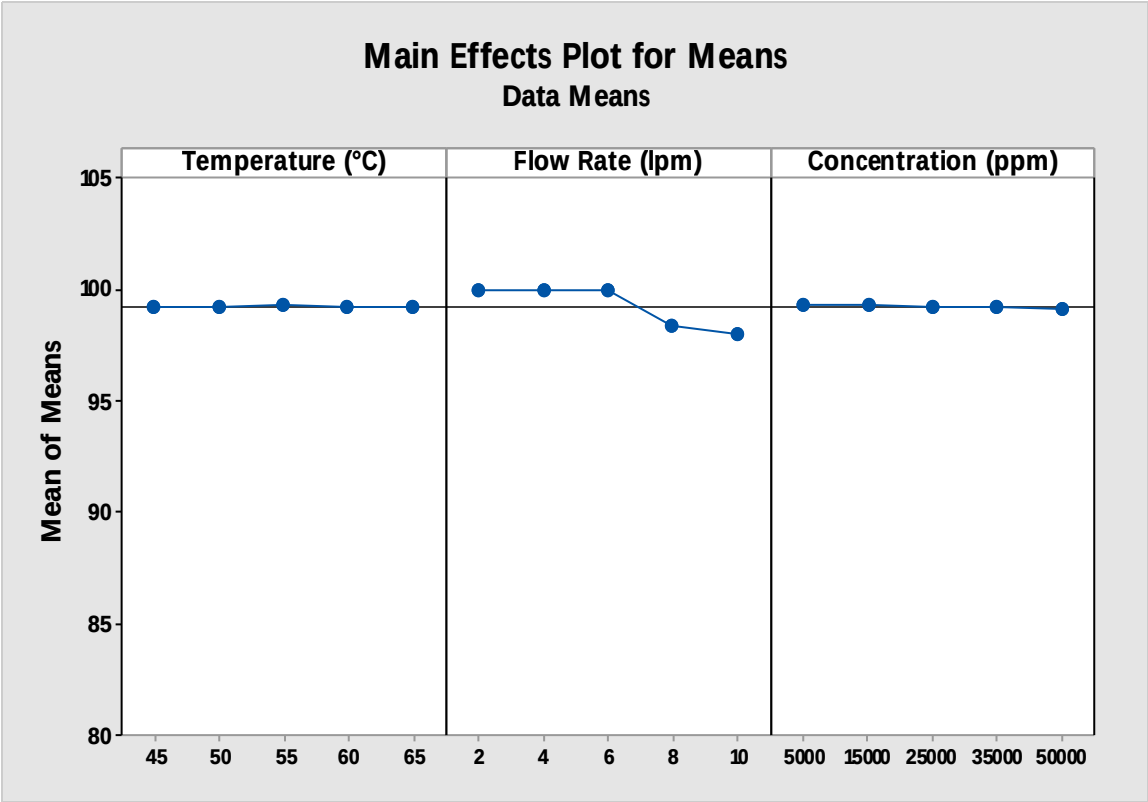

Figure 4.11: Effect of the operating parameters on mean of salt rejection for PVDF membrane (0.22 µm pore size)

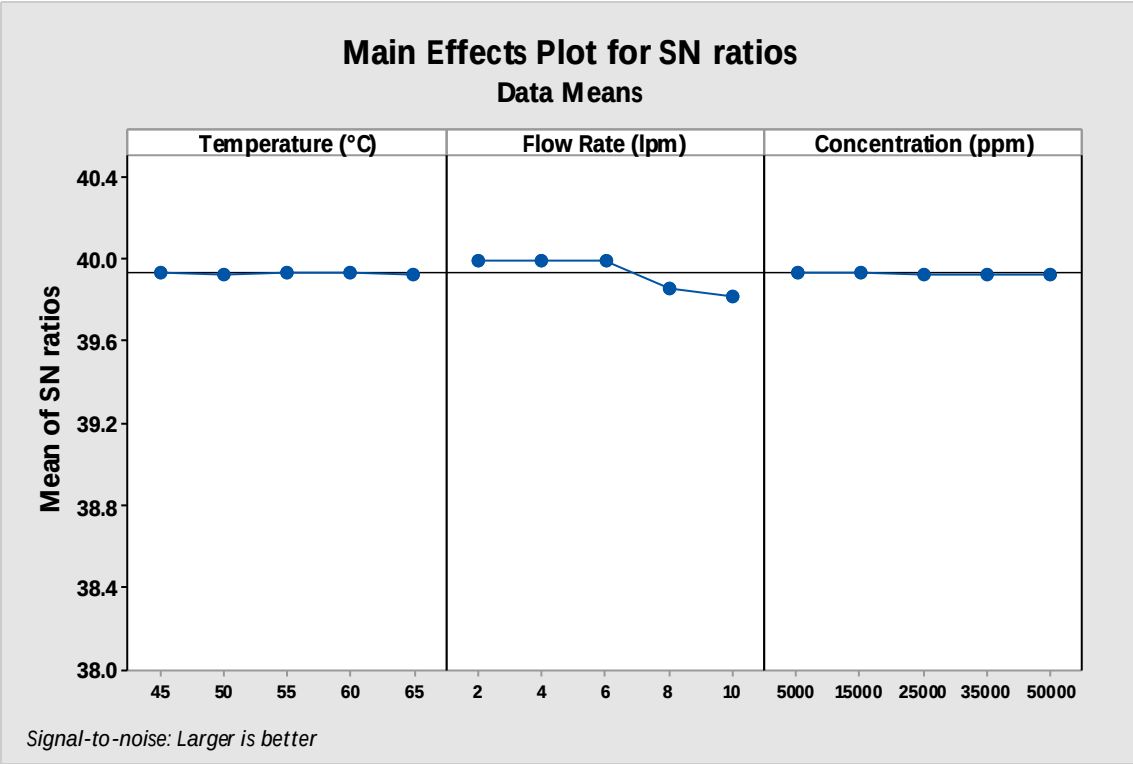

Figure 4.12: Effect of the operating parameters on mean of SN ratio for PVDF membrane (0.22 µm pore size)

4.2.3 Taguchi Approach for salt rejection for PTFE membrane (0.45 µm pore size)

It was found from theFigure 4.13 and Figure 4.14, mean of percentage salt rejection and SN ratio remain almost constant to 91.95 % and 39.22 respectively on increasing the feed bulk inlet temperature from 45 to 65 °C. It can be seen from these figures that temperature has negligible effects on salt rejection. Therefore, 65 °C can be taken as suitable temperature by considering the maximum mean permeate flux and mean percentage rejection. However, remarkable variation in mean of percentage salt rejection is observed from 99.31 % to 77.65 % on increasing the feed flow rate from 1 to 10 lpm. It is also noticed from the figure that mean salt rejection remains almost constant from 1 to 6 lpm and thereafter it decreases steeply. Similar trend has also been observed for SN ratio inFigure 4.14, since its mean value remains constant (39.94) upto 6 lpm and decreases rapidly to 37.80 by increasing the feed flow rate from 6 to 10 lpm. Hence, suitable value for feed flow rate can be understood as 6 lpm since beyond this flow rate rejection suddenly decreased which may be due to membrane getting punctured. Not much variation in mean percentage salt rejection and SN ratio is spotted form the Figure 4.13&Figure 4.14 respectively. However, the lower concentration favors the mean permeate flux as discussed in section 4.6.3. Therefore, the suitable value of salt concentration is 5000 ppm. Hence, at 65°C of feed inlet temperature, 6 lpm of feed flow rate and 5000 ppm of feed NaCl concentration, the experimental percentage salt rejection and permeate flux were found to be 99.5 % and 159.0 kg/m^2 h respectively. Percentage contribution for feed flow rate, feed bulk temperature and feed salt concentration are found to be 99.6%, 0 .016% and 0.19% respectively as given in Table 4.16Table 4.16. This high contribution of feed flow rate is due to the reason the salt rejection starts decreasing tremendously in permeate after 6 lpm. This may also be attributed as hydrostatic pressure approaches to liquid entry pressure on increasing the feed flow rate as a result hydrophobicity for 0.45 µm pore size of PTFE membrane slightly transform into hydrophobicity. Hence, this membrane should not be used beyond 6 lpm feed flow rate since thereafter membrane hydrophobicity deviates sooner at high flow rate which is not demanding for VMD.

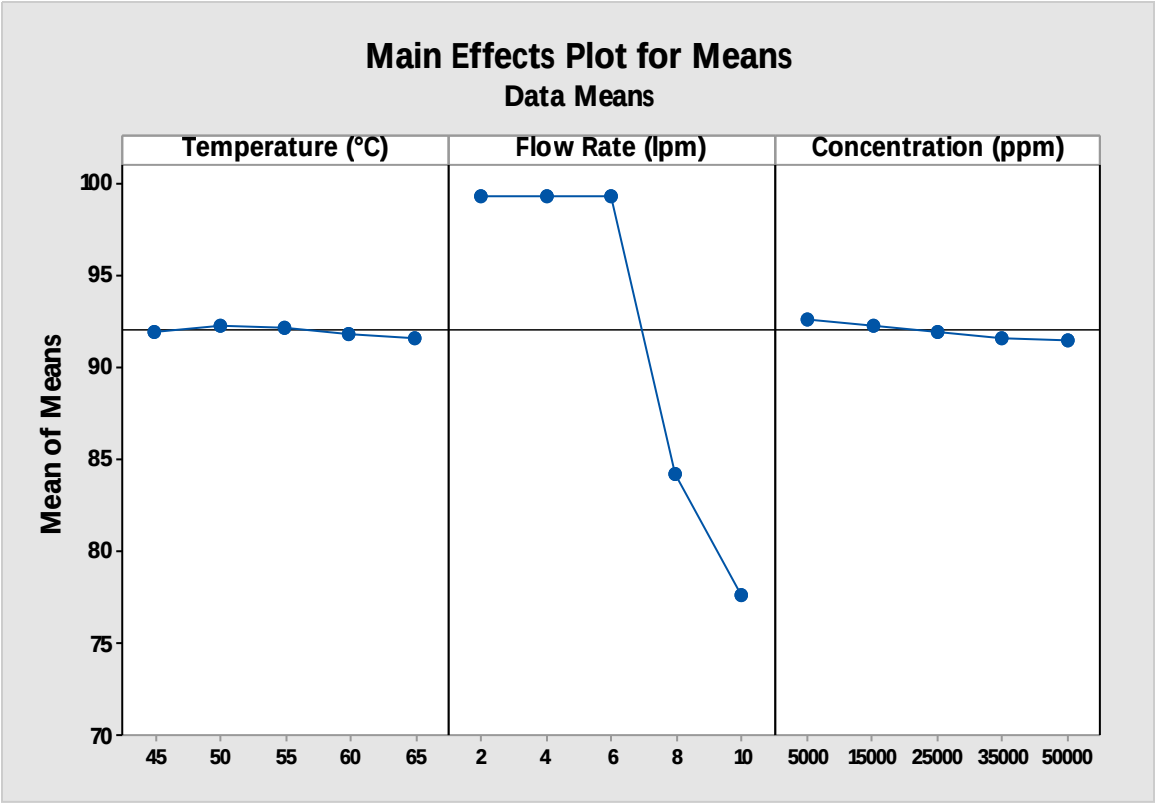

Figure 4.13: Effect of the operating parameters on mean of salt rejection for PTFE membrane (0.45 µm pore size)

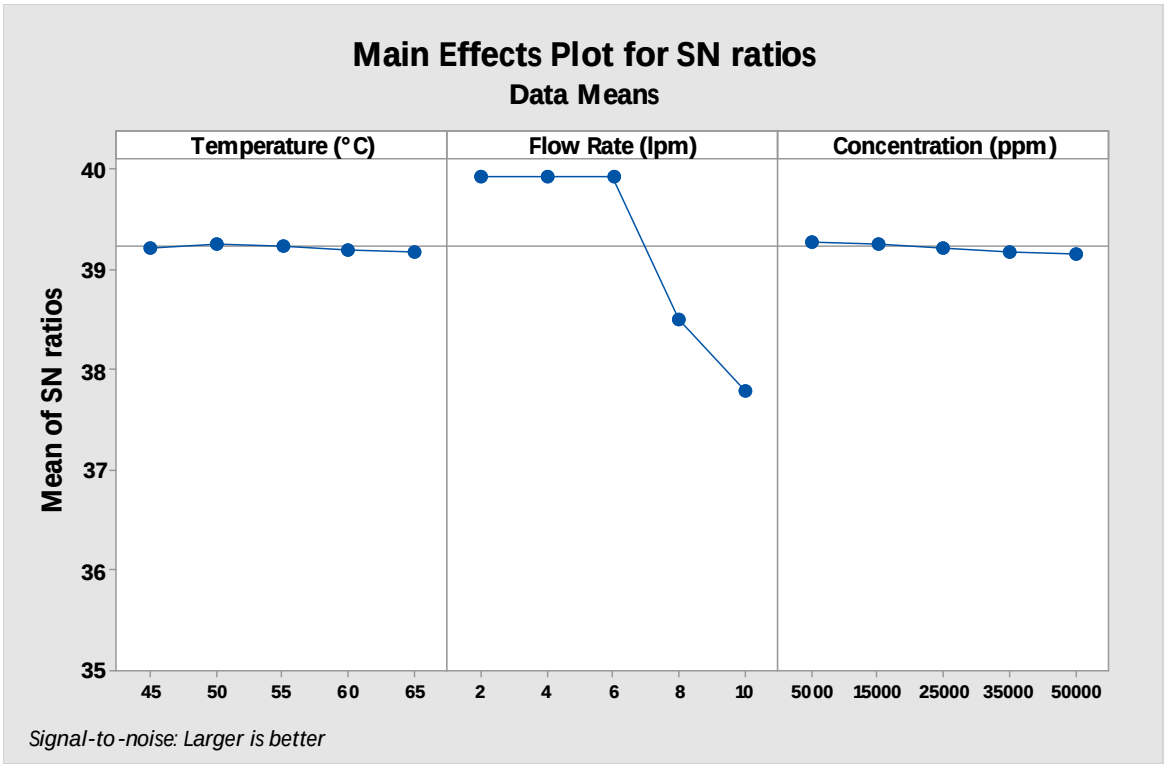

Figure 4.14: Effect of the operating parameters on mean of SN ratio for PTFE membrane (0.45 µm pore size)

Table 4.16: Analysis of variance for percent contribution for experimental salt rejection for 0.45 µm PTFE membrane.

Source	DF	Adj SS	Adj MS	F-Value	% Contribution
Temperature (°C)	4	1.34	0.335	2.44	0.06
Flow rate (lpm)	4	2144.92	536.23	3898.91	99.67
Concentration (ppm)	4	4.13	1.031	7.5	0.19
Error	12	1.65	0.138		
Total	24	2152.04			

4.2.4 Taguchi Approach for salt rejection for PVDF membrane (0.45 µm pore size)

From Figure 4.15 and Figure 4.16, it can be seen that the mean of salt rejection and mean of SN ratio remains almost unchanged on increasing the feed bulk temperature. Therefore, suitable feed bulk temperature can be taken as 45 °C however, higher permeate flux was found at 65 °C as compared to 45 °C as discussed in section 4.1.4. Therefore, 65 °C can be taken as suitable temperature by considering the balance between maximum mean permeate flux and mean percentage rejection. However, very large variation has been observed in mean salt rejection, from 98.71 to 15.17%, on increasing the feed flow rate from 1 to 10 lpm. Further, it can be seen from the figure that salt rejection remains unaffected till 2 lpm and beyond 2 lpm it decreases rapidly to 15.17% at 10 lpm. Almost identical trend was observed for mean SN ratio on increasing the feed flow rate from 1 to 10 lpm. Therefore, most suitable for 0.45µm PVDF membrane may be recommended 2 lpm. Further, it can be seenfrom these figures thatsuitablefeed salt concentration would be 5000 ppm. At 65°C of feed inlet temperature, 2 lpm of feed flow rate and 5000 ppm of feed NaCl concentration, the experimental percentage salt rejection and permeate flux were found to be 98.8% and 322 kg/m^2 h respectively. Percentage contribution for feed flow rate, feed bulk temperature and feed salt concentration on percentage salt rejection are found to be 99.79, 0 .013 and 0.10% respectively as shown inTable 4.17. This high contribution of feed flow rate on percentage salt rejection confirms membrane might have started losingits hydrophobicity beyond 2 lpm and also it might have got punctured at high flow rate since the salt rejection decreaseddrastically in permeate from 98.7% to 15% on increasing the feed flow rate between 2 to 10 lpm. Hence, it can be concluded that PVDF membrane of pore size 0.45 µm is not suitable for VMD at higher feed flow rate.

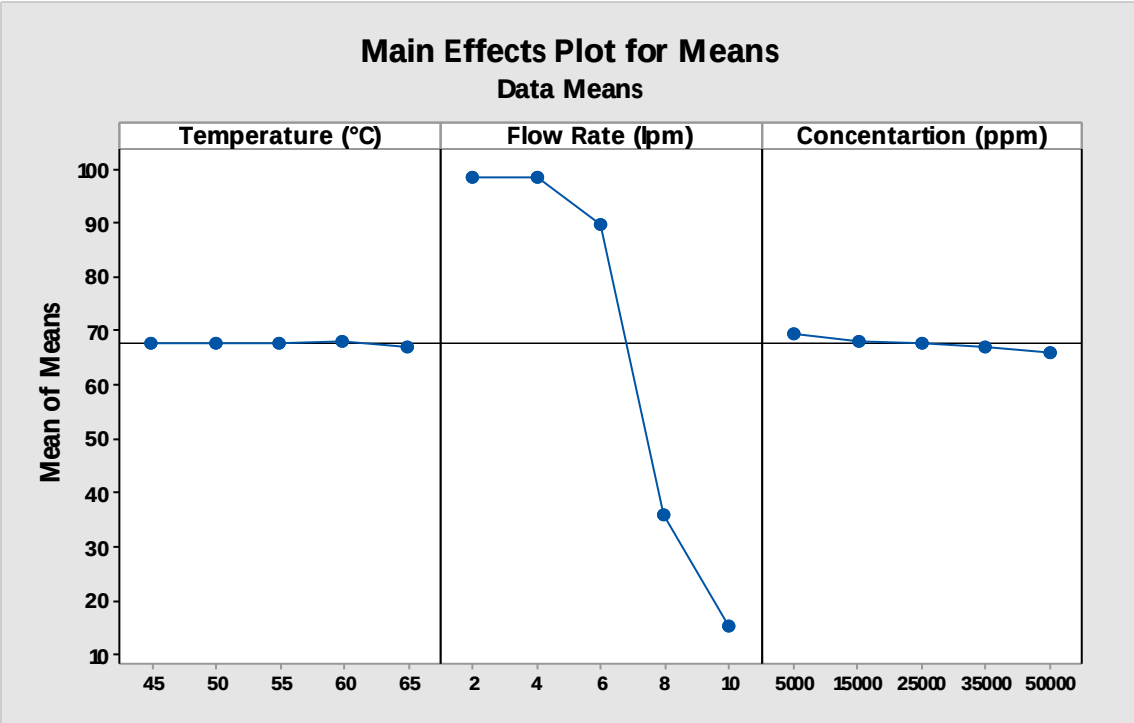

Figure 4.15: Effect of the operating parameters on mean of salt rejection for PVDF membrane (0.45 µm pore size)

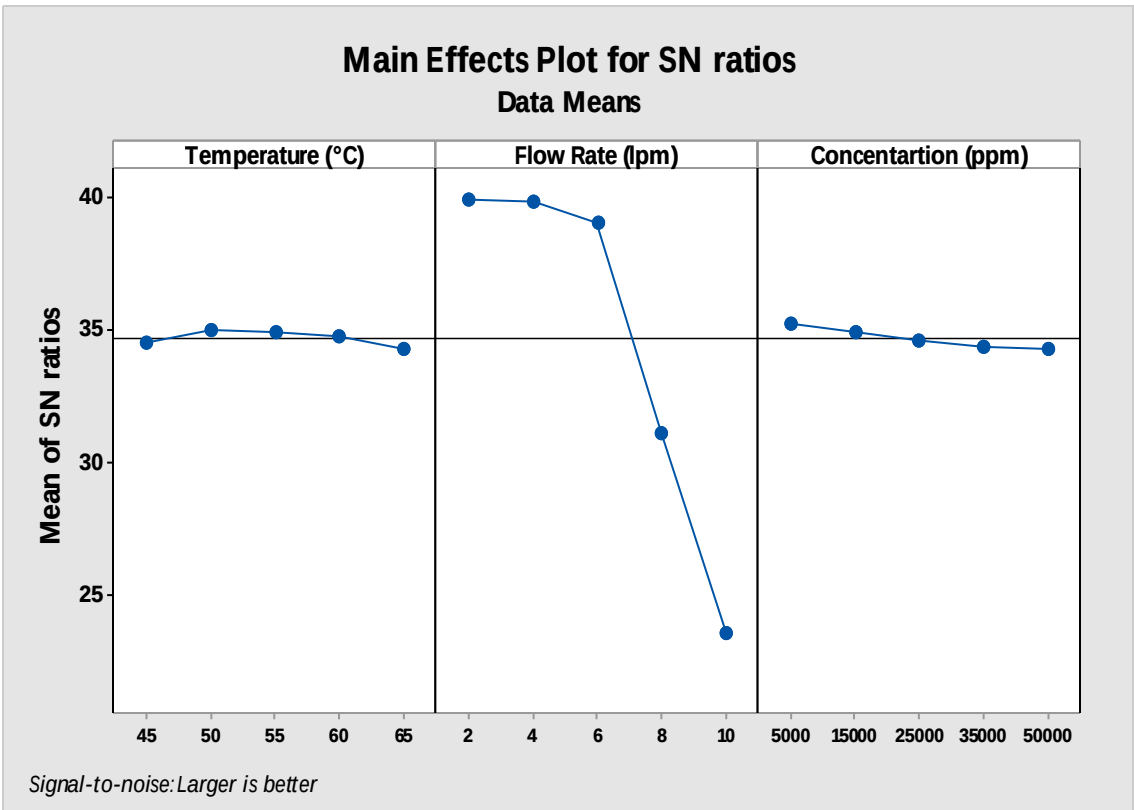

Figure 4.16: Effect of the operating parameters on mean of SN ratio for PVDF membrane (0.45 µm pore size)

Table 4.17: Analysis of variance for percent contribution for experimental salt rejection for 0.45 µm PVDF membrane.

Parameter	DF	Adj SS	Adj MS	F-Value	% Contribution
Temperature (°C)	4	4.1	1.03	0.44	0.01
Flow rate (lpm)	4	30987.2	7746.81	3341.01	99.79
Concentration (ppm)	4	31.5	7.88	3.4	0.10
Error	12	27.8	2.32		
Total	24	31050.7			

Table 4.18: Taguchi analysis for salt rejection

Membrane	Suitable Parameters			Salt Rejection (%)	Permeate Flux ($kg/m^2.hr$)
	Temperature (ºC)	Feed flow rate (lpm)	Feed concentration (ppm)		
PTFE(0.22µm)	65	10	5,000	99.9	98.0
PTFE(0.45 µm)	65	6	5,000	99.5	159
PVDF (0.22 µm)	65	10	5,000	98.0	98.9
PVDF (0.45 µm)	65	2	5,000	98.8	149.8

4.3 Taguchi optimization for Experimental Specific Energy Consumption

From the section 4.1 and 4.2, it is obvious that PTFE and PVDF membranes are suitable for VMD of pore size 0.22 µm rather than 0.45 µm since in the latter case the membrane strength and hydrophobicity deplete at higher flow rate as a result salt rejection decreases. Therefore, Taguchi approach was used for PTFE and PVDF membrane in VMD of 0.22 µm pore size each to determine the suitable operating condition for specific energy consumption. Taguchi orthogonal array were made as shown inTable 4.19 to Table 4.20 representing five level of three factors asfeed bulk temperature (45, 50,55, 60, 65 °C), feed flow rate (2, 4, 6, 8, 10 lpm) and salt concentration level (5000, 15000, 25000, 35000, 50000 g/l) respectively with the corresponding specific energy consumption.

From the Figure 4.17 to Figure 4.20in terms of minimization of mean specific energy consumption and maximization of SN ratio, the suitable condition for specific energy consumption is found to be at feed flow rate of 10 lpm, feed bulk temperature of 65 ºC and 5000 ppm of feed salt inlet concentration of NaCl. At these conditions, the specific energy consumption is found to be 6.5 kWh/kg and 4.4 kWh/kg for PTFE and PVDF membrane of 0.22 µm pore size respectively. It can be seen form ANOVATable 4.21 to Table 4.22, that response of feed bulk temperature is highest on specific energy consumption of 71.28% for PTFE and 77.46 % for PVDF membrane. This may be due to the reason that specific energy consumption is inversely proportional to permeate flux, which increases more rapidly on increasing the feed bulk temperature as discussed in section 4.2.2 and section 4.3.2. Moreover, in this support feed bulk temperature contributes 84.37% and 89.64% as highest contribution to permeate flux for PTFE and PVDF membrane as mentioned in section 4.1.1 and section 4.1.2. Further, from Table 4.21 and Table 4.22 it can be seen that the flow rate contributes to 7.88% and 6.57% as well as feed salt concentration contributes to 20.0% and 15.7% on specific energy consumption for PTFE and PVDF membrane respectively of 0.22 µm pore size.

Table 4.19: Taguchi Orthogonal Array for 0.22 µm PTFE

Temperature (°C)	Flow Rate (lpm)	Concentration (ppm)	Specific Energy Consumption (kWh/kg)		Mean	S/N Ratio
			Trail 1	Trail 2		
45	2	5000	27.68	28.04	27.86	-28.90
45	4	15000	28.78	28.99	28.88	-29.21
45	6	25000	29.32	29.22	29.27	-29.33
45	8	35000	29.36	29.44	29.40	-29.37
45	10	50000	30.56	30.61	30.58	-29.71
50	2	15000	25.46	25.44	25.45	-28.11
50	4	25000	26.36	26.33	26.35	-28.41
50	6	35000	27.35	27.37	27.36	-28.74
50	8	50000	28.87	28.84	28.86	-29.20
50	10	5000	15.79	15.75	15.77	-23.96
55	2	25000	23.44	23.41	23.42	-27.39
55	4	35000	24.01	24.08	24.04	-27.62
55	6	50000	25.57	25.54	25.55	-28.15
55	8	5000	12.56	12.54	12.55	-21.97
55	10	15000	16.19	16.10	16.15	-24.16
60	2	35000	21.12	21.21	21.16	-26.51
60	4	50000	22.96	23.02	22.99	-27.23
60	6	5000	10.45	10.40	10.42	-20.36
60	8	15000	13.22	13.17	13.20	-22.41
60	10	25000	13.67	13.71	13.69	-22.73
65	2	50000	16.72	16.68	16.70	-24.45
65	4	5000	9.04	9.02	9.03	-19.11
65	6	15000	9.89	9.88	9.88	-19.90
65	8	25000	10.16	10.15	10.15	-20.13
65	10	35000	10.33	10.36	10.34	-20.29

Table 4.20: Taguchi Orthogonal Array for 0.22 µm PVDF

Temperature (°C)	Flow Rate (lpm)	Concentration (ppm)	Specific Energy Consumption (kWh/kg)		Mean	S/N Ratio
			Trail 1	Trail 2		
45	2	5000	25.78	25.74	25.76	-28.22
45	4	15000	26.66	26.71	26.68	-28.52
45	6	25000	26.98	26.96	26.97	-28.62
45	8	35000	27.18	27.22	27.20	-28.69
45	10	50000	28.49	28.48	28.48	-29.09
50	2	15000	23.34	23.36	23.35	-27.37
50	4	25000	24.16	24.13	24.15	-27.66
50	6	35000	25.05	25.07	25.06	-27.98
50	8	50000	26.68	26.63	26.66	-28.52
50	10	5000	16.57	16.64	16.60	-24.40
55	2	25000	21.34	21.31	21.32	-26.58
55	4	35000	21.81	21.88	21.84	-26.79
55	6	50000	23.27	23.24	23.25	-27.33
55	8	5000	13.45	13.48	13.47	-22.59
55	10	15000	14.08	14.01	14.05	-22.95
60	2	35000	19.03	19.10	19.06	-25.60
60	4	50000	20.80	20.78	20.79	-26.36
60	6	5000	10.10	10.15	10.12	-20.11
60	8	15000	11.03	10.96	11.00	-20.83
60	10	25000	11.55	11.63	11.59	-21.28
65	2	50000	14.63	14.57	14.60	-23.29
65	4	5000	7.04	7.14	7.09	-17.01
65	6	15000	7.59	7.58	7.58	-17.60
65	8	25000	7.92	7.99	7.95	-18.01
65	10	35000	8.26	8.23	8.24	-18.32

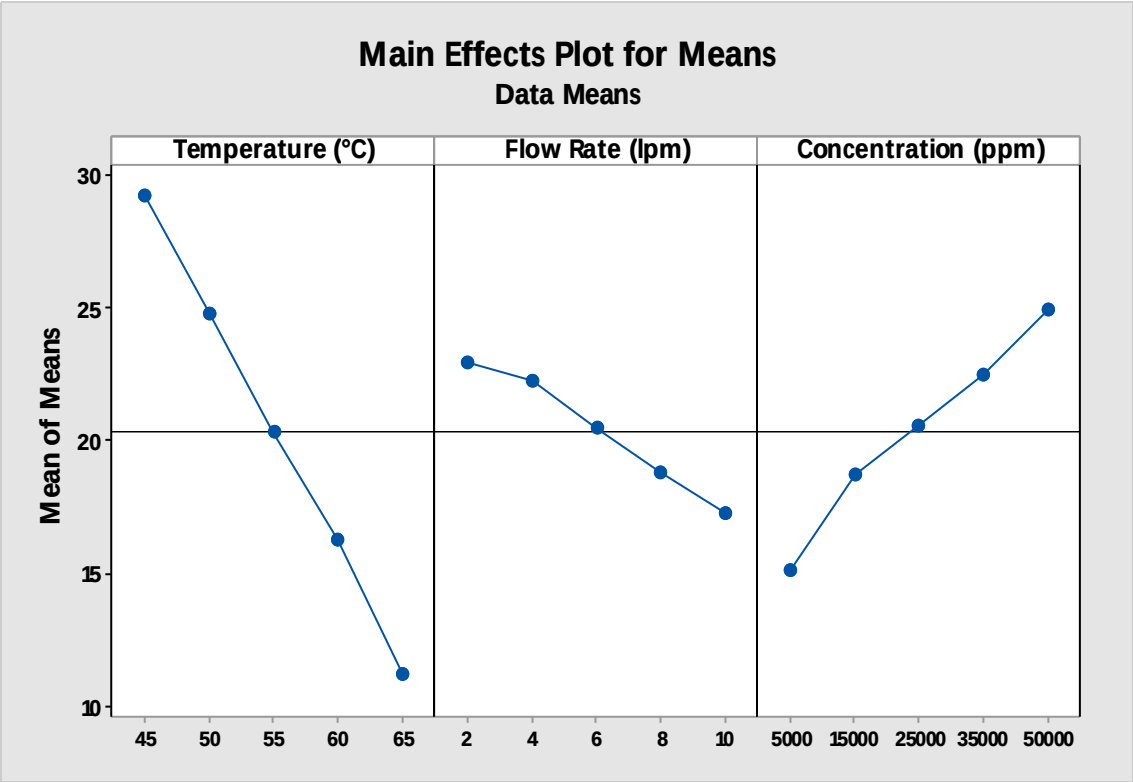

Figure 4.17: Effect of operating parameters on mean of specific energy consumption for PTFE Membrane (0.22µm pore size)

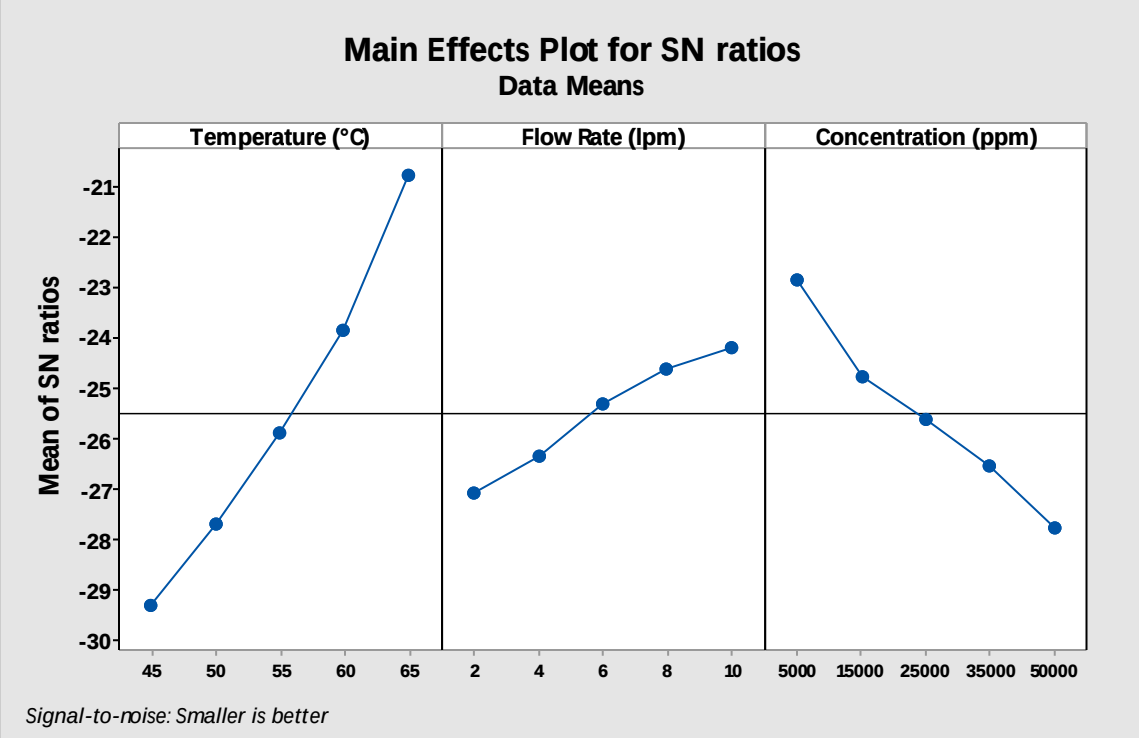

Figure 4.18: Effect of operating parameters on mean of SN ratio on specific energy consumption for PTFE Membrane (0.22 µm pore size)

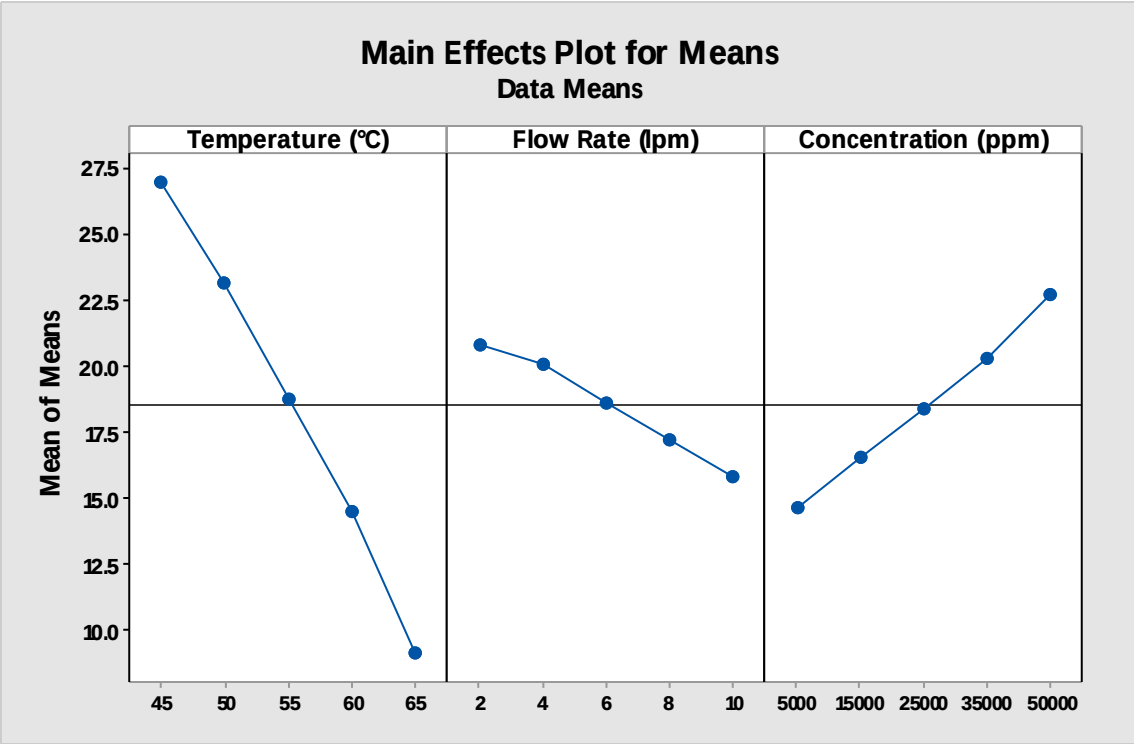

Figure 4.19: Effect of the operating parameters on mean of specific energy consumption for PVDF membrane (0.22 µm pore size)

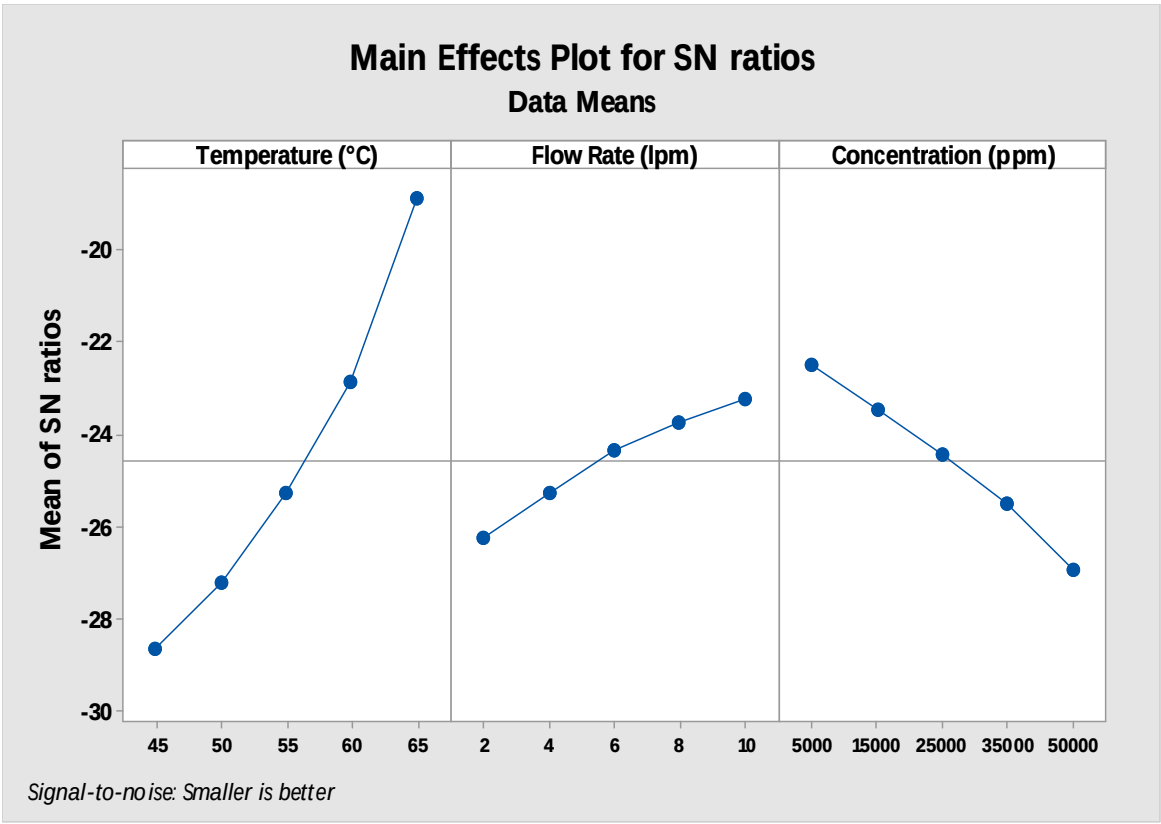

Figure 4.20: Effect of the operating parameters on mean of SN ratio for PVDF membrane (0.22 µm pore size)

Table 4.21: Analysis of variance for percent contribution on experimental specific energy consumption for 0.22 µm PTFE membrane

Parameter	DF	Adj SS	Adj MS	F-Value	% Contribution
Temperature (°C)	4	987.62	246.91	268.36	71.29
Flow rate (lpm)	4	109.19	27.29	29.67	7.88
Concentration (ppm)	4	277.52	69.38	75.41	20.03
Error	12	11.04	0.92		
Total	24	1385.38			

Table 4.22: Analysis of variance for percent contribution on experimental specific energy consumption for 0.22 µm PVDF membrane

Parameter	DF	Adj SS	Adj MS	F-Value	% Contribution
Temperature (°C)	4	993.96	248.49	919.95	77.47
Flow rate (lpm)	4	84.32	21.08	78.04	6.57
Concentration (ppm)	4	201.55	50.38	186.54	15.71
Error	12	3.24	0.27		
Total	24	1283.07			

Table 4.23: Taguchi Analysis for Specific Energy Consumption

Membrane	Suitable Parameters			Specific Energy Consumption (kWh/kg)	Permeate flux ($kg/m^2.h$)	Salt Rejection (%)
	Temperature (°C)	Feed flow rate (lpm)	Feed concentration (ppm)			
PTFE (0.22µm)	65	10	5,000	6.5	98.0	99.9
PVDF (0.22 µm)	65	10	5,000	4.4	98.9	98.0

Table 4.24: Suitable operating conditions for different response like permeate flux, salt rejection, and specific energy consumption

Parameter	P-Value for 0.22 µm PVDF		P-Value for 0.22 µm PTFE		P-Value for 0.45 µm PVDF		P-Value for 0.45 µm PTFE	
Permeate Flux (kg/m^2.h)								
Temperature (°C)	65	**98.9**	65	**98.0**	65	**430**	65	**178**
Flow rate (lpm)	10		10		10		10	
Concentration (ppm)	5000		5000		5000		5000	
Salt Rejection (%)								
Temperature (°C)	65	**98.0**	65	**99.9**	65	**98.8**	65	**99.5**
Flow rate (lpm)	10		10		2		6	
Concentration (ppm)	5000		5000		5000		5000	
Specific Energy Consumption (kWh/kg permeate)								
Temperature (°C)	60	**4.4**	60	**6.5**				
Flow rate (lpm)	10		10					
Concentration (ppm)	5000		5000					

Table 4.25: Contribution of operating parameter on different response, like permeate flux, salt rejection, specific energy consumption.

Source	P-Value for 0.22 µm PVDF	P-Value for 0.22 µm PTFE	P-Value for 0.45 µm PVDF	P-Value for 0.45 µm PTFE
Permeate Flux				
Temperature (°C)	89.64	84.37	70.25	92.23
Flow rate (lpm)	4.21	5.98	26.15	4.94
Concentration (ppm)	5.65	7.84	2.91	2.59
Salt Rejection				
Temperature (°C)	0.22	9.69	0.013	0.06
Flow rate (lpm)	98.63	88.69	99.795	99.67
Concentration (ppm)	0.51	0.40	0.101	0.19
Specific Energy Consumption				
Temperature (°C)	77.47	71.29		
Flow rate (lpm)	6.57	7.88		
Concentration (ppm)	15.71	20.03		

4.4 Effect of Operating Parameters on Permeate Flux for PVDF membrane.

To study the effect of process parameters, experiments have been carried out at different flow rates in the range of 1 to 10 lpm and the feed bulk temperature range of 45°C to 65°C, feed salt concentration of 5000 to 50000 ppm at constant permeate pressure of 9.0 kPa. The effects of individual parameters have been discussed in the subsequent sections.

4.4.1 Effects of feed flow rate on permeate flux of PVDF membrane:

Effect of feed flow rate on permeate flux are shown in Figure 4.21at constant feed salt concentration of 5000 ppm and permeate pressure of 9.0 kPa. It can be observed from the Figure 4.21Figure 4.21 that the permeate flux increases linearly from 78 to 99 kg/m^2.hr and 318 to 430 kg/m^2.hr upon increasing the feed flow rate from 1 to 10 lpm at 65 °C for the membrane of pore size 0.22µm and 0.45µm respectively. This increase in permeate flux is because of decrease in temperature boundary layer thickness and concentration boundary layer thickness which ultimately reduces the resistance to mass transfer of vapor to pass through the membrane in VMD. The decrease in boundary layer thickness occurs due to increase in Reynolds number, i.e., turbulence. The similar behavior of linear increase in permeate flux with feed flow rate is also depicted by many other authors (Tang et al. 2014,Lovineh et al. 2013,Fan and Peng 2012,Tang et al. 2011,Mericq et al. 2009).

The permeate flux of 430 kg/m^2.hr and 99 kg/m^2.hr for 0.45 µmand 0.22µm pore size PVDF membranes, respectively, have been found at feed flow rate of 10 lpm, feed bulk inlet temperature of 65 °C, permeate pressure of 9.0 kPa and feed salt concentration of 5000 ppm. This higher value of permeate flux at 0.45 µm pore size as compared to 0.22 µm pore size at same operating condition is due to the fact that the permeate flux is directly proportional to the square of pore diameter due to poiseuille flow.

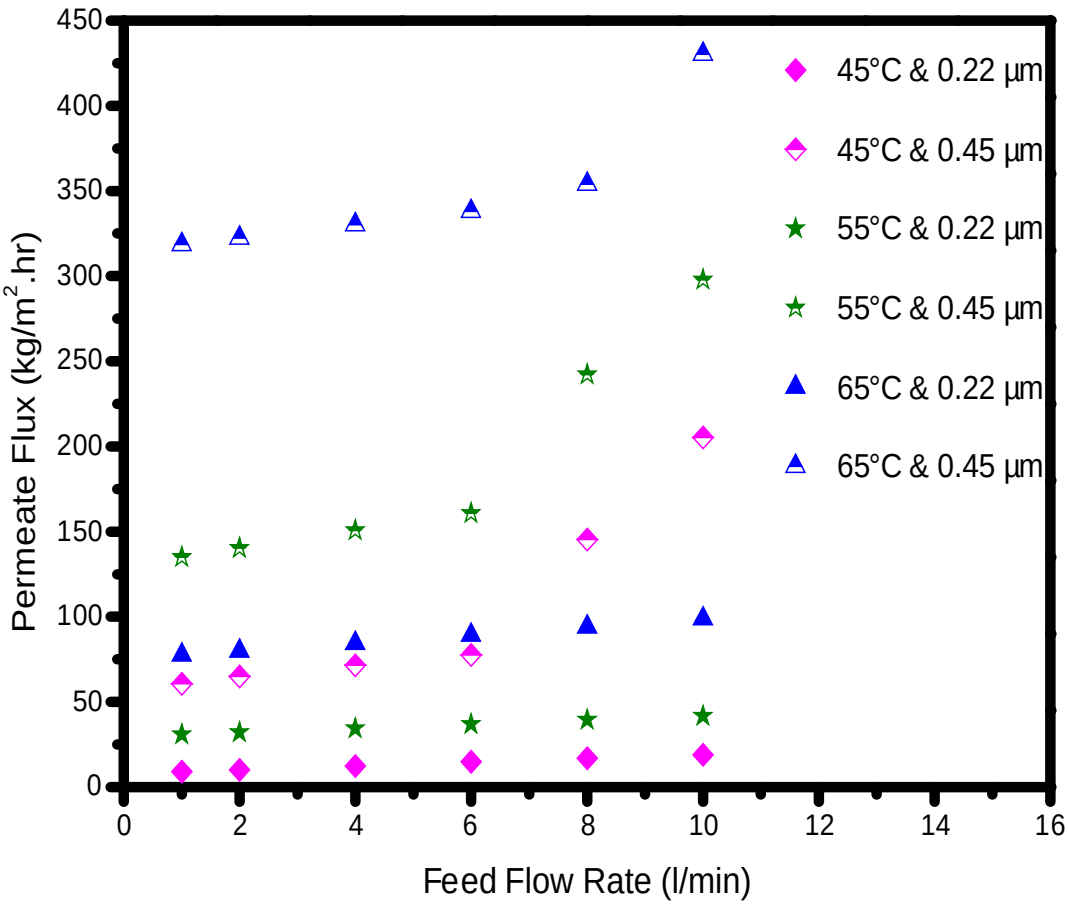

Figure 4.21: Effect of Feed Flow Rate on Permeate Flux [5000 ppm feed salt (NaCl) concentration &9.0 kPa of Permeate Pressure]

4.4.2 Effects of feed inlet temperature on permeate flux for PVDF membrane:

The variation in permeate flux with feed inlet temperature is shown in Figure 4.22.Figure 4.22 Gradual increase was observed in permeate flux from 205kg/m^2·hr to 430 kg/m^2·hr and 19kg/m^2·hr to 99 kg/m^2·hr on increasing the feed bulk temperature from 45 to 65 °C for membrane pore size of 0.45 and 0.22 µm respectively at feed flow rate of 10 lpm, feed salt concentration of 5000 ppm under 9.0 kPa of permeate pressure. This gradual increment in permeate flux is due to the fact that the feed side vapor pressure on membrane increases exponentially according to Antoine relation on increasing the feed bulk temperature which ultimately enhances the driving force for mass transfer. Similar trend is also shown by many other researchers(Lovineh et al. 2013,Tang et al. 2009). However, linear trend in permeate flux is also reported by few authors(Tang et al. 2014,Fan and Peng 2012) on increasing the feed bulk temperature. It can be also visualized from the same figure that the increase in

permeate flux was more on increasing the feed bulk temperature compared to that obtained upon increasing the feed flow rate.

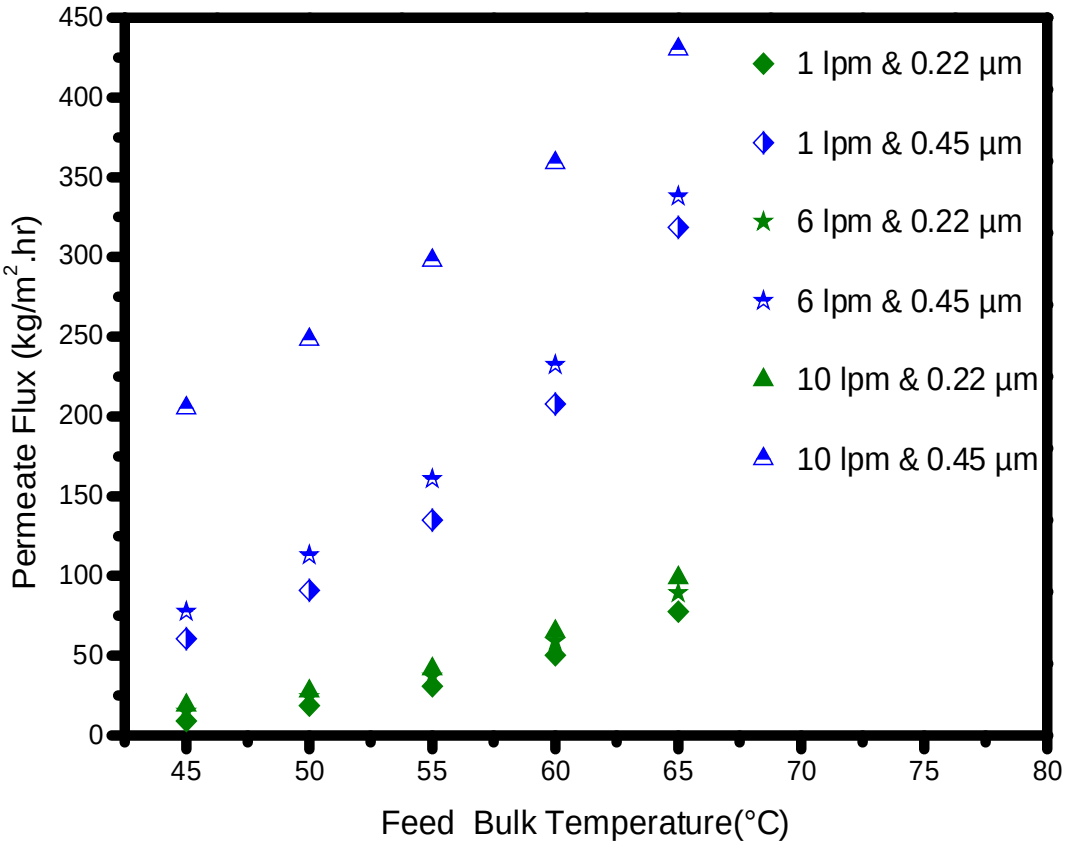

Figure 4.22: Effect of Feed Bulk Temperature on Permeate Flux [5000 ppmfeed salt (NaCl) concentration &9.0 kPa Permeate Pressure]

The temperature polarization coefficient (TPC) is defined as the ratio of feed side membrane surface temperature (feed-membrane interface) to the feed bulk inlet temperature for nonvolatile solute component present in aqueous solution. It is calculated as follows:

$$\theta = \frac{T_{fm}}{T_f} \quad (4.12)$$

It is found from Figure 4.23that TPC decreases with increasing feed bulk inlet temperature at permeate pressure of 9.0 kPa and feed inlet flow rate of 10 lpm, which causes decrease in thermal boundary layer at high feed bulk inlet temperature and subsequent increase in permeate flux.

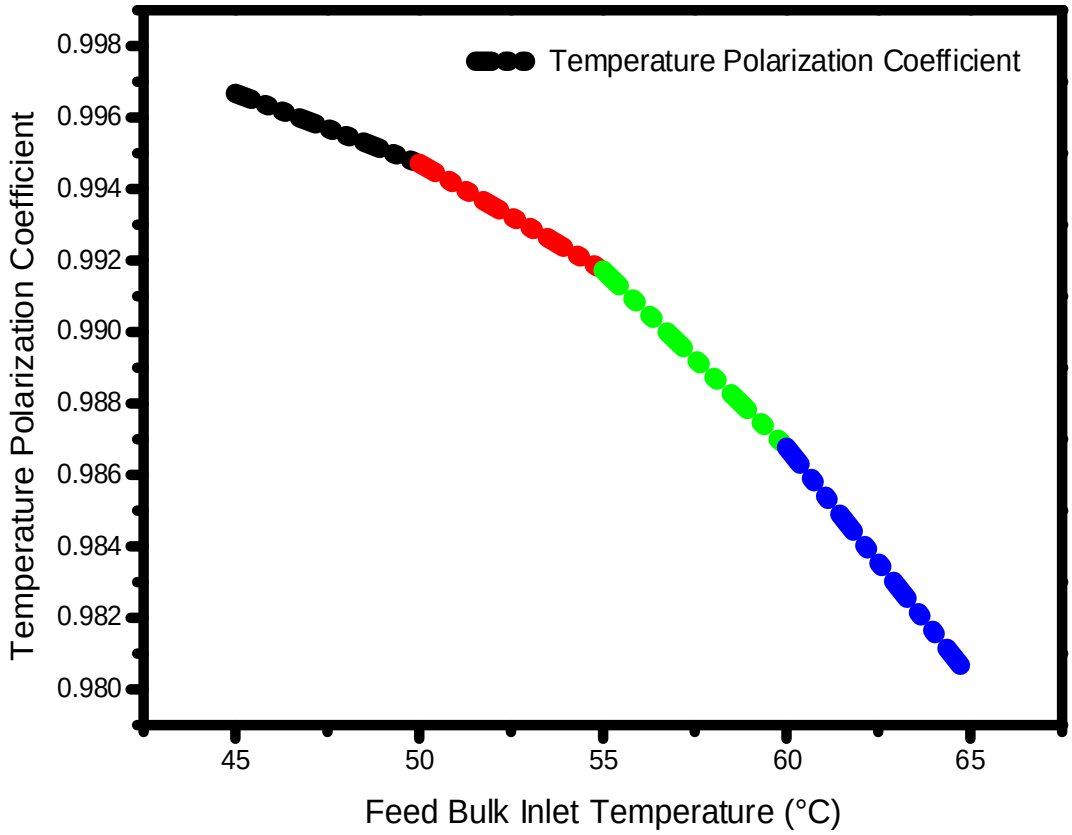

Figure 4.23: Effect of Feed bulk Inlet Temperature on temperature polarization coefficient [9.0 kPa of permeate pressure and feed flow rate 10 lpm for PVDF membrane0.22 µm pore size]

4.4.3 Effect of Feed Concentration on Permeate Flux for PVDF membrane:

The VMD experiment was conducted for different feed salt concentration from 5000 to 50000 ppm at constant feed flow rate of 10 lpm and permeate pressure of 9.0kPa for different pore size of membrane at various feed temperature of 45, 55, and 65 °C. It is evident from Figure 4.24, the permeate flux decreases on increasing the feed salt concentration. This decrease in permeate flux may due to decrease in the vapor pressure with increased salt concentration on the feed side of the membrane and hence, the decrease in mass transfer rate. It was also observed that the permeate flux decreases to 19% and 16% on increasing the feed salt concentration from 5000 to 25000 ppm at 45°C and 65°C respectively for PVDF membrane of pore size 0.22µm . This indicate that the temperature effect on permeate flux on low feed salt concentration is not significant.

However, this decrease in flux becomes significant at higher feed salt concentration and a decrease of 8.7& 4.8% in permeate flux was observed at 45°C and 65 C °respectively for

membrane of pore size 0.45 µm. The same observation of decrease in flux was also reported by many authors (Sun et al. 2014, Drioli et al. 2013) at higher salt concentration range from 40000 to 70000 ppm. Hence, the behavior of membrane was different at low and high salt concentration. This might be due to the fact that the extra concentration boundary layer might have got created on the feed side of the membrane which causes increase in the mass transfer resistance and resulted decline in transmembrane flux. This problem can be overcome by increasing the feed flow rate or by creating the turbulence at feed side of the membrane.

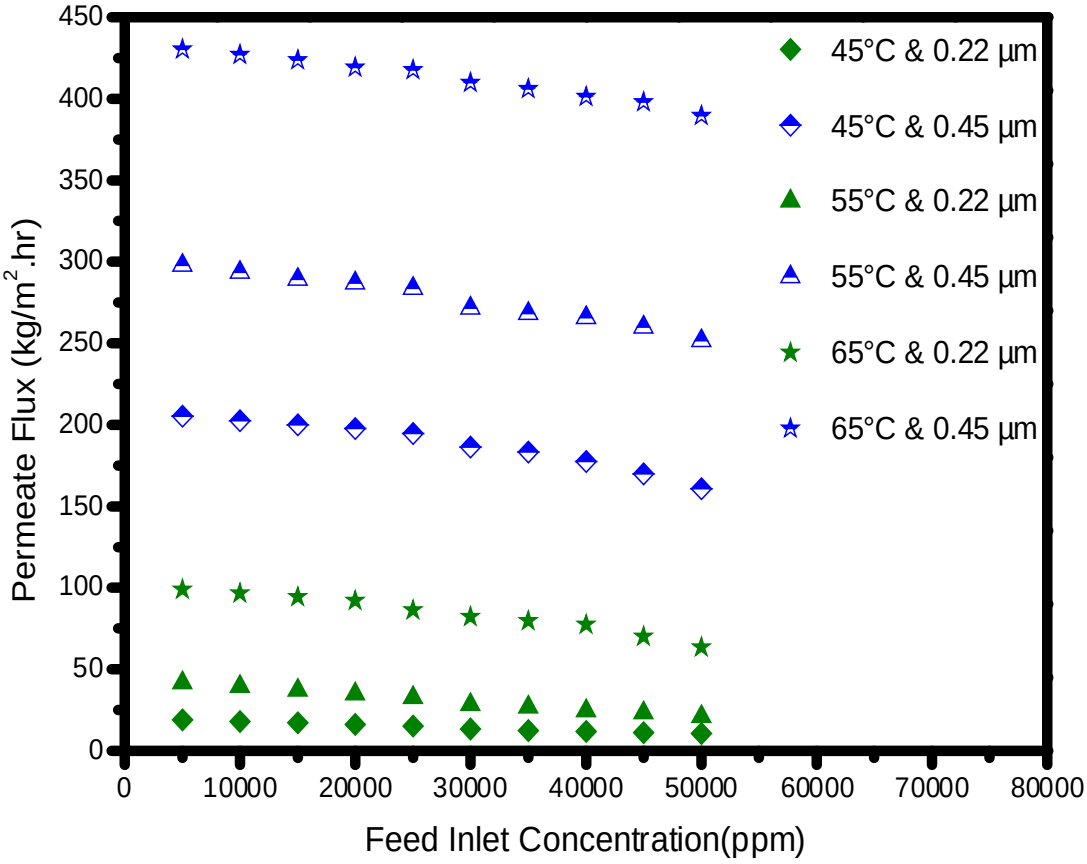

Figure 4.24: Effect of Feed Salt Concentration on Permeate Flux [10 lpm feed flow rate &9.0 kPa of Permeate Pressure]

4.5 Effect of Operating Parameters on Permeate Flux for PTFE membrane.

To study the effect of process parameters, experiments have been carried out at different flow rates in the range of 1-10 l/min and the feed bulk temperature range of 45 °C to 65 °C, feed salt concentration range of 5000 to 50000 ppm at constant permeate pressure. The effect of individual parameters have been discussed in the subsequent sections.

4.5.1 Effect of feed flow rate on permeate flux for PTFE membrane:

Effects of feed flow rate on permeate flux is shown in Figure 4.25at constant feed salt concentration of 5000 ppm and permeate pressure of 9.0 kPa. It can be observed from the Figure 4.25that the permeate flux increases linearly from 77 to 98 kg/m^2·hr and 134 to 178 kg/m^2.hr upon increasing of feed flow rate from 1 to 10 lpm at 65°C for PTFE membrane of pore size 0.22µm and 0.45µm respectively. This increment in permeate flux is because of decrease in temperature boundary layers and concentration boundary layer thickness which ultimately reduces the resistance to mass transfer of vapor to pass through the membrane in VMD, due to increasing in Reynolds number, i.e., turbulence. The same behavior of linear increase in permeate flux with feed flow rate is also reported by many authors (Upadhyaya et al. 2015, Tang et al. 2014, S.P. Chaurasia, Sushant Upadhyaya 2014, Mengual et al. 2004, Mericq et al. 2009). The permeate flux of 178 kg/m^2.hr and 98 kg/m^2.hr is found at feed flow rate of 10 lpm, feed bulk inlet temperature of 65ºC, permeate pressure of 9.0 kPa and feed salt concentration of 5000 ppm was obtained for 0.45µm and 0.22 µm pore size of PTFE membrane. This higher value of permeate flux for 0.45 µm pore size compared to 0.22 µm pore size, at same operating condition is due to the fact that the permeate flux is directly proportional to the square of pore diameter, according to poiseuille flow.

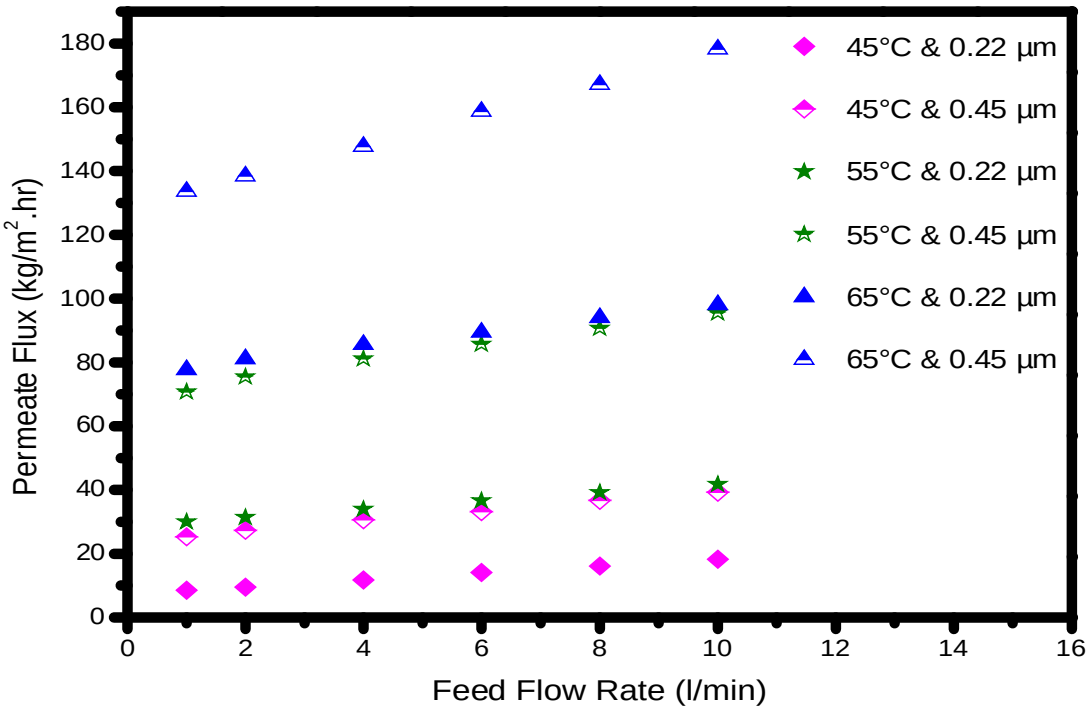

Figure 4.25: Effect of Feed Flow Rate on Permeate Flux [5000 ppm feed salt (NaCl) concentration &9.0 kPa of Permeate Pressure].

4.5.2 Effects of feed inlet temperature on permeate flux for PTFE membrane:

As shown inFigure 4.26, gradual increase was observed in permeate flux from 44 to 178 kg/m^2·hr and 18.2 to 98 kg/m^2·hr on increasing the feed bulk temperature from 45 to 65 °C for PTFE membranes of pore size of 0.45 and 0.22 µm, respectively at feed flow rate of 10 lpm, feed salt concentration of 5000 ppm and9.0 kPa of permeate pressure. This gradual increase in permeate flux is due to the fact that the feed side vapor pressure on membrane increases exponentially by Antoine relation on increasing the feed bulk temperature which ultimately enhances the driving force for mass transfer. The same trend was also shown by many researchers (Upadhyaya et al. 2015,S.P. Chaurasia, Sushant Upadhyaya 2014,Jitendra Singh 2013,Singh et al. 2012. However, linear trend in permeate flux is also reported by few authors(Upadhyaya et al. 2015,Zhang et al. 2015,Chiam and Sarbatly 2013). It can be also visualized from the Figure 4.26that the increase in permeate flux is more rapid on increasing the feed bulk temperature than the feed flow rate.

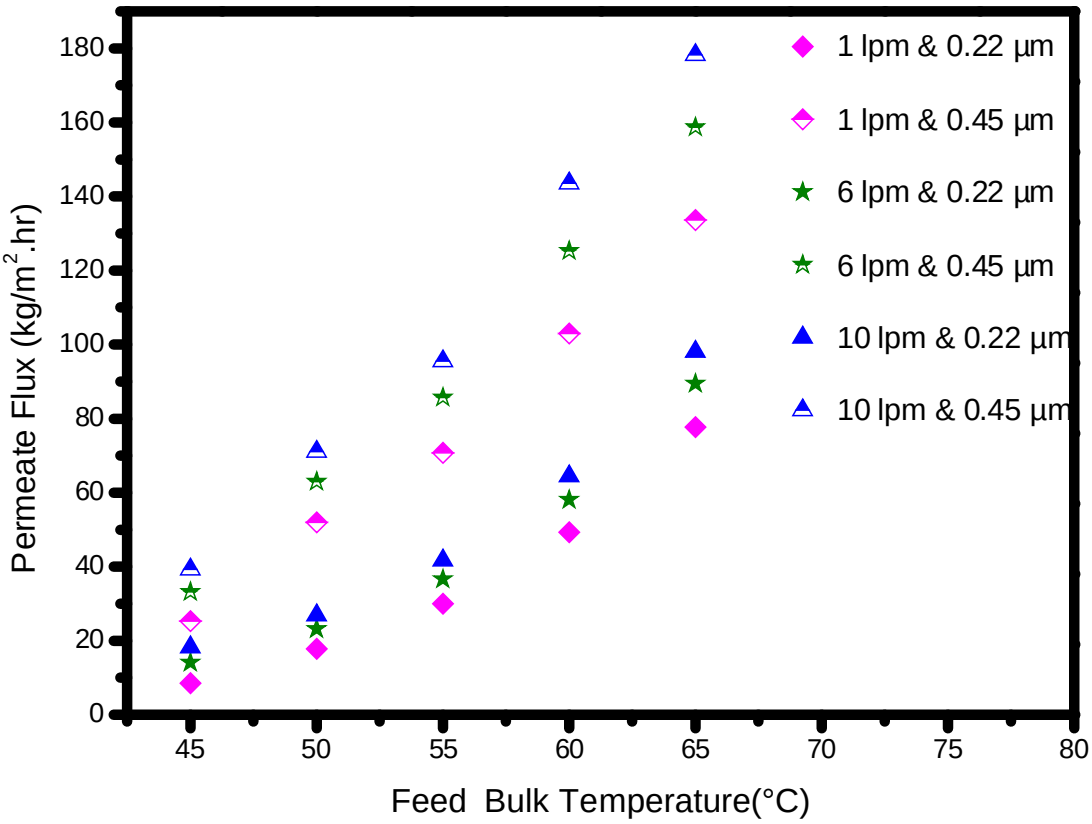

Figure 4.26: Effect of Feed Bulk Temperature on Permeate Flux [5000 ppm feed salt concentration, 9.0 kPa of Permeate Pressure]

It is also observed from Figure 4.27that Temperature Polarization Coefficient (TPC) decreases with increasing feed bulk inlet temperature at permeate pressure of 9.0kPa and feed inlet flow rate of 10 lpm, which causes decrease in thermal boundary layer at high feed bulk inlet temperature and subsequent increase in permeate flux.The same behavior of decrease in TPC with increasing feed bulk temperature is also depicted by other authors (Alsaadi et al. 2014).

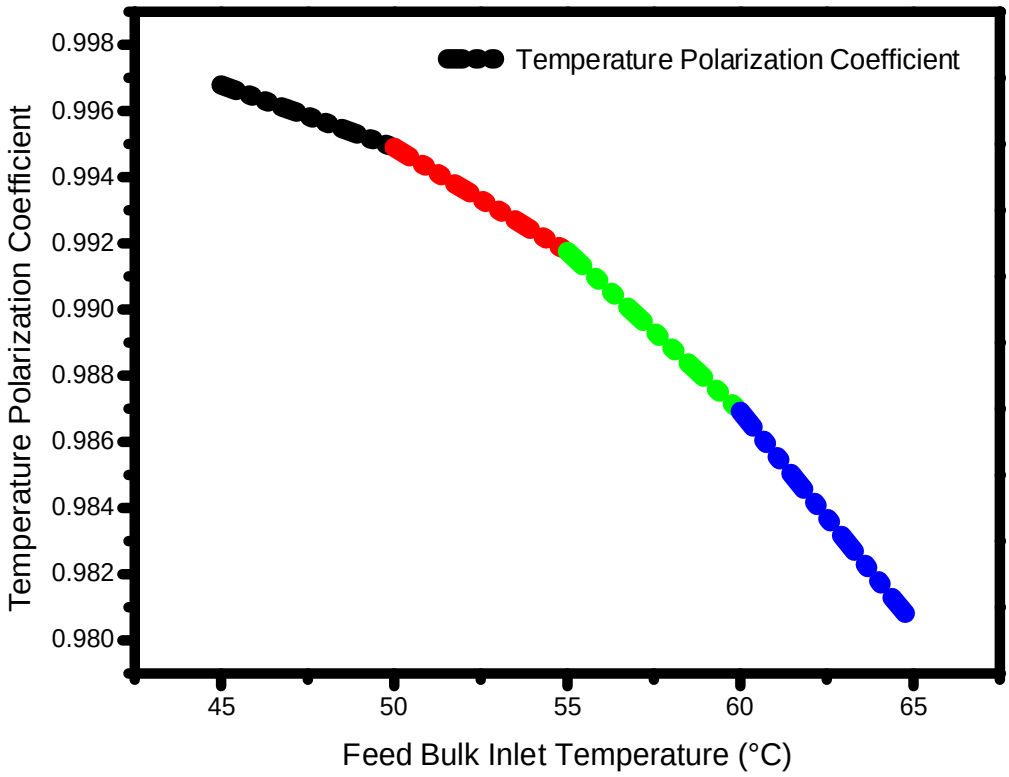

Figure 4.27: Effect of feed bulk inlet temperature on Temperature Polarization Coefficient [9.0 kPa of permeate pressure and feed flow rate 10 lpm].

4.5.3 Effect of Feed Concentration on Permeate Flux for PTFE membrane:

The VMD experiment was conducted for different feed salt concentration from 5000 to 50000 ppm at constant feed flow rate of 10 lpm and permeate pressure of 9.0kPa for different pore size of membrane at various feed temperature of 45°C, 55°C, and 65°C. It is evident from theFigure 4.28, the permeate flux decreasing on increasing the feed salt concentration. This decrease in permeate flux is due to decrease in vapor pressure at the feed side of the membrane after addition of salt and subsequent reduction in mass transfer rate. It was also seen that the permeate flux decreased 18.1% to 16.2 % on increasing the feed salt concentration from 5000 to 25000 ppm at 45°C and 65°C, respectively; for membrane of pore

size 0.22µm. This indicate that the negligible effect on permeate flux on low feed salt concentration.

However, at higher feed salt concentration, decrease in permeate flux has been found to be 11.4% and 5.6%at 45ºC and 65º respectively for membrane of 0.45µmpore size. The same observation of decrease in flux was also reported by many authors(Upadhyaya et al. 2015,Wang et al. 2014, Singh et al. 2012, Pangarkar et al. 2010) at higher salt concentration range from 40000 to 70000 ppm. Hence, the behavior of membrane was different at low and high salt concentration. This might be due to creation of additional boundary layer concentration on the feed side of membrane and further resulting into increased in mass transfer resistance and as a result declination in transmembrane flux. This problem can be overcome by increasing the feed flow rate or by creating the turbulence at feed side of the membrane.

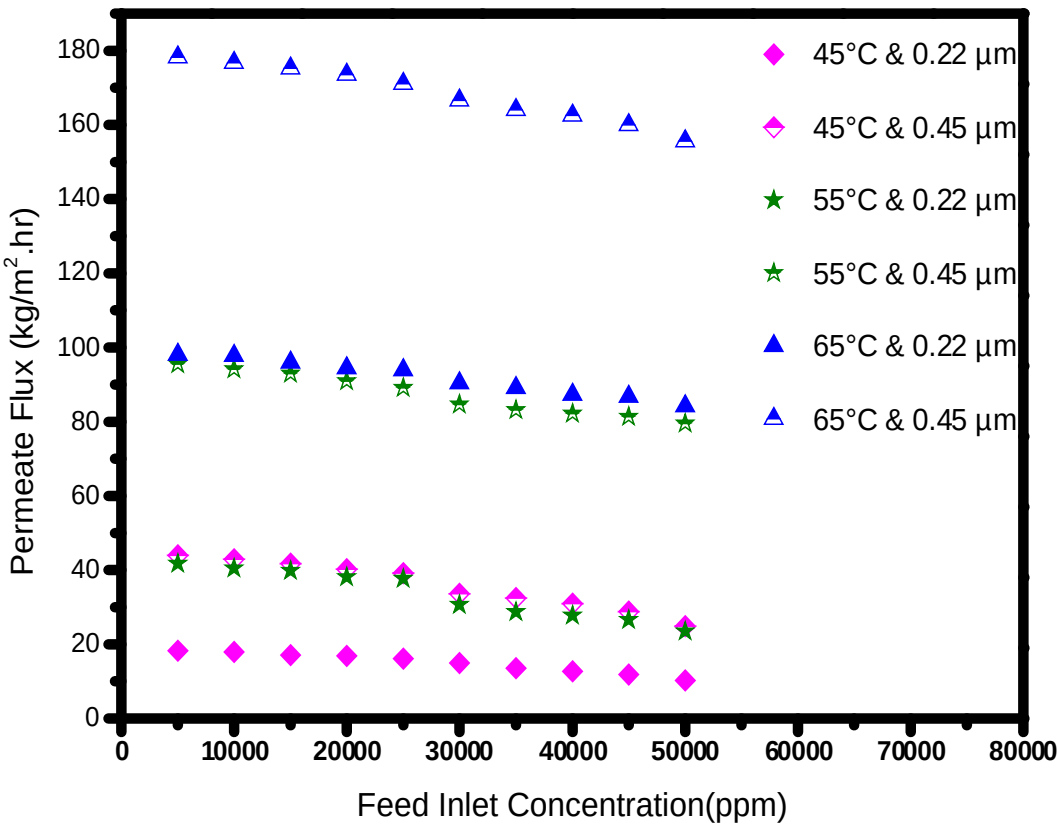

Figure 4.28: Effect of Feed Salt Concentration on Permeate Flux [9.0 kPa of Permeate Pressure and 65°C Feed Bulk Temperature]

4.6 Effects of the operating parameters on saltrejection for PTFE and PVDF membranes

Salt rejection were calculated for both membrane and the effect of operating parameter *viz* feed flow rate, feed bulk temperature and feed salt concentration on salt rejection are shown in Figure 4.29 to Figure 4.34.

4.6.1 Effects of feed flow rate on Salt rejection for PTFE and PVDF Membrane:

As shown in Figure 4.29&Figure 4.30, the rejection of salt was found to be 99.8 % which is constant throughout for PTFE and PVDF for 0.22 µm on increasing the feed flow rate from1 to 10 lpm. However, the rejection of salt was obtained more than 99% for PTFE membrane and PVDF membrane which remains nearly constant on increasing the feed flow rate from 1 to 6 lpm for PTFE and from 1 to 4 lpm for PVDF membrane at 0.45 µm but it was observed that the percentage rejection decreased linearly from 99.5 % to 78.3 % on increasing the feed flow rate beyond 6 to 10 lpm for PTFE membrane and gradually decreased from 98.8 to 16.7 % for PVDF membrane on increasing the feed flow rate from 4 to 10 lpm. The decrease in salt rejection was found to be 21% for PTFE membrane at 0.45 µm pore size.

The decrease in salt rejection was more for PVDF membrane to 82% which might be due to hydrophobicity being directly proportional to mechanical strength of polymer matrix (Norman N. Li). This high level of decrement in percentage rejection may be due to the fact that there might be chance of membrane getting puncture at high flow rate and large pore size.

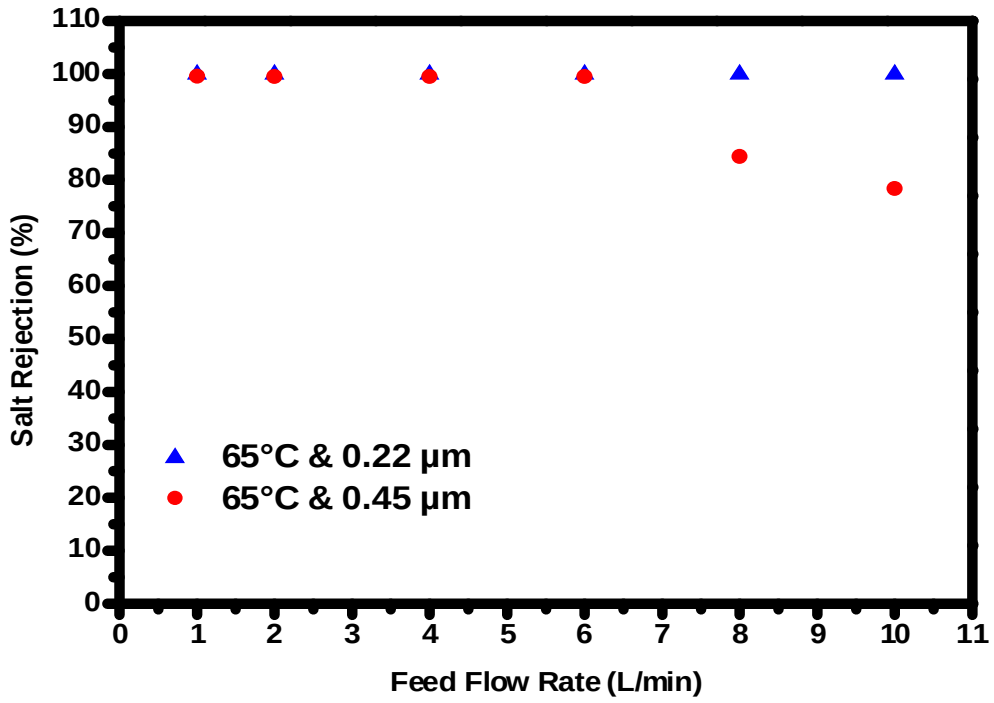

Figure 4.29: Effect of feed flow rate on salt rejection for PTFE membrane [65°C feed bulk inlet temperature, 5000 ppm feed salt (NaCl) concentration & 9.0 kPa permeate pressure]

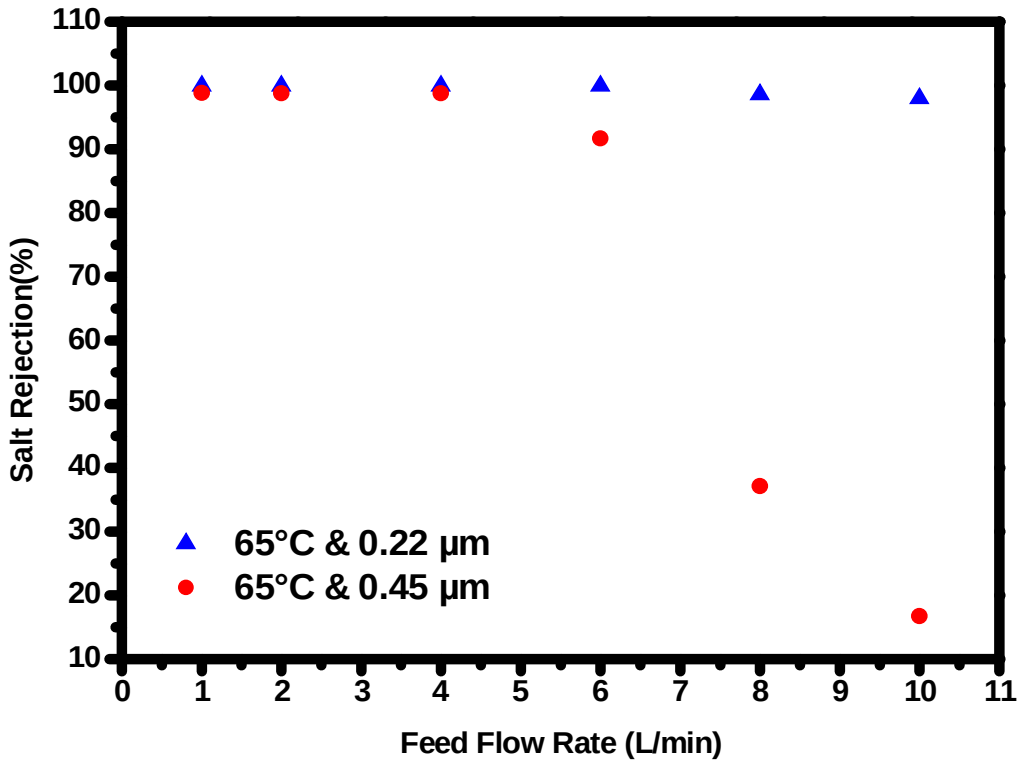

Figure 4.30: Effect of feed flow rate on salt rejection for PVDF membrane [65°C feed bulk inlet temperature, 5000 ppm feed salt (NaCl) concentration & 9.0 kPa permeate pressure]

4.6.2 Effect of the feed bulk inlet temperature on salt rejection for PTFE and PVDF membranes respectively:

It was observed from theFigure 4.31&Figure 4.32 that percentage rejection was more than 99 % for both the membranes (PTFE and PVDF) of pore size 0.22 µm each at feed flow rate of 6 lpm and was constant throughout upon increasing the feed bulk temperature from 45ºC to 65ºC. Moreover, the same level of constant rejection was also encountered for both membranes at feed flow rate 10 lpm for pore size of 0.22 and 0.45 µm respectively by varying the feed bulk temperature from 45 to 65 C. But the percentage rejection for 0.22 µm pore size was more than 99% for both membranes and 78.3% for PTFE whereas 16.7% for PVDF membrane at pore size of 0.45 µm. It is observed that the percentage rejection being constant by varying the feed bulk temperature but got decreased rapidly to 21% and more tremendously to 83% for PTFE and PVDF membrane upon increasing the pore size from 0.22 to 0.45 µm at 10 lpm. This may be due to the fact that the LEP is inversely proportional to pore size of membrane. So, on increasing the pore size, the LEP got decreased which ceases the hydrophobicity of the membrane, as a result at high pore size of 0.45 µm there may be chance of leakage in the membrane subject to high feed flow rate of 10 lpm which ultimately reduces the percentage rejection of salt. Therefore, percentage rejection of 16.7% is found at feed flow rate of 10 lpm at 0.45 µm for PVDF membrane. This shows that the membrane may got punctured.

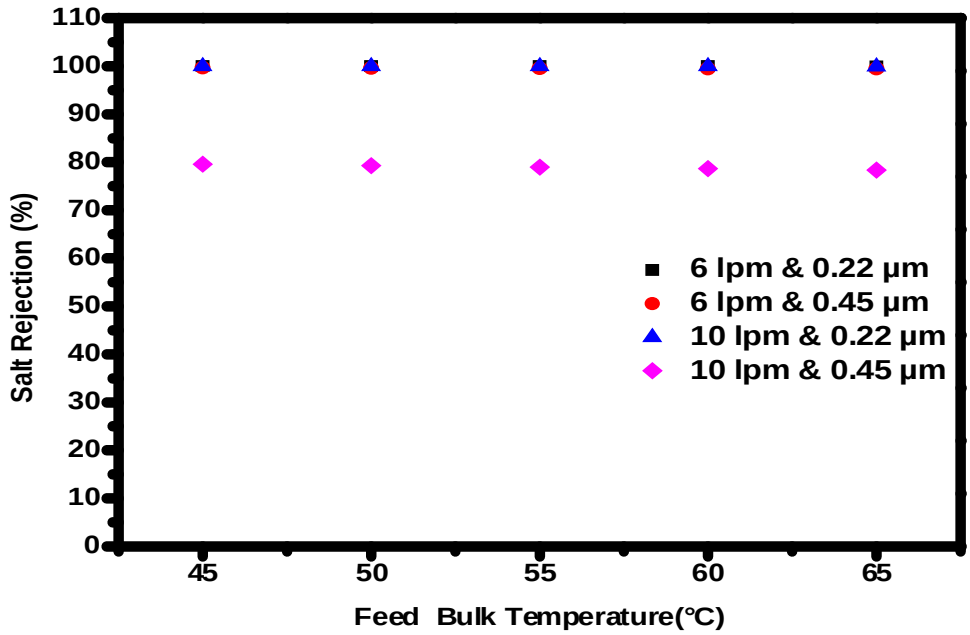

Figure 4.31: Effect of feed bulk temperature on salt rejection for PTFE membrane [feed salt (NaCl) concentration of 5000 ppm & permeate pressure of 9.0 kPa]

4.6.3 Effects of the feed salt concentration on salt rejection for PTFE and PVDF membranes respectively:

The salt rejection was found to be 99.9% as shown in Figure 4.33&Figure 4.34, which is constant on increasing the feed salt concentration from 5,000 ppm to 50,000 ppm for PTFE and PVDF membrane of pore size 0.22 µm at 6 lpm. However, the salt rejection decreased from 91.7% to 84.7% on increasing the feed salt concentration from 5,000 ppm to 50,000 ppm for PVDF membrane of pore size 0.45 µm at 6 lpm. Further, the salt rejection decreased from 78.3% to 5.5% and 16.7% to 10.3% at 10 lpm for 0.45µm PTFE and PVDF membranes, respectively.

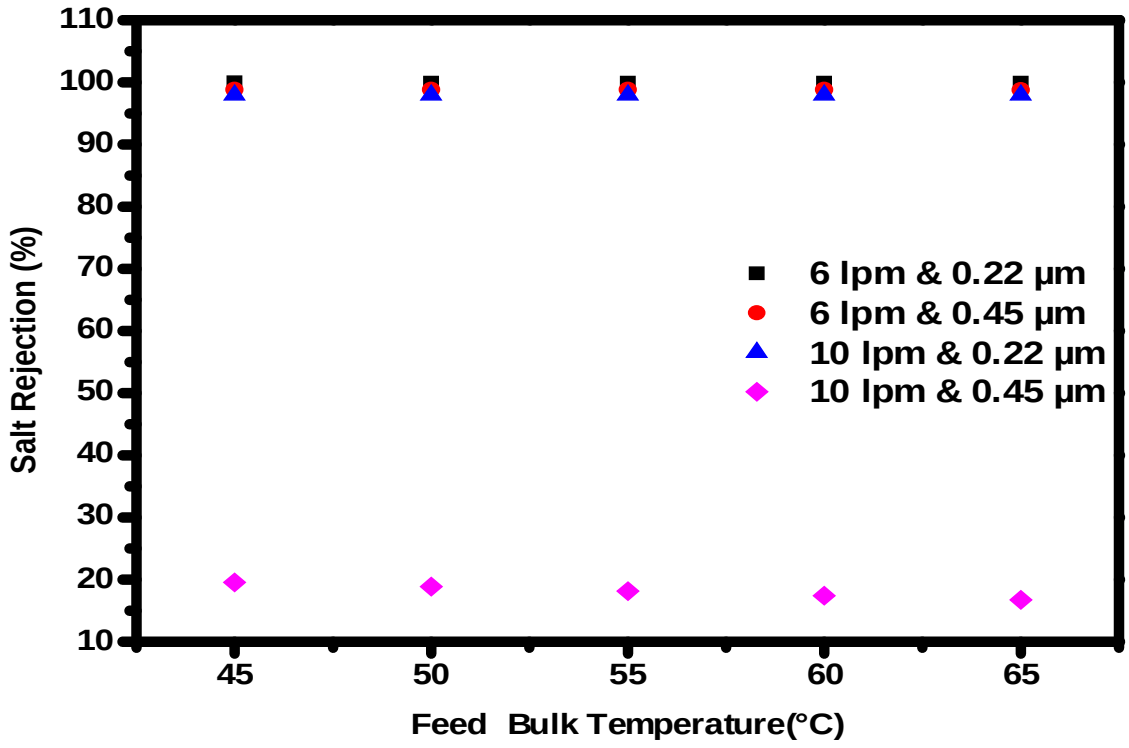

Figure 4.32: Effect of feed bulk temperature on salt rejection for PVDF membrane [feed salt (NaCl) concentration of 5000 ppm & permeate pressure of 9.0 kPa]

4.7 Effects of the operating parameters on Specific Energy Consumption for PTFE and PVDF membranes.

Specific energy consumption were calculated for both membranes and the effect of operating parameter *viz* feed flow rate, feed bulk temperature and feed salt concentration on specific energy consumption have been studied and the results are shown in Figure 4.35 to Figure 4.37as discussed below.

4.7.1 Effects of feed flow rate on energy consumption for PTFE and PVDF membranes:

It can be observed from theFigure 4.35, that specific energy consumption decreased linearly from 10.2 to 6.5 kWh/kg and 8.4 to 4.4 kWh/kg for 0.22 µm for PTFE and 0.22 µm PVDF membranes respectively on increasing the feed flow rate from 1 to 10 lpm. The specific energy consumption is found to be higher for PTFE membrane than PVDF membrane for same pore size. This may be due to the fact that the PTFE is more hydrophobic and has higher thermal conductivity 0.26 W/m.K than PVDF material as both, hydrophobicity and thermal conductivity of material are inversely proportional to the permeate flux (Lovineh et al. 2013). However, the percentage decrease in specific energy consumption for PTFE membrane was found to be 36 % which is lower than the PVDF membrane for which specific energy consumption was found to be 48% on increasing the feed flow rate from 1 to 10 lpm at pore size of 0.22 µm.

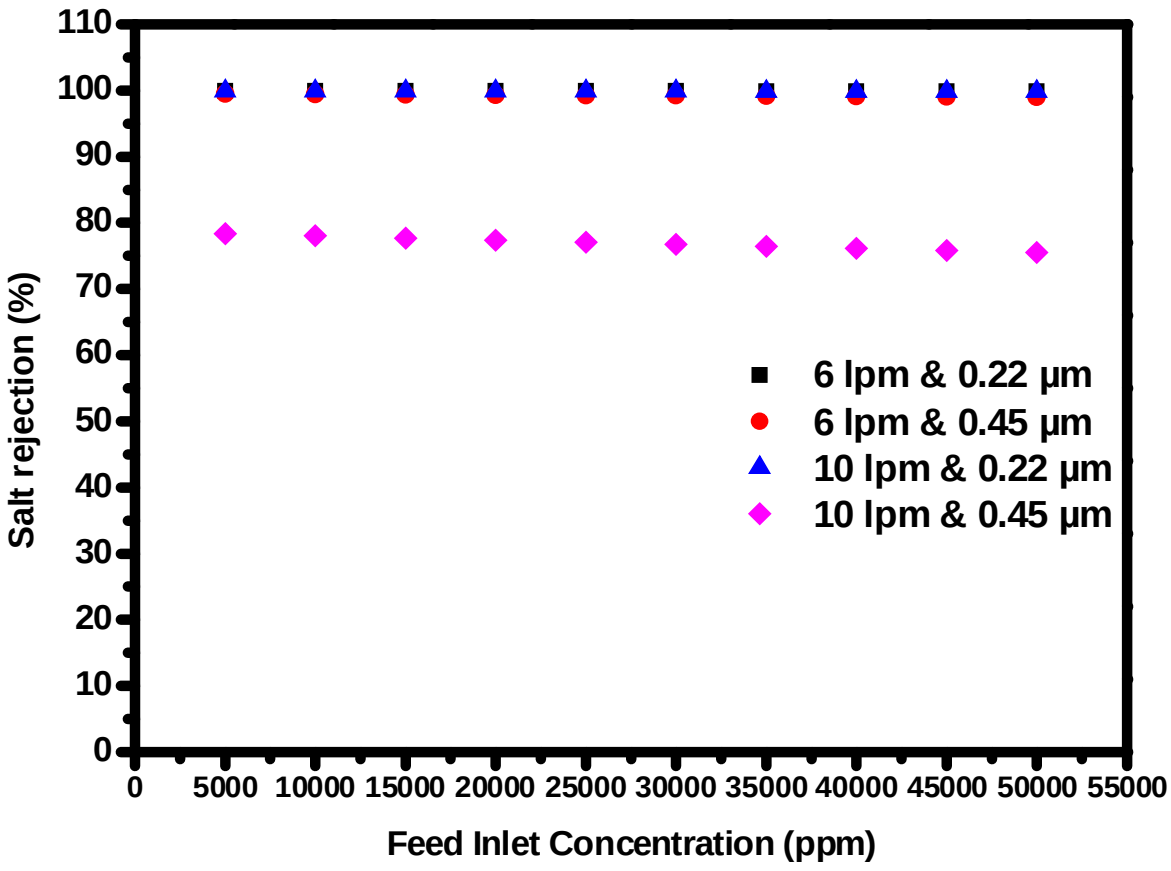

Figure 4.33: Effect of feed inlet concentration on salt rejection for PTFE membrane [65°Cfeed bulk inlet temperature, 5000 ppm feed salt (NaCl) concentration & 9.0 kPa permeate pressure]

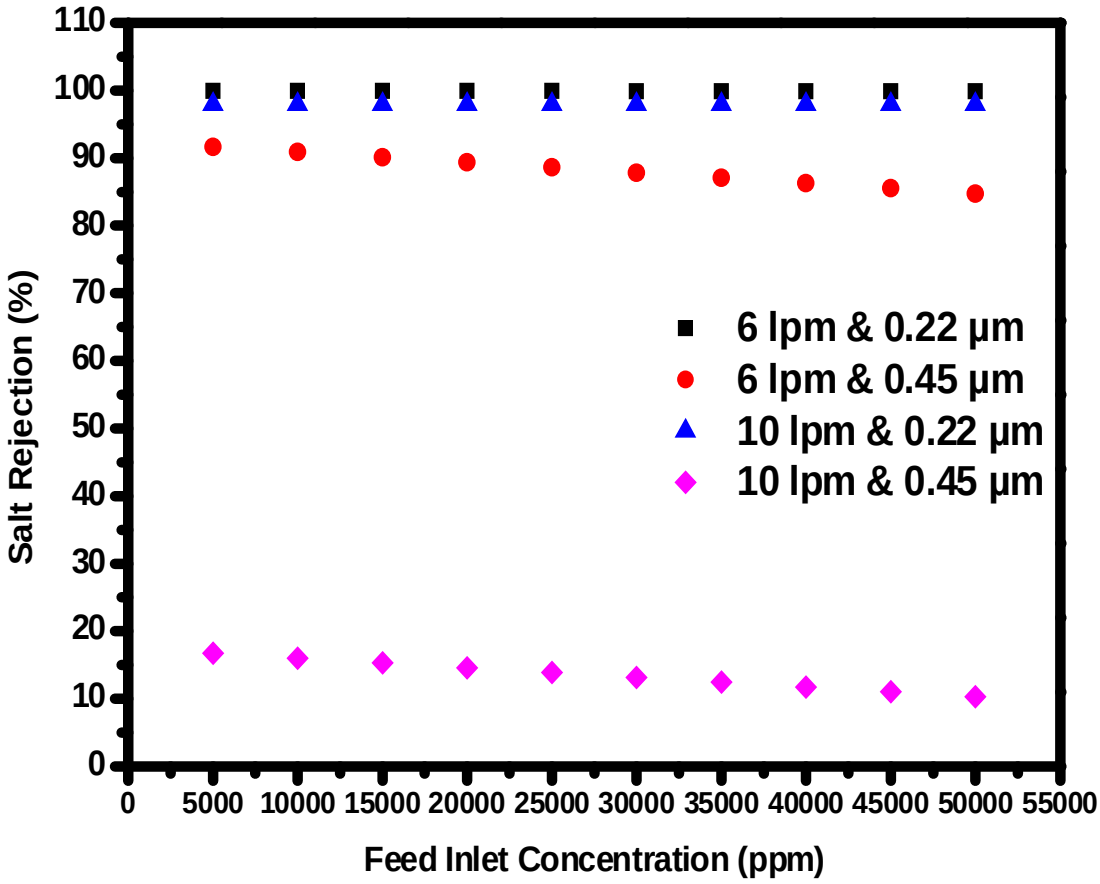

Figure 4.34: Effect of feed inlet concentration on salt rejection for PVDF membrane [65°Cfeed bulk inlet temperature, 5000 ppm feed salt (NaCl) concentration & 9.0 kPa permeate pressure]

4.7.2 Effects of the feed bulk inlet temperature on energy consumption for PTFE and PVDF membranes:

The effect of feed bulk temperature on specific energy consumption is shownFigure 4.36. It was observed that the specific energy consumption has decreased linearly from 20.7 to 8.95 kWh/kg and 18.65 to 4.4 kWh/kg for 0.22 µm of PTFE and PVDF membranes respectively, on increasing the feed bulk temperature from 45°C to 65°C. This may be due to the reason that permeate flux increased on increasing the feed bulk temperature and due to this specific energy decreased. Remarkable decrease in specific energy consumption has been observedfor 0.22 µm PTFE and PVDF, both types of membranes, on increasing the feed bulk temperature from 45 to 65°C, at feed flow rate of 10 lpm and 9.0 kPa permeate pressure.This may be attributed as the discrimination of pore size decreases on permeate flux by increasing the feed bulk temperature as more vapor space is created at high temperature which minimize the effect of pore size on flux.

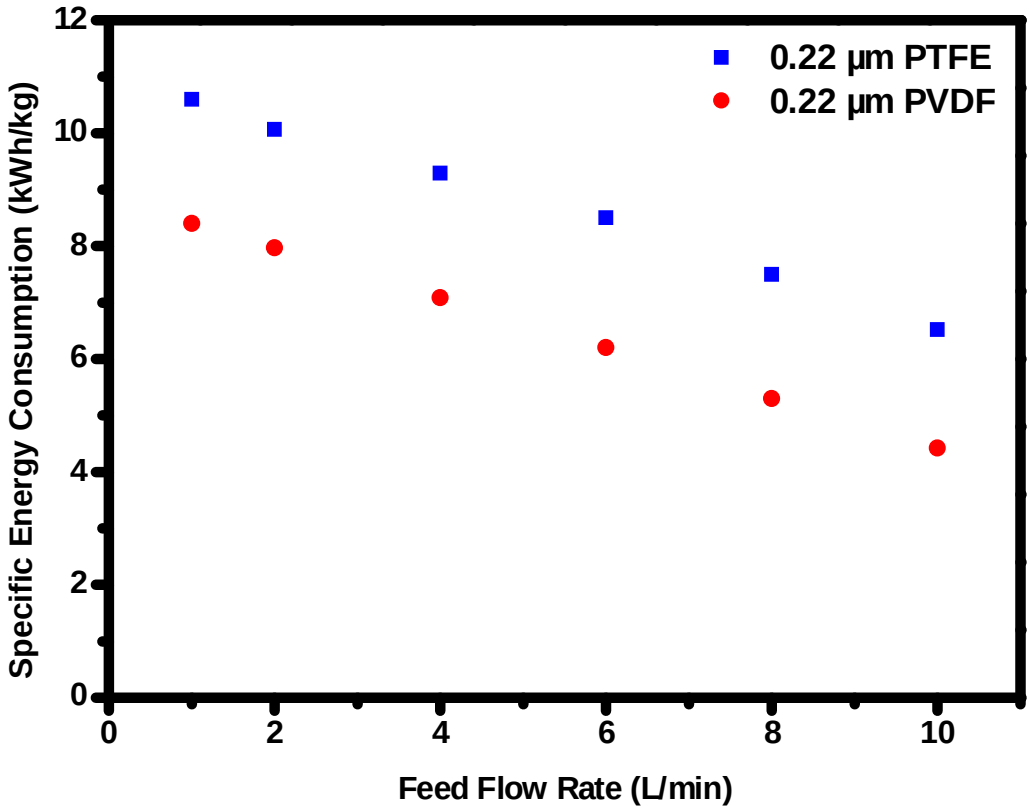

Figure 4.35: Effect of Feed Flow Rate on Specific Energy Consumption [Feed bulk temperature65°C, feed salt (NaCl) concentration5000 ppm& permeate pressure9.0 kPa]

4.7.3 Effect of the feed salt concentration on energy consumption for PTFE and PVDF membranes:

The effects of feed salt concentration on specific energy consumption is shown in Figure. It can be depicted from the figures that the specific energy consumption has increased linearly on increasing the feed salt concentration from 5,000 to 50,000 ppm for PTFE and PVDF membrane of pore size 0.22 µm, at feed flow rate of 10 lpm. This may be due to the fact that activity coefficient decreases as per modified *Raults' law* on increasing the feed concentration as a result driving force for mass transfer declines which ultimately decreases the specific energy consumption. The specific energy consumption at 50000 ppm of NaCl salt concentration was found to be 12.25 kWh/kg for pore size of 0.22 µm PTFE membrane whereas it is 10.14 kWh/kg for 0.22µm pore size of PVDF membrane. Hence, it can be observed that the specific energy consumption is more for PTFE as compared to PVDF which may be due to PVDF membrane being less hydrophobic.

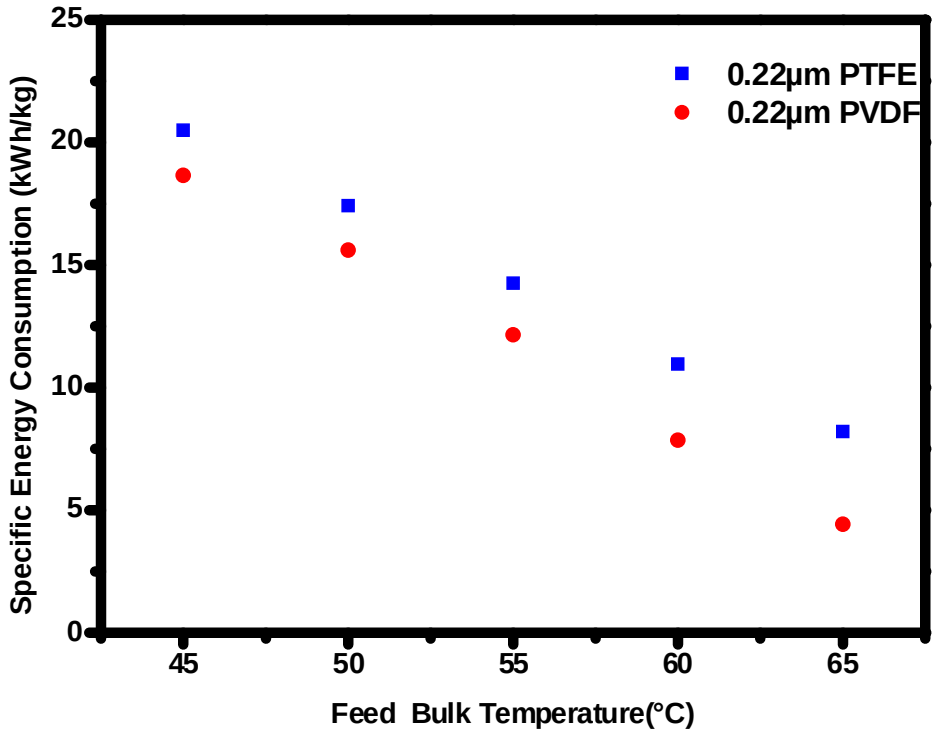

Figure 4.36: Effect of Feed bulk temperature on Specific Energy Consumption [Feed flow rate10 lpm, feed salt (NaCl) concentration5000 ppm& permeate pressure9.0 kPa]

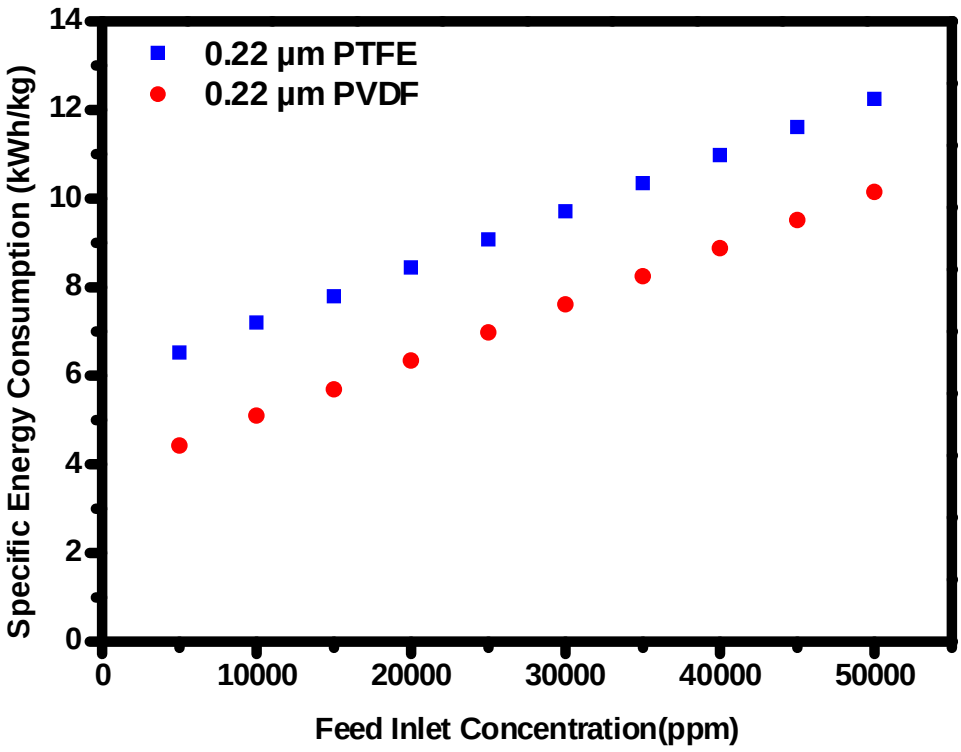

Figure 4.37: Effect of Feed Salt Concentration on Specific Energy Consumption [Feed Bulk Temperature 65°C, feed flow rate 10 lpm& Permeate Pressure9.0 kPa]

4.8 Membrane Material Comparison

Membrane material comparison has been done in the present work by studying the influence of membrane material type and pore diameter on permeate flux and salt rejection.Two different membrane materials *viz* PTFE and PVDF have been studied. The effect of feed flow rate, feed bulk inlet temperature and feed concentration are shown in Figure 4.38 to Figure 4.40for pore diameter of 0.22 µm and in Figure 4.41 to Figure 4.43for pore diameter of 0.45 µm. It is observed from Figure 4.38 to Figure 4.40that the permeate flux remains nearly unchanged for PTFE and PVDF membrane for constant pore diameter of 0.22 µm. However, a dramatic increment in permeate flux were seen in Figure 4.41 to Figure 4.43for different membrane material but of constant pore size of 0.45 µm. This interesting outcome may be due to the fact that the membrane thermal conductivity is more significant at higher pore size (>0.22 µm) and have negligible effect for small pore size (< 0.22 µm). The same inference regarding membrane flux, no significant difference between membrane materials below pore size of 0.2 µm was also reported by author (Lovineh et al. 2013).

The permeate flux for PVDF membrane of thermal conductivity (0.18 W/m.K) is found to be less as compared to PTFE membrane of thermal conductivity (0.26 W/m.K) for constant pore diameter of 0.45 µm. This may be due to the fact that thermal conductivity of membrane material is inversely proportional to permeate flux. Further, since the coefficient of friction (COF) of PTFE membrane material is 0.05 which is less than COF of 0.34 for PVDF membrane. So, PTFE is more hydrophobic than PVDF as COF is inversely proportional to hydrophobicity. As a result, PTFE membrane will restrict the water molecule to pass through membrane pores to a higher extent as compared to PVDF membrane. Henceforth, permeate flux for PTFE membrane is found to be less compared to PVDF membrane at constant pore diameter of 0.45 µm.

In case of 0.45µm pore size membrane, the permeate flux for PVDF membrane was found to be higher than that of PTFE membrane as shown in Figure 4.41 to Figure 4.43. This may be due to the fact that the thermal conductivity of PVDF is 0.18 W/m.K compared to 0.26 W/m.K for PTFE and as the permeate flux is inversely proportional to the thermal conductivity of the membrane material.

The heat loss through the membrane is directly proportionally to thermal conductivity of the membrane material. Therefore, heat loss through PVDF and PTFE membrane under identical conditions can be calculated as

$$\frac{Q_{PTFE}}{Q_{PVDF}} = \frac{K_{PTFE}}{K_{PVDF}} \Rightarrow \frac{0.26}{0.18} = 1.44 \Rightarrow Q_{PTFE} = 1.44 Q_{PVDF} \quad (4.12)$$

Hence, heat loss through PTFE membrane is found to be1.44 time more than PVDF membrane. Moreover, quantitate value of heat loss can be calculated through the membrane as follows

$$HeatLoss = \frac{KA}{\delta}\left(t_{fm} - t_{pm}\right) \quad (4.13)$$

On putting the respective value for PTFE and PVDF membrane in above equation for 0.22µm pore size. The heat loss for PTFE and PVDF membrane is found to be 1.15W and 0.83W respectively.

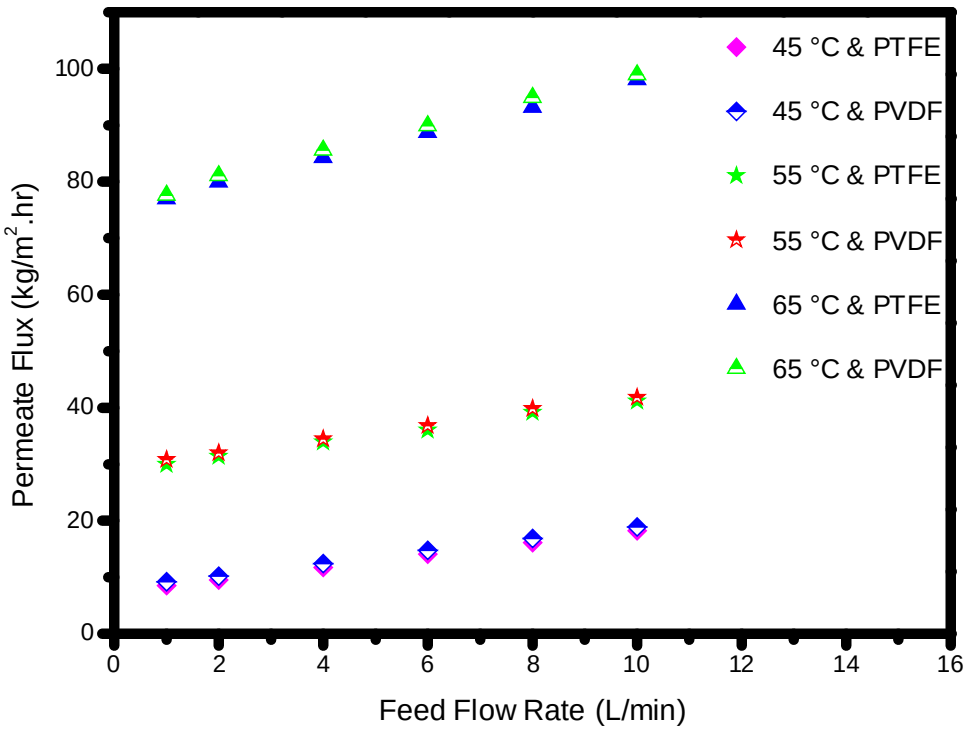

Figure 4.38: Effects of the feed flow rate on permeate flux [feed salt (NaCl) concentration5000 ppm, permeate pressure 9.0 kPa and membrane pore diameter0.22µm]

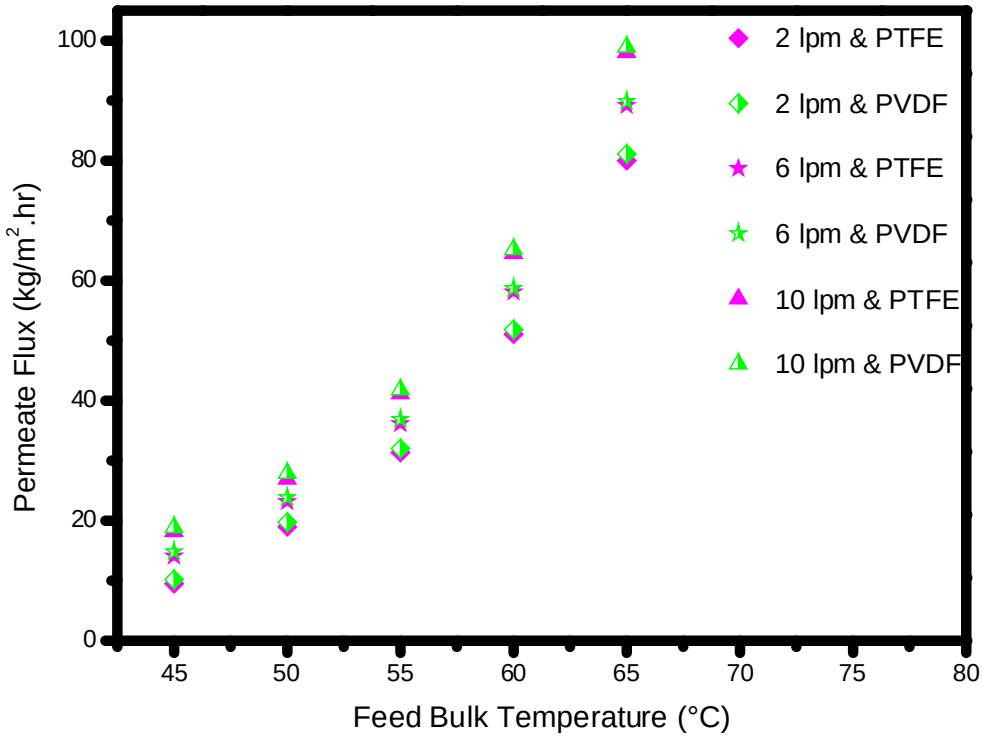

Figure 4.39: Effects of the feed bulk temperature on permeate flux [feed salt (NaCl) concentration5000 ppm, permeate pressure 9.0 kPa and membrane pore diameter0.22µm]

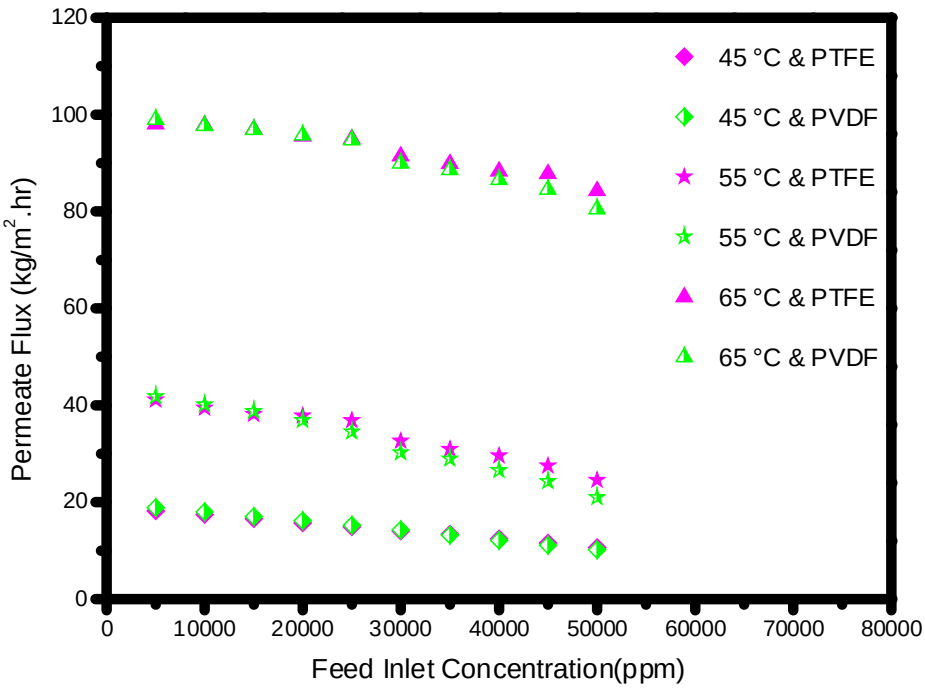

Figure 4.40: Effects of the feed salt concentration on permeate flux [feed flow rate10 lpm, permeate pressure 9.0 kPa and membrane pore diameter0.22µm]

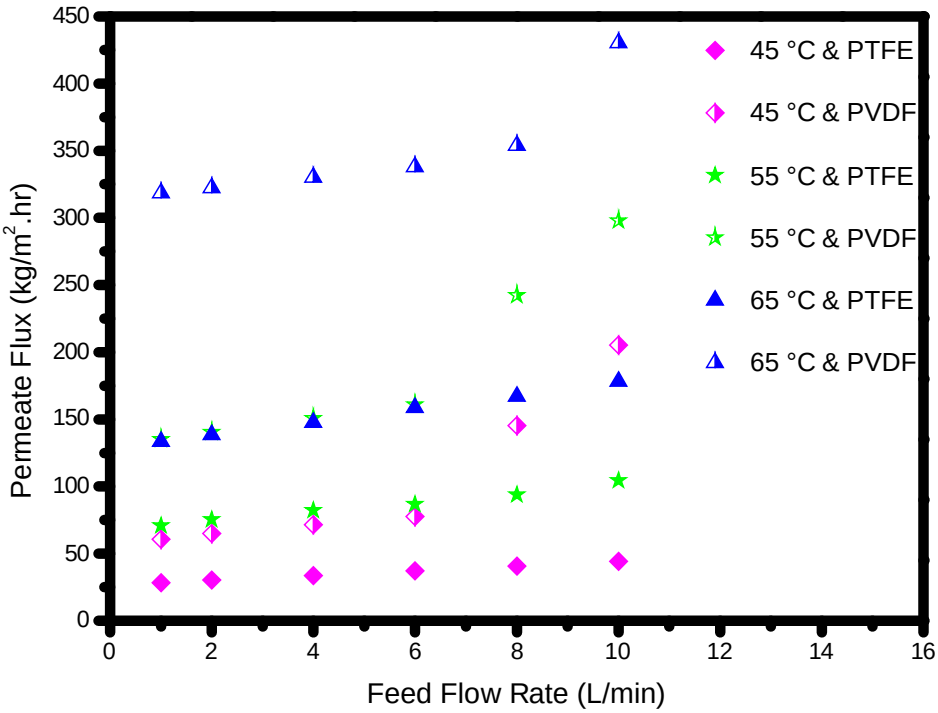

Figure 4.41: Effects of the feed flow rate on permeate flux [feed salt (NaCl) concentration5000 ppm, permeate pressure 9.0 kPa and membrane pore diameter0.45 µm]

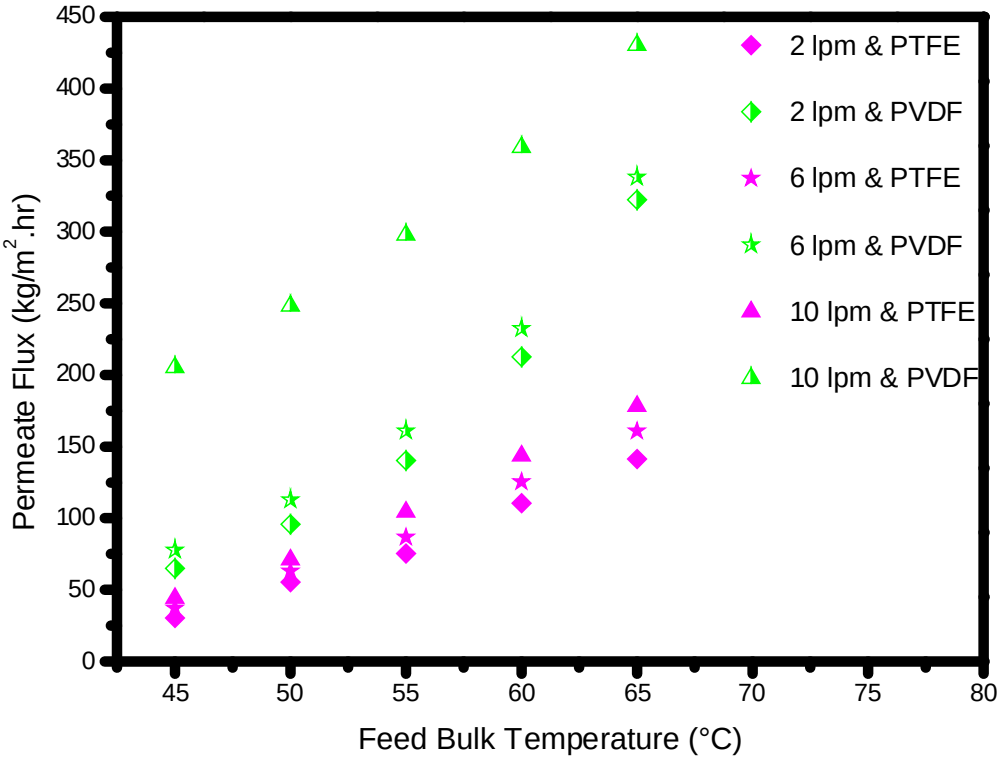

Figure 4.42: Effects of the feed bulk temperature on permeate flux [feed salt (NaCl) concentration5000 ppm, permeate pressure 9.0 kPa and membrane pore diameter0.45 µm]

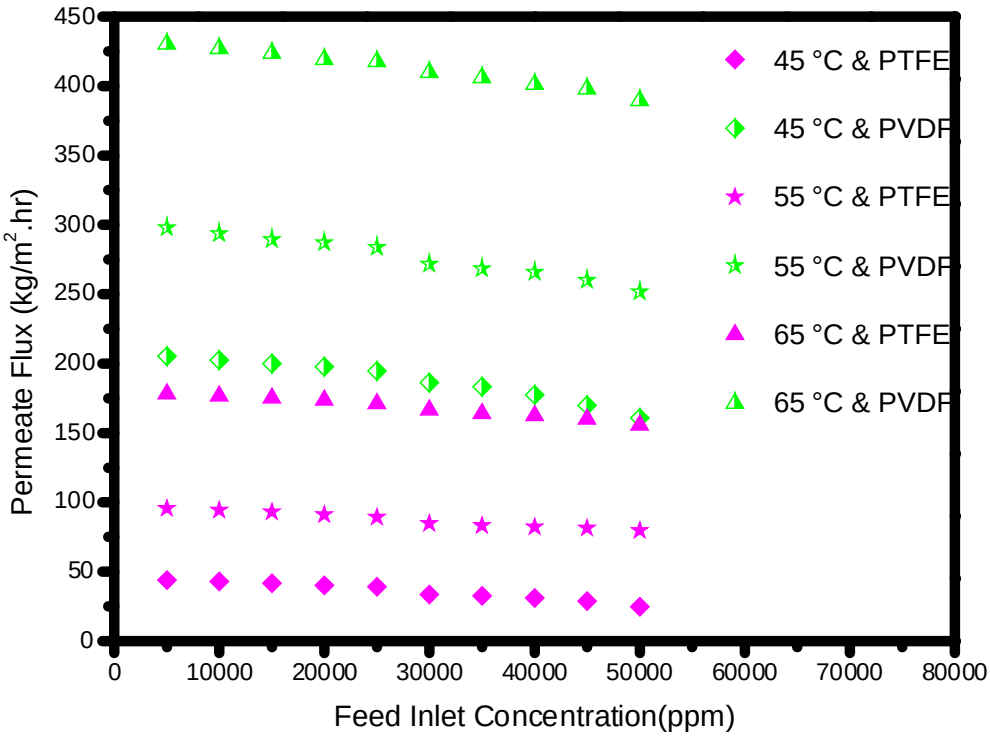

Figure 4.43: Effects of the feed salt concentration on permeate flux [feed flow rate10 lpm,permeate pressure 9.0 kPa and membrane pore diameter0.45 µm]

4.9 Membrane Characterization

4.9.1 Effect of Membrane Fouling on Permeate Flux

In a continuous operation, the salt concentration of 5000 ppm was used as a feed solution for a VMD setup and the trans-membrane permeate flux collected continuously for about 200 hours for PTFE and PVDF membrane respectively at two different pore diameter of 0.22 and 0.45 µm. In 200 hrs of operation the flux remained almost constant for both, PTFE and PVDF membranes of 0.22 µm and 0.45 µm pore size as shown in Figure 4.44. At 338 K, the permeate flux was 89.3 kg/m^{2}hr for PVDF membrane and 89.21 kg/m^{2}hr for PTFE membrane which remained nearly constant till 200 hours at 9.0 kPa permeate pressure and 6 lpm feed flow rate for pore diameter of 0.22 µm. It can be observed from the Figure 4.44, that the flux decreased nearly 4 % for PVDF and 1.7% for PTFE membrane respectively in 200 hours, which may be due to the minor fouling on the membrane surface. After, 200 hours the water washing was done and the membrane performance was checked again and it was observed that the flux regained to about 88.32 kg/m^{2}h for PVDF and 87.88 kg/m^{2}h for PTFE membrane under the same process conditions with 99.9% salt rejection. Further, it is also evident from the Figure 4.44., that the decrease in flux for PTFE membrane is less as compared to PVDF

membrane for both the pore sizes of 0.22 and 0.45 µm which may be because PTFE is more hydrophobic than PVDF. As shown in Figure 4.44, the percentage decrease in permeate flux was more for higher pore size membrane of same membrane material. This may be due to the reason, the probability of solute entrapment inside the membrane pore is more likely, when the pore size of membrane is higher.

4.9.2 Comparison of Membrane Morphology before and after Use of the membranes

The membrane morphology was tested by scanning electron microscope (SEM). The membranes before and after its use in VMD process were analyzed. The SEM micrograph of brand new PVDF and PTFE membrane morphology for two different pore diameter of 0.22 and 0.45 µm are shown inFigure 4.45. It is observed that the new membranes used in SEM study, one pore diameter of PVDF and PTFE membrane found up to 0.35 µm and 0.30µm respectively, whereas the average pore diameter of the PVDF and PTFE membrane were 0.22 µm as per the specifications given by the manufacturer (Millipore). Similarly, from Figure 4.45 (c) and (d), the largest pore for PVDF and PTFE membranes were found to have diameter of 0.59µm and 0.54µm respectively, however, few pore were having diameter of less than 0.45 µm whereas the average pore diameter for the PVDF and PTFE membranes were 0.45 µm as per the manufacturer (Millipore). Hence, it may be concluded that average pore diameter reported by supplier was matching with the pore diameter measured from SEM.The other characteristics of fresh PTFE membranes are given in Table 3.4. Large pores of size 10 µm were also observed through SEM by other researchers Khayet et al. 2004, Tang et al. 2010,Banat and Simandl 1996,Karakulski et al. 2002 inspite the average pore size of accrual PP S6/2 membrane mentioned as 0.22 µm.

The performance of PTFE and PVDF membranes were checked by continuously using the membranes in VMD setup separately under 9.0 kPa of permeate pressure, feed flow rate of 6 lpm, feed inlet temperature of 65 °C and feed salt concentration of 5000 ppm for 200 hr run. The SEM micrograph of these membranes is shown in Figure 4.46(a), (b), (c), (d). Minor fouling/scaling can be observed over the membrane surface. Therefore, little reduction in permeate flux was observed for PTFE membrane of pore diameter 0.22 and 0.45 µm after 200 hours of continuous use of membrane.

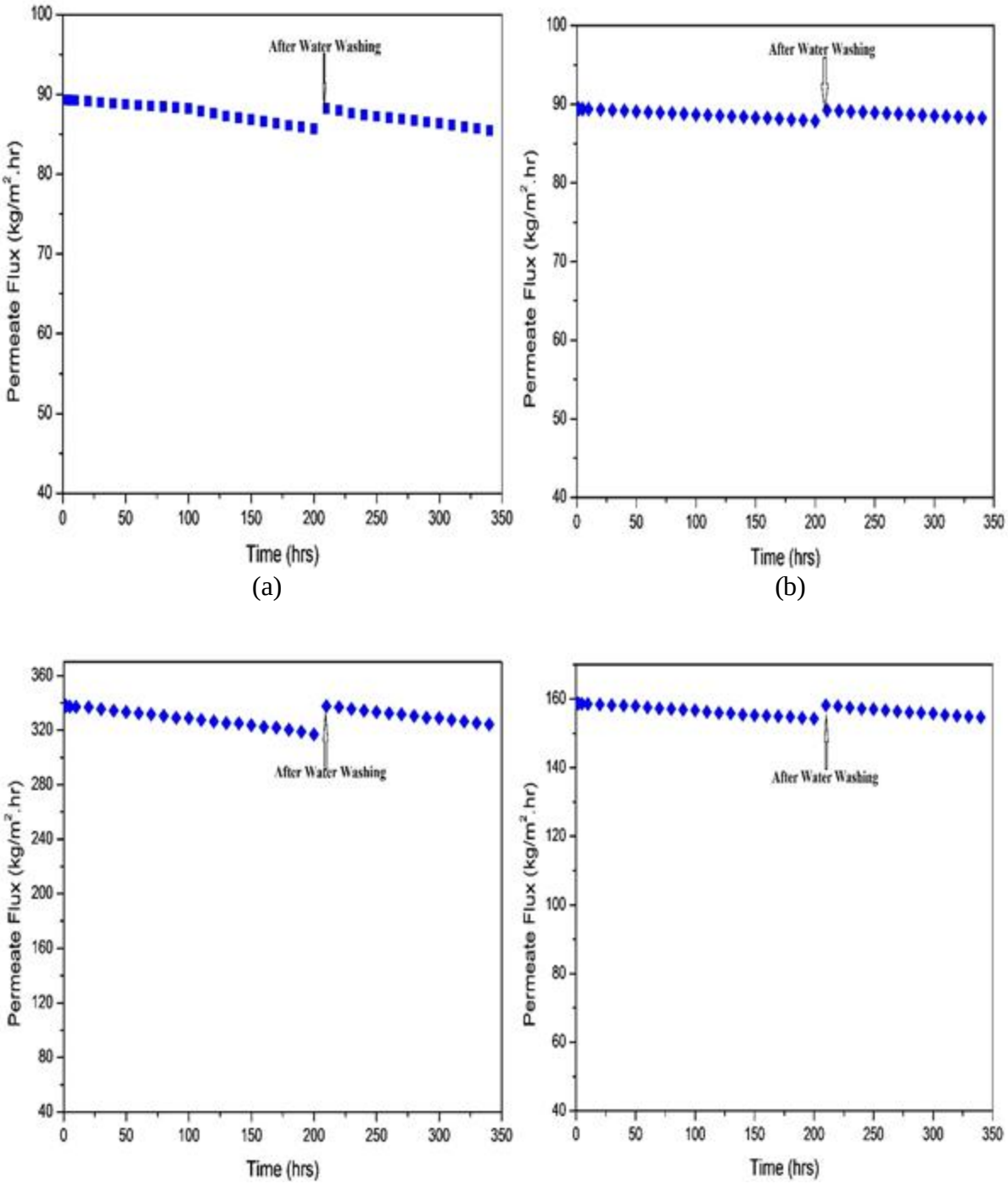

Figure 4.44: Effects of operating time on permeate flux, (a) 0.22 µm PVDF, (b) 0.22 µm PTFE, (c) 0.45 µm PVDF, (d) 0.45 µm PTFE[Feed bulk temperature 65°C, feed salt (NaCl) concentration5000ppm, feed flow rate 6 lpm& permeate pressure 9.0 kPa]

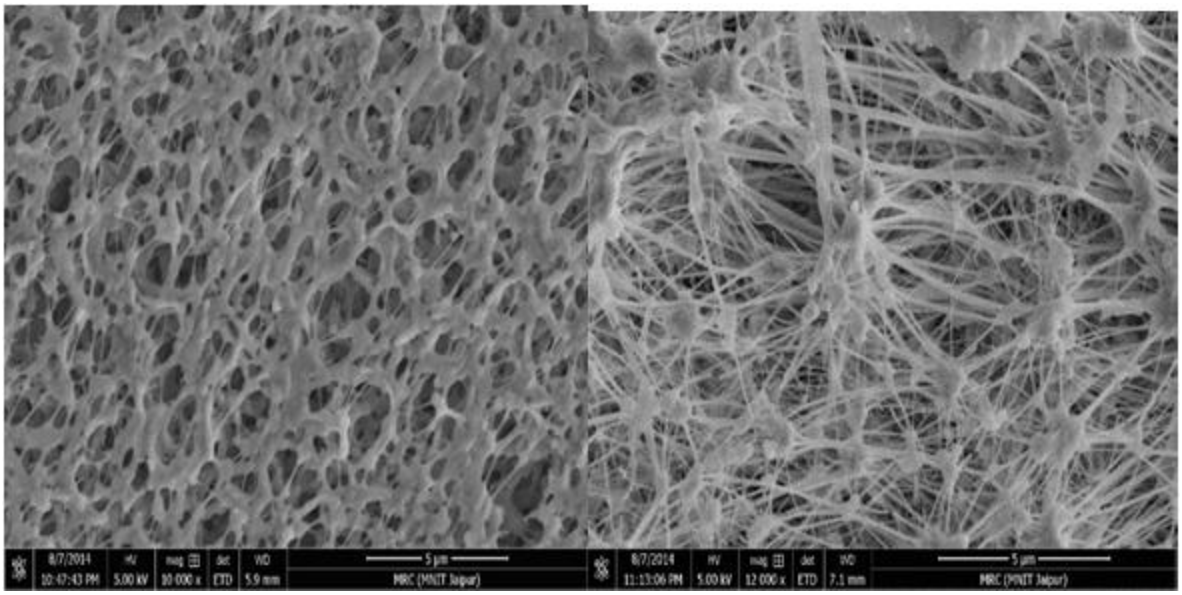

(a) **(b)**

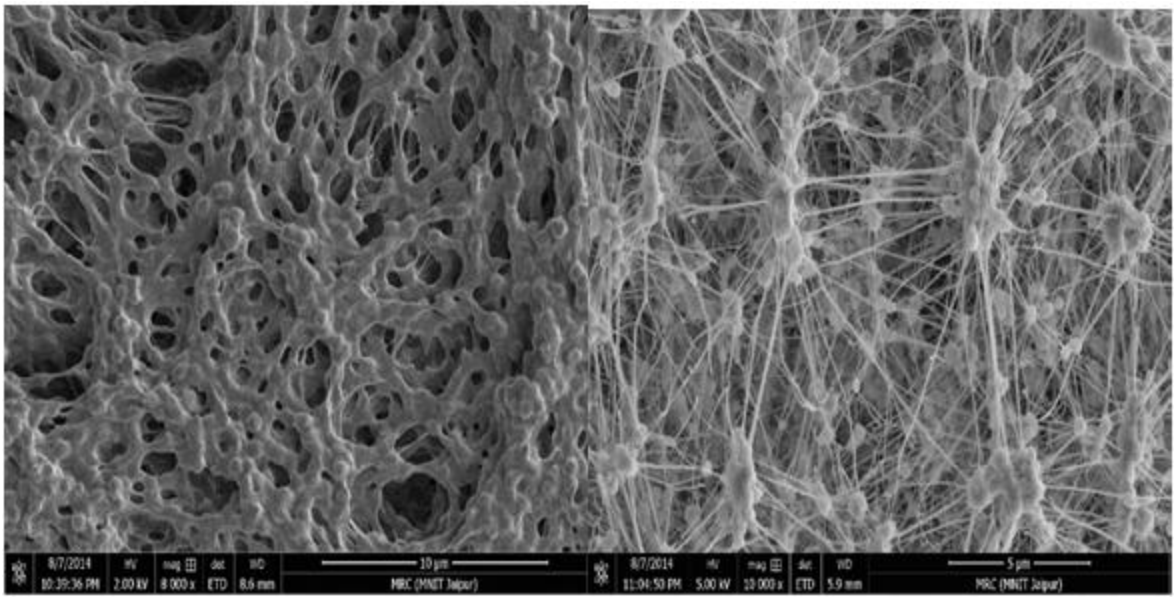

(c)(d)

Figure 4.45: SEM micrograph depicting pore size (new brand) (a) 0.22 µm PVDF (b) 0.22 µm PTFE (c) 0.45 µm PVDF (d) 0.45 µm PTFE.

Similar results were observed for PVDF membrane of pore diameter 0.22 and 0.45 µm also. The flux was almost found to regain its original value after washing the membrane with water. In the present work as shown inFigure 4.46, the decrease in permeate flux is observed to 4% and 6.3 % for PVDF membrane of pore size 0.22 and 0.45 µm respectively and for PTFE membrane of pore size 0.22 and 0.45 µm decline in flux was observed 1.7% and 2.6%, respectively at 5 g/l of feed salt concentration over 200 hour run. Safavi and Mohammadi 2009 have also reported 33.6% decrease in permeate flux for synthetic sea water solution of

salt concentration 300 g/l and about 10% decrease for 34 g/l of salt concentration in feed solution. In the later case, no crystal growth and scale deposit was observed in SEM micrograph.

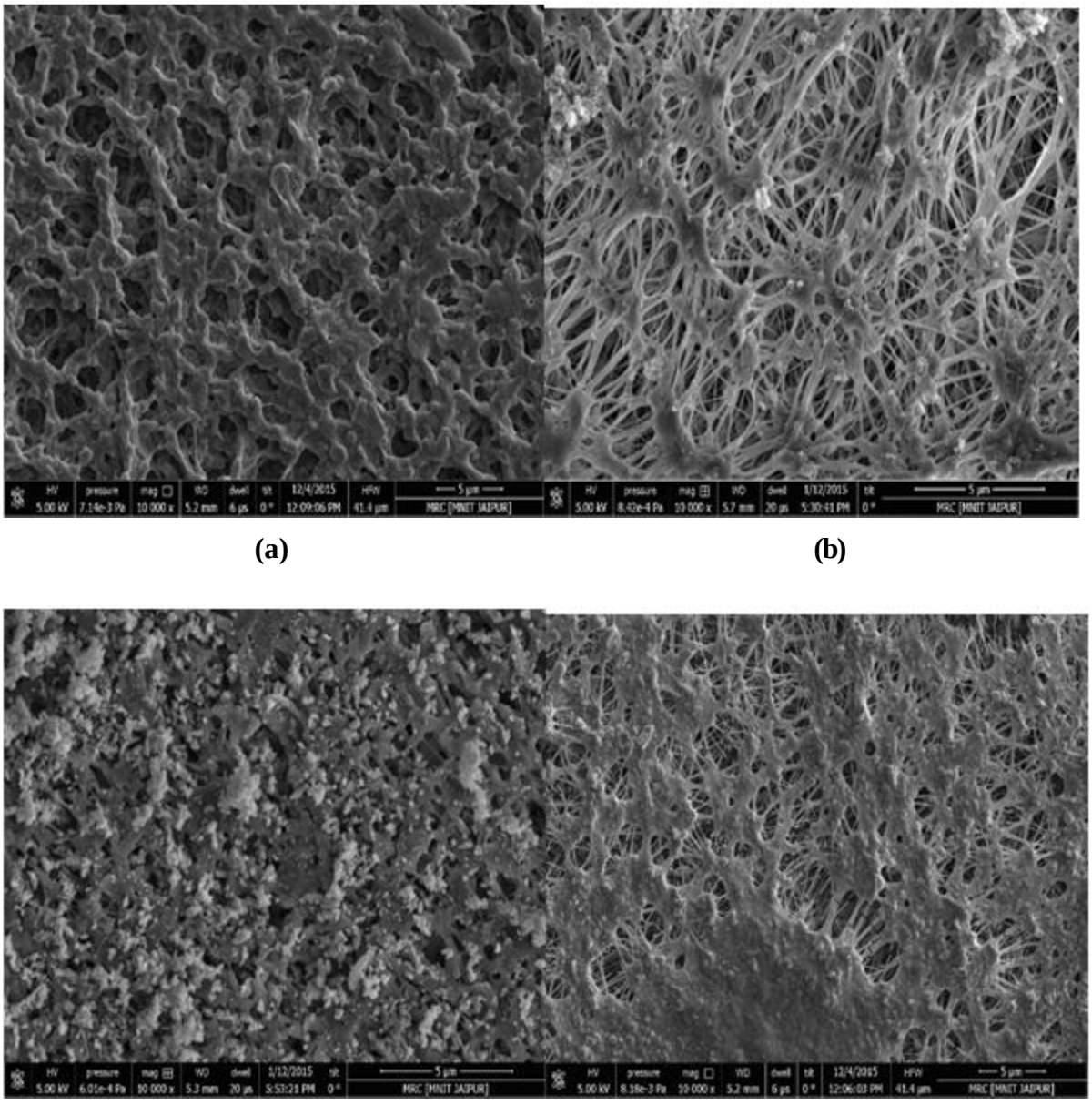

(a) **(b)**

(c) **(d)**

Figure 4.46: SEM image of used (a) 0.22 µm PVDF (b) 0.22 µm PTFE (c) 0.45 µm PVDF (d) 0.45 µm PTFE, after 200 hours run[Feed bulk temperature 65°C, feed flow rate 6 lpm, feed salt (NaCl) concentration 5000 ppm & permeate pressure 9.0 kPa]

The SEM micrograph of PTFE and PVDF hydrophobic membrane of different pore diameter of 0.22 µm and 0.45 µm after use of 340 hours continuously, at 9.0 kPa of permeate pressure, feed flow rate of 6 lpm, feed inlet temperature of 65°C and feed NaCl salt concentration of

5,000 ppm are shown in Figure 4.47 (a) (b) (c) (d). The figure is showing little delta deposition which may be because of high NaCl feed concentration. Also, at this high concentration, the declination of 9% and 4% in permeate flux was observed for PVDF and PTFE membrane respectively for 0.22 µm pore size. On the other hand, the declination in permeate flux was found to be 12.5% and 7.2% for 0.45µm PVDF and PTFE membranes respectively. Thistype of decrease in permeate flux was supported by the SEM picture as NaCl deposit lapped feeble portion of the membrane surface which increases the temperature polarization effect and reduces the membrane permeability due to salt deposition.

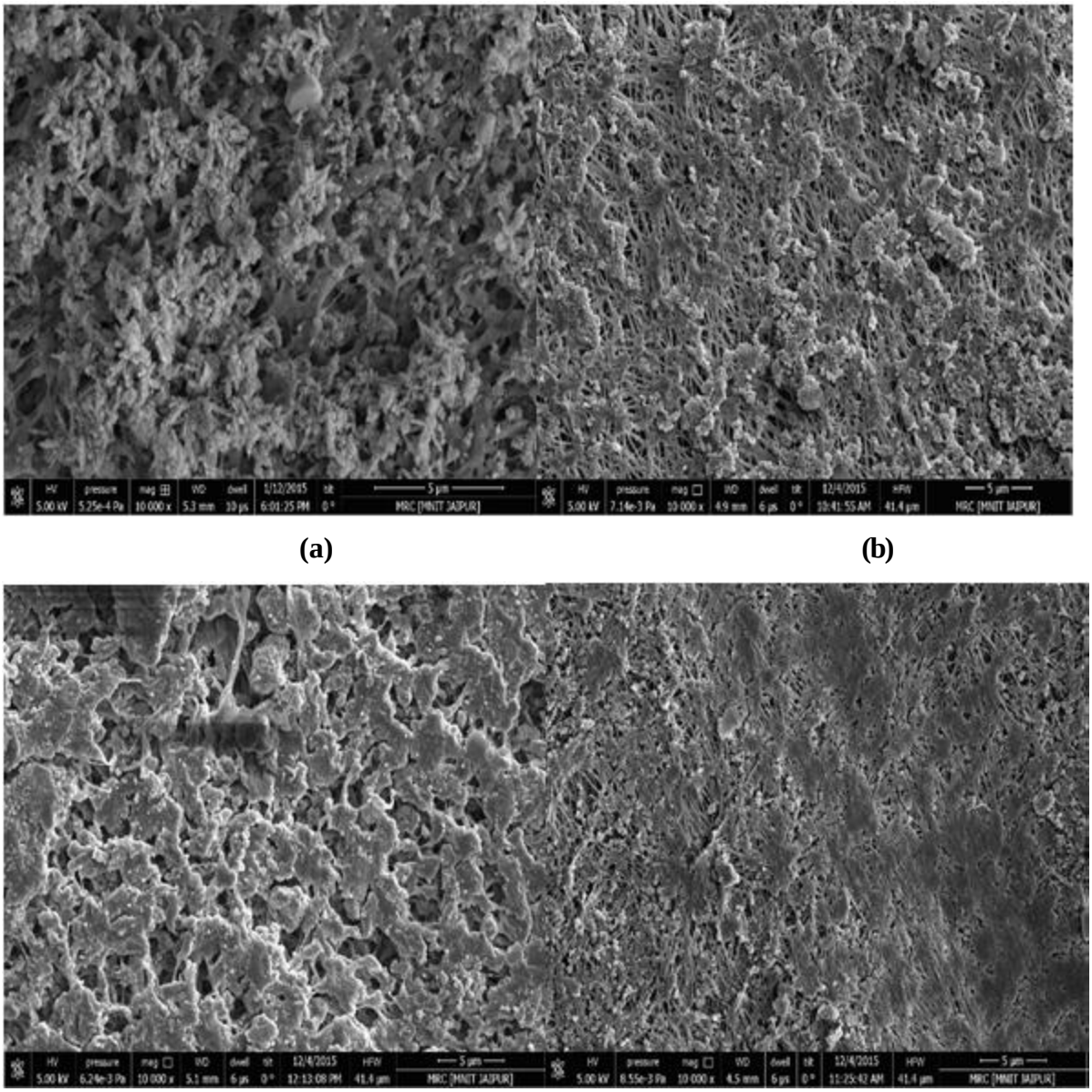

(a) **(b)**

(c) **(d)**

Figure 4.47: SEM image of used (a) 0.22 µm PVDF (b) 0.22 µm PTFE (c) 0.45 µm PVDF (d) 0.45 µm PTFE, after 340 hours run.

Ultimately, the vapor pressure difference was reduced since there is reduction in partial pressure of the water vapor and significant decrease in the permeate flux was observed in the experimental run under the above mentioned condition. The membrane scaling and deposition was also reported by other workers Tang et al. 2010, Hou et al. 2012,Zhou et al. 2014 for tap water purification. Reason for decrease in permeate flux after continuous usage can also be attributed to variation in pore size distribution before and after use of both membranes. SEM images of new membranes, used membranes of PTFE and PVDF were taken to determine the pore size distribution (PSD) using software *ImageJ*. The developed PSD images for PTFE and PVDF membrane are shown in Figure 4.48 and Figure 4.49 respectively. As shown in Figure 4.48, the average pore size for new PTFE membrane of 0.22 µm has reduced to 0.154µm after use of 200 hrs and it further reduced to 0.099µm after use of 340 hrs. This clearly shows that there is blockage of membrane pores with respect to time of its usage which has resulted in reduction of average pore size of the membrane. Similar trend has been observed in case of PVDF membrane also as shown in Figure 4.49. The average pore size has reduced from 0.22µm for a brand new membrane to 0.14µm after using the membrane for 200 hrs. and further reduced to 0.094µm after use of membrane for 340hrs.

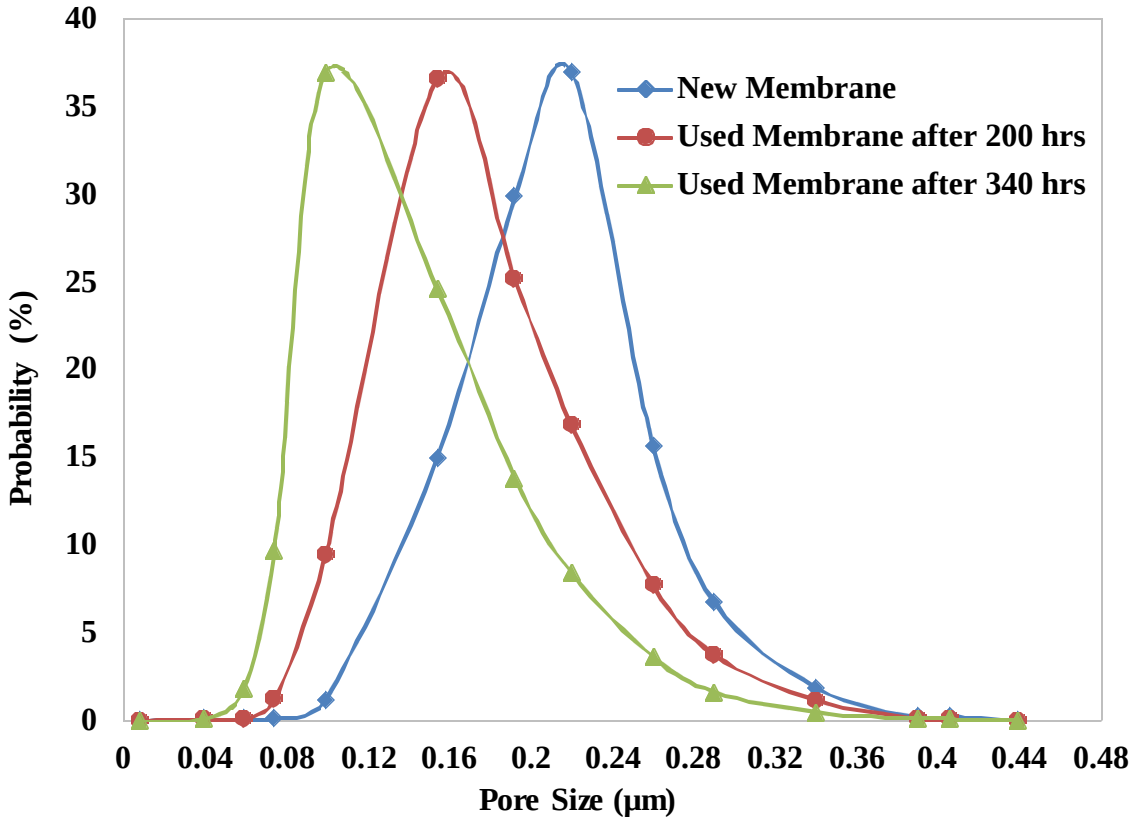

Figure 4.48: Pore size distribution of PTFE membrane before and after use

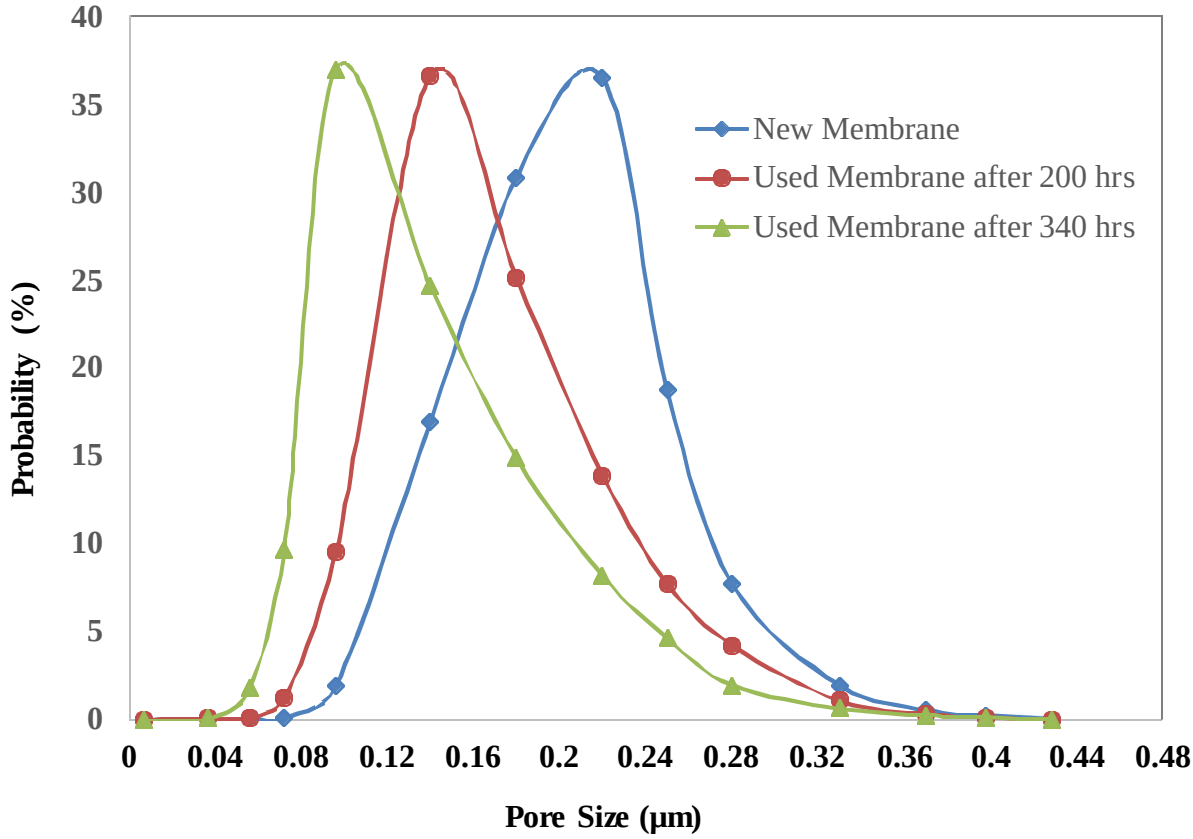

Figure 4.49: Pore size distribution of PVDF membrane before and after use

4.10 Recovery

The water recovery through VMD was calculated theoretically by using unsteady state mass balance on the system. The average permeate flow rate was estimated by carrying out VMD experiment and permeate was collected over a definite period of time which was obtained to be 0.098 kg/hr and it was assumed to be constant at this value for the whole time of operation. The retentate was recycled into the feed tank. The feed flow rate was kept at 1 lpm(Upadhyaya et al. 2016). The initial volume of water in the feed tank was 10 liters with concentration of 45000 ppm of NaCl. The transient salt concentration in the tank was determined experimentally and estimated using MATLAB program as shown in Figure. From the Figure 4.50 it can be seen that salt concentration in the tank goes on increasing and becomes 97,000 ppm at 50 hr. The percent recovery was also calculated as shown inFigure 4.51. It was assumed that the maximum feed concentration can go up to97000 ppm beyond which the tank is refilled with fresh feed on the basis of the minimum volume requirement in the feed tank was 1.7 liter. The percent recovery goes on increasing with time and become 83% at 49 hr. The recovery time is high due to low effective area of the membrane used in the setup, which is 0.00212m^2. The experimental recovery is found to be 81% at 49 hr. It was

also found from the same figure that the mathematical recovery is also well in agreement with the experimental recovery since the R^2 value and MAPE is 0.999and 1.936% respectively. Moreover, it was observed that the concentration of the feed tank increased parabolically from 45000 ppm to 125000 ppm by continuously running the setup till 100 hour.

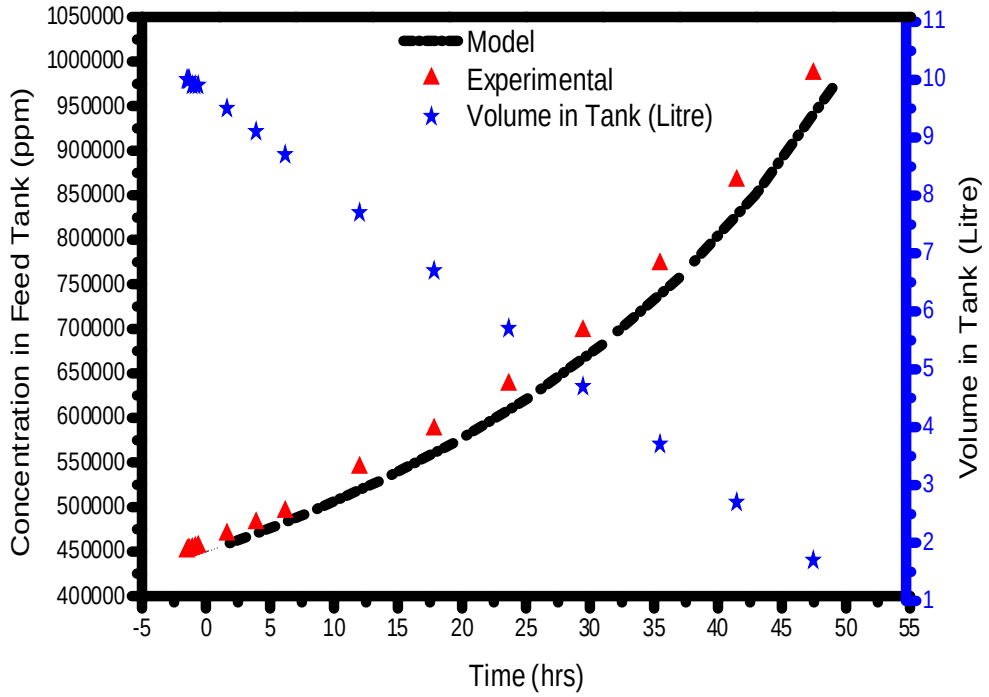

Figure 4.50: Feed Salt Concentration in Tank with Time.

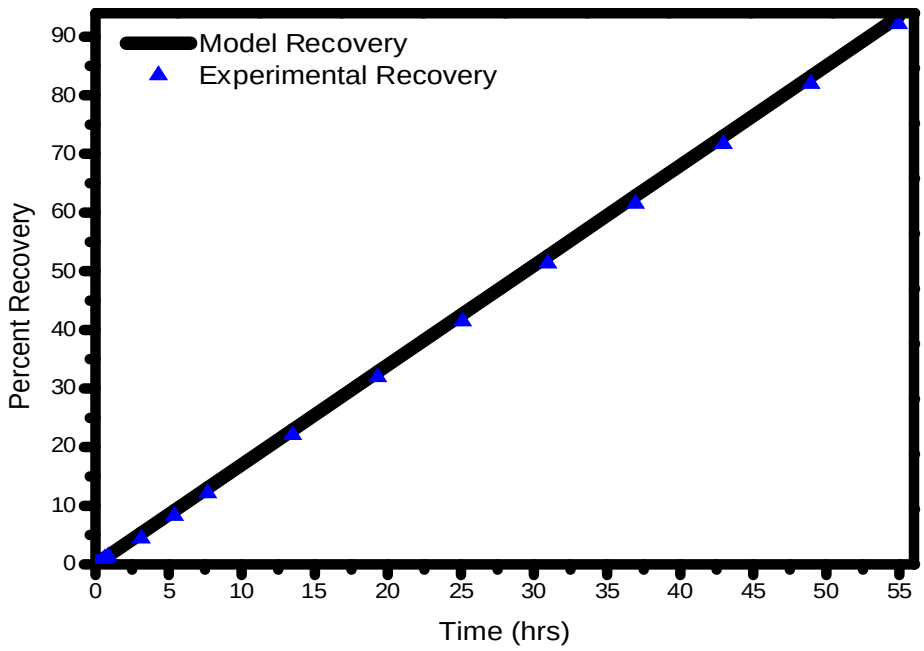

Figure 4.51: Percent Recovery in VMD with Time

Table 4.26: Comparison of experimental and model for concentration in feed tank

Concentration in Feed Tank by Experimental (ppm)	Concentration in Feed Tank by Upadhyaya (2015) model (ppm)	R^2	MAPE
45000	45000	0.999	1.187
45014.4	45134.4		
45037.7	45157.7		
45065.3	45185.3		
45175.3	45295.3		
45287.9	45407.9		
45401.3	45521.3		
46585.7	46899.7		
47832.2	48146.2		
49147.2	49461.2		
52850.1	54393.3		
57139.4	58682.6		
62180.5	63723.7		
68196.5	69739.7		
75719.4	77262.6		
85063	86606.2		
97047.4	98590.6		

Table 4.27: Comparison of experimental and Model recovery

Experimental Recovery (%)	Upadhyaya (2015) model Recovery (%)	R^2	MAPE
0	0	0.999896	11.61647
0.001	0.1062		
0.1072	0.2124		
0.32135	0.3187		
0.75989	0.7041		
0.9844	1.0896		
1.3698	1.475		
4.4536	5.3296		
8.3082	9.1842		
12.1627	13.0387		
22.0572	22.9332		
31.9518	32.8278		
41.4463	42.7223		
51.3408	52.6168		
61.5408	62.8168		
71.7408	73.0168		
81.9408	83.2168		

4.11 Heat Transfer Correlation Development:

The heat transfer coefficients on the boundary layers are usually calculated from well-known heat transfer empirical correlations. These correlations are valid only for non-porous and rigid heat exchangers. However, the membranes are porous in nature. Therefore, there is a difference between the mechanisms of heat transfer in membrane distillation systems and in heat exchangers. Moreover, in a MD system, the heat transfer is coupled with mass transfer (Lawson and Lloyd, 1997). In this work, VMD heat transfer phenomenon was studied using test-cell module consisting of PTFE flat-sheet membrane. Different experimental conditions of feed temperature, feed flow rate at permeate pressure of 9.0 flux is obtained. The temperature polarization effect and the mechanisms of heat and mass transfer through the system have been considered. The experimental heat transfer correlation was obtained in terms of Nusselt, Reynolds and Prandtl numbers at the suitable permeate pressure.

The heat energy needed for the water to vaporize into the membrane pores is provided by the heat transfer through the boundary layer at the feed side. The heat flux is given by

$$q_f = h_f (t_f - t_{fm}) \quad (4.12)$$

Assuming the contribution of both evaporation and conduction, the total heat flux transferred through the membrane

$$q_m = N.\Delta H + h_m (t_{fm} - t_{pm}) \quad (4.13)$$

The value of heat transfer coefficient, h_f was calculated using equation 4.13 and 4.14. The Nusselt number, Nu, was calculated by $N_u = h_f d/k$, where d_e is the effective diameter of membrane and k is the thermal conductivity of water. Reynolds number, Re, was calculated by $\mathrm{Re} = v d_e \rho/\mu$, where v is the approach velocity of water, ρ and μ are the density and viscosity of liquid water, respectively. The heat transfer correlation was developed using a tool *Solver* in MS-Excel and the corresponding calculated data are given in Table 4.28. For varied feed bulk inlet temperature, feed flow rate at permeate pressure of 9.0 kPa.

It is observed from the table that the heat transfer coefficient increases by increasing the feed flow rate and feed bulk inlet temperature. The increment of heat transfer coefficient with respect to feed flow rate and feed bulk inlet temperature can cause the reduction in temperature and concentration polarization effect. This phenomena is due to the temperature of feed side membrane surface approaching towards feed bulk inlet temperature, which consecutively, increases the vapor pressure driving force for mass transfer. The following

empirical correlation was fitted using a tool *Solver* in MS Excel, which gives the suitable values of the constants *a*, *b*, and *c* by minimizing the error between experimental and calculated values using Newton's method.

$$N_u = aR_e^{\,b}P_r^{\,c} \quad (4.14)$$

The correlation after fitting the data was found to be as follows:

$$N_u = 0.158R_e^{0.854}P_r^{0.33} \quad (4.15)$$

The plot of theoretical and experimental values of log ($Nu/Pr^{0.33}$) versus log (Re) is shown inFigure 4.52. It is observed that the theoretical model is in good agreement with the experimental data. The R^2 value was found to be 0.983.

The experimental heat transfer coefficient as a function of feed bulk temperature is shown in Figure 4.53at feed flow rates of 2, 6 and 10 lpm. It is found that the following relationship between the heat transfer coefficient (HTC) and feed bulk inlet temperature holds good.

$$\text{At 2 lpm} \quad h_f = 0.3234T_f^{\,3} - 47.511T_f^{\,2} + 2582.5T_f - 49312 \quad (4.16)$$

$$\text{At 6 lpm} \quad h_f = 0.5701T_f^{\,3} - 90.77T_f^{\,2} + 5188.1T_f - 100674 \quad (4.17)$$

$$\text{At 10 lpm} \quad h_f = 1.2918T_f^{\,3} - 206.26T_f^{\,2} + 11391T_f - 210807 \quad (4.18)$$

The R^2 values were found to be 0.9998, 0.9995 and 0.9998

Table 4.28: Heat Transfer data at Permeate Pressure of 9.0 kPa, Feed Salt Concentration of 20000 ppm

Flow rate (lpm)	Feed inlet temperature T_f (°C)	Experimental Permeate Flux (N) kg/m^2 s	Re	Pr	Model Nu	log Re	Experimental h_f	Experimental Nu
1	45	0.001866808	6.80E+02	4.34E+00	6.38E+01	2.832824499	34.940892	2.86E+00
2	45	0.002096138	1.36E+03	4.34E+00	1.15E+02	3.133854495	162.3861	1.33E+01
4	45	0.002653575	2.72E+03	4.34E+00	2.09E+02	3.43488449	458.68701	3.75E+01
6	45	0.003206974	4.08E+03	4.34E+00	2.95E+02	3.610975749	986.32627	8.06E+01
8	45	0.003747924	5.44E+03	4.34E+00	3.78E+02	3.735914486	1408.7975	1.15E+02
10	45	0.004367584	6.80E+03	4.34E+00	4.57E+02	3.832824499	1845.2285	1.51E+02
1	65	0.018109172	9.54E+02	2.99E+00	7.54E+01	2.97953198	6549.3797	5.18E+02
2	65	0.018874847	1.91E+03	2.99E+00	1.36E+02	3.280561976	7030.7243	5.56E+02
4	65	0.020039781	3.82E+03	2.99E+00	2.47E+02	3.581591972	8084.716	6.40E+02
6	65	0.021316194	5.72E+03	2.99E+00	3.49E+02	3.757683231	10303.664	8.15E+02
8	65	0.022674228	7.63E+03	2.99E+00	4.46E+02	3.882621967	11591.15	9.17E+02
10	65	0.025975991	9.54E+03	2.99E+00	5.40E+02	3.97953198	12631.761	1.00E+03
1	50	0.003511794	7.46E+02	3.56E+00	6.47E+01	2.872988423	1332.5474	1.08E+02
2	50	0.003849143	1.49E+03	3.56E+00	1.17E+02	3.174018419	1600.1769	1.30E+02
4	50	0.004516644	2.99E+03	3.56E+00	2.12E+02	3.475048414	2029.7951	1.64E+02
6	50	0.005172006	4.48E+03	3.56E+00	2.99E+02	3.651139673	3162.9269	2.56E+02
8	50	0.005860444	5.97E+03	3.56E+00	3.83E+02	3.77607841	4035.5772	3.27E+02
10	50	0.006418241	7.46E+03	3.56E+00	4.63E+02	3.872988423	4639.2628	3.76E+02
1	55	0.006661329	8.05E+02	3.56E+00	6.91E+01	2.90596779	1480.2618	1.19E+02
2	55	0.006993541	1.61E+03	3.56E+00	1.25E+02	3.206997786	1723.0892	1.38E+02
4	55	0.007604154	3.22E+03	3.56E+00	2.26E+02	3.508027781	2133.5515	1.71E+02
6	55	0.008272205	4.83E+03	3.56E+00	3.20E+02	3.68411904	3270.4522	2.63E+02
8	55	0.008862221	6.44E+03	3.56E+00	4.09E+02	3.809057777	4039.1417	3.24E+02
10	55	0.009921688	8.05E+03	3.56E+00	4.95E+02	3.90596779	4655.5215	3.74E+02
1	60	0.011195997	8.74E+02	2.99E+00	7.00E+01	2.941658869	4165.9857	3.32E+02
2	60	0.011718011	1.75E+03	2.99E+00	1.27E+02	3.242688864	4527.6321	3.61E+02
4	60	0.012753964	3.50E+03	2.99E+00	2.29E+02	3.54371886	5379.1094	4.29E+02
6	60	0.013846819	5.25E+03	2.99E+00	3.24E+02	3.719810119	7142.1362	5.69E+02
8	60	0.014809347	6.99E+03	2.99E+00	4.14E+02	3.844748856	8215.9265	6.55E+02
10	60	0.015726906	8.74E+03	2.99E+00	5.01E+02	3.941658869	9040.331	7.20E+02

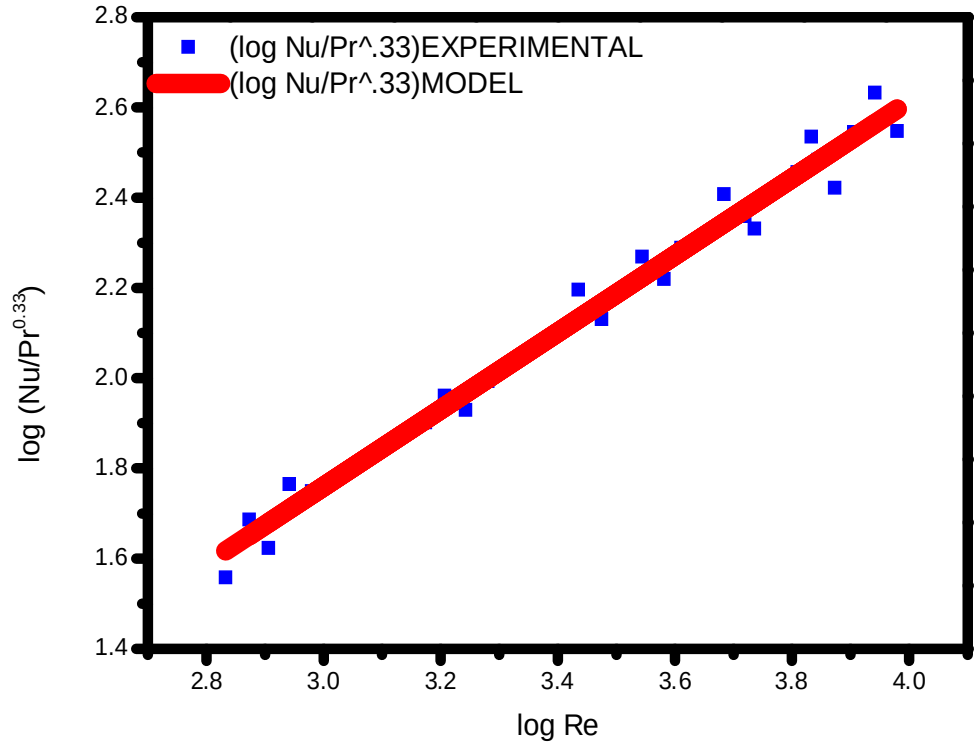

Figure 4.52: Heat Transfer Correlation Fitting at 9.0 kPa Permeate Pressure.

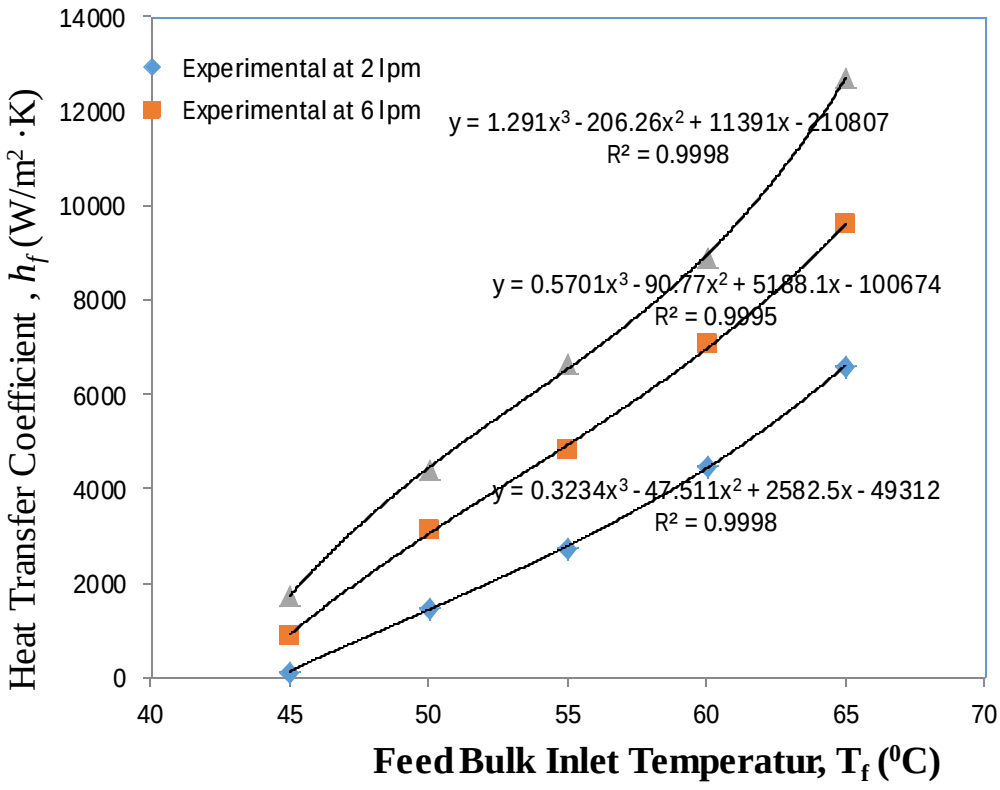

Figure 4.53: HTC as a Function of Feed Bulk Temperature at 9.0 kPa.

4.12 Model Validation

4.12.1 Prediction of Flux by ANN and Mathematical Modelling

Artificial neural networks (ANN) are widely used for predicting the output from the experimental data. Neural networks provide the relationship between two system of data sets i.e., input vector and output vector. An artificial neural network consists of assembly of multiprocessing module connected with one and all by decision weights. Although every artificial neural network is made from this basic building block, the fundamentals may vary. Neural network designing process is based on iterative method. In the present work a general ANN model was created in MATLAB and simulated to determining the effect of various operating parameters on VMD performance in terms of permeate flux.In ANN four input parameters were taken with 10 neurons in hidden layer. Moreover, learning function, learning algorithm performance function and transfer function were assumed as TRAINLM, LEARNGDM, MSE and TANSIG respectively as shown inFigure 4.54to generate the ANN network as shown inFigure 4.55.The input neurons comprise of feed flow rate from 1 to 10 lpm, feed temperature from 45 °C to 65 °C , feed salt concentration of NaCl from 5000 to 50000 ppm and permeate pressure ranges from 7 to 11 kPa. The experimental permeate flux used as output. Intotality, 1500 experimental data were used in ANN modelling out of which 900 data was trained whereas 600 data were used in testing and validation Simulation was converged in 45 epochs showing with performance of 1.56 as shown inFigure 4.56. Computed suitable weights for ANN are represented inTable 4.29. It was observed that ANN model data were well fitted with training, validation and testing data since R^2found to be 0.99881, 0.99901, and 0.99847 for training, validation and testing respectively as depicted inFigure 4.56. Therefore, it can be concluded that ANN modelling can be implemented for prediction of permeate flux in VMD and validation of experimental data.

In terms of theoretical modelling various mathematical models like dusty gas model(Mericq et al. 2009; Pangarkar et al. 2010a)and Knudsen viscous transition model(Lawson and Lloyd 1997; Mengual et al. 2004; Xu et al. 2009)have been reported for prediction of permeate flux and its validation with experimental data. However, the model developed by Upadhyaya et al (2015) has been found to be superior in comparison with all models since Upadhyaya et al (2015) have computed the feed side membrane surface temperature (T_{fm}) using computational fluid dynamics (CFD) which was tedious to calculate by first principle while others(Xu et al. 2009; Shakaib et al. 2011; Upadhyaya et al. 2015) assumes this temperature to be identical with feed inlet temperature in estimation of permeate flux. Moreover, this feed side

membrane surface temperature is essential to be estimated using CFD because feed flow rate will also affect this temperature. In addition to this, following other assumption used inUpadhyaya et al. (2015) model has made it more suitable:

i. Vapour permeates through a porous membrane comprising Knudsen diffusion, molecular diffusion, and Poiseuille flow.
ii. Heat loss through membrane is not negligible.
iii. Effect of salt concentration is considered in terms of activity coefficient using thermodynamic consideration.
iv. Effect of feed flow rate is also incorporated inmodel by taking into account hydrodynamics as well as heat transfer.

Therefore, in the present study developed ANN model is compared with Upadhyaya et al (2015) mathematical model whose boundary condition, initial condition and membrane surface condition in *Fluent* for estimation of feed side membrane surface temperature are taken as mentioned below:

i. *Initial condition*: The feed inlet and outlet region of membrane model was selected to velocity-inlet and pressure outlet respectively. The inlet pressure was kept to 1 atmospheric and the gravitational acceleration was kept to 9.81 m/s^2. The vacuum export was selected to pressure outlet. Moreover, the range of vacuum was taken in between 7 to 11 kPa.
ii. *Boundary Condition*: The velocity gradient of fluid was considered to be zero as well as the outlet temperature was chosen 5 °C lower than feed bulk inlet temperature. The vapor backflow was set to zero.
iii. *Membrane Condition*: The membrane surface was selected under porous jump option. Superficial velocity was used to estimate the flow through porous domain. Wall option was considered for membrane silk surface.

After implementation of all the input conditions and boundary conditions in *fluent* the temperature profiles in the membrane module were generated by simultaneous simulation of all equations*viz*continuity equation, x- velocity, y-velocity, energy, *k*, and epsilon were solved in fluent under varied permeate pressure in the range of 7-11 kPa, feed bulk temperature in the range of 45 - 65 °C and feed flow rate of 1 to 10 lpm. Temperature profiles contour were shown in Figure 4.45 to 4.47 at feed bulk inlet temperature of 45, 55, and 65 °C, respectively at feed flow rate of 10 lpm and 9 kPa of permeate pressure. The estimated temperature by the

Fluent at the feed side membrane surface (T_{fm}) was incorporated in Upadhyaya et al. (2015)model for further calculation of permeate flux. The estimated permeate flux based on Upadhyaya et al. (2015) model at 9 kPa and feed salt concentration of 5000 ppm is shown inTable 4.30. It was observed that ANN model is found to be superior as compared to Upadhyaya et al. (2015) model though R^2 values are same for both model as shown inTable 4.30since MAPE for ANN model is lower than mathematical model.This accuracy of ANN model is due to reason as this model was edify on experimental facts.

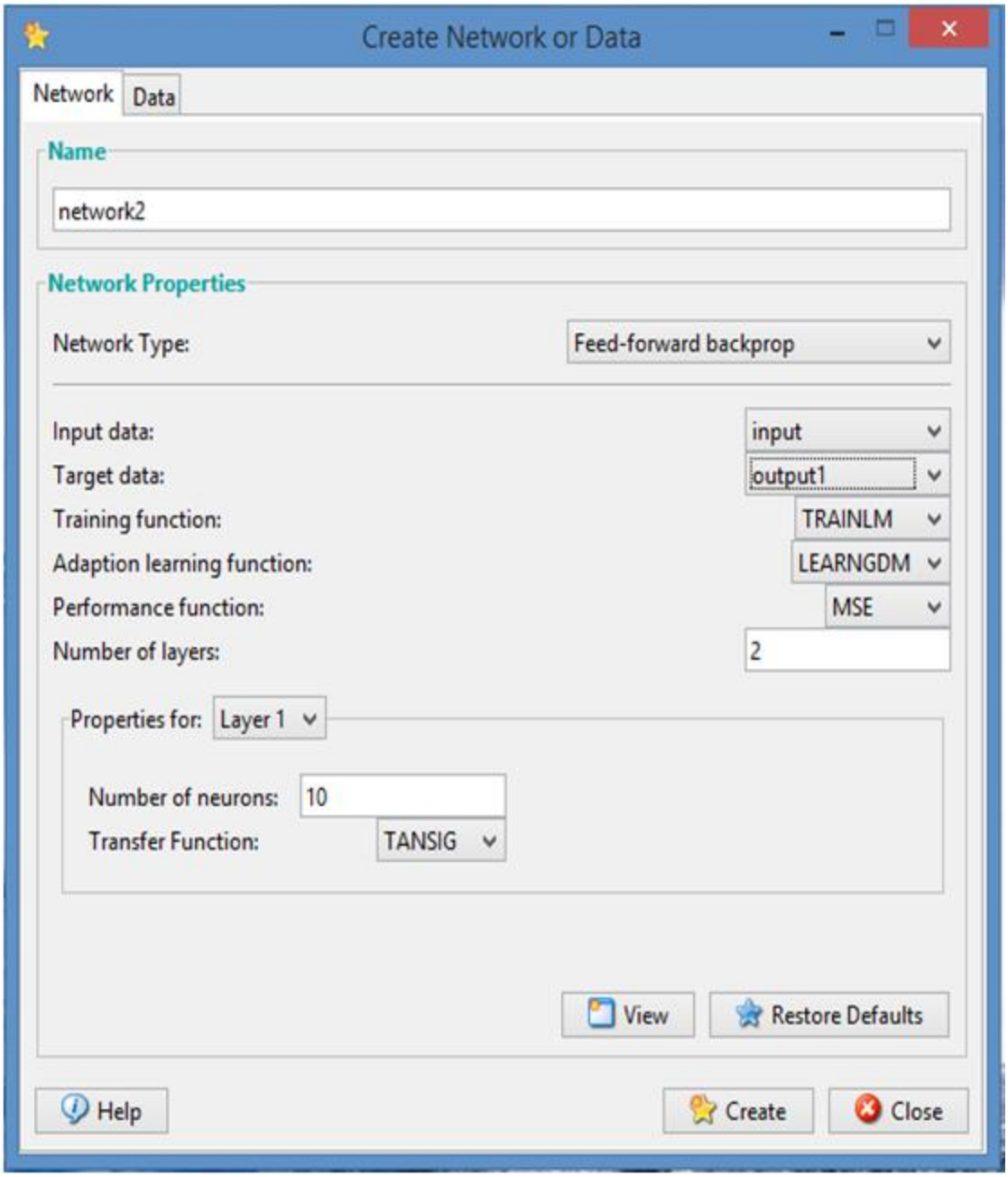

Figure 4.54: Learning Function, Learning Algorithm and Transfer Function generation through Network Data

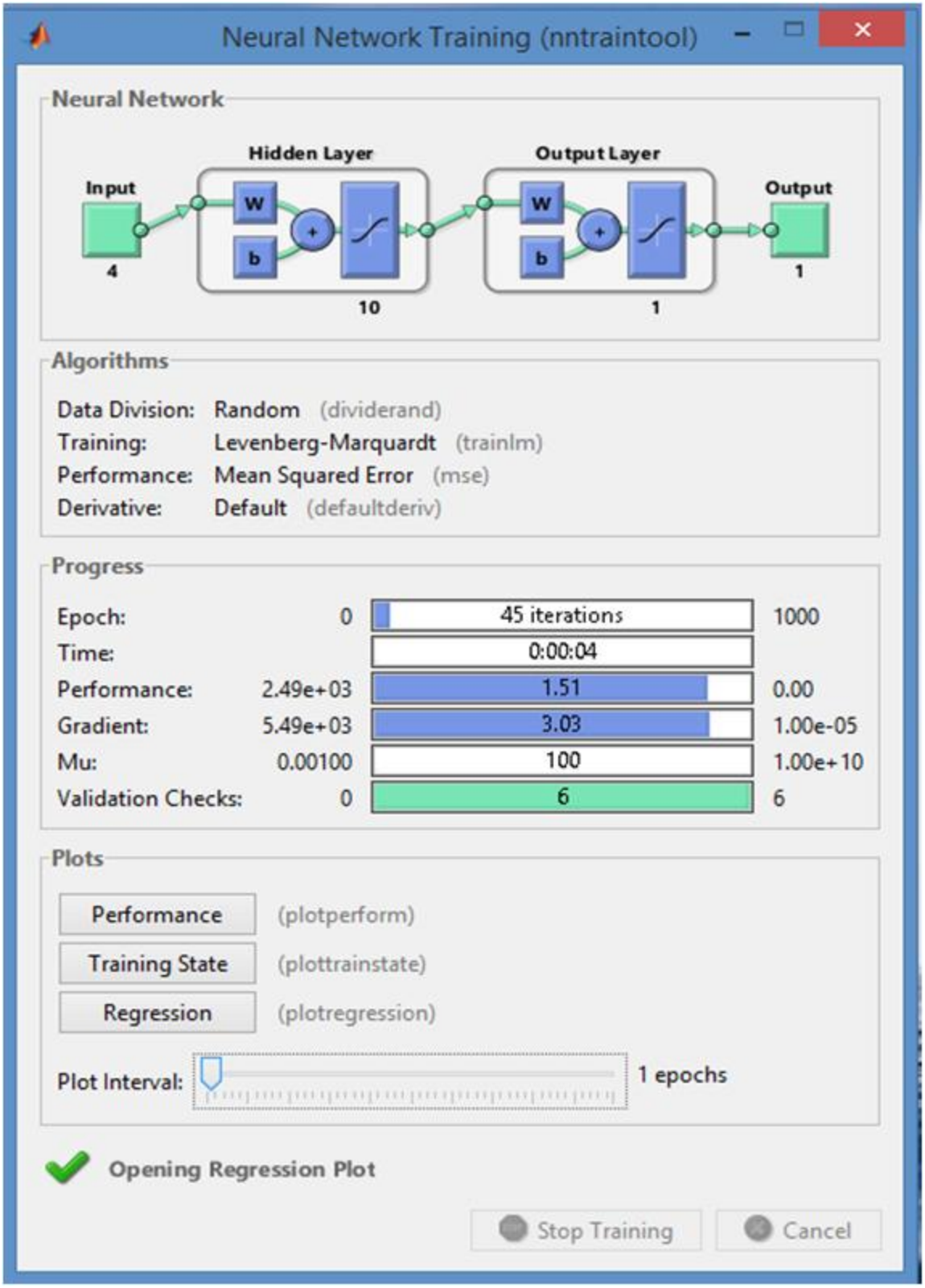

Figure 4.55: Neural Network Training Showing Iteration and Performance.

Table 4.29: Weights for ANN

(a) Input Layer to Hidden Layer used at 9.0 kPA

Weights from Input1 to Hidden Layer	Weights from Input2 to Hidden Layer	Weights from Input3 to Hidden Layer	Weights from Input4 to Hidden Layer
0.13723	-0.052485	0.19417	-0.024642
2.0128	0.38693	-1.68	-1.0012
-2.0921	-1.2971	-1.0463	-3.5427
-1.696	5.0199	-2.8248	2.3291
-0.43648	0.0019531	-0.10718	0.12063
-0.56843	-0.0051012	3.4842	0.69476
3.4083	1.8773	-0.30751	-0.019132
0.28661	-0.53622	-1.0118	-0.57143
3.6581	1.4532	-6.9656	4.5254
3.9804	-10.5183	-1.2351	3.325

(b) Hidden Layer to output Layer weights

-3.1354	0.25566	0.0081818	-0.006957	-3.3097	0.030132	1.8989	-0.167	0.0013005	0.016022

(c) Bias on Hidden Layer

-0.25493	2.6843	1.5996	1.4051	0.62377	-1.0242	-6.3607	1.9051	5.2	6.9316

(d) Bias to Output Layer

[2.318]

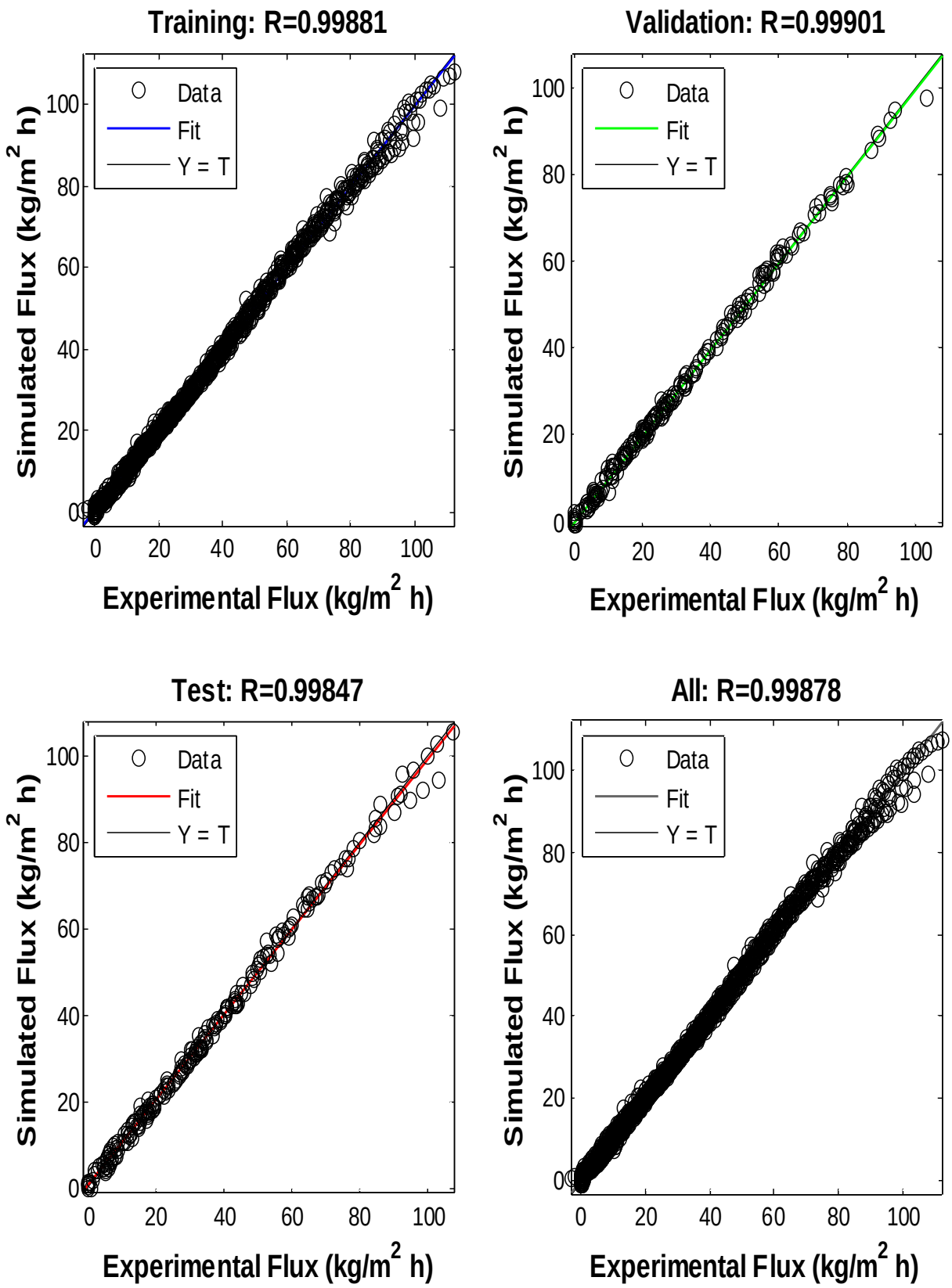

Figure 4.56: ANN Fitting of Experimental Data.

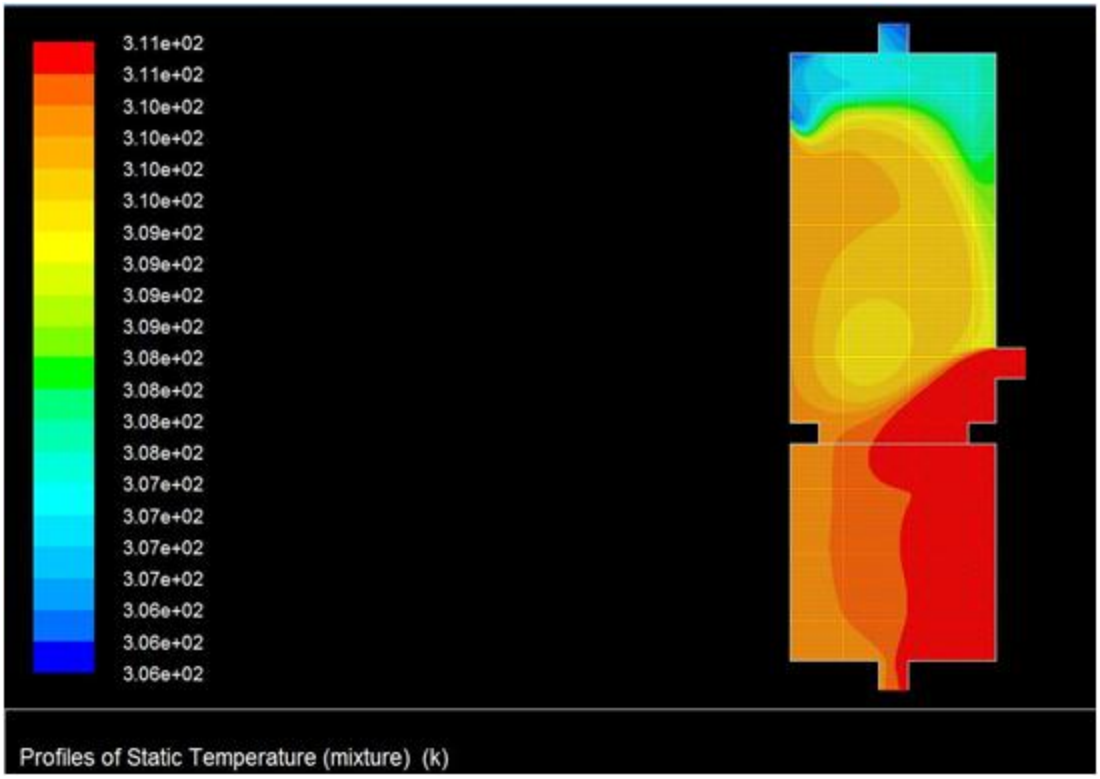

Figure 4.57: Temperature Profile of Membrane Module at 40 °C of Feed Bulk Temperature

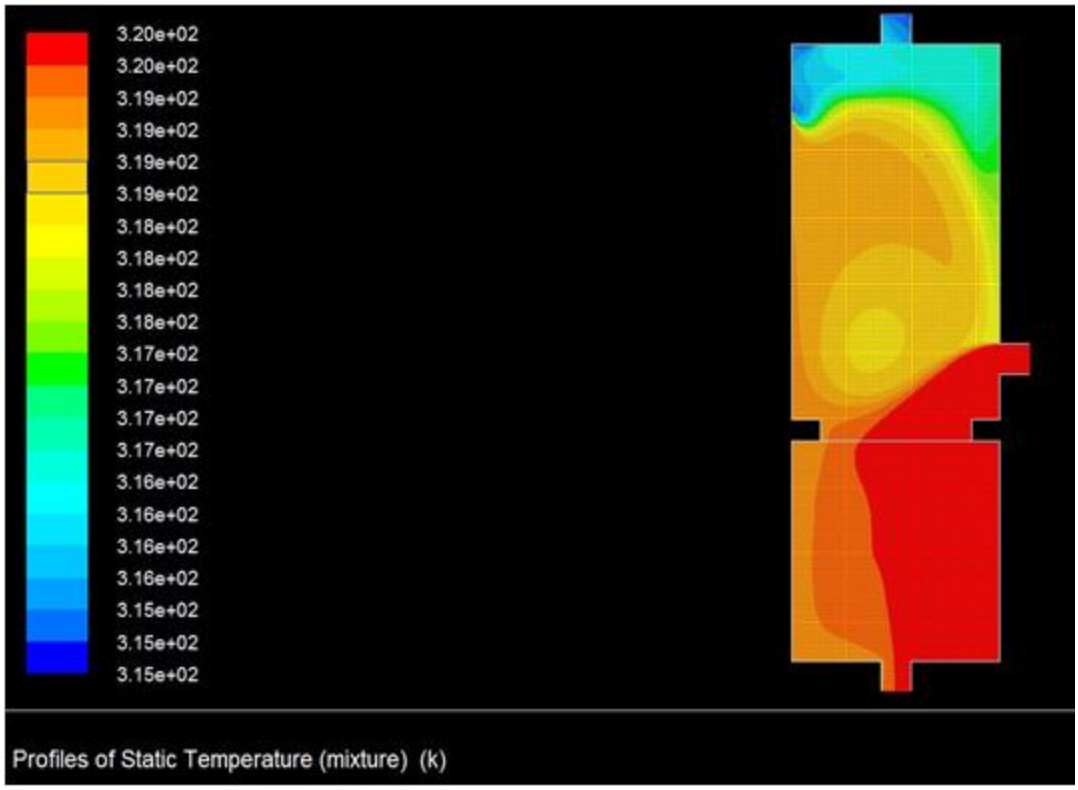

Figure 4.58: Temperature Profile of Membrane Module at 50 °C of Feed Bulk Temperature

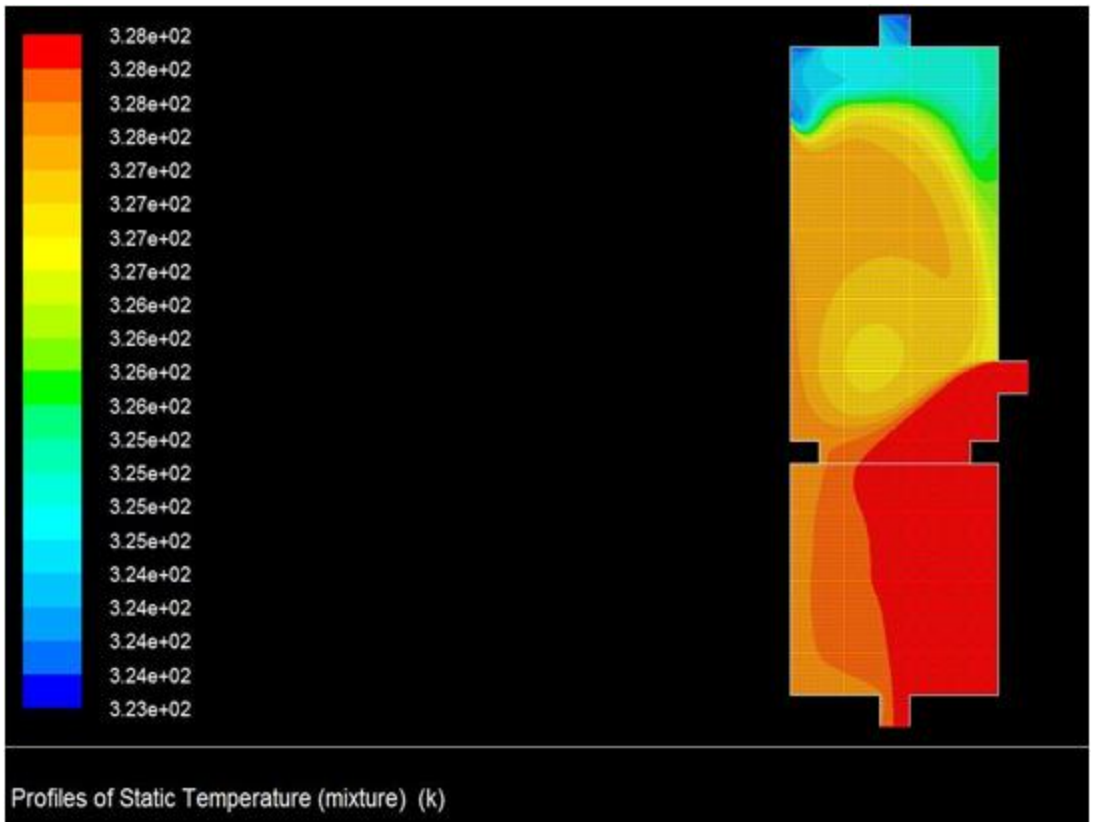

Figure 4.59: Temperature Profile of Membrane Module at 60 °C of Feed Bulk Temperature

Moreover, the ANN model and Upadhyaya et al. (2015) model was also compared on the basis of input parameters like feed flow rate, permeate pressure, feed bulk inlet temperature and feed salt concentration. The effect of feed flow rate is represented in Figure 4.60. It can be seen that the ANN model shows more closeness to experimental data compared to Upadhyaya et al. (2015)model on increasing the feed flow rate from 1 to 10 lpm since the MAPE for ANN model is 0.93 which is less than Upadhyaya et al. (2015)model of MAPE 1.51 inspite the same R^2value of 0.993 as shown in Table 4.31 Further, It can also be observed that ANN model is better fitted with experimental data as compared to Upadhyaya et al. (2015)model as shown in Figure 4.61on increasing the feed bulk temperature from 45°C to 65°C,since MAPE value for ANN model and mathematical model are found to be 1.86 and 5.26 respectively as given in Table 4.31.Similarly, the effect of feed salt concentration from 5000 ppm to 50000 ppm on permeate flux at feed flow rate of 10 lpm, feed bulk inlet temperature of 65 °C and permeate pressure of 9 kPa is shown in Figure 4.62 which indicates ANN model is more accurate than mathematical model since MAPE value of ANN model is

found to be less than MAPE of mathematical model despite of same R^2 value as represented in Table 4.31.

Table 4.30: Comparison of ANN and Mathematical Model

[Permeate Pressure of 9 kPa]

Experimental Flux ($kg/m^2 \cdot h$)	**ANN Flux ($kg/m^2 \cdot h$) (1)**	**Upadhyaya (2015) model Flux ($kg/m^2 \cdot h$) (2)**	**R^2 (1)**	**R^2 (2)**	**MAPE (1)**	**MAPE (2)**
17.795	17.82	17.41	**0.999**	**0.999**	**10.1498**	**18.806**
18.966	18.99	18.21				
21.152	20.96	20.92				
23.207	23.36	22.96				
25.388	25.49	24.95				
26.950	26.99	25.76				
29.998	29.85	30.89				
31.365	31.42	31.85				
33.940	33.12	34.24				
36.646	36.46	37.42				
39.196	38.95	39.71				
41.755	41.66	40.51				
49.312	49.94	49.61				
51.072	51.96	50.94				
54.443	54.99	54.60				
58.120	58.94	59.45				
61.508	61.24	62.94				
64.511	64.33	64.26				
77.70	76.78	76.30				
81.08	79.52	78.98				
85.56	85.14	84.58				
89.42	90.55	90.75				
94.20	94.78	95.25				
98.04	98.17	98.94				

Similarly, the ANN model is also found to have better fitting with experimental data as compared to mathematical model by varying the permeate pressure from 7 to 11 kPa as shown inFigure 4.63, though R^2 value being same. This is because MAPE of ANN model is found to be 0.660 which is less than Upadhyaya et al. (2015)model of MAPE 1.336. Henceforth, it is obvious that ANN model is providing better fitting with experimental data as compared to mathematical model which may be due to the reason that ANN permeate flux were predicted on the basis of experimental data during training. Moreover, the path of membrane is not uniform everywhere along the thickness of membrane whose effect is not considered in mathematical model which might be the reason for higher variation in case of mathematical model predicted data compared to those predicted by ANN.

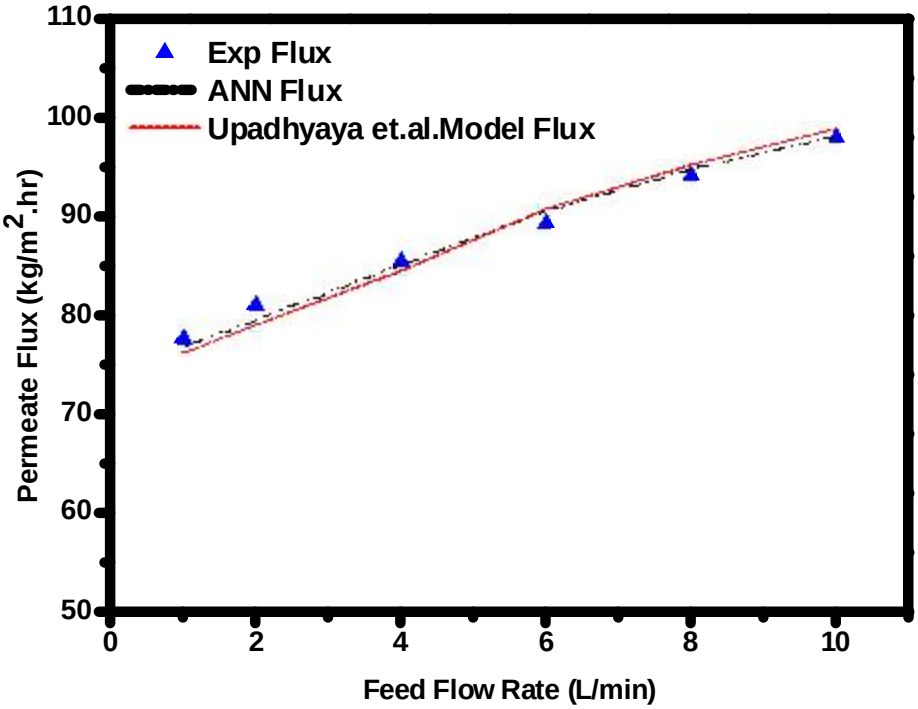

Figure 4.60: Effect of feed flow rate on permeate flux, ANN Flux, Model Flux [65°C feed bulk temperature, 5000 ppm of feed inlet concentration and 9.0 kPa of permeate side pressure]

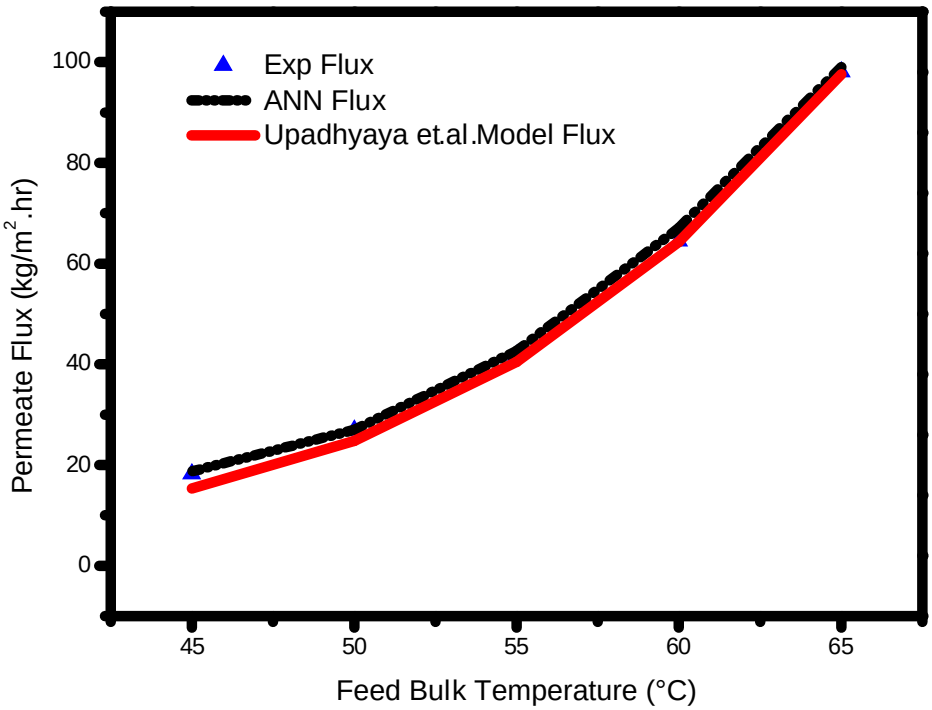

Figure 4.61: Effect of feed bulk temperature on permeate flux, ANN Flux, Model Flux, [10 lpm of feed flow rate, 5000 ppm of feed inlet concentration and 9.0 kPa of permeate side pressure]

Table 4.31: Comparative Study of Effect of Feed Flow Rate, Assumption: Knudsen – Viscous Transition

	Experimental Flux ($kg/m^2 \cdot h$)	**ANN Flux ($kg/m^2 \cdot h$) (1)**	**Upadhyaya (2015) model Flux ($kg/m^2 \cdot h$) (2)**	**R^2 (1)**	**R^2 (2)**	**MAPE (1)**	**MAPE (2)**
Feed Flow Rate (lpm)							
[Feed Bulk Temperature of 65°C, Feed Concentration 5000ppm and Permeate Pressure 9.0kPa]							
1	77.70	76.78	76.30	0.993	0.993	0.93	1.51
2	81.08	79.52	78.98				
4	85.56	85.14	84.58				
6	89.42	90.55	90.75				
8	94.20	94.78	95.25				
10	98.04	98.17	98.94				

Feed Bulk Temperature (°C)							
[Feed Flow Rate 10 lpm, Feed Concentration 5000ppm and Permeate Pressure 9.0kPa]							
45	18.220	18.75	15.35	**0.999**	**0.999**	**1.86**	**5.26**
50	26.950	26.99	24.76				
55	41.755	42.66	40.51				
60	64.511	67.03	64.26				
65	98.044	99.01	97.59				
Feed Salt Concentration (ppm)							
[Feed Bulk Inlet Temperature, Feed Flow Rate 10 lpm and Permeate Pressure 9.0kPa]							
5000	98.04	98.17	98.94	**0.99**	**0.99**	**0.63**	**1.02**
10000	96.806	97.36	96.18				
15000	94.956	95.46	94.69				
20000	93.514	94.20	93.13				
25000	91.969	92.43	91.49				
30000	90.425	91.16	89.77				
35000	88.881	89.70	87.98				
40000	87.337	87.79	86.12				
45000	85.793	86.68	84.19				
50000	84.249	84.75	82.19				
Permeate Pressure (kPa)							
[Feed Bulk Inlet Temperature 65°C, Feed Flow Rate 10 lpm and Feed Concentration 5000 ppm]							
7	112.120	110.69	113.29	**0.996**	**0.996**	**0.660**	**1.336**
8	104.934	104.18	105.44				
9	98.04	98.17	98.94				
10	92.634	92.81	91.17				
11	87.224	86.36	84.90				

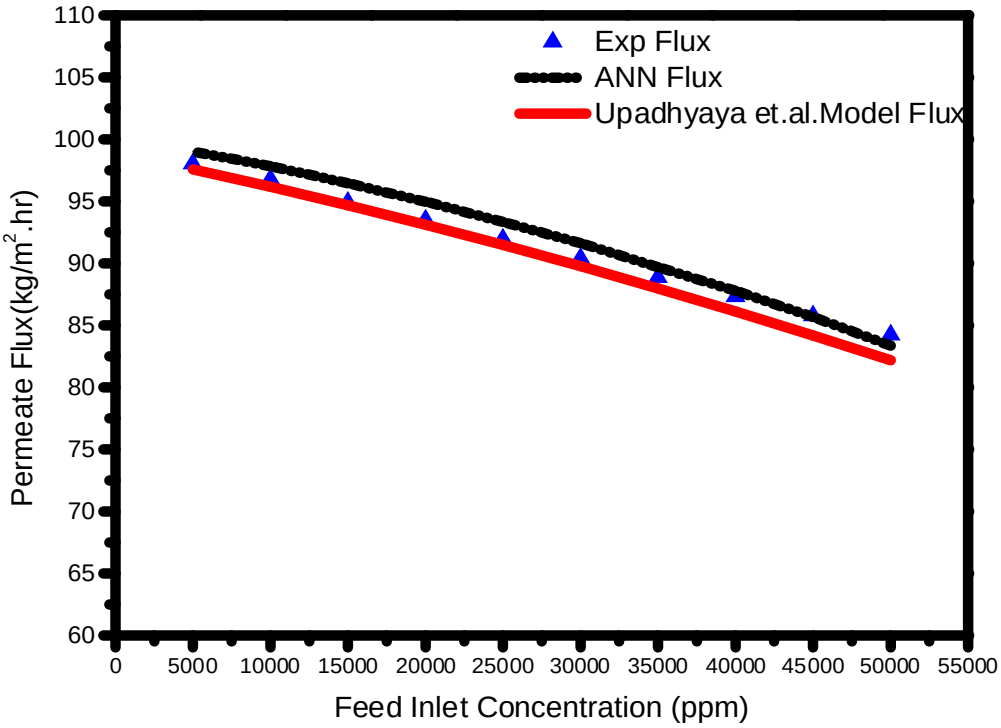

Figure 4.62: Effect of feed inlet concentration on permeate flux, ANN Flux, Model Flux, [65°C of feed bulk temperature, 10 lpm of feed flow rate, and 9.0 kPa of permeate side pressure]

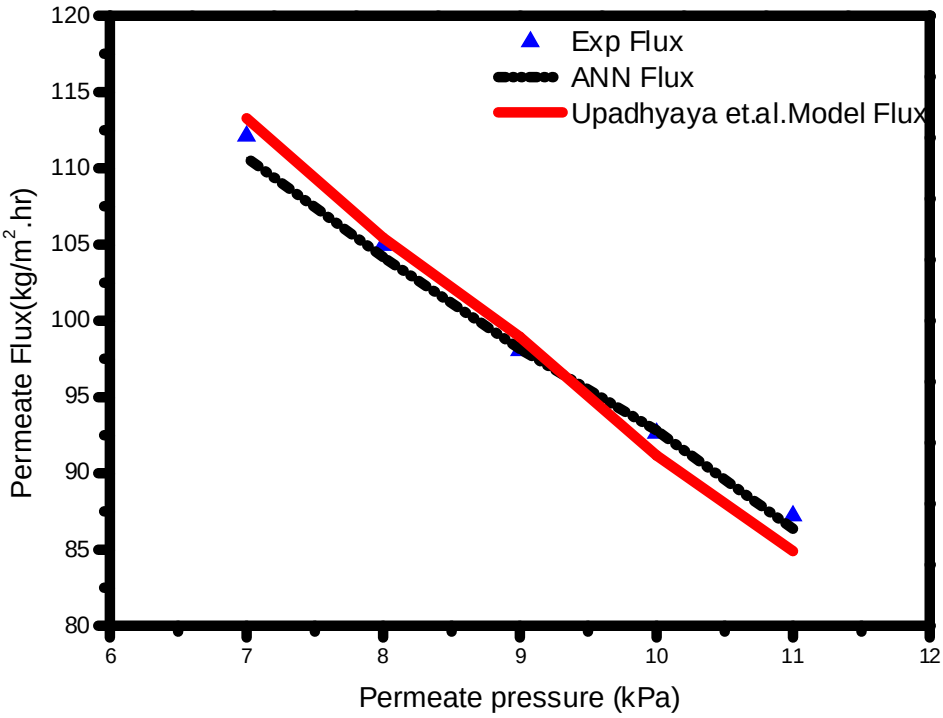

Figure 4.63: Effect of Permeate Pressure on permeate flux, ANN Flux, Model Flux [65°C of feed bulk temperature, 10 lpm of feed flow rate, and 5000 ppm feed salt concentration]

4.13 Comparison between Vacuum Membrane Distillation and Reverse Osmosis

Comparison of VMD with reverse osmosis on the ground of power consumption and percentage recovery is discussed in subsequent section.

4.13.1 Effects of Feed Salt Concentration on Energy Consumption for VMD & RO Process

In this work the differential increase in specific energy consumption in VMD has been compared with the experimental specific energy consumption reported by Ali Al-Karaghouli(2012)for RO with differential increase in feed salt concentration from 5000 to 45000 ppm as shown inFigure 4.64. It was observed that the percentage increase in specific energy consumption for VMD is less compared to RO. This may be due to the reason for every increase in feed salt concentration from 5000 ppm to 45000 ppm increases the requirement of pump water pressure to more as compared to the energy requirement for applying vacuum on permeate side in VMD.

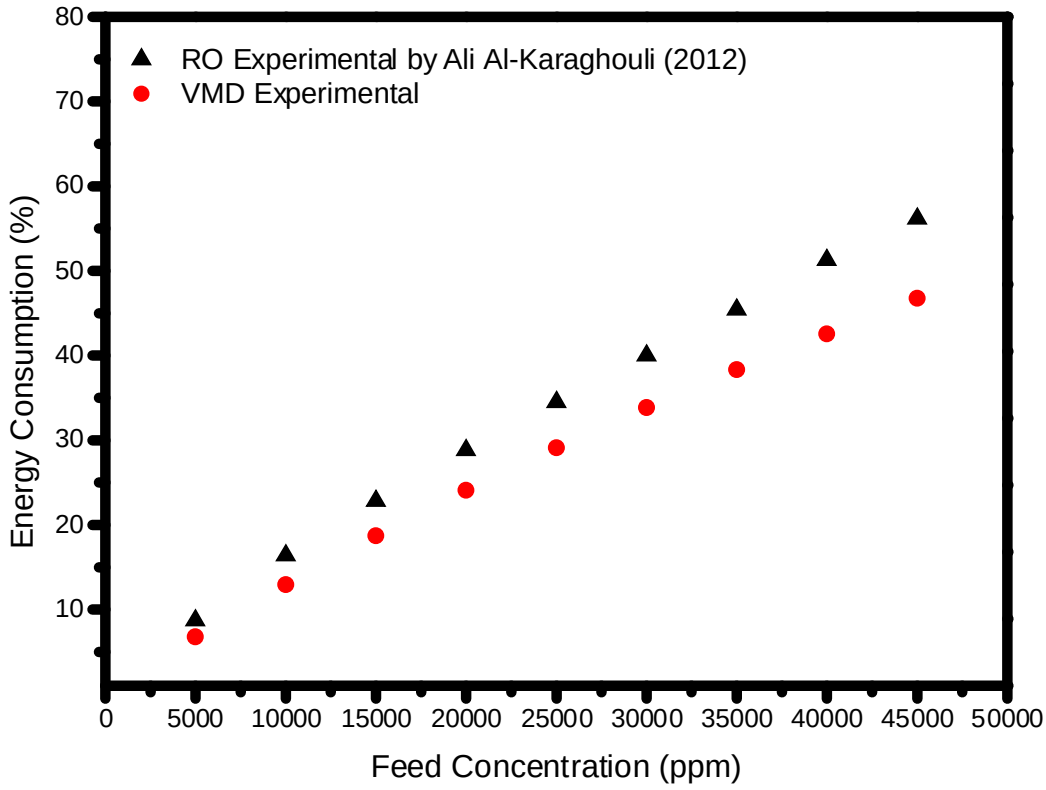

Figure 4.64: Effect of feed salt concentration on energy consumption for RO and VMD

4.13.2 Effect of Feed Salt Concentration on Recovery for VMD and RO Process

The experimental recovery for VMD is estimated using feed salt concentration from 35000 to 45 000 ppm till the feed tank concentration reached up to 60000 ppm in all cases and compared with experimental recovery reported by Ali-AL-Karaghouli (2012) in RO process under same condition of feed salt concentration in feed tank as shown in Table 4.23. It was observed that percentage recovery is higher in VMD than RO. This may be due to the reason that vaporization rate enhances by decreasing the permeate pressure in VMD which allows rapidly to pass through water vapor from membrane thickness. Moreover, scaling on membrane surface is negligible due to which membrane pores remain unaffected from clogging under long run. From Figure 4.65, it can be seen that percentage recovery decreases linearly on increasing the feed salt concentration.

Table 4.32: Recovery for VMD and RO processes.

Feed Concentration (ppm)	Retentate Concentration (ppm)	Recovery (%)	
		RO (1)	VMD (2)
35,000	60,000	42	55
40,000	60,000	33	47.5
45,000	60,000	25	41

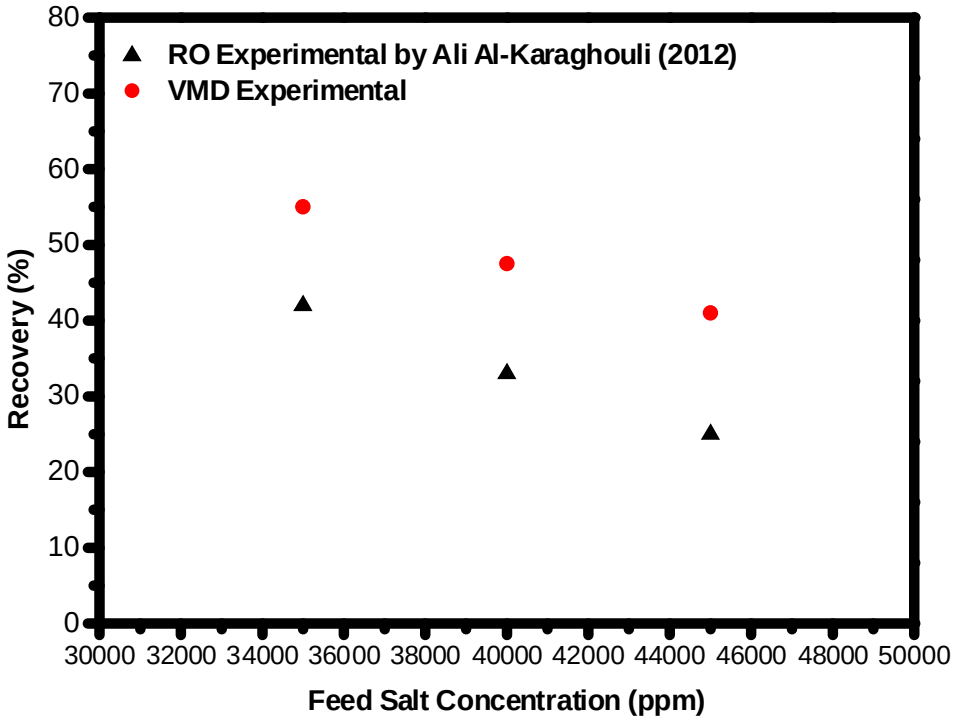

Figure 4.65: Effect of feed salt concentration on recovery for RO and VMD

CHAPTER 5. CONCLUSIONS

Based on the present study, following conclusions may be drawn:

1. Several experimental runs on VMD were conducted by varying the feed flow rate, feed bulk temperature, and salt concentration at constant permeates pressure. It was observed that feed flow rate of 10 lpm, 65°C of feed bulk temperature and 5000 ppm NaCl salt concentration gives the maximum permeate flux

S. No.	Membrane Type	Permeate flux (kg/m^2.h)	Rejection of Sat (%)
1.	PTFE 0.22 µm	98.0	99.9
2.	PVDF 0.22 µm	99.0	98.8
3.	PTFE 0.45 µm	178	78
4.	PVDF 0.45 µm	430	15

2. The permeate flux increased linearly from 77 to 98 kg/m^2·hr and 78 to 99 kg/m^2·hr for PTFE and PVDF membrane of pore size 0.22 µm and 318 to 430 kg/m^2.hr and 134 to 178 kg/m^2.hr for PTFE and PVDF membrane of pore size 0.45 µm upon increasing the feed flow rate from 1 to 10 lpm at feed bulk inlet temperature of 65 °C, feed salt concentration of 5000ppm and permeate pressure of 9 kPa.
3. The gradual increase was found in permeate flux from 18.2 to 98 kg/m^2·hr and 19 to 99 kg/m^2·hrfor PTFE and PVDF membrane of pore size 0.22 µm and 44 to 178 kg/m^2·hr and 205kg/m^2·hr to 430 kg/m^2·hr for PTFE and PVDF membrane of pore size 0.45 µm on increasing the feed bulk temperature from 45 to 65 °C, at feed flow rate of 10 lpm, feed salt concentration of 5000 ppm under 9.0 kPa of permeate pressure.
4. The linear decrease was observed in permeate flux from 98.04 kg/m^2·hr to 84.24 kg/m^2·hr and 98.93 kg/m^2·hr to 63.57 kg/m^2·hr for PTFE and PVDF membrane of pore diameter 0.22 µm and 178.30 kg/m^2·hr to 155.62 kg/m^2·hr and 430.20 kg/m^2·hr to 389.66 kg/m^2·hr for PTFE and PVDF membrane of pore diameter 0.45 µm on increasing the feed inlet salt concentration from 5000 ppm to 50,000 ppm at feed flow rate of 10 lpm, feed bulk inlet temperature of 65 °C under 9.0 kPa of permeate pressure. This decrease in permeate flux might be attributed due to the reason that salt addition will decrease the vapor pressure at the feed side of the membrane and hence, the mass transfer rate.
5. From Taguchi Optimization on percentage salt rejection, it was found that PTFE and PVDF membrane of pore size 0.45 µm was not suitable for use at higher flow rate. Which might be due to decreased membrane hydrophobicity at increased hydrostatic

pressure. The suitable Taguchi results obtained for permeate flux was found to be is 65 °C, 10 lpm and 5000 ppm for PTFE and PVDF membranes of pore size 0.22 µm. The experimental permeate flux under these suitable conditions were found to be 98.04 and 98.9 kg/m^2 .h.

6. The role of pore size for different membrane material was studied in this work and it was observed that permeate flux remains nearly unchanged for PTFE and PVDF membrane for constant pore diameter of 0.22 µm. However, a large variation in permeate flux was observed for PTFE and PVDF membrane of 0.45 µm pore size. This may be due to the fact that the membrane thermal conductivity is more significant at higher pore size (>0.22 µm) and have negligible effect for small pore size (< 0.22 µm).
7. Negligible declination in permeate flux of 1.7 % and 4 % was observed for PTFE and PVDF membranes respectively of pore diameter 0.22 µm after 200 hours continuous run which may be due to the minor scaling on the membrane surface. This minor fouling was also depicted in SEM image as shown in Figure 4.21 (a) & (b). Moreover, this minor scale deposition is also supported from pore size distribution (PSD) as shown in Figure 4.23 and 4.24 which indicate that average pore size in PSD curve shifted from 0.22 µm to 0.18 µm. At 65°C, the permeate flux were found to be 89.42 kg/m^2hr for PVDF membrane and 89.31 kg/m^2hr for PTFE membrane which remain nearly constant till 200 hours at 9.0 kPa of permeate pressure and feed flow rate of 6 lpm for pore diameter of 0.22 µm. Therefore, after every 200 hours the water washing of both membranes was done and the membrane performance was checked again and it was observed that the flux regained to about 98.76% i.e. 88.32 kg/m^2h for PVDF and 98.39% i.e. 87.88 kg/m^2h for PTFE membrane under the same process conditions with 99.9% salt rejection.
8. Percentage salt rejection for PTFE and PVDF membrane of pore size 0.22 µm was found to be constant (99.0%) on increasing the feed flow rate from 1 to 10 lpm. However, percentage salt rejection remains constant to 99% till 6 lpm and beyond 6 lpm to 10 lpm it decreased from 99 to 78.4% for PTFE membrane of 0.45 µm pore. On the other hand, percentage salt rejection remains constant to 99% till 4 lpm and gradual decrease was observed from 99% to 16.7% on increasing the feed flow rate from 4 to 10 lpm for PVDF membrane of 0.45µm pore size. Effect of feed bulk inlet temperature on percentage salt rejection was not observed for PTFE and PVDF membrane of pore size 0.22 µm. The percentage salt rejection was found to be constant throughout to 99% on increasing the feed bulk temperature from 45 to 65 ° C for both membranes of pore size 0.22 µm. Similarly, percentage salt rejection was found to be 99.9 % as constant

throughout on increasing the feed salt concentration from 5000 to 50000 ppm for PTFE and PVDF membrane of 0.22 µm pore size but remarkable variation in salt rejection is observed on increasing the feed salt concentration from 5000 to 50000 ppm for membranes (PTFE & PVDF) of pore size 0.45 µm.

9. The experimental recovery was found to be 81% at 52 hr. It was also found that mathematical recovery was in well agreement with the experimental recovery since the R^2 and MAPE values were found to be 0.999 and 1.936% respectively. Moreover, it was observed that the concentration of the feed tank increased parabolically from 45000 ppm to 125000 ppm by continuously running the setup till 100 hour.
10. Newton Raphson method was used in *solver* to develop heat transfer correlation. It was obtained as $\boldsymbol{Nu=0.158Re^{0.854}Pr^{0.33}}$ at 9.0 kPa permeate pressure at varied flow rate and temperature.
11. The suitable condition for specific energy consumption in VMD was found to be at feed flow rate of 10 lpm, feed bulk temperature of 65°C and 5000 ppm of feed salt inlet concentration of NaCl. Under this condition the specific energy consumption was found to be 6.5 kWh/kg and 4.4 kWh/kg for PTFE and PVDF membrane of 0.22 µm pore size respectively.
12. Linear decrease in specific energy consumption was found from 10.2 to 6.5 kWh/kg and 8.4 to 4.4 kWh/kg for PTFE and PVDF membranes respectively for 0.22 µm pore size on increasing the feed flow rate from 1 to 10 lpm. Further, the specific energy consumption decreases linearly from 20.7 to 8.95 kWh/kg and 18.65 to 4.4 kWh/kg for 0.22 µm pore diameter of PTFE and PVDF membranes respectively, on increasing the feed bulk temperature from 45°C to 65°C. However, linear increase in specific energy consumption was observed on increasing the feed salt concentration from 5,000 to 50,000 ppm for PTFE and PVDF membrane of pore size 0.22 µm at feed flow rate of 10 lpm feed bulk inlet temperature of 65°C and permeate pressure of 9 kPa.
13. VMD was compared with RO on the basis of percentage increment in specific energy consumption and percentage recovery. It was observed that percentage increment in specific energy consumption for VMD was found to be less as compared to RO and percentage recovery was observed higher in VMD than RO. This indicates superiority of VMD over RO.
14. Developed ANN model was found to be well validated with experimental data of VMD as compared to Upadhyaya (2015) model. The R^2 value (0.999) being same for both

models, MAPE value was 10.14% for ANN model which was less than the MAPE value of 18.8% as reported by the mathematical model given by Upadhyaya et al. (2015).

Contribution to Knowledge

1. The effects of operating parameters and membrane parameters on specific energy consumption is done in the present study.
2. The effect of different pore size with same membrane material as well as different membrane materials with same pore size on permeate flux and salt rejection for VMD is studied.
3. Reverse Osmosis and Vacuum Membrane distillation process is compared on the basis of energy consumption and recovery.

Future Recommendations

1. More research is needed to improve the hydrophobicity and liquid entry pressure for PVDF membrane and also to develop new membrane for higher flux.
2. Membrane suitability optimization is needed in terms of membrane characteristics like porosity, pore size, hydrophobicity and membrane material.
3. There is need to find out suitable membrane material and membrane which can provide high flux and the suitability of the membrane with respect to its characteristics like hydrophobicity, porosity, and its physical strength against rupturing.
4. The available mathematical model should be strengthen to understand the microscopic phenomena in the VMD.
5. Fabrication of composite membrane for VMD needs more attention.
6. Heat recovery should be emphasized in process integration to minimize the energy consumption in VMD.
7. Non-conventional energy resources like solar energy, geothermal energy etc. integrated in to vacuum membrane distillation plant for large scale production and to minimize the energy consumption is needed.

References

Abdallah H, Moustafa a. F, AlAnezi AA, El-Sayed HEM (2014) Performance of a newly developed titanium oxide nanotubes/polyethersulfone blend membrane for water desalination using vacuum membrane distillation. Desalination 346:30–36. doi: 10.1016/j.desal.2014.05.003

Abu-Zeid MAE-R, Zhang Y, Dong H, et al (2015) A comprehensive review of vacuum membrane distillation technique. Desalination 356:1–14. doi: 10.1016/j.desal.2014.10.033

Agbekodo KM, Legube B, Cote P (1996) Organics in NF permeate. J AWWA 88:67–74.

Al-Ahmad M, Aleem FA (1993) Scale formation and fouling problems effect on the performance of MSF and RO desalination,plants in Saudi Arabia. Desalination 93:287–310.

Alborzfar M, K. Escande, Allen SJ (1998) Removal of natural organic matter from two types of humic ground waters by nanofiltration. Water Res 32:2970–2983.

Alklaibi AM, Lior N (2004) Membrane-distillation desalination : status and potential. 171:111–131.

Alsaadi AS, Francis L, Amy GL, Ghaffour N (2014) Experimental and theoretical analyses of temperature polarization effect in vacuum membrane distillation. J Memb Sci 471:138–148. doi: 10.1016/j.memsci.2014.08.005

Banat F a., Simandl J (1996) Removal of benzene traces from contaminated water by vacuum membrane distillation. Chem Eng Sci 51:1257–1265. doi: 10.1016/0009-2509(95)00365-7

Bandini S, Saavedra A, Sarti GC (1997) Vacuum membrane distillation: Experiments and modeling. AIChE J 43:398–408. doi: 10.1002/aic.690430213

Berg P, Hagmeyer G, Gimbe R (1997) Removal of pesticides and other micropollutants by nanofiltration. Desalination 113:205–208.

Bergma RA (1996) Cost of membrane softening in Florida. J AWWA 88:32–43.

Bergman R. (1995) Membrane softening versus lime softening in Florida: A cost comparison update. Desalination 102:11–24.

Bhattacharyya D, Williams ME (1992) Reverse Osmosis. In: Membrane Handbook. pp 265–280

Bodell BR (1968) Distillation of Saline Water Using Silicone Rubber Membrane. United State Pat 1–4.

Bray DT (1968) Reverse osmosis purification apparatus. United State Part 1-10.

Bruggen B Van der, Everaert K, Wilms D, et al (2001) The use of nanofiltration for the removal of pesticides from ground water: an evaluation. Water Sci Technol 1:99–106.

Bruggen B Van der, Schaep J, W M, et al (1998) Nanofiltration as a treatment method for the removal of pesticides from ground waters. Desalination 117:139–147.

Bruggen B Van der, Vandecasteele C (2002) Distillation vs. membrane filtration: overview of process evolutions in seawater desalination. Desalination 143:207–218.

Bruggen B Van Der, Vandecasteele C (2003) Removal of pollutants from surface water and groundwater by nanofiltration: Overview of possible applications in the drinking water industry. Environ Pollut 122:435–445. doi: 10.1016/S0269-7491(02)00308-1

Cath TY, Adams VD, Childress AE (2004) Experimental study of desalination using direct contact membrane distillation: a new approach to flux enhancement. J Memb Sci 228:5–16. doi: 10.1016/j.memsci.2003.09.006

Cerneaux S, Strużyńska I, Kujawski WM, et al (2009) Comparison of various membrane distillation methods for desalination using hydrophobic ceramic membranes. J Memb Sci 337:55–60. doi: 10.1016/j.memsci.2009.03.025

Chen J, Zhang Y, Wang Y, et al (2013) Removal of inhibitors from lignocellulosic hydrolyzates by vacuum membrane distillation. Bioresour Technol 144:680–3. doi: 10.1016/j.biortech.2013.07.021

Cheng DY, Wiersma SJ (1983a) Apparatus and method for thermal membrane distillation.

Cheng DY, Wiersma SJ (1983b) Composite membrane for a membrane distillation system.

Chiam C-K, Sarbatly R (2013) Vacuum membrane distillation processes for aqueous solution treatment—A review. Chem Eng Process Process Intensif 74:27–54. doi: 10.1016/j.cep.2013.10.002

Cho JW, Amy G, Pellegrino J (1999) Membrane filtration of natural organic matter: initial comparison of rejection and flux decline characteristics with ultrafiltration and nanofiltration membranes. Water Res 33:2517–2526.

Criscuoli a., Carnevale MC, Drioli E (2013a) Modeling the performance of flat and capillary membrane modules in vacuum membrane distillation. J Memb Sci 447:369–375. doi: 10.1016/j.memsci.2013.07.044

Criscuoli A, Bafaro P, Drioli E (2013b) Vacuum membrane distillation for purifying waters containing arsenic. Desalination 323:17–21. doi: 10.1016/j.desal.2012.08.004

Desalination W, Distillation M (2009) Water Desalination by Membrane Distillation. Desalination, Trends Technol 334.

Drioli E, Ali a., Simone S, et al (2013) Novel PVDF hollow fiber membranes for vacuum and direct contact membrane distillation applications. Sep Purif Technol 115:27–38. doi: 10.1016/j.seppur.2013.04.040

Drioli E, Wu Y, Calabro V (1987) Membrane distillataion in the treatment of aqueous solutions. J Memb Sci 33:277–284. doi: 10.1016/S0376-7388(00)80285-9

Ducom G, Cabassud C (1999) Interests and limitations of nanofiltration for the removal of volatile organic compounds in drinking water production. Desalination 124:115–123.

El-Bourawi MS, Ding Z, Ma R, Khayet M (2006) A framework for better understanding membrane distillation separation process. J Memb Sci 285:4–29. doi: 10.1016/j.memsci.2006.08.002

Ericsson B, Hallberg M, Wachenfeldt J (1996) Nanofiltration of highly colored raw water for drinking water production. Desalination 108:129–141.

Esato K, Oda E, Miyashita H, et al (1979) Expanded polytetrafluoroethylene grafts for small artery replacement. Jpn J Surg 9:164–171.

Escobar IC, Hong S, A. Randall (2000) Removal of assimilable and biodegradable dissolved organic carbon by reverse osmosis and nanofiltration membranes. J Membr Sci 175:1–17.

Everest WR, Malloy SA (2000) Design/build approach to deep aquifer membrane treatment in Southern California. Desalination 132:41–45.

Fan H, Peng Y (2012) Application of PVDF membranes in desalination and comparison of the VMD and DCMD processes. Chem Eng Sci 79:94–102. doi: 10.1016/j.ces.2012.05.052

Ferguson PV (1980) Than. Desalination 32:6–12.

Figoli a., Simone S, Criscuoli a., et al (2014) Hollow fibers for seawater desalination from blends of PVDF with different molecular weights: Morphology, properties and VMD performance. Polym (United Kingdom) 55:1296–1306. doi: 10.1016/j.polymer.2014.01.035

Fu P, Ruiz H, Lozier J, et al (1995) A pilot study on groundwater natural organics removal by low-pressure membranes. Desalination 102:47–56.

García-Payo MC, Essalhi M, Khayet M (2009) Preparation and characterization of PVDF–HFP copolymer hollow fiber membranes for membrane distillation. Desalination 245:469–473. doi: 10.1016/j.desal.2009.02.010

Gorenflo A, Veliizquez-Padrh D, Frimmel FH (2002) Nanofiltration of a German groundwater of high hardness and NOM content: performance and costs,. Desalination 151:253–265.

Gostoli C, Sarti GC (1989) Separation of liquid mixtures by membrane distillation. J Memb Sci 41:211–224. doi: 10.1016/S0376-7388(00)82403-5

Hailin Zhu, Hongjie Wang, FengWang, Yuhai Guo HZ (2013) Preparation and properties of PTFE hollow fiber membranes for desalination through vacuum membrane distillation. J

Memb Sci 446:145–153.

Hasanoğlu a., Rebolledo F, Plaza a., et al (2012) Effect of the operating variables on the extraction and recovery of aroma compounds in an osmotic distillation process coupled to a vacuum membrane distillation system. J Food Eng 111:632–641. doi: 10.1016/j.jfoodeng.2012.03.004

Hilal N, Al-Zoubi H, Darwish NA, et al (2004) A comprehensive review of nanofiltration membranes:Treatment, pretreatment, modelling, and atomic force microscopy. Desalination 170:281–308. doi: 10.1016/j.desal.2004.01.007

Hoop S van, Minnery JG, Mack B (2001) Dead end ultrafiltration as alternative pre treatment to reverse osmosis in seawater desalination: a case study. Desalination 139:161–168.

Horvath AG, Dayton OF, Ieionyv ANI (1931) reverse osmosis. United State Pat 1:631.

Hou D, Wang J, Sun X, et al (2012) Preparation and properties of PVDF composite hollow fiber membranes for desalination through direct contact membrane distillation. J Memb Sci 405–406:185–200. doi: 10.1016/j.memsci.2012.03.008

Jacangelo JG, Trussell RR, Watso M (1997) Roleof membrane technology in drinking water treatment in the United States. Desalination 113:119–127.

Ji Z, Wang J, Hou D, et al (2013) Effect of microwave irradiation on vacuum membrane distillation. J Memb Sci 429:473–479. doi: 10.1016/j.memsci.2012.11.041

Jianhui Z, Ohya H, Negishi Y (1991) Reverse Osmotic Low Concentration of Aqueous Solution of Molecular Weight Organic Solutes. Membrane 16:163–168.

Jitendra Singh SU and SPC (2013) Studies on Separation of NaCl from Water by Vacuum Membrane Distillation. In: International Conference on water desalnation, Treatment and Management by InDACON-2013.

Karakulski K, Gryta M, Morawski A (2002) Membrane processes used for potable water quality improvement. Desalination 145:315–319. doi: 10.1016/S0011-9164(02)00429-0

Khalik A, Praptowidodo VS (2000) Nanofiltration for drinking water production from deep well water. Desalination 132:287–292.

Khayet M (2004) Direct contact membrane distillation of humic acid solutions. J Memb Sci 240:123–128. doi: 10.1016/j.memsci.2004.04.018

Khayet M (2011) Membranes and theoretical modeling of membrane distillation: A review. Adv Colloid Interface Sci 164:56–88. doi: 10.1016/j.cis.2010.09.005

Khayet M, Khulbe K, Matsuura T (2004) Characterization of membranes for membrane distillation by atomic force microscopy and estimation of their water vapor transfer coefficients in vacuum membrane distillation process. J Memb Sci 238:199–211. doi: 10.1016/j.memsci.2004.03.036

Khedr MG (2003) Development of reverse osmosis desalination membranes composition and configuration: Future prospects. Desalination 153:295–304. doi: 10.1016/S0011-9164(02)01149-9

Kimura S, Nakao S-I, Shimatani S-I (1987) Transport phenomena in membrane distillation. J Memb Sci 33:285–298. doi: 10.1016/S0376-7388(00)80286-0

Kiso Y, Mizuno A, Othman RB, et al (2002) Rejection properties of pesticides with a hollow fiber NF membrane (HNF-1). Desalination 143:147–157.

Kiso Y, Nishimura Y, Kitao T, Nishimura K (2000) Rejection properties of non phenylic pesticides with nanofiltration membranes. J Membr Sci 171:229–237.

Kuo C-Y, Lin H-N, Tsai H-A, et al (2008) Fabrication of a high hydrophobic PVDF membrane via nonsolvent induced phase separation. Desalination 233:40–47. doi: 10.1016/j.desal.2007.09.025

Kurbiela J, Rybicki SM (1996) Selection of the best desalination technology for highly saline drainage water from coal mines in southern Poland. 106:415–418.

Lawson KW, Lloyd DR (1997) Membrane distillation. J Membr Sci 124:1–25. doi: 10.1007/s00216-011-4733-9

Lee J-G, Kim W-S (2013) Numerical modeling of the vacuum membrane distillation process. Desalination 331:46–55. doi: 10.1016/j.desal.2013.10.022

Levine B, Madireddi K, Lazarova V, et al (1999) Treatment of trace organic compounds by membrane processes: at the Lake Arrowhead water reuse pilot plant. Water Sci Technol 40:293–301.

Li B, Sirkar KK (2005) Novel membrane and device for vacuum membrane distillation-based desalination process. J Memb Sci 257:60–75. doi: 10.1016/j.memsci.2004.08.040

Li J-M, Xu Z-K, Liu Z-M, et al (2003) Microporous polypropylene and polyethylene hollow fiber membranes. Part 3. Experimental studies on membrane distillation for desalination. Desalination 155:153–156. doi: 10.1016/S0011-9164(03)00292-3

Loeb S (1981) The Loeb-Sourirajan membrane: How it came about [Desalination]. ACS Symp Ser (USA) 153–154.

Lonsdale HK (1982) Reverse Osmosis. Synth Membr Sci Eng Appl 181:307–342.

Lovineh SG, Asghari M, Rajaei B (2013) Numerical simulation and theoretical study on simultaneous effects of operating parameters in vacuum membrane distillation. Desalination 314:59–66. doi: 10.1016/j.desal.2013.01.005

Lu X, Bian X, Shi L (2002) Preparation and characterization of NF composite membrane. J Memb Sci 210:3–11. doi: 10.1016/S0376-7388(02)00120-5

M.E.Findley (1967) Vaporization through Porous Membranes. Ind Eng Chem Process Des

Dev 6:226–230.

Mariah L (2006) MEMBRANE DISTILLATION f OF CONCENTRATED BRINES.

Mariah L, Buckley C a., Brouckaert CJ, et al (2006) Membrane distillation of concentrated brines-Role of water activities in the evaluation of driving force. J Memb Sci 280:937–947. doi: 10.1016/j.memsci.2006.03.014

Mengual JI, Khayet M, Godino MP (2004) Heat and mass transfer in vacuum membrane distillation. Int J Heat Mass Transf 47:865–875. doi: 10.1016/j.ijheatmasstransfer.2002.09.001

Mericq J-P, Laborie S, Cabassud C (2009) Vacuum membrane distillation for an integrated seawater desalination process. Desalin Water Treat 9:287–296. doi: 10.5004/dwt.2009.862

Mohammadi T, Kazemi P, Peydayesh M (2014) Optimization of vacuum membrane distillation parameters for water desalination using Box–Behnken design. Desalin Water Treat 1–10. doi: 10.1080/19443994.2014.961173

Montovay T, Assenmacher M, Frimme FH (1996) Elimination of pesticides from aqueous solution by nanofiltration. Magy Kem folyoriat 102:241–247.

Naidu G, Choi Y, Jeong S, et al (2014) Experiments and modeling of a vacuum membrane distillation for high saline water. J Ind Eng Chem 20:2174–2183. doi: 10.1016/j.jiec.2013.09.048

Ohya H, Suzuki T, Nakao S (2001) Integrated system for complete usage of components in seawater: A proposal of inorganic chemical combinat in seawater. Desalination 134:29–36. doi: 10.1016/S0011-9164(01)00112-6

Oktem H (2007) Materials & Design Application of Taguchi optimization technique in determining plastic injection molding process parameters for a thin-shell part. 28:1271–1278. doi: 10.1016/j.matdes.2005.12.013

P. Fu HR, Thompson K, Spangenber C (1994) Selecting membranes for removing NOM and DBP precursors. J Am Water Work Assoc 86:55–72.

Pangarkar BL, Sane MG, Parjane SB, et al (2010a) The Heat and Mass Transfer Phenomena in Vacuum Membrane Distillation for Desalination. World Acad Sci Eng Technol 33–38.

Pangarkar BL, Thorat P V., Parjane SB, Abhang RM (2010b) Performance evaluation of vacuum membrane distillation for desalination by using a flat sheet membrane. Desalin Water Treat 21:328–334. doi: 10.5004/dwt.2010.1400

Reid C (1966) Principles of reverse osmosis. Desalin by Reverse Osmosis 1–14.

Reid CE, Breton EJ (1959) Water and ion flow across cellulosic membranes. J Appl Polym Sci 1:133–143. doi: 10.1002/app.1959.070010202

Rodgers FA (1968) Distillation under hydrostatic pressure with vapor permeable membrane.

Rodgers FA (1969) Multiple effect distillation with microporous membranes and distillate recirculation. 3.

Roy RK (1990) A Primer on the Taguchi Methods.

S.P. Chaurasia Sushant Upadhyaya Kailash Singh (2013) Water desalination by membrane distillation. In: Desalination, Trends and Technologies. pp 21–40

Safavi M, Mohammadi T (2009) High-salinity water desalination using VMD. Chem Eng J 149:191–195. doi: 10.1016/j.cej.2008.10.021

S Loeb SS (1962) High-flow semipermeable membranes for separation of water from saline solutions. Adv Chem Ser 38:117–132.

Sarbatly R, Chiam CK (2013) Evaluation of geothermal energy in desalination by vacuum membrane distillation. Appl Energy 112:737–746. doi: 10.1016/j.apenergy.2012.12.028

Schaep J, Van Der Bruggen B, Uytterhoeven S, et al (1998) Removal of hardness from groundwater by nanofiltration. Desalination 119:295–302. doi: 10.1016/S0011-9164(98)00172-6

Selvi SR, Baskaran R (2014) Variation of Flux in Membrane Distillation. APCBEE Procedia 9:97–101. doi: 10.1016/j.apcbee.2014.01.018

Shakaib M, Ahmed I, Yunus R (2011) CFD modeling for fluid flow and heat transfer in membrane distillation. Proc Int … 6:265–268.

Shatat M, Riffat S, Ghabayen S (2012) State of Art Water Desalination Technologies Using. 4th Int Eng Conf –Towards Eng 21st century 1–16.

Shi JY, Zhao ZP, Zhu CY (2014) Studies on simulation and experiments of ethanol-water mixture separation by VMD using a PTFE flat membrane module. Sep Purif Technol 123:53–63. doi: 10.1016/j.seppur.2013.12.015

Shim SM, Lee JG, Kim WS (2014) Performance simulation of a multi-VMD desalination process including the recycle flow. Desalination 338:39–48. doi: 10.1016/j.desal.2013.12.009

Sikora J, Hansson C, Ericsson B (1989) Pre-treatment and desalination of mine drainage water in a pilot plant. Desalination 75:363–373.

Singh J, Chaurasia SP, Upadhyaya S, Dohare RK (2012) Studies on Separation of Multi-Ions by Membrane Distillation. In: National Conference on Water Quality Management. pp 4–5

Sivakumar M, Ramezanianpour M, O'Halloran G (2013) Mine Water Treatment Using a Vacuum Membrane Distillation System. APCBEE Procedia 5:157–162. doi: 10.1016/j.apcbee.2013.05.028

Sombekke HDM, Voorhoeve DK, Hiemstra P (1997) Environmental impact assessment of groundwater treatment with nanofiltration. Desalination 113:293–296. doi: 10.1016/S0011-9164(97)00144-6

Soukane S, Chelouche S, Naceur MW (2014) A ballistic transport model for vacuum membrane distillation. J Memb Sci 450:397–406. doi: 10.1016/j.memsci.2013.08.038

Sun AC, Kosar W, Zhang Y, Feng X (2014) Vacuum membrane distillation for desalination of water using hollow fiber membranes. J Memb Sci 455:131–142. doi: 10.1016/j.memsci.2013.12.055

Sushant Upadhyaya, S.P.Chaurasia KS and JKS (2012) Desalination of water by Vacuum membrane distillation for sustainable development. Int J Environ Eng Manag 3:349–352.

Tang N, Cheng P, Wang X, Zhang H (2009) Study on the vacuum membrane distillation performances of PVDF Hollow Fiber membranes for aqueous NaCl solution. Chem Eng Trans 17:1537–1542. doi: 10.3303/CET0917257

Tang N, Jia Q, Zhang H, et al (2010) Preparation and morphological characterization of narrow pore size distributed polypropylene hydrophobic membranes for vacuum membrane distillation via thermally induced phase separation. Desalination 256:27–36. doi: 10.1016/j.desal.2010.02.024

Tang N, Peng Y, Jia Z, et al (2014) Vacuum membrane distillation simulation of desalination using polypropylene hydrophobic microporous membrane. J Appl Polym Sci 41632:n/a-n/a. doi: 10.1002/app.41632

Tang N, Zhang H, Wang W (2011) Computational fluid dynamics numerical simulation of vacuum membrane distillation for aqueous NaCl solution. Desalination 274:120–129. doi: 10.1016/j.desal.2011.01.078

Tavakolmoghadam M, Safavi M (2012) An Optimized Neural Network Model of Desalination by Vacuum Membrane Distillation Using Genetic Algorithm. Procedia Eng 42:106–112. doi: 10.1016/j.proeng.2012.07.400

Upadhyaya S (2013) Mathematical Modeling and Experimental Study of Vacuum Membrane Distillation for Desalination. Malaviya National Institute of Technology Jaipur

Upadhyaya S, Singh K, Chaurasia SP, et al (2015) Mathematical and CFD modeling of vacuum membrane distillation for desalination. Desalin Water Treat 3994:1–16. doi: 10.1080/19443994.2015.1048306

Upadhyaya S, Singh K, Chaurasia SP, et al (2016) Recovery and development of correlations for heat and mass transfer in vacuum membrane distillation for desalination. Desalin Water Treat 3994:1–13. doi: 10.1080/19443994.2016.1189245

van de Lisdonk C a. C, van Paassen J a. M, Schippers JC (2000) Monitoring scaling in nanofiltration and reverse osmosis membrane systems. Desalination 132:101–108. doi:

10.1016/S0011-9164(00)00139-9

Visvanathan C, Marsono B, Basu B (1998) Removal of THMP by nanofiltration: effects of interference parameters. Water Res 32:3527–3538.

Vrouwenvelder HS, Van Paassen JAM, Folmer HC, et al (1998) Biofouling of membranes for drinking water production. Desalination 118:157–166. doi: 10.1016/S0011-9164(98)00116-7

Walton J, Lu H, Turner C (2000) Solar and Waste Heat Desalination by Membrane Distillation.

Wang L, Li B, Gao X, et al (2014) Study of membrane fouling in cross-flow vacuum membrane distillation. Sep Purif Technol 122:133–143. doi: 10.1016/j.seppur.2013.10.031

Watson B., Hornburg CD (1989) Low-energy membrane nanofiltration for removal of color, organics and hardness from drinking-water supplies. Desalination 72:11–22.

Westmoreland Julius C (1968) SPIRALLY WRAPPED REVERSE OSMOSIS MEMBRANE CELL.

Weyl PK (1967) Recovery of demineralized water from saline waters.

William J Conlon SAM (1989) Membrane softening: a treatment process comes of age. J Am Water Work Assoc 81:47–51.

Wittmann E, Cote P, Medici C, et al (1998) Treatment of a hard borehole water containing low levels of pesticide by nanofiltration. Desalination 119:347–352.

Wu B, Teo WK (2004) Preparation and application of PVDF hollow fiber membranes for TCA removal from aqueous solutions by vacuum membrane distillation.

Xu Y, Zhu BK, Xu YY (2006) Pilot test of vacuum membrane distillation for seawater desalination on a ship. Desalination 189:165–169. doi: 10.1016/j.desal.2005.06.024

Xu Z, Pan Y, Yu Y (2009) CFD simulation on membrane distillation of NaCl solution. Front Chem Eng China 3:293–297. doi: 10.1007/s11705-009-0204-7

Yeh H, Tseng I, Kao S, et al (2000) Comparison of the finished water quality among an integrated membrane process, conventional and other advanced treatment processes. Desalination 131:237–244.

Zhang J, Gray S, Li J De (2012) Modelling heat and mass transfers in DCMD using compressible membranes. J Memb Sci 387–388:7–16. doi: 10.1016/j.memsci.2011.08.034

Zhang J, Li J De, Duke M, et al (2013) Modelling of vacuum membrane distillation. J Memb Sci 434:1–9. doi: 10.1016/j.memsci.2013.01.048

Zhang L, Xiang J, Cheng PG, et al (2015) Three-dimensional numerical simulation of

aqueous NaCl solution in vacuum membrane distillation process. Chem Eng Process Process Intensif 87:9–15. doi: 10.1016/j.cep.2014.11.002

Zhao K, Heinzl W, Wenzel M, et al (2013a) Experimental study of the memsys vacuum-multi-effect-membrane-distillation (V-MEMD) module. Desalination 323:150–160. doi: 10.1016/j.desal.2012.12.003

Zhao Z-P, Xu L, Shang X, Chen K (2013b) Water regeneration from human urine by vacuum membrane distillation and analysis of membrane fouling characteristics. Sep Purif Technol 118:369–376. doi: 10.1016/j.seppur.2013.07.021

Zhou T, Yao Y, Xiang R, Wu Y (2014) Formation and characterization of polytetrafluoroethylene nanofiber membranes for vacuum membrane distillation. J Memb Sci 453:402–408. doi: 10.1016/j.memsci.2013.11.027

Zuo G, Guan G, Wang R (2014) Numerical modeling and optimization of vacuum membrane distillation module for low-cost water production. Desalination 339:1–9. doi: 10.1016/j.desal.2014.02.005

Appendices

Experimental error calculation

$$N_A = \frac{m_A}{\pi r_e^2 t} \qquad \text{A.1}$$

$$dN_A = \frac{1}{\pi r_e^2 t}\mathrm{dm}_A - \frac{2m_A}{\pi r_e^3 t}\mathrm{dr}_e - \frac{m_A}{\pi r_e^2 t^2}\mathrm{dt} \qquad \text{A.2}$$

$$\frac{dN_A}{N_A} = \frac{r_e^2}{m_A}\left[\frac{1}{r_e^2 t}\mathrm{dm}_A - \frac{2m_A}{r_e^3 t}\mathrm{dr}_e - \frac{m_A}{r_e^2 t^2}\mathrm{dt}\right] \qquad \text{A.3}$$

$$\frac{dN_A}{N_A} = \frac{r_e^2}{m_A}\left[\frac{1}{r_e^2 t}\left|\mathrm{dm}_A\right| + \frac{2m_A}{r_e^3 t}\left|\mathrm{dr}_e\right| + \frac{m_A}{r_e^2 t^2}\left|\mathrm{dt}\right|\right] \qquad \text{A.4}$$

$$\textit{Maximum Error } \% = \frac{dN_A}{N_A} \times 100 \qquad \text{A.5}$$